APRIL 1983
ENVIRONMENTAL SCIENCE & TECHNOLOGY

ES&T

Water analyses: Improving the results

174A

A New ACS Audio Course to help you understand and solve industrial and municipal waste-water problems . . . .

ACTIVATED SLUDGE:

Stoichiometry, Kinetics, and Mass Balances

Whether you're a chemist or chemical engineer, a biological scientist or civil engineer, if you need to understand aerobic, suspended growth, mixed culture systems, ACTIVATED SLUDGE will give you the most up-to-date information.

The bulk of the course focuses on the development of mass balance principles and their application to biological reactors. Using these principles, you'll learn how to apply stoichiometric and kinetic relationships to select appropriate system sizing, oxygen needs, nutrient levels and sludge-disposal methods.

In addition to treating common industrial waste problems, the author introduces advanced concepts and procedures required to analyze more complex problems.

To test your understanding, numerous problems are presented with detailed solutions.

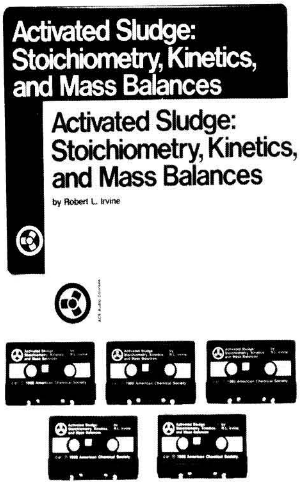

INSTRUCTOR

Dr. Robert L. Irvine, Professor of Civil Engineering, University of Notre Dame, is a recognized expert on biological treatment in sequencing batch reactors.

COURSE MATERIALS

Five audiotape cassettes (6.2 hours playing time) and a 127-page manual, \$275.00. Additional manuals for group use, 1 to 9 copies . . . \$16.00 each; 10 or more copies . . . \$12.80 each. (Catalog no. Z-57.)

NO-RISK GUARANTEE

Order now! If you're not completely satisfied, just return the course within ten days for a full refund or cancellation of invoice.

Please allow six weeks for delivery.

Please send _____ copy(ies) of

Activated Sludge: Stoichiometry, Kinetics, and Mass Balances at \$275.00 each to:

Also send _____ additional manuals for group study.

Name __________

Organization __________

Address __________

City/State/Zip __________

☐ Purchase order enclosed. ☐ Payment enclosed.

Charge my ☐ VISA ☐ MasterCard Expiration Date __________

Account No. __________

Interbank Code __________ (MasterCard Only)

Signature __________

☐ Please ship by air (billed at cost) ☐ Please send free catalog.

American Chemical Society
Education Department
1155 Sixteenth Street, N.W.
Washington, D.C., 20036
(202) 874-4588

NEW
LOWER PRICES!

Man and Molecules

Dimensions in Science

Man and Molecules Cassettes:

An easy way to keep up with what's happening in science.

Outstanding scientists are interviewed in language that everyone can understand. Each cassette has two 15-minute programs.

Single Cassette	**$3.50**
Any Four — Nineteen Cassettes	**$3.00**/Cassette
Any 20 or more cassettes to one address	**$2.50**/Cassette

10% discount if payment accompanies order

California residents please add 6% State Use Tax.

Name ______________________________

Address ______________________________

____

City ______________________________

State ____________ Zip ____________

Annual Cassette Subscriptions also available

Select your choices and mail to:

American Chemical Society
1155 Sixteenth St., N.W.
Washington, D.C. 20036
Dept. M&M

Science and Society

☐ **World Energy** Dr. Glenn T. Seaborg
The Recycle Society Dr. Glenn T. Seaborg

☐ **Science and the Future** Dr. Linus Pauling
Society and the Future Dr. Linus Pauling

☐ **Chemrawn 2 — World Hunger Problems** Dr. Bryant Rossiter
Chemrawn 2 — World Hunger Solutions Dr. Bryant Rossiter

☐ **The Robots are Coming** Mr. R. Behler and Mr. R. Malczewski
The R&D Gap Dr. Herbert Striner and Rep. George Brown

☐ **Feeding the World** Dr. Norman Borlaug
Fighting World Famine Dr. Jean Mayer

☐ **Good News on Organic Farming** Dr. Garth Youngberg
Foods for the Future Dr. Robert Wiley

Health and Medicine

☐ **Vitamins — More is not Better** Dr. Victor Herbert
Evolution of the Human Diet Dr. Glynn Isaac

☐ **Sickle Cell Update** Dr. Clarice Reid
Antibiotics: The Vicious Circle Dr. Richard Novick

☐ **New Promise for Preemies** Dr. Shlomo Shinnar
New Developments in Dentistry Dr. Rayfael Bowen

☐ **Update on the Pill** Mr. Ward Rinehart
Ring Around the Collar Dr. Kay Obendorf

☐ **Rhythmic Humans I** Dr. Thomas Wehr
Rhythmic Humans II Dr. Thomas Wehr

☐ **The Organized Brain** Dr. Ronald MacGregor
Windows to the Brain Dr. Terry Bahill

☐ **The Science of Pain I** Drs. Edward Huskisson and William Beaver
The Science of Pain II Drs. John Bonica and Gerald Aronoff

☐ **The Frozen Cell: Cryobiology** Dr. Harold Meryman
How Blood Clots Dr. Russell Doolitle

☐ **Folk Medicine** Dr. Ned Heindel
Nuclear Medicine Dr. Ned Heindel

☐ **Vision and the Nervous System** Dr. Arthur Sanderson
Cataract: The Clouded Eye Dr. Abraham Spector

☐ **Trace Metals and Aging** Dr. Gunther Eichhorn
Diabetes: The Receptor Problem Dr. Jesse Roth

☐ **Halting Emphysema** Dr. James Powers
Pulmonary Fibrosis Dr. Ronald Crystal

☐ **The Stopped Heart: Assessing CPR** Dr. Myron Weisfeldt
Chemistry of the Sickled Cell Drs. Wm. Eaton and James Hofrichter

Science

☐ **Laser Age** Mr. John Walters
Verifying Art — It's a Science Dr. George Reilly

☐ **Delving into Dreams** Dr. Robert McCarley
Earthquake Clues Drs. Mark Shapiro and Kate Hutton

☐ **Chemical Weapons** Dr. Arthur Westing
Tracing Breezes and Bombs Dr. Russell Dietz

☐ **Scientists Responsibility to Public** Dr. Harlyn Halvorson
Who Controls Scientific Data? Dr. Stephen Fienberg

☐ **Composite Materials** Prof. Byron Pipes
Fiber Optics Dr. Suzanne Nagel

☐ **Crime Fighting with Chemistry** Mr. Roger Aaron
Chemistry and Sherlock Holmes Dr. Samuel Gerber

☐ **Symmetry, Antimatter and the Big Bang** Drs. J. Cronin and B. Winstein
Atomic Movies Dr. Albert Crewe

The Natural World

☐ **Animals' Biological Compass** Dr. Joseph Kirschvink
The Horned Faced Bee Dr. Suzanne Batra

☐ **Bioluminescence** Dr. John Warner
Plants that Fight Back Dr. David Rhoades

☐ **A Sea of Chemicals** Dr. William Fenical
The Chemical Tree Dr. John Rowe

☐ **Animal Talk** Dr. Eugene Morton
The Defensive World of Insects Dr. Thomas Eisner

☐ **Problems in Weather Forecasting** Dr. Richard Somerville
Life on the Sea Floor Dr. Robert Hessler

☐ **The Unsteady Sun** Dr. J. Murray Mitchell
Climatic History On Ice Dr. Bruce Parker

☐ **Plants: Chemical Treasure Chest** Dr. Leon Zaikov
The Flowering Mystery Dr. Charles Cleland

☐ **Climate and Food** Dr. Wayne Decker
Plants and Temperature Dr. Judith St. John

Energy

☐ **More Energy from Less** Drs. Meyers, Harris, Meier
Alfalfa: Fuel and Food Dr. Bruce Dale

☐ **A New Look at Solar Economics** Mr. William Wilhelm
Water Weakens Glass Dr. Stephen Freiman

☐ **The Electric Car** Dr. John Hartman
Saving Energy with Batteries Mr. Kurt Kluner

☐ **Synfuels: The Uncertain Solution** Dr. Mark Hanson
Special Essay on Energy Essay Report

☐ **Saving Energy in Buildings** Mr. Christopher Flavin
The Sun's Heat Can Cool Mr. Dennis Schlepp

☐ **The New Age of Materials** Mr. Christopher Flavin
Synthetics: The Petroleum Connection Mr. Christopher Flavin

☐ **Solar Cells: Improving Materials** Mr. Donald Carmichael
Solar Cells: Performance Testing Mr. Donald Carmichael

Space

☐ **Cosmology by Experiment** Drs. Howell Pugh and Paul Richards
The Search for Gravity Waves Drs. Ronald Drever and Stanley Whitcomb

☐ **From Sputnik to Space Shuttle** Dr. Alan Needell
Landsat IV Dr. Vincent Salomonson

☐ **The Rings of Saturn** Dr. Larry Esposito
Saturn and its Moons Dr. Larry Esposito

☐ **Looking at Solar Explosions** Mr. Ken Frost
Jupiter and Beyond Dr. Edward Stone

☐ **Stars and the Elements** Dr. Michael Zelik
Archaeoastronomy: Sky and Culture Dr. Edwin Kurpp

☐ **Universe of Questions** Dr. John Wheeler
Resources from Space Dr. James Arnold

☐ **The Expanding Universe** Dr. Victor Viola
Interstellar Molecules Dr. Eric Herbst

Environment

☐ **Acid Rain Update** Essay Report
Academia's Chemical Waste Dr. Jack Gerlovich

☐ **Coal Questions** Dr. K.P. Ananth
Fire Toxicity Mr. Gordon Vickery

☐ **Chemicals and Health: Biological Tests** Dr. Benjamin Barnhart, Ms. Ann Grow
Chemicals and Health: Toxic Dumps Dr. William Lowrance

☐ **Taking the Hazard Out of Waste** Dr. Robert Pojasek
What to Do With Hazardous Wastes Mr. Thomas Williams

☐ **New Target in Water Pollution** Mr. Joseph Krivak
Environment Doctors Dr. Richard Perrine

☐ **Air Pollution: The Human Factor** Dr. Ralph Stacy
Indoor Air Pollution Mr. John Yocom

☐ **Water Weeds** Dr. Dean Martin
The Red Tide Dr. Dean Martin

☐ **Drinking Water Worries** Dr. John O'Conner
Water Chlorination Problems Dr. William Glaze

Popular Older Programs

☐ **The Vanishing Soil** Mr. Lester Brown
The Not So Limitless Oceans Dr. Joel Goldman

☐ **How Times Has Changed** Sir George Porter
Analyzing with Light Dr. Richard Nathan

☐ **Taking Earth's Temperature From Space** Dr. John Price
Probing the Earth's Magnetosphere Dr. Erwin Schmerling

☐ **Solar Thermal Energy** Mr. J.D. Walton
Coal Furnaces: Think Small Dr. Arthur Squires

☐ **Energy-Efficient Autos** Dr. Gene Mannella
Fuel Cells: Problems and Progress Dr. John Belding

☐ **New Light on Myasthenia Gravis** Dr. Daniel Drachman
Hormones and Aging Dr. George Roth

☐ **Nutrition and the Brain** Dr. John Fernstrom
Chemical Look at Mental Illness Dr. Seymour Kety

☐ **The Brain's Own Morphine** Dr. Solomon Snyder
Narcotics and the Brain Dr. Avram Goldstein

☐ **Plants and Air Pollution** Dr. Howard Heggestad
Particulate Air Pollution Dr. Glen Gordon

☐ **Genetic Engineering in Agriculture** Drs. P. Carlson and I. Zelitch
Jojoba Power Dr. Milton Harris

☐ **Chemistry of the Mind: Schizophrenia** Dr. Larry Stein
Chemistry of the Mind: Depression Dr. Joel Elkes

☐ **Cancer and Chemicals Part I** Dr. Charles Heidelberger
Cancer and Chemicals Part II Dr. Charles Heidelberger

ห้องสมุดกรมวิทยาศาสตร์บริการ
26 ก.พ. 2526

ES&T

CONTENTS

Volume 17, Number 4, April 1983

165A

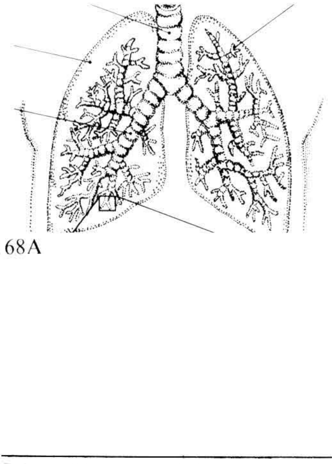

168A

OUTLOOK

REGULATORY FOCUS

FEATURE

RESEARCH

Environmental Science & Technology

"*Environmental Science & Technology* ES&T (ISSN 0013-936X) is published monthly by the American Chemical Society at 1155 16th Street, N.W., Washington, D.C. 20036. Second-class postage paid at Washington, D.C. and at additional mailing offices. POSTMASTER: Send address changes to Membership & Subscription Services, PO Box 3337, Columbus, OH, 43210."

SUBSCRIPTION PRICES 1983: Members, $20 per year; nonmembers (for personal use), $25 per year; institutions, $110 per year. Foreign postage, $8 additional per year/Air freight add $30; multiple year rates available on request. Single issues $8.00 for current year; $9.00 for prior years. Back volumes $96. Rates above do not apply to nonmember subscribers in Japan, who must enter subscription orders with Maruzen Company Ltd., 3-10 Nihon bashi 2-chome, Chuo-ku, Tokyo 103, Japan. Tel: (03) 272-7211.

SUBSCRIPTION SERVICE: Orders for new subscriptions, single issues, back volumes, and microfiche and microform editions should be sent with payment to Office of the Treasurer, Financial Operations, ACS, 1155 16th St., N.W., Washington, D.C. 20036. Phone orders may be placed, using Visa or Master Card, by calling toll free (800) 424-6747 from anywhere in the continental U.S. Changes of address, subscription renewals, claims for missing issues, and inquiries concerning records and accounts should be directed to Manager, Membership and Subscription Services, ACS, P.O. Box 3337, Columbus, Ohio 43210. Changes of address should allow six weeks and be accompanied by old and new addresses and a recent mailing label. Claims for missing issues will not be allowed if loss was due to: insufficient notice of change of address, if claim is dated more than 90 days after the issue date for North American subscribers or more than one year for foreign subscribers, or if the reason given is "missing from files."

Credits: p. 169A, p. 171A, *ES&T*'s Julian Josephson

Cover: UNIPHOTO. Bruce Waters

ESTHAG 17(4) 157A-190A
187-250 (1983)
ISSN 0013-936X

211
Mass transfer coefficient correlations for volatilization of organic solutes from water. Donald Mackay* and Andrew T. K. Yeun

The data confirm the validity of the two-resistance model for mass transfer and show that no interaction occurs when solutes are volatilized simultaneously.

217
Chemical changes in concentrated, acidic, metal-bearing wastewaters when treated with lime. Dennis R. Jenke, Gordon K. Pagenkopf,* and Frank E. Diebold

Of the chemical changes that occur, precipitation is predominant with complexation, oxidation, and adsorption playing major roles.

224
Photochemical ozone formation in urban and point-source plumes. Ken Sexton* and Hal Westberg

NMHC/NO_x ratios indicate ozone production, or depletion in the case of power-plant effluents, was consistent with the HC-NO_x-UV light model.

227
Partition equilibria of nonionic organic compounds between soil organic matter and water. Cary T. Chiou,* Paul E. Porter, and David W. Schmedding

The sorption of some aromatic compounds from both single-solute and binary-solute aqueous solutions on a Woodburn soil is investigated.

231
Partitioning of strontium-90 among aqueous and mineral species in a contaminated aquifer. Richard E. Jackson* and Karen J. Inch

The geochemical partitioning of ^{90}Sr during its migration through a shallow sand aquifer is discussed.

237
Effect of natural organic coatings on the coagulation of particles. Ronald J. Gibbs

These experiments show that natural coated samples coagulate significantly more slowly than samples with the coatings removed.

NOTES

240
Reductive destruction of hydrazines as an approach to hazard control. George Lunn, Eric B. Sansone, and Larry K. Keefer*

Nickel-based reductive methods are shown to hold promise as an approach to preventing environmental pollution by hydrazines.

244
Impact of fossil fuel combustion on sediments of Lake Michigan: a reprise. John J. Griffin and Edward D. Goldberg*

Concentrations, morphologies, and size distributions of charcoals are identified and may be used to reconstruct burning histories.

245
Electrolytic preparation of [^{36}Cl]-chlorine dioxide from H^{36}Cl. Hossein A. Ghanbari,* Willis B. Wheeler, and James R. Kirk

This procedure is an effective preparation of $^{36}ClO_2$ and is characterized by high yield, purity, and specific activity.

248
Application of γ-γ-directional correlation measurements for speciation studies in environmental research. Marcel de Bruin* and Peter Bode

The technique of PDC measurements is shown to have potential in studying trace-element behavior in living systems.

* To whom correspondence should be addressed.

DEPARTMENTS

Published by the
AMERICAN CHEMICAL SOCIETY
1155 16th Street, N.W.
Washington, D.C. 20036
(202) 872-4600

BOOKS AND JOURNALS DIVISION
Director: D. H. Michael Bowen

Head, Journals Department: Charles R. Bertsch
Head, Production Department: Elmer M. Pusey
Head, Research and Development Department: Seldon W. Terrant
Head, Marketing and Sales Department: Claud K. Robinson
Manager, Circulation Development: Cynthia Smith

ADVERTISING MANAGEMENT
Centcom, Ltd.
For officers and advertisers, see page 188A.

Please send *research* manuscripts to Manuscript Reviewing, *feature* manuscripts to Managing Editor. For author's guide and editorial policy, see the January 1983 issue, page 57A, or write Janice L. Fleming, Manuscript Reviewing Office, *ES&T*. A sample copyright transfer form, which may be copied, appears on the inside back cover of the January 1983 issue.

LETTERS

Environmental toxicology

Dear Sir: Michigan State University is seeking candidates for its interdisciplinary doctoral program leading to joint PhD degrees in environmental toxicology and in a traditional department. This program, which is open to bachelor's degree recipients, provides much flexibility in choosing areas for study. Faculty advisors may be drawn from a variety of units including the Colleges of Agriculture, Human Medicine, Osteopathic Medicine, Veterinary Medicine, Engineering and Natural Science, the Institute for Water Research, and the Pesticide Research Center. Fields of study include the molecular aspects of environmental toxicology, clinical toxicology of animals and humans, and the degradation and fate of chemicals in the environment. Each student's course of study is planned with that individual's particular interests, capabilities, and professional goals in mind. Applications are welcome at any time. Potential candidates should contact the Center for Environmental Toxicology, C-231 Holden Hall, Michigan State University, East Lansing, Mich. 48824; (517) 353-6469.

Jerry B. Hook, Director
Michigan State University
East Lansing, Mich. 48824

Biological diversity

Dear Sir: "Why maintain biological diversity?" (*ES&T*, February 1982, p. 94A) cites the California Gene Resources Program (CGRP) as a force, active since the early 1970s, working to maintain plant biological diversity. CGRP was actually started in 1980 by the state of California in response to reported losses of bioresources vital to the state. Its scope extends well beyond the genetic diversity of plants, including wild and domesticated animals, microorganisms, agricultural tree and field crops, and commercial timber species important to California.

The California Gene Resources Program, the first such program in the nation, is conducted by the National Council on Gene Resources. The National Council was founded to help generate the kinds of support necessary for the adequate management, conservation, and utilization of gene resources essential to the U.S.

The council brings together public and private decision makers, provides them with the specific technical and policy-related information necessary to justify changes in their policies and budgets, and helps establish the financial and organizational arrangements required for additional support.

Obtaining adequate long-term private and governmental support for gene resource activities and focusing greater attention on gene-resource-related issues at the state, regional, national, and international levels are central concerns of the National Council. Safeguarding the gene resources essential to the continued success of American agriculture, forestry, fisheries, and pharmaceutics should concern us all.

For additional information on the activities and publications of the National Council on Gene Resources, please contact: NCGR, 2855 Telegraph Ave., Suite 209, Berkeley, Calif. 94705.

David Whitman
Associate Education Director
National Council on Gene Resources
Berkeley, Calif. 94705

Dear Sir: I am responding to Julian Josephson's article on biological diversity and Professor Blair's letter (*ES&T*, July 1982, p. 367A).

Biological diversity, with the multitude of biological systems and their interrelations, results from the evolutionary process leading from simple to complex systems. This diversity developed under a great variety of living conditions on this planet.

Unquestionably, conservation of the diverse biological systems that have evolved over millions of years is important to humanity. However, a problem is the choice between meeting human needs harmonious with the conservation of living nature, and others whose satisfaction is in opposition to conservation goals. More often, people emphasize the latter type of needs. As a result, relations between humans and the biosphere become increasingly distant from a balanced state of nature. A consequence is the destruction of many ecosystems, leading not only to the decrease in biological diversity, but even to threats to the existence of the biosphere itself.

This trend is normally ascribed to the unwise or inexperienced behavior of humans, who have not yet learned to live in harmony with nature. But I believe that a more satisfactory explanation involves a theory that distinguishes the biological component of man, which must depend upon and interact with other portions of the biosphere, from the psychosocial component of man, which can exist independently of the biosphere, at a certain stage of its evolution. A concrete example of the psychosocial component of human beings can be seen in machines of artificial intelligence, which are not dependent upon the biosphere.

This contradiction between the biological and psychosocial components results in the divergence of the evolutionary trends of these two components. They separate human psychic processes from the biological side of man. A main cause of damage to the biosphere, and to the biological functions of human beings, I believe, is found in this dichotomy between our biological and psychosocial development.

Petr Molík
Okružní 103/III
392 01 Soběslav
Czechoslovakia

ES&T

EDITORIAL

Manuscript processing time

The utility of the refereed scientific literature is strongly related to the speed with which the results of research appear in print. This same factor is one of the vital signs of the current status of research in a particular field, along with the number of submitted manuscripts and their overall quality.

I have to conclude that the field of environmental science is strong, as indicated by the numbers of scientists, engineers, and other professionals engaged in research bearing on environmental issues. Other indicators of vitality include the fact that our manuscript receipts at *ES&T* have risen from a level of 280 per year in 1977 to approximately 350 in the past two years. Also, the number of competitive environmental journals has increased as has the number of national environmental societies. Our efforts to make *ES&T* a truly useful reflection of this vitality require that it be a forum for "current" scientific deliberation. Therefore, we need to focus on reducing manuscript processing time to a minimum. Effective reduction of this time cannot be done by a single person, since the journal belongs to all of us—the publishers, the staff, the editors, the reviewers, and the authors.

I am pleased to report that the management of the Books and Journals Division of ACS, the ACS staff in our Manuscript Reviewing Office and Columbus Editorial Office, and the members of the journal's Editorial Advisory Board have been actively interested in analyzing the time factors associated with producing the journal. Improvements have been made in both the "receipt to acceptance" and "acceptance to publication" time categories.

The bottom line is that all those working directly for the journal or the Society have succeeded in trimming approximately 9 to 11 weeks from the median processing times recorded in 1978–79.

What can you do to help? The most important thing, of course, is to send us your very best work. Our experience, not surprisingly, shows that the highest quality articles are the ones that are processed most rapidly. Their value tends to be recognized immediately by reviewers, and revisions, if any, are minor. Another important contribution you can make is to realize that over half of our processing time is taken by reviewers' and/or authors' efforts at revision. Our requests for reviews ask that manuscripts be returned in a three-week period, and if all reviewers were attentive to the significance of this period, our times would be dramatically reduced. The same, of course, applies to authors who have received the reviewer comments and editorial requests for revision. Since August 1981, only approximately 60% of all manuscripts accepted fell into the fastest category (accepted directly after review or after minor revision). The remainder constitutes a significant pool from which time savings can be exacted.

We are quite fortunate at *ES&T* to have a dedicated and highly trained staff in the Manuscript Reviewing Office. Jan Fleming, Monica Creamer, Yvonne Curry, and Mary Ellen Provencher are all willing and anxious to work swiftly with authors and reviewers. Your efforts coupled with ours will move us toward the goal of keeping the journal's Research section truly current.

R F Christman

0013-936X/83/0916-0161A$01.50/0

ES&T

CURRENTS

INTERNATIONAL

To help Third World countries solve industrial pollution problems, 14 U.S. corporations have agreed to provide free technical assistance. A five-year program will be funded equally by U.S. industry and the U.S. Agency for International Development. The World Environment Center (New York, N.Y.) will administer the program through its International Environment and Development Service, established in February. An expert would visit a country to inspect industrial sites and recommend remedial measures. Local authorities or plant management would take any necessary follow-up action. Tunisia has already requested this assistance.

The Justice Department has turned three documentaries made by the National Film Board of Canada into instant box office hits. Two of the films concern acid rain; the third is about nuclear war. In late February, the Justice Department decided that the films are political propaganda and cannot be shown without a disclaimer saying that the U.S. government disapproves of them. Justice acted under the 1938 Foreign Agents Registration Act, which was written to force undercover lobbyists or dummy front organizations to name their true sponsorship. The sponsorship of these films is clearly known, however—the Canadians. Before the Justice Department action, there was little interest in these films. In early March, however, hundreds of people lined up at a Washington, D.C., theater to see them.

WASHINGTON

The EPA removed more than 50 scientists from its science advisory boards after conservative groups provided lists that characterized dozens of these scientists with such expressions as "horrible," "a real activist," or "bleeding-heart liberal." A political evaluation of more than 90 EPA scientists was released by Sen. Gary Hart (D-Colo.) and others on Capitol Hill in early March. In a break with tradition, EPA Administrator Anne M. Burford did not reappoint several dozen members of the EPA's science advisory panels when their fixed terms expired. Several EPA officials say these were replaced with scientists who have a reputation for being politically conservative. However, advisory board director Terry Yosie said the advisory boards still include balanced viewpoints.

Synar: *Superfund used as a slush fund*

Superfund monies amounting to $53.6 million are not accounted for properly in EPA records, according to a draft audit report on the federal program prepared by former EPA Inspector General Matthew Novick. Part of this money was apparently used to pay the costs of other programs. Rep. Mike Synar (D-Okla.) said the draft audit suggested that EPA used Superfund as a "slush" fund to make up for deficient funds in other programs. However, an EPA statement asserted that the audit was preliminary and was drafted so that program managers would have an opportunity to correct auditing errors. The inspector general's audit for fiscal 1981 also said that tighter accounting procedures were needed for the Superfund program.

EPA officials have drafted a proposal for particulate matter that would set the average annual primary standard at 55 $\mu g/m^3$ and the 24-h standard at 180 $\mu g/m^3$ for particles less than 10 μm in diameter. This represents a relaxation of 41% in the annual standard and 18% in the 24-h standard. The current annual standard is 75 $\mu g/m^3$, and the 24-h standard is 260 $\mu g/m^3$. These apply to total suspended particulates. Therefore, although the numbers look smaller and stricter in the new standards, they represent a significant relaxation because particles 10 μm and smaller constitute 46% of the total suspended particulates.

The EPA is now attempting to assess substantial penalties against the Thriftway Company for violations of the rules that limit the lead content of gasoline. Company lawyers allege that EPA Administrator Anne Burford made an unequivocal commitment in December 1981 that EPA would not enforce the lead standard against Thriftway during the time when EPA was considering a relaxation in the lead standard. Last year the EPA's inspector general investigated the meeting at which the alleged commitment was made, and a report of the investigation was sent to the White House counsel for review. Early last month, the president's deputy counsel, Richard A. Hauser, said, "We reviewed the report . . . and felt no disciplinary action was required by the White House."

EPA Administrator Anne M. Burford resigned last month and three other top EPA officials have left the agency. On Feb. 7, Rita M. La-

0013-936X/83/0916-0162A$01.50/0

velle, assistant administrator in charge of the toxic waste cleanup program, was discharged after she refused to resign at the request of Burford. Inspector General Matthew N. Novick and Assistant Administrator for Administration John P. Horton resigned on Feb. 23. On March 9, Burford resigned, following many weeks of intense criticism during which a number of Congressional leaders from both parties asked for her resignation and several White House aides suggested that she leave the agency. All four officials are under investigation. Lee M. Thomas was chosen as a replacement for Lavelle, Charles Dempsey was named inspector general, and Alfred M. Zack replaced Horton.

Dingell: *the documents reveal failure*

The EPA has reduced money and personnel needed for hazardous waste enforcement, according to agency documents released in late February. One document warned that the enforcement division did not have enough funds and personnel to initiate new cases and that the number of lawyers had been cut by a third. Another said that the agency's goals could not be met with current funding. Rep. John D. Dingell (D-Mich.) said the documents revealed "continued failure to protect the American people from the ill effects of exposure to hazardous wastes."

STATES

Levels of 2,3,7,8-TCDD, commonly known as dioxin, in certain fish taken from lakes and rivers throughout southern Michigan are far higher than those recommended for human consumption by the Food and Drug Administration (FDA), according to an unpublished project conducted at Michigan State University. The contamination was found in the edible fillets of carp and suckers throughout the heavily industrialized southern part of Michigan. Matthew J. Zabic, who headed the research, said that these studies are not conclusive. He found traces of TCDD in fish ranging from 17–586 parts per trillion (ppt) with most of the findings in the range of 100–200 ppt. The FDA has ruled that fish containing more than 50 ppt of dioxin should not be eaten at all.

The state of Maryland is being criticized for using herbicides to control weeds along roadsides by a coalition of environmentalists, watermen, hunters, road workers, and commissioners of the three southern Maryland counties of Calvert, Charles, and St. Marys. Tordon and 2,4-D are among the chemicals being used at present. 2,4,5-T was used until the EPA banned it three years ago. The coalition believes that using herbicides along roadsides threatens plant and animal life in the streams and rivers, kills birds and small animals, and may be a threat to human health. The three counties requested that the state stop spraying herbicides on their roadsides. Highway officials ceased using herbicides on county roads but not on state roads.

Both legislative and legal action will be used by the U.S. Conference of Mayors in an effort to stop EPA's proposed sanctions against 213 counties that did not meet the clean air standards by December 1982. The mayors believe that if cities are making a good faith effort to implement plans aimed at achieving ambient air quality standards, then sanctions should not apply. The mayors adopted a statement in mid-February saying that "EPA is attempting to use the nation's cities as a club to persuade Congress to weaken the Clean Air Act." The mayors favor a strong Clean Air Act and assert that they will not allow the cities to be used in this way.

EPA has relaxed sulfur dioxide emission limits for eight sources in North Carolina. These sources are presently operating under a limit of 1.6 lb per million units of heat input. Unless opposing comments are submitted, a new limit of 2.3 lb per million units of heat input will take effect on April 11. The change will be incorporated into the North Carolina state implementation plan.

SCIENCE

Wood-stove "nostalgia" can be a health hazard, warns Sidney Benson of the University of Southern California's Hydrocarbon Research Institute. "Wood stoves produce more carbon monoxide than the internal combustion engine," he observes, adding that improperly ventilated wood stoves have caused fatalities. Benson also says that wood-stove ventilation problems can expose the user to several carcinogenic compounds, "including many of those identified as lung cancer agents in tobacco smoke." He notes that particulate matter from wood smoke carries these compounds. Benson calls for better ventilation and careful selection of woods to be burned.

An experimental insecticide that is harmful to most plant-eating insects but harmless to other forms of life has been developed by researchers in biotechnology from the State University of New York at Stony Brook. The scientists took plant products called phytosterols and added fluorine to the substances to produce compounds called 29-fluorophytosterols. Enzymes present only in plant-eating insects metabolize the chemicals and release deadly fluoroacetate. Most other forms of life cannot break down the chemicals and thus are not affected by them.

Fears of contracting cancer from drinking groundwater contaminated with chemicals, such as trichoroethylene and carbon tetrachloride, "have been overstated," says Paul Newberne of the Massachusetts Institute of Technology. He adds that "cancer risk is minimal, particularly in the light of the huge doses given to test animals in the laboratory to develop cancer." And Harry Demopoulos of New York University suggests that only 1–5% of cancers in the U.S. are caused by contamination; he blames the rest on factors such as diet and lifestyle.

Vapor movement in air depends not only on air currents, but also on the weight and size of the molecules involved, say scientists from the U.S. Department of Agriculture and the University of Maryland. They acknowledge that their theory is controversial and needs more verification, but if borne out it could require revisions of ideas on how gases disperse in the atmosphere. The scientists found this "unexpected" vapor behavior while measuring how much pesticide vaporizes after application to the ground. They worked with more than 3000 samples of six pesticides, taken 2–72 in. above ground level, and concluded that smaller molecules rose faster than larger ones.

TECHNOLOGY

Converting raw coal to clean-burning liquid fuel might be done with 25–40% less hydrogen than previously needed for coal liquefaction, says William Harrison of the Southern Company. He adds that lower hydrogen consumption makes the process more efficient and allows up to two-thirds of the raw coal to be recovered as clean liquid fuel. Raw coal is mixed with a small amount of hydrogen and a solvent derived from the coal and then heated to about 825 °F. Sulfur goes out as a gas, and solid mineral residues, which would have become ash, are separated. Next, hydrotreatment with a catalyst leads to liquid and some solid fuels with about 0.25% sulfur.

A special facility to incinerate low-level β- and γ-emitting wastes was established at Studsvik, Sweden, in 1976. The amount of wastes burned there rose from 76 metric tons (tonnes) in 1977 to about 300 in 1981. Principal items burned are plastics, cloth, wood, paper, and rubber from nuclear plants and research stations, hospitals, and other places where radioactive materials are used. Reportedly, the waste is reduced in mass by a factor of six and in volume by a factor of 50. Ash residue is then encased in concrete for eventual proper disposal. This incineration know-how is now available for marketing by Studsvik Energieteknik AB.

To enhance activated-carbon wastewater treatment system performance, a small device will simulate the operation of a full-scale carbon adsorption system for removing pesticides. This device is the core of the "Dynamic Mini-Column Adsorption Technique" (DMCAT) for which EPA's Industrial Environmental Research Laboratory awarded a $294 440 contract to Environmental Science and Engineering, Inc. (Gainesville, Fla.). The DMCAT is being field-tested to validate it. It will then be used to improve the operation of carbon systems for wastewater at three selected pesticide manufacturing plants.

Aeration powered by wind energy could clean up canals, says Peter Freeman, a consulting engineer and inventor of the Wind Energy Water Aeration and Circulation device (WEWAC). The WEWAC is being tested by scientists with the Marine Sciences Consortium (Wallops Island, Va.). Tests started in 1979. After three years, canals equipped with WEWAC appeared to show a return of oxygen to waters and sediments. Freeman believes that wind power makes the canal aeration scheme more economical; electrical equipment for this purpose would be costly to buy and operate.

Incineration system

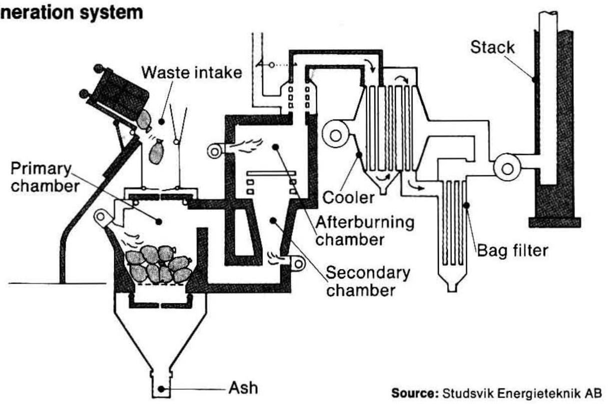

Source: Studsvik Energieteknik AB

INDUSTRY

The Aluminum Company of America (Alcoa) has agreed to spend $1.5 million to clean up a toxic waste site at Olney, Ill. An agreement with EPA instructs Alcoa to remove all liquids, sludges, and other wastes, some of which are contaminated with polychlorinated biphenyls. The company also agreed to clean up underground pollution at the site and to ascertain the extent of contamination of nearby groundwater supplies. EPA also filed suit to have McDonnell Douglas Corporation clean up an approximately four-acre site in Greenup, Ill. Both sites were operated by A&F Materials Inc., a waste disposal firm now out of business.

With the aim of commercializing a process to make methane from liquid industrial wastes, the Gas Developments Corporation (GDC, Chicago, Ill.), a component of the Institute of Gas Technology, signed a licensing agreement with VIMAG, Inc., a Maryland firm associated with Belgian interests. The two-phase process uses acid- and methane-phase digestors, which GDC says offer improved biogasification efficiency. In other work, GDC is seeking improved inocula for the anaerobic fermentation of wood to produce methane. GDC believes that the potential for usable energy from terrestrial biomass will be 12–17 quads by the year 2000.

"Chemical companies are committed to reducing chemical hazards and to finding solutions to health and environmental issues," says Robert Roland, president of the Chemical Manufacturers Association (CMA, Washington, D.C.). CMA commissioned an accounting firm to survey the industry and document this statement. The survey found that each chemical firm spent an average of almost $2 million on toxicity testing and recordkeeping in 1981. Recycling and incineration have become hazardous waste management approaches for nearly 75% of the 112 companies surveyed. Strong efforts were also put forth in the areas of safety, communications, and government compliance, Roland said.

ES&T
OUTLOOK

Environmental dispute resolution

Can mediation provide better solutions than litigation to environmental disputes while reducing the time and expense required?

"To facilitate the negotiations, all participants have agreed to refrain absolutely from any further disclosure of what may be taking place on the other side of the conference-room door."

Drawing by Ed Fisher; © 1982 The New Yorker Magazine, Inc.

The U.S. is a litigious society. The courts throughout the country are faced with a heavy case load of environmental actions. Not only do these cases tend to be expensive, but they frequently alienate the opposing parties even further. Before building almost any large plant in a new location, industry has to anticipate one or more legal challenges.

Although mediation and other forms of conflict resolution could possibly replace litigation for resolving certain disputes in many areas of society, mediation is often particularly appropriate for resolving environmental conflicts. This possibility was discussed at length at the National Conference on Environmental Dispute Resolution, sponsored by the Conservation Foundation and held in Washington, D.C., in late January. Conference participants gave many reasons why the courtroom is often a less-than-satisfactory vehicle for resolving environmental conflicts.

John Larsen, vice-president of the Weyerhaeuser Company, said that the parties in an environmental dispute are not "individuals seeking justice—but, in effect, varied and diverse groups pursuing often abstract concepts concerning economic health, energy, and environmental quality." Environmental suits are almost always tied to specific points of law. They may have little to do with what the plaintiff is attempting to accomplish. For example, an interest group might sue over the adequacy of an environmental impact statement when what it really wants is an agreement to protect the rural nature of the proposed project site.

Another drawback of litigation is that it often creates a winner and a loser. In contrast, mediation seeks a solution that makes both sides winners. Furthermore, when a court is forced to find a solution, this sometimes results in placing the burden of running an environmental agency or fishery, for instance, on the court—which does not have the appropriate expertise. Another reason mediation is useful is that the courts have become overloaded with environmental disputes.

Conference speakers pointed out that mediation, which was first attempted for environmental conflicts in 1975, has already been used to resolve about 70 disputes and predicted that its use would grow in coming years. Eight states now have organizations that provide environmental dispute resolution services, and there is an increasing number of professional mediators with experience in environmental matters.

Although several alternatives to litigation, such as structured dialogue and negotiation, have been tried for resolving environmental conflicts, mediation is the method most commonly used. It is a formal procedure in which a neutral outsider is employed to mediate between the opposing fac-

0013-936X/83/0916-0165A$01.50/0

tions, organize formal negotiations, encourage the disputants to work together to resolve the conflict, and try to bring the dispute to a resolution satisfactory to both sides. Mediation has been used to settle conflicts in a wide variety of areas such as labor disputes.

Important benefits

The advantages mediation provides for resolving environmental disputes are numerous. As already mentioned, mediation allows the disputants to focus on the substantive issues, rather than on peripheral points of law. John L. Watson, a lawyer with the firm of Kirkland and Ellis (Denver, Colo.) pointed out that because the parties in a mediated dispute are not forced to tie their arguments to the law, they are free to express and try to gain their real objectives. Thus, mediation provides the disputants with an opportunity to engage in direct dialogue on specific issues. In addition, environmentalists as well as developers may find that mediation frequently obtains results more favorable than what a court could order.

Furthermore, mediation may restrain the tendency of conflicting parties to advocate an extreme position in anticipation of being forced into a compromise. In ordinary litigation, each side brings up the evidence that is favorable to its goal and neglects to mention the unfavorable reports and the gray evidence—the inconclusive research studies, for instance, that are relevant to almost any conflict. In mediation, the opposing parties are encouraged to discuss and consider all the information that relates to the dispute. They usually educate each other in the process and discover many points of agreement. After a conflict is resolved by mediation, the parties may feel much less rancor toward each other than if a solution had been handed down by a court. Many conference participants expressed the opinion that mediation is generally less costly and time-consuming than litigation, although no comparative studies have been done to test this theory.

Not a panacea

Mediation has many advantages, but it cannot substitute for litigation in some kinds of environmental disputes. To be resolved by mediation, a conflict must meet certain criteria. Conference participants seemed to agree on nearly all of these. Jay D. Hair, executive vice-president of the National Wildlife Federation, noted that "mediation, to be effective, must focus primarily on local resource disputes that can be brokered, not values which cannot." As Washington, D.C., attorney Phillip J. Harter wrote last year in the *Georgetown Law Journal*, "Most of these [environmental] negotiations have involved a specific dispute over the environmental consequences of a particular action at a specific site." Where and how to build a power plant or a mine or a highway are examples of the types of disputes that have been solved by mediation. Because nearly all disputes involve values of one kind or another, it is probably incorrect to say that a dispute must not concern values if it is to be mediated. One of the benefits mediation provides is the political balancing of competing values. But if the dispute is solely over deeply held values—the value or lack of value of the Clinch River breeder reactor project, for example—the dispute cannot be solved by mediation.


Hair: *Mediation will be used increasingly to resolve environmental disputes.*

A second criterion is that each side must have enough power so that no side can take unilateral action without incurring an unacceptable burden of lawsuits from the other side. When one side has no power to interfere in a dispute, there is no motivation to solve the dispute by mediation. There must also be some pressure of time. If one of the opposing sides feels that it can let the conflict drag on for years with no harm done, it will not feel any pressure to engage in mediation. Another requirement is that the parties must be able to deliver on their agreements. If one party has no power, alone or in conjunction with other parties, to carry out the agreements it makes, then there is no point in trying to resolve a dispute with mediation. Mediation must be started rather early in the conflict, before lawsuits are filed, but late enough so that the issues are well-known and the interested parties have emerged.

Two other criteria mentioned by John A. S. McGlennon of Clark-McGlennon Associates in Boston are that the parties should have nothing to gain by not settling a dispute and should have some degree of countervailing power. In some conflicts, each of the opposing factions has the erroneous impression that it has no power. In this case, the mediator may be able to help the parties to understand the power they possess.

Necessary ingredients

In addition to these criteria a dispute must meet, the mediation process itself must fulfill certain general requirements. Gov. Richard D. Lamm of Colorado, who has had extensive experience with mediation, pointed out that "the hardest problem is to decide who is represented at the mediation table." Implicit in Governor Lamm's statement is the idea that all significantly affected parties should be represented. If one interested group is not included in the negotiation process, it may be dissatisfied with the agreement that is reached and institute a lawsuit afterward. The mediator in a dispute has to be acceptable to the parties and be seen as neutral. For example, a mediator with a vested interest in a corporation engaged in the dispute would not be perceived as neutral.

Another requirement for successful mediation is continuity—the participants should be willing to participate throughout the proceedings. Replacing a negotiator with a substitute is harmful to the process.

Confidentiality is also very important during much of the mediation process. If each meeting is open to the press, the parties will not feel free to discuss the issues and explore alternative solutions openly. As Glenn Paulson, vice-president for science of the National Audubon Society, said, "It is important for the participants to agree on when to report the proceedings to the media." A final important criterion noted by Gerald W. Cormick, executive director of the Institute for Environmental Mediation (Seattle, Wash.), is that the mediator should make sure the parties don't just "blunder into agreements but that they be reached on the basis of informed self-interest."

Obstacles

Experience with mediation has shown it to be a good way to resolve conflicts if they meet the criteria mentioned. There are several impediments to mediation, however, that must be overcome if it is to be used to resolve a substantial percentage of environmental disputes. One of the primary obstacles is funding. At present, there is no institutional means to fund mediation. In the past, foundations have financed mediation for some conflicts. But if it is to be used widely, state and federal governments may need to play an important role in funding, as Madeleine Crohn, president of the National Institute for Dispute Resolution (Washington, D.C.) pointed out.

Related to funding is another problem that environmental groups often face when contemplating the use of mediation. This is a lack of expert advice on technical issues. If adequate funds are available, however, the required technical advice can be purchased. Robert J. Golton of the National Wildlife Federation said that "until people can supply themselves with the technical expertise they need, they will use the courts."

A third obstacle is the difficulty of communication. Attorney John Watson pointed out that "those actually participating in mediation are likely to find that their understanding of the issues develops so rapidly that it leaves their clients and colleagues behind." Consensus building within many grass-roots environmental organizations takes place through a democratic process, frequently involving open give-and-take debate. Much hard work, including careful communication, is required of a representative of such an organization in a mediation effort if the individual is to truly represent the organization and not his or her own views in arriving at a mediated compromise.

Leah K. Patton, director of Mediation Services at the Institute for Environmental Mediation (Seattle, Wash.), listed a number of fears that hinder mediation and may cause parties to use the courts instead. One of these is a fear on the part of one party that in the process of negotiating, it will lose the support of its constituency. A hard-and-fast position may seem to preserve more support than does the flexibility required in successful mediation. The mere fact that it is negotiating may cause a disputant to fear that it appears to be compromising or giving in to the "enemy." A second fear is that mediation will cause the party to lose in the conflict. Rather than exploring through mediation what alternative paths are available to achieve its final goal, an interest group may incorrectly think that if it doesn't achieve a certain tactical objective, it will not achieve its ultimate goal. Often a party will believe that it has a better chance of winning in the courtroom when in fact the probable outcome is quite different. A third fear is a lack of trust that the opposite side will abide by any settlement that results from mediation.

Negotiated rule making

The rule-making process is now bitterly adversarial. Several participants at the conference expressed the idea that mediation might be used in rule making to produce regulations that give rise to fewer lawsuits after they are promulgated. In some other countries, such as Canada and Japan, these rule-making proceedings are considerably less adversarial.

Joseph A. Cannon, associate administrator for Policy and Resource Management at EPA, described EPA's current plans for two experimental projects in negotiated rule making. He noted that the steps in the present rule-making process are: an internal memorandum describing the proposed rule, advance notice of proposed rule making, notice of proposed rule making, and final rule making. "Then," he said, "everyone sues us." In fact, negotiation is always a part of

Organizations for environmental dispute resolution

New England

Center for Negotiation and Public Policy
Boston, Mass.

Clark McGlennon Associates, Inc.
Boston, Mass.

Environmental Law Center
Vermont Law School
South Royalton, Vt.

Environmental Negotiation Program
Massachusetts Institute of Technology
Cambridge, Mass.

New England Environmental Mediation Center
Boston, Mass.

East

American Arbitration Association
Washington, D.C.

The Conservation Foundation
Washington, D.C.

Federal Mediation and Conciliation Service
Office of Mediation Services
Washington, D.C.

Institute for Environmental Negotiation
University of Virginia
Charlottesville, Va.

Institute for Mediation and Conflict Resolution
New York, N.Y.

Public Mediation Service
Falls Church, Va.

Scientists' Institute for Public Information
New York, N.Y.

Central

Illinois Environmental Consensus Forum
Institute of Government & Public Affairs
Urbana, Ill.

Institute for Environmental Mediation
Madison, Wis.

Rocky Mountains

Adaptive Environmental Assessment
Ft. Collins, Colo.

ROMCOE, Center for Environmental Problem Solving
Boulder, Colo.

Keystone Center
Keystone, Colo.

West

The Center for Collaborative Problem Solving
San Francisco, Calif.

Center for Conflict Resolution
Neighborhood Justice Center
Honolulu, Hawaii

Forum on Community and the Environment
Palo Alto, Calif.

Institute for Environmental Mediation
Seattle, Wash.

Interaction Associates, Inc.
San Francisco, Calif.

Shorett and Associates
Seattle, Wash.

Western Network
Santa Fe, N.M.

Canada

Environmental Mediation International
Ottawa, Ontario

the present process, but it is sequential negotiation, and it takes place after the final rule making. At this time, each party meets with the agency individually and tries to convince it to change its rules to more nearly match the position of the party.

Sequential negotiation is quite different from mediation, as Phillip Harter noted, because "such negotiation is merely one form of the adversary process itself; each party attempts to sway the decision maker to a favorable disposition," and in the process opposing parties "tend to take extreme positions expecting that they may be pushed toward the middle." Unlike mediation, the parties in sequential negotiation do not deal directly with one another. Each of them makes an individual presentation to the rule maker. Just as in a courtroom, the parties usually feel reluctant to reveal weaknesses in their extreme positions and refuse to reveal data that do not support them.

For some types of rule making, Cannon is optimistic that mediated rule making will work. With this approach, the negotiations will take place earlier in the rule-making process and their nature will be changed to a form of mediation. But when describing the two experimental projects EPA will be carrying out in this area, he stressed that mediated rule making is "fraught with peril." One unresolved question is how the agency will run this project with a sense of impartiality and fairness and have its own representatives at the bargaining table. Another important problem is confidentiality. For mediated rule making to be successful, not all sessions can be open to the press because this would prevent candid discussions from taking place. But the Federal Advisory Committee Act (FACA) and the Administrative Procedure Act (APA), which apply to all-party, face-to-face negotiations that occur in the process of rule making, allow closed meetings only under limited circumstances. Therefore, the EPA experiments in negotiated rule making will include both open and closed meetings as FACA and APA permit. Much experimentation and some changes in laws may be required before negotiated rule making can be successful.

Future prospects

The optimistic attitude of the participants at the National Conference on Environmental Dispute Resolution showed that many professionals in the area are confident that mediation can be used to solve a growing number of environmental conflicts. Jay Hair predicted that in 10 years "more environmental disputes will be mediated than litigated." Weyerhaeuser's John Larsen, who sees "the increasingly adversarial nature of American public life" as a great problem for this country, said that industry has a responsibility to help with this problem by a "willingness to explore new approaches to conflict resolution—particularly in the environmental area." William K. Reilly, president of the Conservation Foundation, stated that he can't recall a time when there has been as much acrimony concerning the environment. Perhaps mediation can be used to dispel some of this.

—Bette Hileman

Additional reading

(1) Baldwin, Pamela. "Environmental Mediation: An Effective Alternative?" Report of a Conference held in Reston, Va., Jan. 11-13, 1978. Available from The Conservation Foundation.

(2) Harter, Philip J. "Negotiating Regulations: A Cure for Malaise" *Georgetown Law Journal* **1982,** *71*(1), 1-118.

(3) Talbot, Allan R. "Settling Things, Six Case Studies in Environmental Mediation"; The Conservation Foundation: Washington, D.C., 1983.

Exposure pathways of workplace contaminants

Respiration is the principal, though not exclusive route. More needs to be learned about how the lungs and other body organs and functions come to be at risk

Human exposure to toxic substances in the workplace can occur through entry routes such as the skin or by ingestion of particles too large to enter the lung. Increasingly, these routes are being studied. However, the respiratory system is considered the dominant pathway for the entry of contaminant gases and aerosols.

The lungs are often the target organ for a given contaminant or group of contaminants. However, the chemical(s) may affect other organs or body functions after entry through the pulmonary system. In the case of aerosols, the particles may be toxic, whether in liquid or solid form, or they may be inert. An inert particle may carry a dissolved or adsorbed vapor contaminant that is toxic to respiratory tract sites that it could not otherwise reach.

One example of a gas to which a worker might be exposed through inhalation is vinyl chloride monomer (VCM). Its concentration in the workplace atmosphere is now severely limited by regulation. On the basis of animal tests conducted during the early 1970s, inhaled VCM became suspected of having links to angiosarcoma, a very rare, but virulent liver cancer that appears to be 100% fatal. However, in the vinyl chloride industry, only 16 known or suspected cases have appeared worldwide as of 1974.

What is an aerosol?

The term "aerosol" refers to solid or liquid particles suspended in a gas such as air. Technically an aerosol is defined as a two-phase system that includes both the particles and the gas in which they are suspended. Klaus Willeke of the University of Cincinnati explains that the term "carries a connotation that the suspension is relatively stable and that the particles will remain suspended for some significant period of time. However, the length of time for being considered an aerosol has not been agreed upon by scientists."

0013-936X/83/0916-0168A$01.50/0

Certain airborne particles, such as asbestos, are suspected of causing mesothelioma, a deadly cancer of the tissue lining the lungs and peritoneum (membrane covering the abdominal cavity). Other materials with possible links to cancer or other permanently or temporarily debilitating afflictions are polynuclear aromatic hydrocarbons (PAHs), polychlorinated dibenzodioxins and -furans, bis(chloromethyl) ether, heavy-metal-containing dusts, and numerous other materials.

Future research on exposure to chemicals in the workplace will put greater emphasis on routes of exposure from the nose and mouth all the way to the alveoli and on the contaminants that attack the human organism by these routes. The biological and biochemical nature of these insults and the mechanisms that the body employs to "fight back" will also be of growing interest to occupational health experts.

A departure from custom

"People often expect retired professors, such as myself, to tend to look to the past," said Anna Baetjer, Emerita Professor of Environmental Health Sciences at The Johns Hopkins University School of Hygiene (Baltimore, Md.). "But I will depart from this custom and try to predict what future needs will be for research in toxicology and respiratory diseases," she told the First Theodore F. Hatch Symposium on Recent Advances in Occupational Health, held at the University of Pittsburgh in September.

"A very important need will be for toxicological studies of multiple chemicals," Baetjer said. She explained that "while it is much simpler to study single chemicals, they often do not reflect 'real life.' We will also need to know about factors in man that may affect his susceptibility, and what his stress factors are. Another important study field will be the response of man to chemicals at concentrations normally encountered, rather than at the extremely high doses used today," Baetjer added.

With respect to respiratory ailments brought about by exposure to toxic chemicals, "we need to determine the role of macrophages [a type of phagocyte] and their enzymes in alveolar clearance, especially with regard to dust particles deep in the respiratory tract. We will want to know more about pulmonary effects of surfactant compounds, or of fresh fumes of, say, cadmium oxide, or how gases such as ozone or others affect the deep lung tissue," Baetjer suggested. Also, "does an exposed person become acclimated to various contaminants and, if so, how, and what happens? Are there allergic or immunological reactions in the respiratory tract?"

The "exposure curve"

The symposium at the University of Pittsburgh was named after Theodore F. Hatch, one of the pioneers and "elder statesmen" of the field of occupational health. He is also a founder of the University of Pittsburgh's Graduate School of Public Health (GSPH). Today, Hatch is a professor emeritus who came to attend the first symposium in his honor and to award the first Hatch fellowship to Daniel Goon, a student at the GSPH.

One of Hatch's accomplishments was the development of a curve from which the effects of exposure of a living organism to varying amounts of a contaminant could be explained. Nurtan Esmen of the University of Pittsburgh observes that this curve is not, by itself, a quantitative tool. Nevertheless, the curve suggests that if the dose of a contaminant were sufficiently low, one would expect homeostasis. In this case, the body repairs all damage to the lungs, for example, caused by the exposure, and recovery is complete.

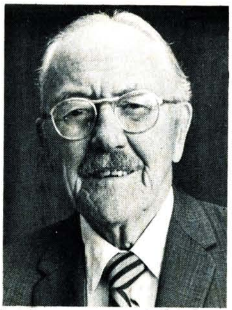

***Hatch:** symposium in his honor*

When the dose is larger, the phenomenon of "adaptation" could occur. Yves Alarie of the University of Pittsburgh explained why adaptation may be deceptive for certain agents. What happens is that a chemical may initially cause respiratory symptoms. Although the exposure remains unabated, the symptoms seem to disappear; the worker has "adapted" or "acclimated" to his or her exposure and feels nothing. Alarie warns that this lack of symptoms should not be taken to be equivalent to homeostasis. He says that some damage to the lungs, for example, could have oc-

The Hatch curve for dose–response[a]

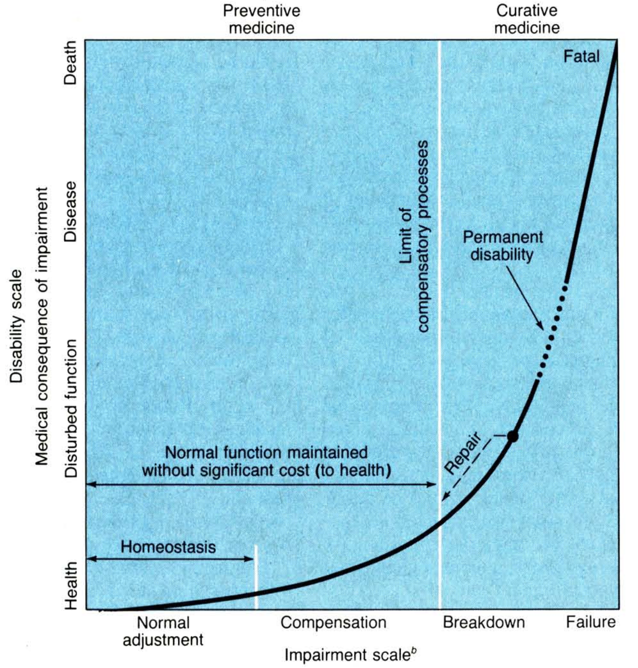

[a] Suggested relationship between impairment and disability

[b] Impairment increases with aging, as a residual of illness, and from excessive environmental stress

Source: Hatch, T.F. "Changing Objectives in Occupational Health," *Amer. Ind. Hyg. Assoc. J.* **1962,** *23,* 1–7.

curred—even if it is not felt, or seen in X-ray pictures or even in exploratory surgery or forensic pathology.

Alarie singled out formaldehyde and SO_2 as chemicals to which workers "are especially subject to 'adaptation.' This is dangerous to the worker, because even though he or she no longer feels irritation, the lungs are damaged all the same." As the dose increases further, adaptation gives way to chronic symptoms that increase in severity. The Hatch curve continues up to acute effects ranging from injury through morbidity to mortality. Esmen cautions that transition between effects along the Hatch curve should be regarded as depending upon "various, and generally quite complicated relationships between the agent(s) and the host."

What should the TLV be?

The TLV is the threshold limit value, the maximum concentration of an air pollutant to which an individual may be exposed for a long period of time without harmful effects. Since different individuals are susceptible to varying degrees, some may be affected by exposures to lower concentrations. Prepared by government industrial hygienists, TLVs are used as guidelines for controlling workplace health hazards.

For a contaminant that a worker may be expected to encounter, Alarie proposes that the TLV be set below the "adaptation" dose of the Hatch curve, if such a value can be determined. A means that he suggests for estimating this value might be derived from calibrated and validated animal models. For example, Alarie presented an animal model to evaluate the potency of airborne chemicals having sensory irritation effects on the eyes, nose, and throat.

From this animal model, it was shown that reasonable predictions for TLVs could be made for 40 industrial chemicals. One major exception was for formaldehyde, with the animal model predicting a much lower value than the current TLV. Alarie noted that "this is the first animal model to predict safe exposure in industry." He urged that "models should be developed for major health effects categories such as lung cancer, pulmonary hypersensitivity, methemoglobinemia (a blood ailment), and other such diseases.

Conducting airways in the human respiratory tract[a]

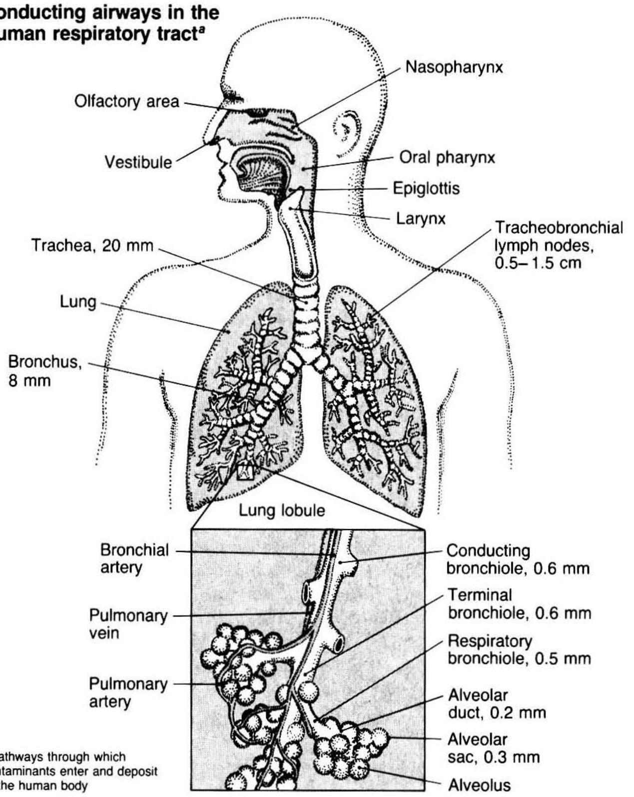

[a] Pathways through which contaminants enter and deposit in the human body

Aerosol deposition

Visualize the lungs as a hollow, upside-down tree. Roughly, the larynx and trachea would be equivalent to the main trunk. The bronchi or airways could be likened to the principal and lesser branches and twigs. The lesser branches and twigs in the lung's lobes might be taken to be the conducting, terminal, and respiratory bronchioles. The alveoli or air sacs may be imagined as leaves.

Morton Lippmann, director of the Aerosol and Inhalation Research Laboratory of the New York University Medical Center, said that before 1950 little was known about the quantitative aspects of the deposition of aerosols—many types of which are encountered in different industries—in the lungs. Research since that time indicates that much aerosol deposition, particularly in the >3-μm-diameter range, is concentrated in the lobar bronchi, or "the lesser branches and twigs." Some of the smaller particles, <3 μm, find their way to the alveoli.

Lippmann has carried out studies of intrabronchial particle deposition in hollow airways of animals and human beings, the latter studies made on a postmortem basis. He has devised a formula relating the size of aerosol particles deposited in the bronchi to the flow rate of the air entering and leaving the lungs. Lippmann observed that deposition "hot spots" at bifurcations of the larger airways play a role in cancer formation, possibly even with nonsmokers.

Clearance

If aerosol particles are deposited in the lungs, how many clear out via the several available pathways? How long does it take? To answer these questions, tests of respiratory function and rates of particle clearance are needed. Selected radionuclides can be used to trace the paths of particles from the lungs, Lippmann explained. Once these isotopically labeled particles have reached various portions of the lungs, the pathways for them to clear out and the length of time it takes depend upon the location of the particle in the lung and the nature of the particle itself.

In certain parts of the bronchi, there exist ciliated cells that produce mucus. From these bronchial regions, clearance times can vary between about 2–20 h, Lippmann noted, adding that the reasons for such a wide variation are not known. In the bronchial or airway portions approaching the alveoli, alveolar macrophages play a vital role in the clearance function. These are mononuclear phagocytes, which essentially are cells that try to engulf and destroy foreign materials in the body. Since cells in the near-alveolar bronchial areas are not ciliated, this portion clears more slowly. Insoluble particles not cleared by macrophages can have residence times up to "many years," Lippmann points out.

Paul Morrow of the University of Rochester (N.Y.) described a hypothetical lung retention curve for insoluble particles. He proposed that a fraction of the deposited particles are removed in up to one day from tracheal and bronchial airways. Next, there is a more "protracted clearance phase" for the balance of the particles—those retained in the lung alveoli. Alveolar retention, Morrow said, may range very widely "from minutes to years"; for instance, small particles of polystyrene may remain in the alveoli "for several years." The alveolar rate of clearance is considered to be the slowest rate overall.

When aerosol particles reach the lungs, little is known about their absorption by pulmonary tissue, but a bit more is understood about mucociliary removal. This process involves ciliated cells in the airways carrying particles off to the gastrointestinal tract. Also, macrophages are brought to the alveoli through the pulmonary circulation system; they "can act as a work force," as Morrow put it, to remove some "insoluble" (solid) particles. He added that the quantitative measurement of particle retention in the lungs may make possible a more accurate determination of permissible doses and TLVs.

Measuring aerosols

Aerosols or atmospheric particles from about 10^{-3} μm to over 10^{2} μm in particle diameter are of interest in the occupational environment, as these can deposit anywhere in the respiratory tract from the nasal passages to the alveoli. Those that deposit in the alveoli are known as "inspirable aerosols," and range from <0.1 μm to nearly 10 μm in aerodynamic diameter.

Klaus Willeke of the University of Cincinnati (Ohio) explains that inhalable aerosols can be divided into three specific subfractions, reflecting portions of the respiratory tract's anatomic regions where they may lodge. These comprise the extrathoracic subfraction (~5–200 μm diameter, "caught" above the larynx), the tracheobronchial subfraction (~1–30 μm), and the alveolar subfraction (<0.1–~10 μm).

***Willeke:** "separate aerosols like the body does it"*

Clearance model[a]

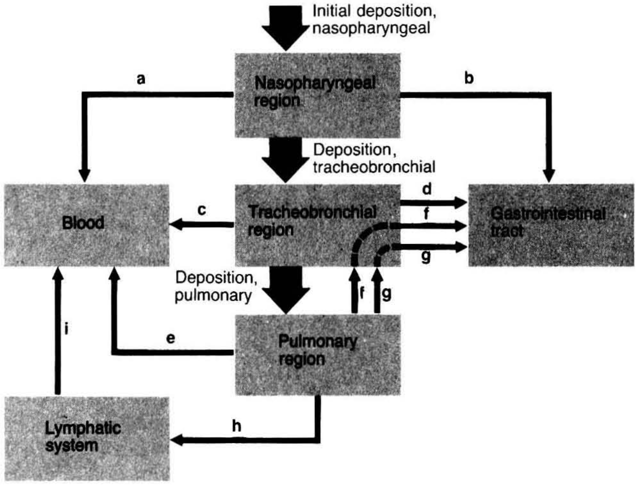

a—Material is taken up into bloodstream
b—Material is rapidly cleared by mucociliary transport
c—Material is rapidly absorbed into systemic circulation
d—Material is rapidly cleared by mucociliary transport to gastrointestinal tract
e—Material is translocated or absorbed to bloodstream
f—This is a rapid clearance phase, most likely by macrophages and mucociliary activity
g—This is a slower pulmonary clearance phase, dependent upon endocytosis and mucociliary transport
h, i—These are pathways for clearance through the lymphatic system

[a] After the International Commission on Radiological Protection, *Health Phys.* **1966,** *12,* 173–207.

Willeke recommends that to assess risk to humans, one should measure only the subfraction of aerosols deposited in the anatomical region of interest (such as tracheobronchial or alveoli). Perhaps this is because different types of particles lodged in each region could vary considerably in their effects on those regions and differ as to clearance rates and paths to other body parts, or out of the body.

There are instruments with which such deposition can be simulated. Such an instrument's inlet would differentiate or "classify" particle size distribution in a manner similar to that in which the respiratory tract performs this function, Willeke explains. For example, if one wishes to capture particles of the alveolar subfraction and eliminate all other sizes, cyclonic, elutriative, impactive, and centripetal removal methods are available. To collect the tracheobronchial subfraction, aerosols are drawn into a stilling chamber through an annular slit, and size classification is accomplished by impaction or cyclonic removal.

Personal and fixed monitors

Both aerosol and gas monitors can be personal or fixed. "Portable" monitors combine features of personal and fixed monitors. The personal monitor is generally a sensor or collector a worker wears in his or her breathing zone. For measuring aerosols, this sensor is normally coupled to a very small pump carried on the worker's belt, Willeke points out. Sensors equipped with optical scattering measuring components have recently become available; these sensors do not require pumps. The monitor records personal aerosol (or gas) exposure, generally during an entire work shift. In most cases, aerosol material is col-

Collecting the tracheobronchial subfraction[a]

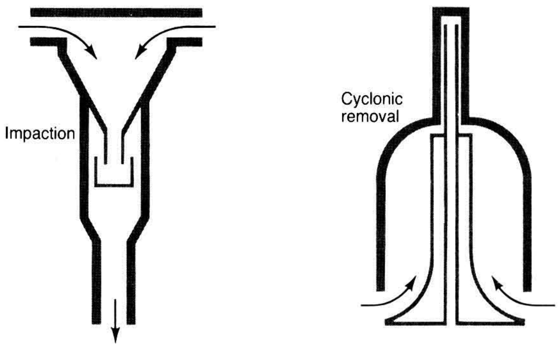

[a] These methods simulate the upper size limit or "cut" of the tracheobronchial fraction, reckoned in μm particle diameter
Source: Symposium presentation by Klaus Willeke of the University of Cincinnati

lected by filtration or impaction for subsequent laboratory extraction and analysis.

Some new technologies involving miniaturization are leading to personal monitors with built-in analysis capabilities. Although these are more costly, they provide "instantaneous exposure data," Willeke says.

Fixed monitors record aerosol concentration variations in a work area as a function of time. But while a fixed instrument gives details of time-varying aerosol generation, it will not necessarily reflect aerosol exposure that a worker experiences. Thus, personal monitors are preferred for regulatory purposes, Willeke explains.

An active gas monitor includes a pump, and therefore could function as an aerosol-capturing instrument. With passive gas monitors, diffusion or convection generally does not transport aerosols into the monitor without some size selectivity.

The lung and beyond

The lung is a principal organ through which workplace contaminants enter the human body, but it is not the only one. Willeke notes that the "extrathoracic fraction" of aerosols (the fraction depositing immediately after entering the nose or mouth, and above the larynx) may be ingested, and become hazardous to the digestive, metabolic, circulatory, and excretory systems. He says that this fraction and mode of entry are gaining increased attention on the part of occupational health scientists and engineers.

Also, either through respiration, ingestion, or topical exposure, a chemical might attack the lung or go on to affect other body organs and functions (or perhaps do both). For example, inhaled vinyl chloride monomer is suspected not of affecting the lung, but of being carried to the liver and eventually causing angiosarcoma, as a result of biochemical reactions subsequent to inhalation.

Cancer evaluations

I. Bernard Weinstein of the Cancer Center of Columbia University notes that industrial chemicals such as benzidine, 4-aminobiphenyl, and 2-naphthylamine are implicated in human bladder tumors. He told the American Cancer Society that inhaled benzene vapors are believed to cause a type of leukemia. Soots and tars are often linked to tumors at various body sites. It is suspected that such tumors are attributable to metabolites of the polynuclear aromatic hydrocarbon "family" contained in soots and tars. Other industrial "cancer-suspect" chemicals and processes Weinstein cites are arsenic, chromium, bis(chloromethyl) ether (BCME), nickel refining, and isopropyl alcohol manufacture by the strong acid process.

To determine longer term risks of workplace chemicals to humans, Weinstein calls for both short-term and in vivo studies. For short-term tests, he recommends the Ames *Salmonella typhimurium* test, studies of yeast and of *Drosophila melanogaster* (a fruit fly), and mammalian cell cultures. Assays for cell transformation; DNA binding (and binding to other macromolecules), damage, and repair; chromosomal abnormalities and sister chromatid exchange (*ES&T*, October 1982, p. 569A); and studies on metabolic activation are also suggested. In vivo studies would include clinical observations and follow-up "by astute physicians and patients," epidemiological studies, and long-term bioassays in experimental animals.

The question is often asked: How reliable are animal bioassays? Weinstein believes that for several chemicals the carcinogenic activity in rodents approaches that of humans.

He reminded *ES&T* that there are 23 specific chemicals that are definitely linked to cancer causation in humans. In addition, he said that seven industrial processes have the same effect; however, the "guilty chemicals are not yet known." Weinstein said that of the 23 chemicals, two—arsenic and benzene—were originally thought not to cause cancer in rodents, but recent evidence indicates that rodents are at risk of cancer from these two substances. Moreover, animal studies have predicted human carcinogens such as BCME, vinyl chloride monomer, and several other industrial chemicals or contaminants.

Weinstein adds that of about 143 known rodent carcinogens, none have been proven to be noncarcinogenic in humans. He stresses the need to employ newly developed laboratory methods in clinical and epidemiological studies on human cancer causation, an approach he calls "molecular epidemiology."

The common bond between toxic gas and aerosol monitoring and analysis, epidemiological assessments, animal and human studies, carcinogenesis evaluations, and the like is found in the objective of protecting the worker from hazardous chemical and biological materials. One way is to determine safe exposures, if any; promulgate regulations based upon this information; and apply science and engineering to the task of constructing workplaces in which undesired substances remain below certain levels. A future approach may use knowledge of biomolecular effects. In that case, the aim could be to ascertain the mechanisms of effects such as carcino-, muta-, and teratogenicity. The goal could be to find chromosomal- and genetic-level means of arresting or even reversing these effects.

Proceedings from the Hatch Symposium are due to be published in September in a volume entitled the "First Hatch Symposium on Occupational Health." The publisher is Princeton Scientific (formerly Princeton University Press) for the Series of Advances in Modern Environmental Toxicology.

—Julian Josephson

Additional reading

"Effects of Inhaled Particles on Human Health: Influence of Particle Size and Shape," NRCC No. 18564; National Research Council Canada. Publications NRCC/CNRC: Ottawa, Ontario K1A OR6, Canada, 1982.

EPA's cancer policy

Michael R. Deland

Hidden behind the headlines on the continuing controversy at EPA and the recent resignation of its administrator is a story with serious implications for the health of the American public. Knowledgeable observers contend that EPA is subtly—without providing an opportunity for public comment or hearing—changing its cancer policy by relaxing regulation of suspected carcinogens.

Roy Albert, professor of environmental medicine at the New York University Medical Center and since 1976 chairman of EPA's Carcinogen Assessment Group (CAG), recently testified before a House agriculture subcommittee, chaired by Rep. George Brown (D-Calif.). He stated that while "there have been no major recent departures from the broad framework set out by the EPA Guidelines for Carcinogen Assessment" there has been a "tuning" of the guidelines "to give them a slant consistent with the philosophy of the present administration." As an example, he cited permethrin, which, based on data from animal tests, would have been regulated as a carcinogen in former years but is not now controlled. He added that "previous administrations tended to be overprotective; the current administration tends to be underprotective" and concluded that "there has never been a federal cancer policy that really works."

Karim Ahmed, senior staff scientist at the National Resources Defense Council (NRDC), testified that changes in EPA's policies have resulted in raising the "acceptance of cancer risks for the U.S. population to at least 100 times the levels which were sanctioned by former administrations."

John Todhunter, assistant administrator for Pesticides and Toxic Substances at EPA, denied that there have been dramatic changes at EPA, stating that "Risk assessment at EPA today is a cautious evolutionary product of past practice and growing sophistication."

EPA's policy

EPA's first articulation of a cancer policy was in a 1972 legal brief in which statements of expert witnesses were referred to as "cancer principles." They conveyed the concept that the only permissible degree of regulation was a total ban on exposures. This policy was widely criticized, leading to the adoption in 1976 of formal guidelines predicated on a "weight of the evidence" approach.

Last fall the White House Office of Science and Technology Policy (OSTP) circulated a draft document on the scientific basis of risk assessment. OSTP is currently refining that effort and preparing guidelines to be used by the various regulatory agencies. Its work is proceeding slowly, and participants will only project that they "hope it is completed this year."

NRDC suit

Distressed by the direction of EPA's policy and finding no reassurance in OSTP's efforts, NRDC recently filed suit against EPA. The suit seeks to force the agency to initiate regulatory action under the Toxic Substances Control Act (TSCA) to reduce the significant risks of cancer posed to humans by exposure to the chemical formaldehyde, or to publish in the *Federal Register* a finding that the risk is not unreasonable. Ironically, in the spring of 1981, EPA staff found that its data on formaldehyde, including studies by the Chemical Industry Institute of Toxicology and the National Toxicology Program, did warrant action under TSCA and prepared a notice for the administrator's signature. Instead, NRDC charges, following a series of private, unannounced "science courts" to which industry representatives but not members of the public were invited, the agency concluded that formaldehyde was not subject to TSCA "at this time." Agency spokesmen now argue that the onus for regulating formaldehyde falls on other agencies such as OSHA.

NAS report

Meanwhile, the National Research Council, the operating arm of the National Academy of Sciences (NAS), last month released a report, "Risk Assessment in the Federal Government: Managing the Process," which could provide a helpful perspective on the ongoing cancer policy debate. Among the major recommendations of the report was that Congress establish a Board on Risk Assessment Methods within the National Academy of Sciences. The Board would assume the lead in all government activity relating to the regulation of carcinogens. Key congressmen such as Representative Brown have hailed the report as timely and extremely helpful and are likely to link it to legislation being drafted in their committees.

A decade has passed since the articulation of EPA's initial "cancer principles." Long overdue is a formally promulgated EPA "cancer policy" that bears the benefit of public participation. Sorely needed as well is a mechanism to coordinate EPA's efforts with those of other government agencies. Current activity by environmentalists, the courts, and Congress could be the catalyst needed to refine the regulation of carcinogens.

Deland writes this column monthly and is counsel to ERT, Concord, Mass.

0013-936X/83/0916-0173A$01.50/0

ES&T
FEATURE

Quality control in water analyses

The definitions and principles underlying the practice of quality control need to be critically evaluated

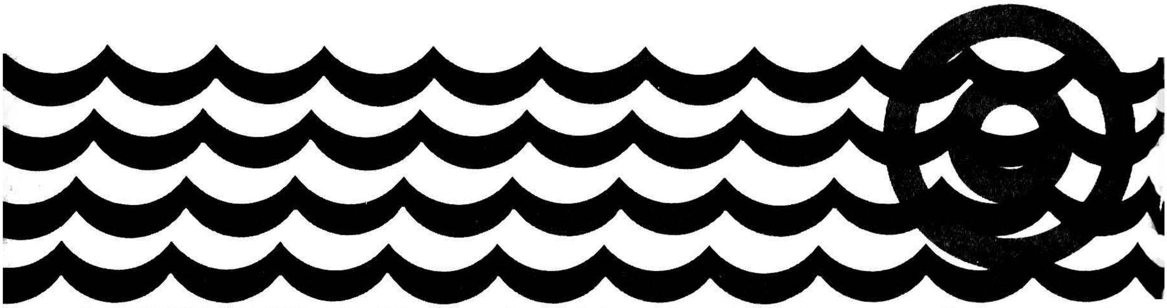

Cliff J. Kirchmer
Roy F. Weston, Inc.
West Chester, Pa. 19380

Until the late 1960s, there was only limited official recognition of the need for analytical quality control in water analyses. In January 1967, the Federal Water Pollution Control Administration (FWPCA) held its first meeting on the subject and established the Committee on Methods Validation and Analytical Quality Control. An analytical quality control laboratory was subsequently established in the FWPCA's Division of Research (the FWPCA was later replaced by the Environmental Protection Agency). This laboratory has evolved into what is now the Environmental Monitoring and Support Laboratory. Throughout its existence, it has played an important role in providing the necessary leadership for developing analytical quality control procedures and encouraging their use in environmental laboratories.

In 1971, the EPA published the "Handbook for Analytical Quality Control in Water and Wastewater Laboratories," which has since undergone several revisions. It provided the first comprehensive discussion of factors that can influence the quality of data in water analyses and was written so that it could be used by a laboratory for self-evaluation. Also, recent editions of "Standard Methods for the Analysis of Water and Wastewater" have included expanded sections that have contributed to the development of criteria and methodology for analytical quality control.

Even though the importance of quality control has been recognized, some of the more commonly used definitions in this subject area need to be clarified, and principles that have been established but are not uniformly applied in practice need to be emphasized. This article discusses these definitions and principles and makes specific recommendations for their application.

Accuracy

The expression "accuracy and precision" is used commonly to characterize the performance of analytical methods. There is no general agreement regarding the meaning of this phrase, however. Churchill Eisenhart referred to this problem when he wrote: "It is most unfortunate that in everyday parlance we often speak of 'accuracy and precision' because accuracy requires precision, but precision does not necessarily imply accuracy" (*1*).

R. B. Murphy compared the situation to a marksman aiming at a target: "We would call him a precise marksman if in firing a sequence of rounds, he were able to place all his shots in a rather small circle on the target. Any other rifleman unable to group his shots in such a small circle would naturally be regarded as less precise. Most people would accept this characterization whether either rifleman hits the bull's-eye or not" (*2*). Precision in water measurements has been defined by the EPA as "the degree of mutual agreement among individual measurements made under prescribed conditions" with a "single test procedure" (*3*). While there is general agreement about the meaning of precision, there is less agreement about the meaning of accuracy and its relationship to precision.

The problem in defining the term "accuracy" is the discrepancy between the accuracy of "individual analytical measurements" and the accuracy of "average values" obtained from a number of replicate measurements. In terms of the bull's-eye analogy, Murphy states that "one school of thought on the subject of accuracy insists that if a marksman hits the bull's-eye 'on

0013-936X/83/0916-0174A$01.50/0

the average,' then he is accurate even though [he] may have a wavering aim so that his shots scatter. The point is that accuracy in this sense is determined solely by the behavior of the long-run average of the shots. The position of the average shot is assumed, of course, to be the centroid of the bullet holes in the target: few shots might actually hit or nearly hit the bull's-eye.

"The second school of thought on accuracy would insist that if the [marksman] is unlikely to be very close to the bull's-eye, he should be termed an inaccurate shot. That is, the second school holds to the belief that accuracy should imply that any given shot is very likely to be in the bull's-eye or very near to it" (*2*).

It is difficult to say which of these definitions is more correct, but it may be possible to decide which is more useful when applied to water analysis. Reported results of analyses are usually based on "individual analytical measurements" rather than "averages" of replicate determinations. Duplicate determinations are made on perhaps 5–10% of the samples as a quality control measure, but extensive replication is not economically feasible. Thus, we are concerned with the "accuracy" of these individual analytical measurements.

It is interesting to note that while statisticians in the U.S. have clearly recognized the two ways of defining accuracy, the definition that equates accuracy with bias or systematic error has been commonly used in water analyses. For example, the EPA has defined accuracy as "the difference between an average value and the true value when the latter is known or assumed" (*3*).

In contrast, the Water Research Centre in England bases its definition of accuracy on individual analytical measurements. The error, E, of an analytical result, R, is defined as: $E = R - \tau$ where τ is the true value. Accuracy is then defined as the total error of a result; that is, accuracy represents the combined random and systematic errors of results and is said to improve as the total error decreases (*4*).

The Water Research Centre defines systematic error as follows. The mean of n analytical results on the same sample approaches a definite value, μ, as the number of results is increased indefinitely. When μ differs from the true value, τ, results are said to be subject to systematic error of magnitude B, where $B = \mu - \tau$. The term "bias" is used synonymously with systematic error.

Note that in the Water Research Centre definition, precision (which is a measure of random error) is a part of accuracy. One then speaks of precision and bias (the two components of accuracy) rather than precision and accuracy. Also, under this definition, it is impossible to speak of measurements being accurate but not precise, since precision is a component of accuracy.

In statistical terminology, common practice in the U.S. has been to define accuracy by comparing the mean of n measurements with the true value, and to define precision separately as the standard deviation, s, of n analytical measurements (*3, 5*). The Water Research Centre approach is more realistic in that it defines accuracy as the difference between individual analytical measurements and the true value, this difference corresponding to the sum of bias (systematic) and random errors.

The bull's-eye analogy described by R. B. Murphy has been used in both the U.S. and Great Britain to graphically illustrate the types of error that

FIGURE 1
Water Research Centre interpretation of the bull's-eye analogy for describing analytical error

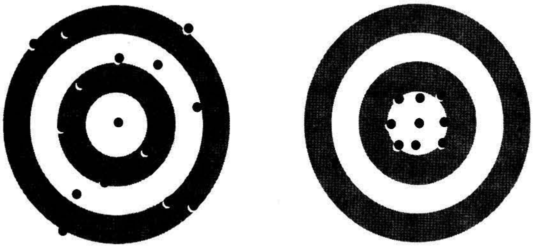

(a) Large random errors, no systematic errors

(b) Small random errors, no systematic errors

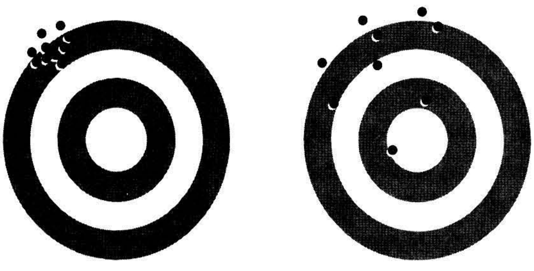

(c) Small random errors, large systematic errors

(d) Large random errors, large systematic errors

Source: Reference 4

can occur in water analysis. The first school of thought has dominated the interpretation of this bull's-eye analogy in the U.S. and has been included even in government training manuals (*6*). In contrast, the Water Research Centre subscribes to the second school of thought; its interpretation of the bull's-eye analogy is illustrated in Figure 1 (*4*). The major difference of interpretation is shown in Figure 1a, which represents "accurate but imprecise" data in the U.S. (*6*). The Water Research Centre avoids the terms accuracy and precision entirely, referring only to random and systematic errors.

Using an appropriate definition of accuracy has important practical consequences. With the definition commonly used in the U.S., methods giving very imprecise results can be characterized as accurate, when individual analytical measurements are clearly not accurate. A definition of accuracy based on individual analytical measurements, which includes the effects of random as well as systematic errors, is clearly more useful.

Analytical method

Before discussing the subject of bias in water analysis, it is useful to define "analytical method." The following definition has been proposed by A. L. Wilson: "An analytical method is to be regarded as the set of written instructions completely defining the procedure to be adopted by the analyst in order to obtain the required analytical result" (*7*).

Wilson states that this definition has two important consequences: A distinction must be made between the errors of analytical methods and the errors of results, and great emphasis must be placed on specifying methods accurately and completely. Under this definition, it is clear that one should not make such statements as "the precision of the method is. . . ." The correct form would be "when the method was followed, analytical results were obtained with a precision of. . . ."

A number of terms have been used to indicate the status of a method (i.e., "standard" method, "tentative" method, "approved" method) or hierarchy of a method (i.e., technique, method, procedure, protocol). There is probably a place for these terms within the classifications of standard methods devised by committees or regulatory agencies. The relative merits of these terms will not be discussed further, however, since the aim of this article is to emphasize the importance of the performance of individual laboratories.

The Water Research Centre has emphasized the value of supplying quantitative evidence about the performance of an analytical method. It recommends that a summary of performance characteristics, using clearly defined criteria, be included at the beginning of each published method. With this approach, methods are not classified arbitrarily, and one is able to answer the basic question: Does this method meet my analytical requirements? A representative tabulation of performance characteristics used by the Water Research Centre is given in Table 1 (*8*).

Bias

It has been stated that there are six possible sources of bias or systematic error in water analyses (*4*):

- unrepresentative sampling,
- instability of samples between sampling and analysis,
- interference effects,
- biased calibration,
- a biased blank correction, and
- inability to determine all forms of the determinand (that which is to be determined). For example, if "total iron" is to be measured, the method should give "total iron" and not soluble ferrous iron.

Because they are more directly associated with the problems of definitions and principles in analytical quality control, the third, fourth, and fifth items are the only ones discussed here.

Calibration bias. Related to the definition of analytical method is the Water Research Centre's insistence that blanks, standards, and samples be analyzed by exactly the same procedure. Failure to do this may result in either a biased blank correction or a biased calibration. Different procedures are acceptable only if there is experimental evidence that they produce results that differ by a negligible amount.

A survey of "standard methods" and "government-approved methods" of water analyses in the U.S. indicates that the possibility of biased calibration curves or biased calibration factors resulting from the use of different analytical procedures for standards and samples is not widely recognized. It is common for calibration standards

TABLE I

Example of tabulation of performance characteristics used by the Water Research Centre

1. Substance determined	Those forms of manganese reacting with formaldoxime after collection of the sample into acid.	
2. Type of sample	Fresh and treated waters.	
3. Basis of method	Manganese reacts with formaldoxime to form a colored complex whose concentration is measured absorptiometrically.	
4. Range of application[a]	Tested over the range 0–0.5 mg Mn/L.	
5. Calibration curve[a]	At 450 nm the curve is linear to at least 1.0 mg Mn/L	
6. Total standard deviation (S_t)[a,b]	Manganese concentration (mg Mn/L)	Total S_t (mg Mn/L)
	0.05	0.002
	0.1	0.004
	0.2	0.008
	0.5	0.011
	1.0	0.022
7. Criterion of detection[a]	0.001 mg Mn/L.	
8. Sensitivity[a]	0.5 mg Mn/L corresponds to 0.19 optical density units.	
9. Bias	No bias detected except when interferences occur.	
10. Interferences	Large concentrations of ferrous and ferric iron may interfere.	
11. Time required for analysis	For six samples, the analytical and operator times are both approximately 75 min.	

[a] These data were obtained at the Water Research Centre using a Hilger Uvispek spectrophotometer with 40-mm cuvettes at 450 nm.

[b] The data refer to standard solutions in distilled water; certain samples may tend to give worse precision.

to be subjected only to the final step in an analytical procedure. This is justified as being the only "practical" approach to analysis, particularly for those methods involving long and complex concentration and separation procedures. According to A. L. Wilson, however, these methods present the greatest possibility for bias due to improper calibration procedures (*9*).

While "bias in the calibration procedure" is usually not recognized by that name in the U.S., procedures have been recommended to estimate this error. They are usually termed "procedures for estimating recovery." For example, the recently published "Guidelines for Data Acquisition and Data Quality Evaluation in Environmental Chemistry" states that "the recovery of a method is derived from the measurement of spiked blanks" (*10*). The difference between the actual recovery and theoretical recovery of 100% corresponds to the bias in the calibration procedure. For methods that give very low recoveries, changes in the calibration procedure should be made whenever possible to correct for this source of bias.

An alternative approach would be to use recovery estimates to correct for the calibration bias. Unfortunately, many methods prohibit this type of correction, although it would clearly permit a better estimate of the true concentration in the water sample. For example, EPA Method 608 for organochlorine pesticides and PCBs says to "report results in micrograms per liter without correction for recovery data." A similar restriction in EPA Method 615 for chlorinated herbicides states that one should "report results in micrograms per liter as the acid equivalent without correction for recovery data." These methods seem intended to measure the quantities of pollutant in the final extracts, rather than in the original water samples.

While not as critical to the analytical results, the use of the increasingly common term "spiked blank" is not recommended. When a known amount of an element or compound is added to a known amount of water, this is a standard solution, not a "spiked blank." Standard solutions can be used either for calibration (calibration standards) or as a check on precision or calibration bias (check standards). Thus, instead of writing that "the recovery of a method is derived from the measurement of spiked blanks," it is preferable to state that the calibration bias of a method can be estimated by the analysis of check standard solutions (where the check standard solutions are analyzed exactly as the samples are analyzed).

Blank correction bias. To obtain accurate analytical results, particularly when performing trace analyses, it is necessary to make a blank correction of sample responses. O'Haver has stated that "in strictest terms, the blank is a solution that contains everything in the sample solution except the analyte" (*11*). Blank correction of individual samples—that is, subtracting a separately determined blank response from each sample response—is the recommended procedure based on statistical considerations, and it is generally accepted in principle, although sometimes ignored in practice. At a minimum, a blank should be analyzed along with each batch of samples. (Subtracting blank response from sample response is valid only for procedures in which calibration is of the form $A = \alpha + \beta C$ where A = response, C = concentration, and α and β are constants. Only these types of procedures are considered in this article.)

It is equally important to recognize that blank determinations should be made by exactly the same procedure as that used for the samples. For example, according to O'Haver, "in analytical procedures involving sample preparation, separation, or preconcentration steps, it is almost always essential that a blank be carried through the entire procedure" (*11*). If this is done, then blank-corrected results for water analyses should not present any problem of bias due to the blank, provided that the concentration of the determinand in the water used for the blank is negligible. On the other hand, when the concentration of the determinand in the water used for the blank is not negligible, it is essential to determine its concentration and make an appropriate correction in the blank value.

Bias due to interference. As indicated previously, the term "recovery" has been used in the methods for measuring the bias of the calibration procedure. More commonly (and correctly), the term recovery has been used to indicate the percent "recovered" when a sample is spiked with a known amount of compound. Recovery is the difference between the analytical results before and after spiking, divided by the known amount of spiking compound and multiplied by 100 to convert to percentage. The difference between the actual recovery and theoretical recovery (100%) is considered to be caused by interference. In other words, the recovery test is used to determine the presence of bias due to interference. The term recovery should be limited to this usage only and not to the evaluation of bias in the calibration procedure.

The recovery test is not very powerful in a statistical sense. The experimental recovery is obtained from the difference between two measurements (sample and spiked sample), each of which is subject to random error. Even in the absence of interference effects, significant deviations from 100% recovery are common. For example, Water Research Centre Technical Report 66 indicates that if the standard deviations of spiked and unspiked samples are equal and the amount of spiking material is 10 times the standard deviation, the expected recovery would lie between 72% and 128% at the 95% confidence level, even in the absence of interference (*4*). In addition, the recovery test does not detect interfering species whose effects are independent of the determinand concentration. This can be another important limitation.

Control charts

A common procedure for analytical quality control is to analyze check standards, duplicates, and spiked samples in amounts corresponding to approximately 10% of the samples analyzed (*3*). As subsequent data are accumulated, these analyses should be used to prepare control charts defining accuracy and precision. As already noted, when referring to tests for interference, accuracy control charts are better termed bias control charts.

Because laboratories operate under budget constraints and limited time, some order of priority should be assigned to the different kinds of control tests. In some European laboratories (*4, 12*), first priority has been given to precision control charts based on the analysis of standard solutions. (These standard solutions should be prepared independently of the calibration standards to provide a truly independent check, including the accuracy and stability of the stock calibration standard solution.) The next priority is the preparation of precision control charts based on duplicate analyses of actual samples. Bias control charts based on the recovery of spiked samples are the third priority. Finally, control charts based on blanks can be plotted to detect changes in the quality of reagents, etc. The latter are not true control charts since there are no control limits. Using this priority listing contrasts sharply with the common practice of devoting equal time to the analysis of standards, duplicate samples, and spiked samples.

It should be added, however, that the order of priority for control charts depends somewhat on the determinand. For example, one may not be able to prepare appropriate standard solutions for "suspended solids" and biochemical oxygen demand; for such determinands, the other types of control tests may be more important.

Several kinds of quality control charts have been recommended, including Cumulative-Summation (CuSum) and Shewhart charts (*3*). But if the emphasis is on the accuracy of individual analytical results, it is sufficient to simply plot the measured values on a chart in which $\mu \pm 2\sigma$ defines the "warning limits" and $\mu \pm 3\sigma$ defines the "action limits," where μ is the arithmetic mean and σ is the standard deviation. This type of chart has been described in "Standard Methods" (*5*), and detailed instructions for construction of the four previously mentioned categories of charts have been given in a publication by the World Health Organization Regional Office for Europe (*12*). An example of the most commonly used control chart, based on the use of standard solutions, is given in Figure 2. Note that the control limits in this chart are based on estimates of standard deviations and, as such, must be updated periodically by "pooling" preliminary and recent estimates. Note also that the warning and action limits in this case are plotted symmetrically around the expected mean concentration. This is because the true concentration of the solution is known. Any trend indicating that the statistical mean is higher or lower than the expected mean would signify that calibration bias probably affects the measurements.

Method validation

In the U.S., tests are often performed before a laboratory begins to use a method for routine sample analyses. These tests are commonly called "method validation" procedures. Few guidelines have been written, however, that provide optimal experimental designs for method validation.

In general, a good experimental design would enable the laboratory to estimate precision for the analysis of both standard solutions and real samples, to estimate bias due to interference in the analysis of real samples, and to estimate a lower limit of detection for the method.

Wilson has proposed an experimental design using analysis of variance to give a preliminary estimate of precision (*13*). This design was later expanded to include estimates of some sources of bias as well as limits of detection (*4*). The design specifies that analyses be performed in several batches over a period of one to two weeks. Each batch consists of replicate analyses of blanks, standard solutions, samples, and "spiked" samples. In general, to estimate precision over a range of concentrations, at least two standard solutions are recommended with the upper and lower concentrations of interest. This is necessary because it is common for precision to worsen with increasing concentration, and therefore the standard deviation at one concentration will not necessarily be the same as the standard deviation at another. A detailed discussion of experimental design is beyond the scope of this article, but clearly there is a need to apply these techniques more often in our laboratories and to be more critical of the approaches to "method validation" now being used.

Limit of detection

Many definitions of the term "limit of detection" or "detection limit" have been proposed in the literature. In recent years, however, there have been indications that some consensus is being reached. It is generally agreed that in qualitative terms, limit of de-

FIGURE 2

Example of a control chart for a standard solution

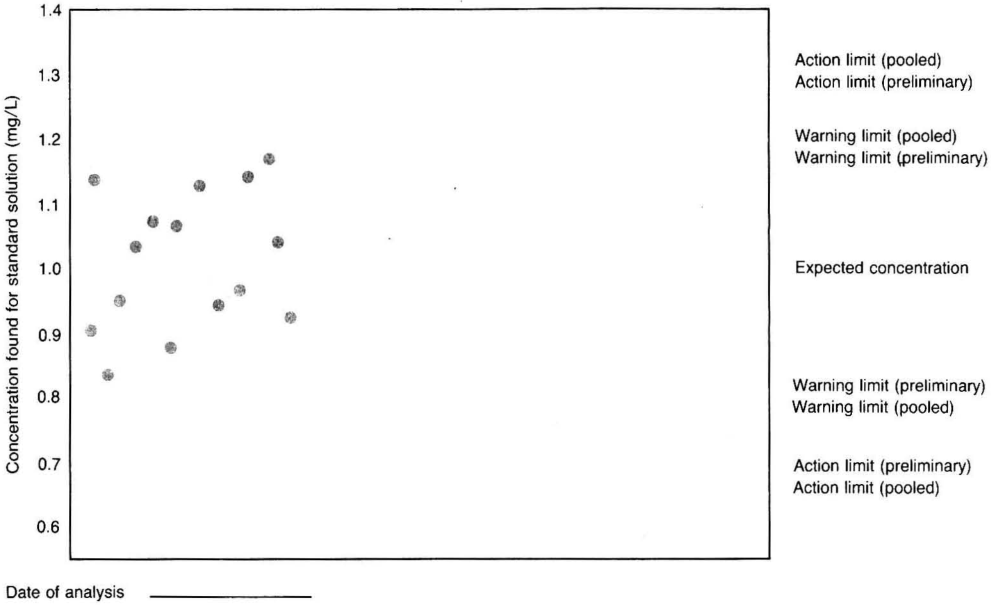

FIGURE 3
Statistical basis for detecting small concentrations

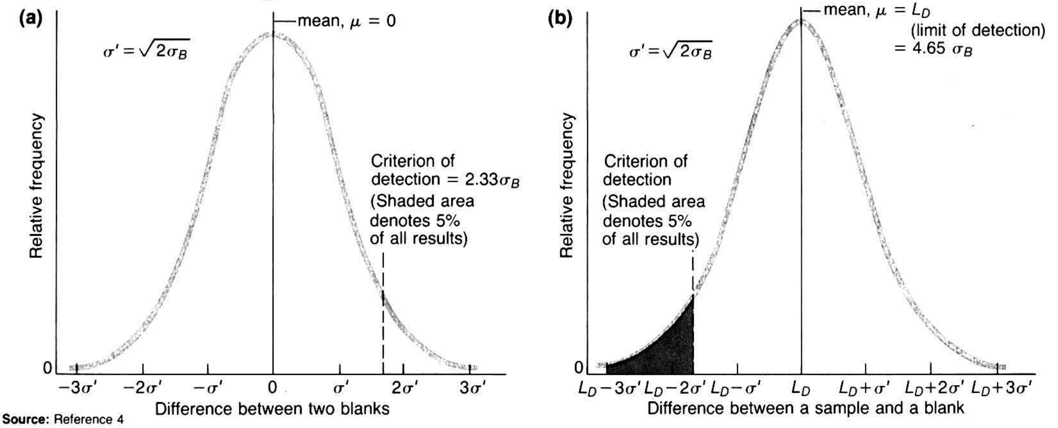

Source: Reference 4

tection is the lowest concentration of determinand that the analytical process can reliably detect. Because an analytical result is generally equal to the difference between the responses obtained for sample and blank, the variability of the blank response has been recognized as the determining factor for estimating the limit of detection for many methods.

The following general equation has recently been accepted by several authors for defining the limit of detection (*10*, *14*, *15*):

$$L_D = K_d\sigma_B \qquad (1)$$

where L_D = limit of detection, K_d = constant obtained from a statistical evaluation of blank responses, and σ_B = the within-batch standard deviation of the blank.

When the limit of detection is treated statistically, it is assumed that analytical results follow a normal distribution. Figure 3a illustrates the distribution of results for the differences of pairs of blank determinations, each pair of blanks being measured in the same batch of analyses. The distribution has a mean of zero and a standard deviation of $\sqrt{2}\ \sigma_B$. (Note: the property of additivity of variances results in the standard deviation of the differences between blank determinations being $\sqrt{2}$ greater than the standard deviations of the blank responses themselves.) Thus the difference of $+1.65\ \sqrt{2}\ \sigma_B$ ($=2.33\ \sigma_B$) will be exceeded, on the average, only once in every 20 occasions. The analytical result (R) is obtained by subtracting the result of a blank determination (B) from that of a sample (S), i.e., R = S − B. If we now analyze a sample and a blank in the same batch and the difference (S − B) is greater than 2.33 σ_B, there is less than a 5% chance that the sample contains the same concentration of the determinand as the blank. This value, 2.33 σ_B, has been called the criterion of detection and is based on an evaluation of the risk of an *error of the first kind* (that is, the error of accepting an apparent effect arising by chance as a real effect).

FIGURE 4
Illustration of the relationship between the criterion of detection and the limit of detection

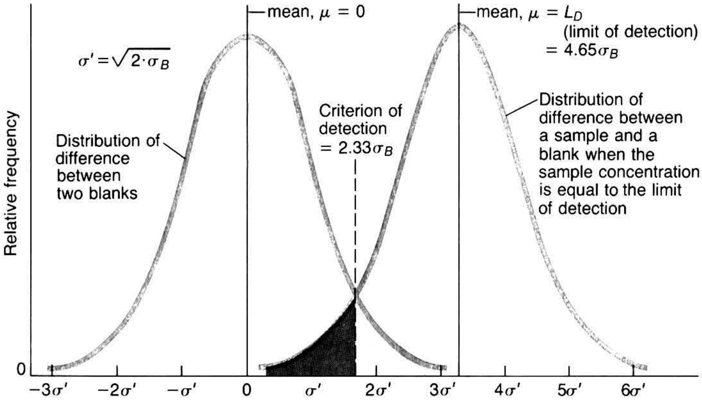

There is also the *error of the second kind*, corresponding to the error of failing to recognize a real effect. In the problem under consideration, this would correspond to concluding that the sample contains the same concentration of the determinand as the blank, when in reality the determinand concentration is greater in the sample.

If we assume a case where the sample concentration is equal to the previously defined criteria of detection, it is apparent that there is a 50% chance of an error of the second kind.

The limit of detection is defined such that the error of the second kind has a lower value (that is, in Figure 3b, the significance level associated with the error of the second kind is equal to 5%) and the limit of detection is 4.65 σ_B. Both Currie (*14*) and Wilson (*15*) suggest this value for defining the detection limit.

Figure 4 summarizes and illustrates the relationship between the criterion of detection and the limit of detection.

Values other than 5% have been chosen for the significance levels associated with errors of the first and second kinds, resulting in different values for K_d in the general equation for limit of detection. For example, the

American Chemical Society's Subcommittee on Environmental Chemistry has recommended using a value of 3 for K_d. This treatment is apparently based, however, on the use of a "well-known" blank rather than paired observations; for paired observations, $K_d = 4.23$. This value is said to imply definite risks of 7% for false positives and false negatives. (The precise value is 6.68%.)

When standard deviation values for a population are known, it is not critical whether a 5% or a 7% risk level is chosen. But in real situations, the limit of detection (L_D) must be estimated from a restricted number of blank measurements, and the following equation is recommended:

$$L_D = 2\sqrt{2}\,t\,s_B \qquad (2)$$

where t = the 5% point of the single-sided t statistic and s_B = estimated within-batch standard deviation of the blank.

While t values corresponding to the 5% confidence level are usually listed in statistical tables, those corresponding to the 7% confidence level are not. Thus, it would appear that the detection limit expression of Currie and Wilson is more easily applied in practice. It is important to recognize the weaknesses of this definition. These include the following assumptions:

- The within-batch standard deviations of both the blank and samples containing very small concentrations of determinand are the same.
- The analytical response is not zero for finite concentrations of the determinand.
- The sample and blank are not biased with respect to each other, (that is, there are no interfering substances in the sample or the blank).

If any one of these assumptions is not true, then the detection limit cannot be calculated using the equations given previously.

It has been stressed that the limit of detection should apply to a complete analytical procedure and not to a given instrument or instrumental method (*11*, *16*). O'Haver also states that a concentration at the detection limit can only be detected, as the term "detection limit" implies, and not measured quantitatively (*11*). In fact, when using Currie and Wilson's definition, the random error at the limit of detection is equal to approximately 66% of the limit of detection at the 95% confidence level.

As a consequence of this high random error for concentrations at or approaching the limit of detection, L_D, Currie suggested the use of another term, the determination limit, L_Q, for which the relative standard deviation is 10% (that is, $L_Q = 14.1\ \sigma_B$). For practical purposes, the following three principal analytical regions defined by Currie can be applied in water analyses:

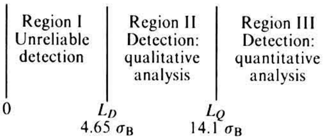

In using these definitions, when a measured value is below the limit of detection, it is reported as such (i.e., $<L_D$). When the measured value is between the limit of detection and the limit of quantification, it is reported as being qualitatively detected but no

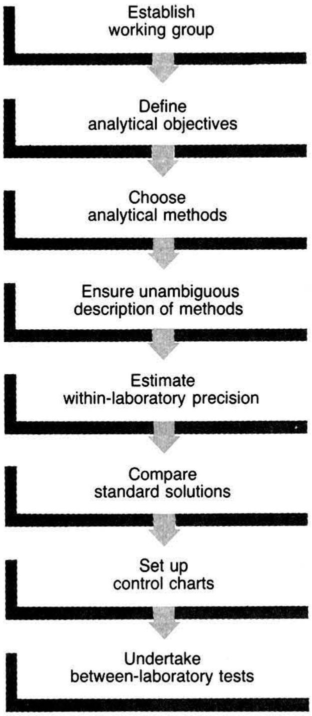

FIGURE 5
Flow chart for achieving comparable analytical results from a group of laboratories

Define the determinand, limit of detection, and accuracy required.

Choose analytical methods with satisfactorily small sources of bias and adequate precision. When suitable methods are not available, improved methods should be developed.

Ensure that the chosen methods are completely and unambiguously specified and that they will be followed as far as possible by all laboratories.

Estimate the standard deviation of analytical results and, if necessary, improve the precision until the target value is achieved.

Ensure that the standard solutions used by all laboratories are in satisfactory agreement.

Establish a control chart and regularly analyze solutions of known concentration to ensure that the precision remains adequate.

Estimate the bias of each laboratory and, if necessary, improve until the target value is achieved.

value is given. If the measured value exceeds L_Q, it is reported as such—that is, the quantitative result is reported.

When it is essential to provide quantitative estimates at low concentrations, the method recommended by the Water Research Centre probably supplies the most information (*4*). The Centre suggests reporting the actual analytical results together with their 95% confidence limits because this gives all relevant information.

Precision of measurement has been described by A. L. Wilson as one of the "performance characteristics" of an analytical method. It is widely recognized that a laboratory using a given method may obtain one precision when applying a method to the analysis of standard solutions and another when applying it to real samples. It should not be surprising, therefore, that the detection limit as determined from repeated measurements on blanks may not always be the same as that obtained when real samples are analyzed. However, while it is fairly easy to determine precision on real samples, it is not so easy to determine the limit of detection on real samples when, for example, the sample contains interfering substances (that is, the sample and blank are biased with respect to each other). Despite the limitations of the limit-of-detection concept in practice, it is still useful, just as determining the precision of measurements of standard solutions is of use.

Finally, it is important to place the limit-of-detection problem into perspective in terms of real analytical needs. Wilson has recommended that analytical objectives be established for each measurement program. These goals include the need to define the determinand, the required accuracy, and the required limit of detection. In other words, the required limit of detection should be distinguished from the experimental limit of detection. In many cases, it will be clear that the method used in the laboratory is capable of measuring below the required limit of detection, whether that be on standard solutions or real samples. In this case, in order not to expend resources in obtaining information unrelated to the objectives of the measurement program, all results less than the required limit of detection can simply be recorded as such (i.e., less than the required L_D).

Between-laboratory control

The concepts discussed thus far relate principally to within-laboratory quality control (also known as intralaboratory or internal quality control). Accurate analyses depend primarily on the implementation of a well-conceived within-laboratory quality control program involving two stages (*4*):

- preliminary error estimation (i.e., method validation), and
- routine quality control through the use of appropriate control charts.

Between-laboratory quality control (also known as interlaboratory or external quality control) is also useful for several purposes. From the standpoint of the individual laboratory, the analysis of standard solutions or samples prepared by another laboratory (for example, EPA quality control samples or standard reference materials of the National Bureau of Standards) can serve as a check on the efficiency of its within-laboratory quality control program. From a broader perspective, between-laboratory collaborative tests may be necessary for several reasons: to evaluate analytical methods or to determine individual and group laboratory performance, for example.

Between-laboratory tests should involve two stages (*4*):

- comparison of standard solutions used by each laboratory with a standard distributed by a coordinating laboratory and, when all standards are in satisfactory agreement, and
- collaborative analysis of samples distributed to all laboratories by a coordinating laboratory.

It is important to stress that between-laboratory quality control can only complement, and not be a substitute for, an efficient within-laboratory quality control program. Figure 5 illustrates the approach to analytical quality control recommended by the Water Research Centre (*4*). Note that in this step-wise approach, between-laboratory quality control is initiated after the individual laboratories have completed within-laboratory tests. Essentially the same approach is used to control the accuracy of a single laboratory and to achieve comparability of results from a group of laboratories by controlling the accuracy of each.

Summary

Although quality control has become an accepted and even required practice in water analysis laboratories, the definitions and principles underlying the practice of quality control still need to be critically evaluated. In evaluating quality control practices in the U.S., the experience of European laboratories, particularly the Water Research Centre in Great Britain, appears most useful.

References

(1) Eisenhart, C. "Realistic Evaluation of the Precision and Accuracy of Instrument Calibration Systems," Paper 1.2 in National Bureau of Standards Special Publication 300, 1969; Vol. 1.

(2) Murphy, R. B. "On the Meaning of Precision and Accuracy," Paper 6.1 in National Bureau of Standards Special Publication 300, 1969; Vol. 1.

(3) Environmental Monitoring and Support Laboratory, U.S. EPA, Office of Research and Development. "Handbook for Analytical Quality Control in Water and Wastewater Laboratories," EPA-600/4-79-019.

(4) Cheeseman, R. V.; Wilson, A. L. "Manual on Analytical Quality Control for the Water Industry," Technical Report TR66, Water Research Centre, 1978.

(5) "Standard Methods for the Examination of Water and Wastewater," 15th ed.; 1980, APHA, AWWA, WPCF.

(6) U.S. Department of the Interior, Federal Water Pollution Control Administration. "Chemical Analyses for Water Quality Training Course Manual"; 1969.

(7) Wilson, A. L. *Talanta* **1970,** *17*, 21–29.

(8) Cheeseman, R. V.; Wilson, A. L. "A Method for the Determination of Manganese in Water," Technical Paper TP85, Water Research Centre, 1972.

(9) Wilson, A. L. "The Chemical Analysis of Water," Analytical Sciences Monograph No. 2, The Society for Analytical Chemistry: London, 1976.

(10) ACS Committee on Environmental Improvement. *Anal. Chem.* **1980,** *52*, 2242–49.

(11) O'Haver, T. C. In "Trace Analysis—Spectroscopic Methods for Elements"; Winefordner, J. D., Ed.; John Wiley and Sons: New York, 1976; Chapter 2.

(12) Ekedahl, G.; Rondell, B.; Wilson, A. L. In "Manual on Analysis for Water Pollution Control"; World Health Organization, Regional Office for Europe, 1974.

(13) Wilson, A. L. *Talanta* **1970,** *17*, 31.

(14) Currie, L. A. *Anal. Chem.* **1968,** *40* (3), 586–93.

(15) Wilson, A. L. *Talanta* **1973,** *20*, 725.

(16) Kaiser, H. "Two Papers on the Limit of Detection of a Complete Analytical Procedure"; Adam Hilger, Ltd.: London, 1968.

__Cliff Joseph Kirchmer__ is presently assigned to a Weston technical assistance team providing support to the EPA Region VII Laboratory, with responsibilities for quality assurance/quality control for the Missouri dioxin studies. Previous positions have been as quality assurance manager for Envirodyne Engineers, Inc., in St. Louis, Mo., and as regional adviser in water chemistry and laboratories with the Pan American Health Organization. Kirchmer received an MST in chemistry and a PhD in environmental sciences from the University of Florida.

ES&T PRODUCTS

Software program
Program is used in conjunction with a plasma emission spectrometer to determine the concentrations of 29 common elements within 8 min. The spectrum around each emission peak is shown graphically and can be printed out to indicate potential spectral interference. The program can be modified from the keyboard to add or delete elements or change analytical lines. Instrumentation Laboratory **101**

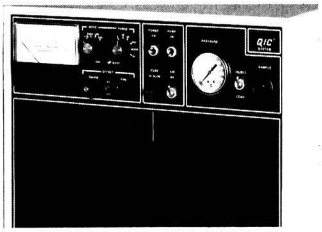

Anion analyzer
Single-channel instrument analyzes anions including fluoride, chloride, nitrite, nitrate, phosphate, and sulfate in water, air, and soils. Total analysis typically takes less than 20 min because minimal sample preparation is required. Dionex **102**

Pyranometer
This weatherproof instrument having a sensitivity of $100\ mV/1000\ W/m^2$ of solar irradiance, may be left in the open environment indefinitely. It has a response time of 1 ms, temperature compensation of ±1.5% from −20 to 50 °C, a cosine response of ±2% from 0 to 70° of incidence, and a linearity of ±1.0% up to 1400 W/m^2. Hollis Geosystems **103**

Dissolved oxygen sensors
Available as general-purpose models or as autoclavable models, these membrane sensors measure percent saturation, oxygen pressure, and oxygen concentration in mg/L. Yellow Springs Instrument **104**

Need more information about any items? If so, just circle the appropriate numbers on one of the reader service cards bound into this issue and mail in the card. No stamp is necessary.

Oscillographic chart recorder
Standard features of this instrument include: an event marker, preset recording time or shot length, trace identification, grid lines, timing lines, and remote control capabilities. It has 6–24 channels and a maximum writing speed of 2000 m/s. Paper speeds vary from 10 cm/min to 4 m/s. Soltec **105**

High-capacity stack sampler
Instrument collects gram quantities without overloading, provides size data in four size ranges from 1.5 to 11 μm, fits a 3-in. sampling port, and may be used in temperatures up to 1500 °F. Andersen Samplers **106**

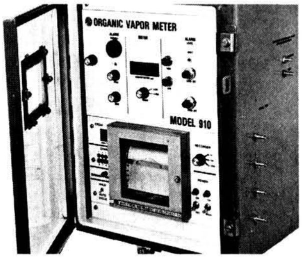

Organic vapor meter
Meter uses a photoionization detection system to measure organic vapors in as many as 10 remote locations in ranges from 0.01 to 2000 ppm. An optional recorder provides a permanent record of all measured concentrations. Analytical Instrument Development **107**

Laboratory controller
Multipurpose controller combines timing, equipment controlling, metric conversion, and calculating functions into a single unit. Three independently programmable channels have countdown capability from 100 h to 1 s. They also sound visual and audible alarms, turn lab appliances on and off, make unit and metric conversions, and perform calculations. Chemtrix **108**

***Companies interested in a listing** in this department should send their releases directly to* Environmental Science & Technology, *Attn: Products, 1155 16th St., N.W., Washington, D.C. 20036*

Solar-powered weather station
Electronic station can measure up to six parameters, including wind speed, wind direction, relative humidity, solar radiation, and precipitation. It is powered by 2-, 4-, or 9-W solar panels with a rechargeable battery. The station is available with these optional measurements: dew point, barometric pressure, soil temperature, water temperature, wind run, and heated precipitation. Climatronics **109**

Transducer
This is designed for measuring extremely low differential pressures. It is available in ranges from 0–2 in. H_2O to 0–100 psid. Applications include combustion analysis, stack draft monitoring, and pump-suction measurement. The device uses a linear variable differential transformer to measure the deflection of a pressure capsule. Schaevitz Engineering **112**

Temperature controls
Designed for on-off or time-proportioning control, these controls provide fast temperature sensing in ranges from 0 to 1000 °F. A replaceable, plug-in 10-amp relay and a field-convertible 115–230 V ac voltage supply are included. United Electric Controls **113**

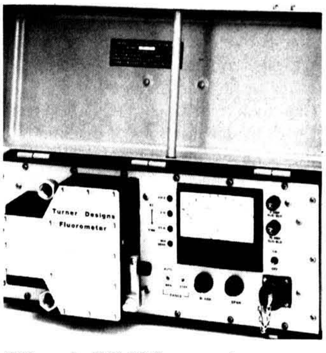

Chlorophyll field fluorometer
Accessory converts the Turner field fluorometer into a portable chlorophyll-measuring instrument, capable of detection down to 5 ppt. Algae, phytoplankton, diatoms, and dissolved organic matter can be measured onsite. Turner Designs **114**

Chlorine test kit
Determines free or total chlorine in water with a method that is free of interference from chromate. The kit includes vacuum-sealed, disposable ampules containing the premeasured reagent DDPD in stable liquid form. CHEMetrics **115**

Slurry packing system
This unit can pack HPLC columns in the upward or downward positions. Three different solvents can be used during the packing process. HPLC Technology **116**

Air velocity meters
Portable units are available in a dozen models with both English and metric units. These meters measure air velocity, temperature, and pressure. Air velocity ranges from 0 to 60 m/s, gas temperature from −40 to 250 °C, and static air pressure from 0 to 5 in. water can be measured. High-temperature models allow operation up to 500 °F. Sierra Instruments **117**

NO, NO_2, NO_x analyzer
This instrument detects concentrations in the 2 ppb–5.0 ppm range. It exceeds all present EPA requirements governing monitors for oxides of nitrogen. Performance specifications are guaranteed over the temperature range of 10 to 40 °C. The analyzer may be operated unattended for at least seven days. Columbia Scientific Industries **118**

Personal computer
Desk-top model has a CRT that displays 80 characters and 25 lines. The memory capacity is 64 kilobytes of RAM. The basic computer includes an RS-232 serial port, a parallel port, and an RS-232 modem port. Cromemco **119**

Waste disposal service
Purchase of a combination storage and shipping container for hazardous waste includes the right to ship the waste to an EPA-approved disposal company and have it disposed of by the company. The container consists of a 4-L glass bottle filled with an absorbent and foamed into place in an outer fiberboard box. Lab Safety Supply **120**

HPLC pulse dampeners
Three different sizes rated at 4000 psi, 6000 psi, and 10 000 psi are available. They are compact and hook up with standard 1/16-in. fittings. ANSPEC **121**

H_2S gas monitor
Pocket-sized personal monitor incorporates a state-of-the-art sensor and an alarm to warn the user of dangerous concentrations of H_2S. It operates up to 2500 h on one 9-V battery. Texas Analytical Controls **122**

Electronic recorder
Housed in a compact case, this monitor continuously records low-level direct current signals. Selectable pen response provides standard response of one full second for full-scale pen travel or an adjustable pen response of 2–20 s. Robertshaw Controls **123**

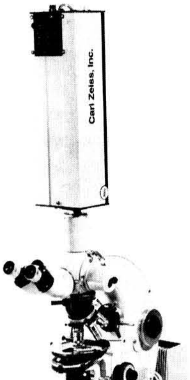

Venus TV cameras
According to the manufacturer, these cameras expand video microscopy capabilities by producing high-resolution, high-contrast images at ultra-low light levels. Light- and heat-sensitive live material can be studied with in vivo and in vitro microscopy. Phase contrast, differential interference contrast, and polarizing microscopy can be employed for motion studies. Carl Zeiss **124**

Digital thermometer
According to the manufacturer, this meter has an accuracy of ±0.1 °C over its entire range of −100 to 850 °C. It has a large 3½-digit LCD display. A 9-V battery provides up to 300 h of continuous operation. Available accessories include a calibration unit, multiple-probe switch box, carrying case, and variety of interchangeable probes. Owen Instruments **125**

Standardized concentrates
These are formulated for more than 75 volumetric solutions to eliminate the drying, weighing, and titrating that are usually required in the preparation of volumetric solutions. Hellige **126**

HPLC systems
Two models are available, each with a reliable solvent delivery system, high-pressure sampling valve, and 254-nm, fixed-wavelength stable UV detector. Model 80-650 has a solvent delivery system with a single-piston reciprocating pump and built-in phase dampener. Model 80-700 has a solvent delivery system with a dual-piston drive mechanism. GOW-MAC Instrument **127**

Video cassette data recorder
Portable recorder has a self-contained microcomputer to control a number of processes. Because it uses a video cassette, this instrument is capable of recording 14 channels. It is designed for use in the field and is resistant to vibration. Six tape speeds range from 38.1 to 1.19 cm/s, and calibration voltages range from 0.2 to 8 V peak. Kyowa Dengyo **128**

Stack sampling train
This is designed to sample gas stream effluents isokinetically in accordance with EPA standards. Recently a number of changes have been incorporated, including a digital readout, modular Pitot tube tip, and a 1-in. manometer mounted on the front panel for calibration of the magnehelics. Andersen Samplers **129**

Portable polarimeter
Useful for the determination of sugars, amino acids, steroids, and other optically active substances, the polarimeter includes several measuring tubes with varying lengths for specific applications. It employs a sodium lamp, spiral focusing adjustment, and a circular metal dial with vernier to permit readings accurate to ±0.1°. PolyScience **130**

ES&T

LITERATURE

Tissue culture. Brochure describes broad line of apparatus for tissue culture, with spinner flasks and slow-speed magnetic stirrers featured. Other equipment is also listed. Wheaton Scientific **174**

Centrifugal sifter. Bulletin CS-82 describes high-capacity centrifugal filter for the continuous separation of dry or moist materials. Can retain particles as small as 37 μm. Kason **175**

Internal deposition detection. Brochure describes chordal thermocouples for instrumenting boilers in order to detect internal deposition. Babcock & Wilcox **176**

Diaphragm valves. Bulletin 4250-DQ4B describes ¼-turn diaphragm valves for fluid shut-off at up to 3000 psig. Parker Hannifin **177**

Fuel cell systems. Technical brochure gives an overview of basic types of fuel cell systems, and a detailed description of a solid polymer electrolyte-phosphoric acid fuel cell system. Engelhard **178**

CO monitor. Brochure describes the Land 8000 carbon monoxide (CO) monitor and explains its application in situations in which cost-effective combustion monitoring is essential. Sensitive to fuel-air ratio changes. Land Combustion **179**

Water conservation in coolers. Bulletin RC explains why recirculating coolant enhances temperature control more reliably than tap water, and can conserve water, and reduce "down time" for cleaning or water shortages. FTS Systems **180**

Water treatment glossary. Booklet, Item TS-69, defines water treatment terms from "absolute pressure" to "zeolite." Mogul **181**

Need more information about any items? If so, just circle the appropriate numbers on one of the reader service cards bound into this issue and mail in the card. No stamp is necessary.

Filtration systems. Booklet features full line of medium- and high-technology filtration systems that meet a broad range of specifications. Disposable or reusable filter elements are offered; many industrial needs are met. Brunswick Technetics **182**

Sample preparation. Data sheet PDS-0982 describes sample grinding, blending, and briquetting additives and techniques to give a preweighed capsule or bulk powder. Chemplex Industries **183**

Solar fiberglass. Brochure describes SUN-LITE, a fiberglass-reinforced material originally made for solar heating. It is useful for aquaculture tanks, industrial research, and other applications. Solar Components **184**

Sodium aluminate. Brochure tells why sodium aluminate can be more effective than lime for wastewater treatment and why it cuts chemical costs and produces far less sludge. Vinings Chemical **185**

Portable instruments. Brochure lists line of instruments for air sampling, air velocity, mass flow, and other uses. Kurz Instruments **186**

Radioactivity SRMs. Release announces availability of standard reference materials (SRMs) for radioactivity such as technetium-99. Office of Standard Reference Materials, B311 Chemistry, National Bureau of Standards, Washington, D.C. 20234 (write direct).

Wood fuel: A threat? "Wood as Home Fuel: A Source of Air Pollution" explains why and how. American Council on Science and Health, 47 Maple St., Summit N.J. 07901 (write direct).

Innovative energy efforts. Directory lists innovative energy efforts by utilities. Madalyn Cafruny, American Public Power Association, 2301 M St., N.W., Washington, D.C. 20037 (write direct).

"Priority products." Advertising section in *ES&T* will help user reach 87 500 readers at low cost. CENTCOM, Ltd., P.O. Box 231, Westport, Conn. 06881 (write direct, or phone 203-226-7131).

Renewable energy's side effects. Study, "Side Effects of Renewable Energy," shows where environmental problems could crop up. Science Division, National Audubon Society, 950 Third Ave., New York, N.Y. 10022 (write direct).

Water conservation. DWR Bulletin 198-82 sets forth recommended water conservation steps for the present and future. California Department of Water Resources, Room 1115-16, Resources Building, 1416 Ninth St., Sacramento, Calif. 95814 (write direct, or phone 916-445-4501).

Industry studies. Brochures list industry studies scheduled for 1983. Predicasts, 11001 Cedar Ave., Cleveland, Ohio 44106 (write direct).

Solvent recovery. Flyer announces study, "Solvent Recovery in the U.S.—Demand, Capacity, and Pricing, 1980-1995." First comprehensive look at this field. Victor Johnson, Harding Lawson Associates, 6300 Westpark Dr., Suite 100, Houston, Tex. 77057 (write direct).

RCRA financial requirements. Pamphlet summarizes federal financial requirements for hazardous waste facilities, pursuant to RCRA, that came into effect in 1982. Single copies available. Office of Solid Waste and Emergency Response, U.S. EPA, Washington, D.C. 20460 (write direct, or phone 800-424-9346; 382-3000 in Washington, D.C.).

Companies interested in a listing *in this department should send their releases directly to* Environmental Science & Technology, *Attn: Literature, 1155 16th St., N.W., Washington, D.C. 20036*

ES&T BOOKS

The Clean Water Act: The Second Decade. Morris A. Ward. 54 pages. E. Bruce Harrison Co., Inc., Suite 900, 605 14th St., N.W., Washington, D.C. 20005. 1982. $11.95.

This book presents a section-by-section analysis of the existing water law and its regulations in layman's language. It also gives a history of U.S. water resources legislation and a summary of water resource and quality issues that will be increasingly discussed.

Manual on Water (STP 442A). C. E. Hamilton. Contains 18 papers, 471 pages. ASTM, 1916 Race St., Philadelphia, Pa. 19103. 1982. $28.50 (20% discount for ASTM members).

This manual consists of information on the influence of water on various industries. It is a guide to the kind of water planning needed at executive and investment levels of management. Certain operations, such as sampling under various conditions, are included.

Indoor Air Pollution. Richard A. Wadden, Peter A. Scheff. 213 pages. John Wiley & Sons, Inc., 605 Third Ave., New York, N.Y. 10158. 1983. $39.95, hardcover.

More than 80% of most individuals' time is spent indoors. With tighter insulation in buildings, pollution concentrations in internal spaces could rise to hazardous levels, the authors say. They look at the dangers posed by cigarette smoke, particle board, cement, and other materials, and by oven exhausts and other sources.

Ionizing Radiation: Sources and Biological Effects. 773 pages. United Nations Industrial Development Organization, P.O. Box 300, A-1400 Vienna, Austria. 1982. Inquire as to price. Paper.

Ionizing radiation emanates from both natural and man-made sources. This work examines these sources and assesses levels and dosages. It also discusses both genetic and somatic effects of ionizing radiation, under the heading of new developments in radiobiology.

Carcinogens and Mutagens in the Environment. Vol. I, "Food Products." Hans F. Stich, Ed. 320 pages. CRC Press, Inc., 2000 Corporate Blvd., N.W., Boca Raton, Fla. 33431. 1982. $89.50, hardcover.

This work discusses epidemiological evidence, carcinogens and mutagens in food, and methodological and regulatory issues. Among more detailed topics covered are life-style and cancer etiology, dietary fat relationships to cancer, metabolic activation, mycotoxins, analysis, and regulatory approaches.

Trace Elements in Coal. Vlado Valković, Ed. 272 pages (Vol. 1) and 304 pages (Vol. 2)., CRC Press, Inc., 2000 Corporate Blvd., N.W., Boca Raton, Fla. 33431, 1983. Vol. 1, $74; Vol. 2, $81 (prepublication). Outside U.S., $85 and $93, respectively, hardcover.

These volumes discuss the nature and mode of trace-element occurrence, analysis, concentrations, and environmental implications. These trace elements can also contain radionuclides. The need for environmentally acceptable coal utilization techiques is strongly emphasized.

Solar Age. Bruce Anderson. Executive Ed. Monthly periodical. P.O. Box 985, Farmingdale, N.Y. 11737. $24/y, or $59 for 3 y.

This magazine looks at active and passive homes, retrofit homes, solar cooling, performance ratings, and many other aspects of solar energy from a technical and business standpoint.

Journal of Atmospheric Chemistry. P. J. Crutzen, D. H. Ehhalt, Eds. Periodical. D. Reidel Publishing Co., P.O. Box 17, 3300 AA Dordrecht, The Netherlands, $34/y, personal; $74/y, institutional.

This journal will publish original work on modeling, physicochemical processes, roles of biogeochemical cycles, laboratory studies, transformation processes, instrumentation, and other subjects devoted to the chemistry of the atmosphere from the earth's surface to about 100 km in altitude.

Carbon Dioxide: Friend or Foe? Sherwood B. Idso. 96 pages. IBR Press, 631 East Laguna Dr., Tempe, Ariz. 85282. 1982. $9.95, paper.

This book examines the controversy as to whether increased atmospheric carbon dioxide will alter the earth's climate. It also discusses agricultural matters.

Floc Property Effects on Sludge Dewatering Characteristics. William R. Knocke, Douglas L. Wakeland. Bulletin 133. 65 pages. Virginia Water Resources Research Center, 617 North Main St., Blacksburg, Va. 24060-3397. 1982. $6 ($8 if billed); single copies free within Virginia.

Topics covered include floc particle size, water content analysis, waste source descriptions, tests to determine if sludge can be properly handled, solids determination, and other aspects.

Environmental Health Perspectives. Vol. 46, December 1982. "Drinking Water Disinfectants." George W. Lucier, Gary E. R. Hook, Eds. 241 pages. Superintendent of Documents, U.S. Government Printing Office, Washington, D.C. 20402. 1982. $8, paper.

Among subjects considered are chlorine dioxide, *N*-chloramines, mutagenic activity by disinfectant reaction products, trihalomethane and behavioral toxicity, and carcinogenic risk estimation. There are 27 papers on these and related topics. The volume stems from a symposium on drinking water disinfectants and disinfectant by-products.

Ozonization Manual for Water and Wastewater Treatment. W. J. Masschelein, Ed. xi + 324 pages. John Wiley & Sons, Inc., 605 Third Ave., New York, N.Y. 10016. 1982. $41.95, hardcover.

This book is divided into parts discussing ozone generation, water ozonization principles, practical aspects, and ozone analysis. Critical questions in ozone practice, costs, new developments, and flow sheets are also presented. The editor is president of the European Committee of the International Ozone Association.

ES&T MEETINGS

April 21 Washington, D.C.
Complying with New Requirements for Radioactive Materials Transport. Hazardous Materials Advisory Council

Write: HMAC, 1100 17th St., N.W., Washington, D.C. 20036; (202) 223-1271

April 25–27 Roanoke, Va.
37th Annual Meeting. Virginia Water Pollution Control Association (VWPCA)

Write: G. David Waltrip, VWPCA, P.O. Box 5000, Virginia Beach, Va. 23455; (804) 460-2661

April 26 Bear Mountain, N.Y.
Alternatives to Land Burial—A Review of Innovative Hazardous Waste Management Techniques. New York State Environmental Facilities Corp. and others

Write: Diana M. Hinchcliff, New York State Environmental Facilities Corp., 50 Wolf Rd., Albany, N.Y. 12205; (518) 457-4222

May 2–4 Pittsburgh, Pa.
4th Annual Symposium of Environmental Epidemiology. University of Pittsburgh

Write: Josephine B. Hatley, Graduate School of Public Health, University of Pittsburgh, Pittsburgh, Pa. 15261; (412) 624-1559

May 2–4 Fort Mitchell, Ky.
9th Annual Research Symposium on Land Disposal, Incineration, and Treatment of Hazardous Waste. EPA

Write: David Shultz or Cathy Murillo, Southwest Research Institute, P.O. Drawer 28510, San Antonio, Tex. 78284; (512) 684-5111

May 9 West Lafayette, Ind.
Particles in Water: Surfaces and Interactions. Association of Environmental Engineering Professors

Write: Desmond Lawler, Department of Civil Engineering ECJ 8.6, University of Texas, Austin, Tex. 78712

May 10–12 West Lafayette, Ind.
38th Annual Purdue Industrial Waste Conference. Purdue University

Write: J. D. Wolszon, Purdue Industrial Waste Conference, Civil Engineering Bldg., Purdue University, West Lafayette, Ind. 47907; (317) 494-2194

May 12–13 Las Vegas, Nev.
The Management and Disposal of Hazardous and Chemical Wastes. J. T. Baker Chemical Co.

Write: Anne Logan, J. T. Baker Chemical Co., 222 Red School Lane, Phillipsburg, N.J. 08865; (201) 454-2500

May 16–17 Arlington, Va.
Superfund Update: Cleanup Lessons Learned. Center for Energy and Environmental Management (CEEM)

Write: Penny Dimler, CEEM, P.O. Box 536, Fairfax, Va. 22030; (800) 424-9068 or (703) 250-5900

May 16–18 Jekyll Island, Ga.
13th Annual Symposium on the Analytical Chemistry of Pollutants. EPA and others

Write: Elaine McGarity, U.S. Environmental Protection Agency, Environmental Research Laboratory, Athens, Ga. 30613; (404) 546-3184

May 18–19 Grand Forks, N.D.
12th Biennial Lignite Symposium. University of North Dakota

Write: Dawn Botsford, Division of Continuing Education, Box 8277, University Station, Grand Forks, N.D. 58202; (701) 777-2663

May 22–26 Washington, D.C.
6th Ozone World Congress. International Ozone Association

Write: Kathleen Loomis, International Ozone Association, Tower Suite 510, 301 Maple Ave. West, Vienna, Va. 22180; (703) 255-2210

May 23–24 San Francisco, Calif.
Siting New Industry: Solving the Environmental Equation. The Conservation Foundation

Write: The Conservation Foundation, 1717 Massachusetts Ave., N.W., Washington, D.C. 20036; (202) 797-4300

May 25–26 Minnetonka, Minn.
Water Purification Seminar. Osmonics, Inc.

Write: Natalie Hahn, Osmonics, Inc., 5951 Clearwater Dr., Minnetonka, Minn. 55343; (612) 933-2277

May 26–31 Detroit, Mich.
149th National Meeting: Science and Engineering—Toward a National Renaissance. American Association for the Advancement of Science

Write: Joan Wrather, American Association for the Advancement of Science, 1515 Massachusetts Ave., N.W., Washington, D.C. 20036 (202) 467-5441

May 30 Baltimore, Md.
Symposium on Groundwater Flow and Solute Transport in Fractured Rocks. American Geophysical Union

This symposium is a part of the AGU Spring Annual Meeting. *Write:* American Geophysical Union, 2000 Florida Ave., N.W., Washington, D.C. 20009; (202) 462-6903

June 10–12 Plattsburgh, N.Y.
Acid Rain Symposium. Plattsburgh State University

Write: Bette S. Brohel, State University, Plattsburgh, N.Y. 12091; (518) 564-2050

June 20–24 Atlanta, Ga.
76th Air Pollution Control Association (APCA) Annual Meeting & Exhibition. APCA

Write: Air Pollution Control Association, P.O. Box 2861, Pittsburgh, Pa. 15230-2861; (412) 621-1090

COURSES

April 21–22 Arlington, Va.
Environmental Laws and Regulations–Update Course. Government Institutes, Inc.

Fee: $565. *Write:* Governmental Institutes, Inc., 966 Hungerford Dr., No. 24, Rockville, Md. 20850; (301) 251-9250

April 25–26 Madison, Wis.
Transport, Storage, Handling, and Cleaning of Drums at Industrial and Hazardous Waste Facilities. University of Wisconsin—Extension

Fee: $255. *Write:* John T. Quigley, Department of Engineering, University of Wisconsin—Extension, 432 North Lake St., Madison, Wis. 53706; (608) 262-0820

May 4–7 Lake Geneva, Wis.
Short Course on Co-oxidation, Autooxidation, Selenium, Anti-oxidation, and Cancer. American Oil Chemists Society (AOCS)

Write: Meetings Coordinator, AOCS, 508 South Sixth St., Champaign, Ill. 61820; (217) 359-2344

May 16–20 Cincinnati, Ohio
Environmental Analysis by Atomic Spectroscopy. Janet Van Doren, Finnigan MAT Institute

Fee: $850. *Write:* Nancy Kranpitz, Registrar, Finnigan MAT Institute, 11 Triangle Park Dr., Cincinnati, Ohio 45246; (513) 772-5500

May 17–18 Kansas City, Mo.
Controlling Air Pollution. University of Missouri and others

Fee: $225. *Write:* Brenda Bryson, University of Missouri, 1020A Engineering Bldg., Columbia, Mo. 65211; (314) 882-3088

(*continued on p. 188A*)

professional consulting services directory

Since 1885
Service to industry
Stearns-Roger

COMPLETE ENVIRONMENTAL SERVICES:

Environmental impact assessments . . . Pollutant emission, air quality & water quality monitoring . . . Dispersion estimates . . . Ecological consulting . . . Meteorological field studies & consulting services. Contact

ENVIRONMENTAL SCIENCES DIVISION
(303) 758-1122
P. O. Box 5888
Denver, Colorado 80217

Havens and Emerson
Consulting Environmental Engineers

Cleveland St. Louis Atlanta Saddle Brook Boston Gary

WESTON
DESIGNERS CONSULTANTS

HEADQUARTERS West Chester, PA 19380 • 215-692-3030
OFFICES Atlanta, GA • Boston, MA • Camden, NJ
Chicago, IL • Cleveland, OH • Concord, NH
Houston, TX • Nashville, TN • New Orleans, LA
New York, NY • Richmond, VA • St. Paul, MN
Washington, DC • Amman, Jordan • Cairo, Egypt

CONSULTING GROUND-WATER GEOLOGISTS
ROUX ASSOCIATES INC

ROUX

- RCRA Monitoring
- Superfund Response
- Site Evaluation
- Aquifer Clean-Up

50 NORTH NEW YORK AVENUE
PO BOX 266, HUNTINGTON, NEW YORK 11743 516 673-4921

BC *Laboratories*

EPA Drinking Water Stds. & Priority Pollutants
Haloforms, PCB's—Gases, TOC, Solid Waste
Extractions, Heavy Metals
4100 Pierce Road (805) 327-4911
Bakersfield, California 93308

Ground Water Associates, Inc.

Water Supply Geologists and Engineers

- **Quantitative and qualitative ground water evaluations**
- **Iron removal by VYREDOX process**

P.O. Box 280
Westerville, Ohio 43081
614/882-3136

Cranford, New Jersey
Arlington, Massachusettes

The Professionals
ENTROPY
ENVIRONMENTALISTS, INC.

- Source Emissions Testing
- In-Plant Air Studies
- Continuous Emissions Monitoring
- Technical Consulting

Box 12291E • Research Triangle Park, NC 27709
Call: 1-800-ENTROPY

TRC Environmental Consultants, Inc

Environmental Planning and Problem Solving for Industry and Government

•AIR •WATER •SOLIDS •NOISE •ODOR

•MEASUREMENT •IMPACT ASSESSMENT
•CONTROL •INFORMATION SYSTEMS
•MODELING •PERMIT PLANNING

800 Connecticut Blvd., E. Hartford, CT 06108
(203) 289-8631
•EAST HARTFORD •DENVER •SAN DIEGO

Clayton Environmental Consultants, Inc.

- Emission and Ambient Air Surveys
- Hazardous Waste Management
- Engineering Design
- Industrial Hygiene Surveys
- Accredited Laboratories
- GC/MS, HPLC, X-Ray, AA and SEM/EDS
- Environmental Audits

Main Office:	*Laboratories:*	*Branch Offices:*
25711 Southfield Road Southfield, MI 48075 (313) 424-8860	Southfield, MI Edison, NJ	Atlanta, GA Edison, NJ Windsor, Ontario

A Technical Service of Marsh & McLennan

DATA
Digitized–Analyzed–Processed

- **Strip charts digitized**
- **Calibration factors applied**
- **Chart/tape/disk data analyzed & processed**
- **Tape, diskette, or hard-copy output**
- **Standard or customized printouts**

Currently processing more than 300 continuous data channels for more than 20 clients

LOW COST • HIGHEST QUALITY
QUICK TURNAROUND

WEST ORANGE, NJ **DENVER, CO**
(201) 325-1544 **(303) 989-5061**

ENVIROPLAN

Woodward-Clyde Consultants

- Site Selection Studies
- Impact Assessment Evaluation
- Decision and Risk Analyses
- Environmental Field and Laboratory Studies

San Francisco • Denver • Houston • Chicago
New York • Anchorage • Kansas City
Wayne, NJ • Plymouth Meeting, PA
Other offices in principal U.S. cities

Dames & Moore

- **Environmental Impact Assessment**
- **Geotechnical and Environmental Engineering**
- **Meteorology and Air Quality Monitoring**
- **Water Pollution Control Engineering**
- **Modelling and Numerical Analyses**
- **Permitting and Licensing Consultation**
- **Solid and Hazardous Waste Management**

San Francisco • Denver • Chicago
Cincinnati • Atlanta

Offices in Principal Cities
Throughout the World

Complete Analytical Services
SINCE 1919

- Screening of Industrial Waste for EPA Priority Pollutants using Finnigan OWA-30 GC/MS.
- NPDES & SPDES Organic & Inorganic Testing.
- Drinking Water Analysis to EPA Standards.
- Bioassay, Bioaccumulation & Toxicity Studies of Industrial Waste, Municipal Sludge & Dredge Spoils.
- Leachate Potential Studies & Analysis.
- Total Instrumental Analysis: A.A., GC/MS, G.C., I.R., TOC & TOD.
- RCRA Hazardous Waste Testing.

NEW YORK TESTING LABORATORIES
81 Urban Avenue, Westbury, N.Y. 11590
(516) 334-7770

ACOUSTIC TECHNOLOGY, INC.

ACOUSTIC CONSULTANTS

- **Environmental Noise Impact Assessment**
- **Ambient Noise Monitoring**
- **Computerized Acoustic Modeling and Analysis**

240 Commercial Street,
Boston, MA 02109

Telephone:
(617) 367-0164

Scott Environmental Technology, Inc.

The Air Pollution Specialists
• Research and Consulting •
• Source Emissions Testing •
• Control Device Efficiency •
• Continuous Source Monitoring •
• Ambient Monitoring •
• Fuel Additive & Automotive Testing •

Route 611, Plumsteadville, PA 18949
215 – 766-8861
2600 Cajon Blvd., San Bernardino, CA 92411
714 – 887-2571
1290 Combermere St., Troy, MI 48084
313 – 589-2950

SIRRINE
ENVIRONMENTAL CONSULTANTS

-Permit Assistance
-Air & Water Quality Modeling
-Site Selection Studies
-Laboratory Analyses
-Environmental Impact Assessments
-Hazardous Solid Waste Management
-Complete Design Services
-Construction Management

Greenville, SC 29606
Houston, TX 77042
Research Triangle Park, NC 27709

DAVID KEITH TODD
CONSULTING ENGINEERS, INC.

Groundwater Planning, Development, Management, and Protection

2914 Domingo Avenue
Berkeley, California 94705 415/841-2091

USE THE CONSULTANTS' DIRECTORY

May 17–20 Seattle, Wash.
Quality Assurance for Ambient Air Monitoring. Northrop Environmental Training

Fee: $585. *Write:* Registrar, Northrop Environmental Training, P.O. Box 12313, Research Triangle Park, N.C. 27709; (919) 549-0652

May 18–19 St. John's, Newfoundland, Canada
Occupational Health and Safety. Memorial University of Newfoundland

Write: Director, Continuing Engineering Education Center, Memorial University of Newfoundland, St. John's, Newfoundland A1B 3X5, Canada; (709) 737-7467

May 18–20 Philadelphia, Pa.
3-Day Stack Sampling and Particle Sizing Seminar. Andersen Samplers Inc.

Fee: $395. *Write:* Ralph Bulger, Andersen Samplers Inc., 4215 Wendell Dr., Atlanta, Ga., 30336; (800) 241-6898

May 23–25 Washington, D.C.
Computer Analysis of Satellite Data for Vegetation Mapping and Environmental Monitoring. The George Washington University

Fee: $685. *Write:* The George Washington University, School of Engineering and Applied Science, Washington, D.C., 20052; (202) 676-6106 or (800) 424-9773

May 24–26 Washington, D.C.
Practical Environmental Law. University of Denver College of Law

Fee: $675. *Write:* J. K. Van Wycks, Seminar Division Office, 5th Floor South, 1120 20th St., N.W., Washington, D.C. 20036; (202) 337-7000

May 26–27 Bronx, N.Y.
Quality Models of Natural Water Systems. Manhattan College

Fee: $200. *Write:* Kathryn King, Program Coordinator, Environmental Engineering & Science Program, Manhattan College, Bronx, N.Y. 10471; (212) 920-0277

June 14–17 Quebec City, Canada
Acid Rain and Forest Resources Conference. Canadian Forestry Service and others

Write: Claude Gendreau, chairman, Arrangements Committee, Acid Rain and Forest Resources Conference, Lauretian Forest Research Centre, Environment Canada, P.O. Box 3800, 1080 Route du Vallon, Sainte-Foy, Quebec G1V 4C7, Canada

August 17–24 Estes Park, Colo.
International Humic Substances Society Meeting. USDA, Soil Conservation Service, U.S. EPA, USGS, and International Humic Substances Society

Write: Ronald L. Malcolm, U.S. Geological Survey, Box 25046, MS 407, Denver, Colo. 80225; (303) 234-3975

INTERNATIONAL

May 17–19 Geneva, Switzerland
Second International Conference on Photovoltaic Business Development. Monegon, Ltd.

Fee: $1200. *Write:* Peter Grambs, Monegon, Ltd., Photovoltaics Business Development Conference, 4 Professional Dr., Gaithersburg, Md., 20879; (301) 258-7540

May 24–26 Jerusalem, Israel
2nd International Conference on Ecology and Environmental Quality. The Israel Ecological Society

Write: H. Shuval, chairman, Israel Ecological Society, Hebrew University-Hadassah Medical School, P.O. Box 1172, Jerusalem, Israel

May 30–June 3 Parkville, Victoria, Australia
International Conference on Chromatographic Detectors. C.S.I.R.O., Melbourne University, and others

Write: The Secretary, International Conference on Chromatographic Detectors, University of Melbourne, Parkville, Victoria, Australia 3052

INDEX TO THE ADVERTISERS IN THIS ISSUE

CIRCLE INQUIRY NO.		PAGE NO.
1	**Martek Instruments, Inc.** Tekmar Marketing Services	**OBC**

PROFESSIONAL CONSULTING SERVICES DIRECTORY **187A**

Advertising Management for the
American Chemical Society Publications

CENTCOM, LTD.

Thomas N. J. Koerwer, President
James A. Byrne, Vice President
Alfred L. Gregory, Vice President
Clay S. Holden, Vice President
Benjamin W. Jones, Vice President
Robert L. Voepel, Vice President
Joseph P. Stenza, Production Director

25 Sylvan Road, South
P.O. Box 231
Westport, Connecticut 06881
(Area Code 203) 226-7131
Telex No. 643-310

ADVERTISING SALES MANAGER
JAMES A. BYRNE

ADVERTISING PRODUCTION MANAGER
GERI P. ANASTASIA

SALES REPRESENTATIVES

Philadelphia, Pa. . . . CENTCOM, LTD., GSB Building, Suite 425, 1 Belmont Ave., Bala Cynwyd, Pa 19004 (Area Code 215) 667-9666

New York, N.Y. . . . CENTCOM, LTD., 60 E. 42nd Street, New York 10165 (Area Code 212) 972-9660

Westport, Ct. . . . CENTCOM, LTD., 25 Sylvan Road South, P.O. Box 231, Westport, Ct 06881 (Area Code 203) 226-7131

Cleveland, Oh. . . . Bruce Poorman, CENTCOM, LTD., 325 Front St., Suite 2, Berea, OH 44017 (Area Code 216) 234-1333

Chicago, Ill. . . . Bruce Poorman, CENTCOM, LTD., 540 Frontage Rd., Northfield, Ill 60093 (Area Code 312) 441-6383

Houston, Tx. . . . Dean A. Baldwin, CENTCOM, LTD., (Area Code 713) 667-9666

San Francisco, Ca. . . . Paul M. Butts, CENTCOM, LTD., Suite 112, 1499 Bayshore Highway, Burlingame, CA 90410. Telephone 415-692-1218

Los Angeles, Ca. . . . Clay S. Holden, CENTCOM, LTD., 3142 Pacific Coast Highway, Suite 200, Torrance, CA 90505 (Area Code 213) 325-1903

Boston, Ma. . . . CENTCOM, LTD. (Area Code 212) 972-9660

Atlanta, Ga. . . Donald B. Davis, CENTCOM, LTD., Phone (Area Code 203) 226-7131

Denver, Co. . . . Clay S. Holden, CENTCOM, LTD. (Area Code 213) 325-1903

United Kingdom:
Reading, England—Technomedia, Ltd. . . . Wood Cottage, Shurlock Row, Reading RG10 OQE, Berkshire, England 0734-343302
Lancashire, England—Technomedia, Ltd. . . . c/o Meconomics Ltd., Meconomics House, 31 Old Street, Ashton Under Lyne, Lancashire, England 061-308-3025

Continental Europe . . . Andre Jamar, Rue Mallar 1, 4800 Verviers, Belgium. Telephone (087) 22-53-85. Telex No. 49263

Tokyo, Japan . . . Shigeo Aoki, International Media Representatives Ltd., 2-29, Toranomon 1-Chrome, Minatoku, Tokyo 105 Japan. Telephone: 502-0656

Distribution Profiles of Chloroform, Weak Organic Acids, and PCBs on Granular Activated Carbon Columns from Waterford, New York

Katherine Alben* and Eugene Shpirt

Center for Laboratories and Research, New York State Department of Health, Albany, New York

■ Profiles are given for the distribution of chloroform, weak organic acids, and polychlorinated biphenyls (PCBs) on granular activated carbon (GAC) samples from four pilot columns, placed in series and operated for 26 weeks at Waterford, NY. Chloroform and the weak organic acids are found at or near saturation through most of the GAC system, whereas the PCBs are accumulated only at the inlet. The extent of saturation achieved by these compounds is consistent with differences in their mass inputs and GAC capacities. However, irregularities in adsorption of these substances are evident in localized depletions of chloroform and the weak organic acids at the inlet to the system. Displacement of chloroform from the GAC inlet after 26 weeks' operation is confirmed by analysis of breakthrough data for the trihalomethanes.

Granular activated carbon (GAC) is often monitored for evidence of column breakthrough based on comparative analyses of influent and effluent water samples. This strategy is appropriate to assess final water quality and the overall efficiency of the GAC adsorber. In the case of a potable water supply being treated for compounds whose maximum contaminant levels are defined, such information is essential. It is the purpose of this paper to show that detailed examination of GAC samples, as much as the analysis of water samples, can be used to advantage to understand GAC performance under complex treatment plant conditions.

From a mass transfer viewpoint, the saturation of an adsorbent such as GAC parallels breakthrough to the effluent. The saturation of a GAC bed can be deduced from breakthrough data by analyzing water samples collected along the length of a column. This approach has been used to study mass transfer zones for phenolic compounds (*1*) and for volatile trichloroethylene (*2*) through fixed beds of GAC.

Direct analysis of GAC samples, also taken along the length of a column, is an alternative approach. Distribution profiles have been obtained for volatile and semivolatile organics obtained in solvent extracts of GAC samples (*3, 4*). Cases have also been reported where the distribution profile for total organic halogen was determined from microcoulometric analysis of pyrolyzed GAC samples (*3, 5, 6*). Generally the highest surface concentrations were found at the inlet to the columns studied. However, in a few instances, depletions of chloroform, dichloroethane, dichloropropane, trichloroethylene, bis(2-chloroisopropyl) ether (*3*), and total organic halogen (*5*) were observed at the column inlet. These results indicate that uniform saturation of a GAC bed is not necessarily achieved in a chemically complex system.

For this project, similar postrun analyses were performed on GAC samples taken from pilot columns at the Waterford, NY, potable water treatment plant. Methods of sample preparation and instrumental analysis were selected (or developed, when necessary) to study the diversity of organics adsorbed on the GAC pilot columns: chloroform and other volatile organics; semivolatile Aroclors 1016 and 1254 added as a spike to the GAC influent; polar nonvolatile organic acids. Sample chromatograms were inspected to identify compounds whose concentrations changed as a function of distance through the GAC columns. Distribution profiles were constructed for the different compounds to obtain a case history for GAC saturation and to look for evidence of displacement.

Experimental Section

Design and Operation of Pilot Columns. The pilot columns at Waterford, NY, have been described elsewhere (*7, 8*). Data for this paper were obtained from samples taken from four columns (10 cm i.d., 212 cm long) operated in series. The columns were each filled with 3900 g of Calgon F400 to a bed depth of 120 cm. Water from the Hudson River was taken after prechlorination and sand filtration and pumped onto the columns at a rate of 76 L/h, resulting in a total empty-bed contact time of 30 min. The GAC influent was continuously spiked at 1 μg/L with a 50:50 mixture of Aroclors 1016 and 1254, until the last week, when their influent concentration was increased to 10 μg/L. The pilot column experiments were terminated after 26 weeks' operation.

Sample Collection. When the pilot columns were shut down, they were divided into 20-cm sections and labeled for sampling. At a given distance, six samples were taken from a column cross section for replicate thermal desorption analyses (*8*). A custom-made auger was used to work through the columns in increments of 20 cm; the sections of intervening material were stored in a refrigerator for related analyses (e.g., elemental distributions by energy-dispersive X-ray fluorescence, and bacterial distributions (*9*)).

Volatile Organics. Several methods were used to analyze the GAC samples for volatile organics. The first set was analyzed by thermal desorption-packed column GC, and results were confirmed by mass spectrometry (MS) (*8*).

For comparison, a second set of samples were solvent extracted by a microscale analytical procedure. Approx-

0013-936X/83/0917-0187$01.50/0

imately 25 mg of GAC was weighed into a glass capillary tube (2 mm i.d., 6 mm 0.d., 12.7 cm long) sealed at one end. Methylene chloride (30 μL) was added, and the sample end of the tube was frozen in liquid nitrogen. The tube was quickly sealed at its other end and placed in an ultrasonic bath for 30 min. Just prior to analysis the tube was broken with a sharp file and 2 μL of extract withdrawn in a syringe. Data were acquired on a Perkin-Elmer Sigma 1 GC with a flame ionization detector. Organics were separated on a 40-m SF 96 glass capillary column, held at −30 °C for 5 min and then heated by a programmed temperature change from 5 to 200 °C at 6 °C/min. Helium carrier gas was supplied at 20 psi to achieve a linear velocity of about 25 cm/s.

In addition, influent and effluent water samples for each of the four GAC columns were independently analyzed for total (instantaneous) trihalomethanes (*7*), following established procedures (*10*).

Polychlorinated Biphenyls (PCBs). To determine the concentration of Aroclors 1016 and 1254, GAC samples (approximately 20 g) were Soxhlet-extracted overnight in methylene chloride. The extracts were concentrated with a Kuderna–Danish and Snyder column, and the methylene chloride was exchanged for hexane. The PCBs were further separated from interferring background material by a Florisil cleanup procedure, and the final hexane extracts were analyzed by extablished GC methods with electron-capture detection (*11*).

Organic Acids. Acids were eluted from the carbon samples (approximately 40 g each) with three 25-mL aliquots of 0.1 N NaOH, allowing 15-min contact time each. The extracts were analyzed by pH gradient HPLC, following a procedure developed for separation of humic substances into characteristic fractions of weak and strong organic acids (*12*). A 100-cm column of XAD-8, ground and sieved between 45 and 75 μm, was slurry packed in methanol and installed in a Spectra Physics 8000 liquid chromatograph. After sample injection (25 μL) the column was eluted at 1 mL/min with a linear gradient from 0.1 N H_3PO_4 (held for 1 min) to 0.1 N NaOH at 30 min (held for 15 min). The column effluent was monitored by measuring the UV absorbance at 254 nm.

Quantitation of the organic acids was based on measurements of dissolved organic carbon. GAC fines were removed from sodium hydroxide extracts of GAC samples by using 0.45-μm membrane filters. The filtrates were analyzed for dissolved organic carbon (DOC) on an Oceanography International carbon analyzer, following standard procedures (*13*).

For additional characterization of the organic acids, 0.1 N sodium hydroxide extracts were chlorinated with commercial solutions of sodium hypochlorite at chlorine to carbon mole ratios of 0.7–2.2. The initial and final concentration of hypochlorite were determined by titration (*14*). After 3 days, chlorinated samples and blanks were analyzed for trihalomethanes by liquid–liquid extraction with electron-capture gas chromatography (*10*).

Results and Discussion

Volatile Organics: Chloroform. Chromatograms for replicate GAC samples, analyzed for volatile organics by thermal desorption–packed-column GC and solvent extraction–capillary column GC, are given in Figures 1 and 2. Regardless of the methods of sample preparation and analysis, chloroform was the major volatile organic compound found on the GAC samples.

Profiles for the distribution of chloroform obtained by the two GC procedures are compared in Figure 3. The results are qualitatively the same. Chloroform was at or near saturation in all of the columns except the first. However, the chloroform concentration was lowest (ap-

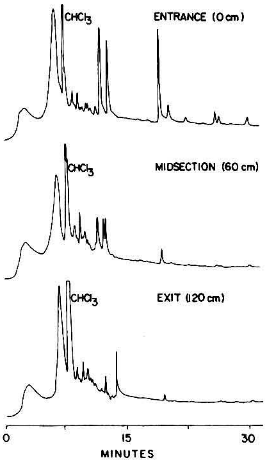

Figure 1. Thermal desorption–packed-column gas chromatograms for volatiles adsorbed on GAC samples from column 1.

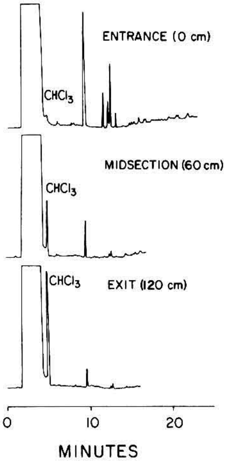

Figure 2. Solvent extraction–capillary-column gas chromatograms for volatiles adsorbed on GAC samples from column 1.

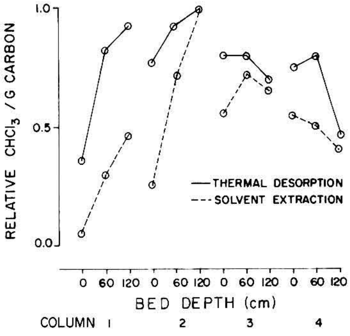

Figure 3. Profiles for distribution of chloroform on columns 1–4. Results from thermal desorption–packed column GC analysis were obtained 1 month after the pilot column shut down. Results from solvent extraction–capillary column GC analysis were obtained 9 months after shutdown.

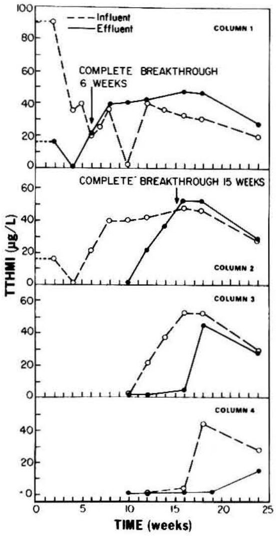

Figure 4. Breakthrough data for TTHMs on pilot columns 1–4, based on data from ref 7, Figure 12.

proximately 5–36% of saturation) at the inlet to the first column.

Quantitatively, the maximum GAC surface concentration for chloroform in Figure 3 was determined to be 2.3 ± 0.2 mg of $CHCl_3$/g of GAC by thermal desorption and 1.5 ± 0.2 mg of $CHCl_3$/g of GAC by solvent extraction. The difference between our two values for the chloroform–GAC surface concentrations could be the result of sample losses during the 8 months between determinations and/or of better resolution of chloroform by the capillary system used to analyze the solvent extracts. Evidence has also been found that chloroform concentrations are 15–45% greater in water samples analyzed by direct injection than in replicates analyzed by the purge-and-trap procedure (*14*). In this case, the difference was attributed to thermal decomposition of nonpurgeable organics in the hot injection port of the GC. In a similar manner, thermal decomposition could have resulted in enhancement of chloroform determined by thermal desorption of GAC samples, compared to solvent extraction.

For comparison, equilibrium capacities of 0.2–2 mg of $CHCl_3$/g of GAC have been reported elsewhere for solutions containing 10–100 µg of $CHCl_3$/L (*15*). We have also recently determined adsorption isotherms for chloroform on Calgon F400, 100–200 mesh, allowing 7 days to achieve equilibrium (*15*). The results were fit by a log–log plot of GAC surface concentration (mg/g) vs. solution concentration (µg/L) with a coefficient of linearity of 0.95 for $N = 24$ experimental points: the Freundlich constants were $1/n = 0.75$ and $K_F = 0.096$ (*16*). Thus our results give equilibrium capacities of 0.5–3.0 mg of $CHCl_3$/g of GAC for solutions containing 10–100 µg of $CHCl_3$/L.

Other compounds less volatile than chloroform are noted from the sample chromatograms to be concentrated primarily at the inlet to the GAC columns (Figures 1 and 2). Some of these compounds have been tentatively identified by thermal desorption–GC–MS analysis as butanamide, pyridine, toluene, chlorobenzene, chlorofluorobenzene, and ethylbenzene–xylene isomers (*8*). Since different columns were used for GC and GC–MS analyses, peaks other than chloroform are not identified in the GC–FID chromatograms. However, some of these compounds have been recently reported elsewhere in similar GC–MS analyses by thermal desorption and solvent extraction of GAC samples (*17*).

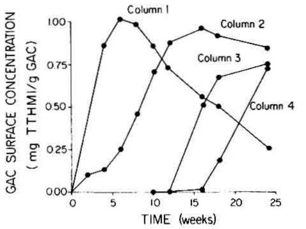

Figure 5. Cumulative adsorption of TTHMs on pilot columns 1–4, based on data from ref 7 Figure 12.

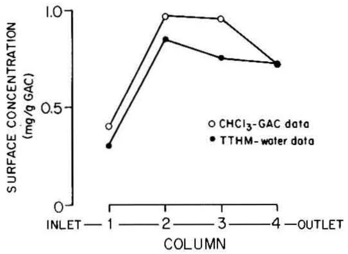

Figure 6. Comparison of distribution profiles obtained for chloroform (based on solvent extraction capillary GC-FID data in Figure 3) and TTHMs (based on data from ref 7, Figure 12).

For comparison to the chloroform distribution profiles, the breakthrough curves for total (instantaneous) trihalomethanes (TTHMs) are given in Figure 4 (*7*). The first and second columns are noted to have reached complete breakthrough (effluent = influent) at 6 and 15 weeks, respectively, whereas the third and fourth columns were near complete breakthrough at 24 weeks.

Average TTHM–GAC surface concentrations as a function of time are given in Figure 5. To obtain these results, the mg of TTHM applied were calculated by integrating each column's influent and effluent breakthrough curves, taking the difference, and multiplying by the total volume of water treated (1.27×10^4 L/week). The mg of TTHM applied were then divided by the amount of GAC in a column (3900 g) to determine the average GAC surface concentration.

The results in Figure 5 show qualitatively that trends in TTHM–GAC surface concentrations for the four columns resemble trends in the chloroform–GAC data. The first and second columns are noted to have a relatively high TTHM–GAC surface concentration when they initially reached complete breakthrough at 6 and 15 weeks, respectively. However, after 24 weeks the average TTHM–GAC surface concentration of the first column had dramatically decreased.

In Figure 6 the final $CHCl_3$ and TTHM distribution profiles from the different methods of analysis are compared. Points for the $CHCl_3$ profile represent the average of three points plotted for each column in Figure 3 by using the solvent extraction–capillary GC–FID data. Reasons for using this set of data have been discussed above. Points for the TTHM profile are taken from results in Figure 5, corresponding to 24 weeks' operation. Both distribution profiles provide evidence for $CHCl_3$ depletion from the first column.

Differences in quantitative values for trihalomethane–GAC surface concentrations shown in Figure 6 are remarkably small. The maximum TTHM–GAC surface

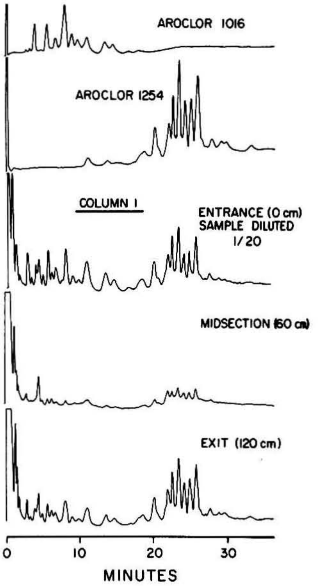

Figure 7. Chromatograms for Aroclors 1016 and 1254 compared to PCBs adsorbed on GAC samples from column 1.

concentration (0.85 mg of TTHM/g of GAC, column 2), based on analysis of water samples concurrent with pilot column operation, is close to the $CHCl_3$–GAC surface concentration (0.98 mg of $CHCl_3$/g of GAC, column 2 average, solvent extraction capillary GC–FID data). Less agreement between the two sets of data would not have been surprising, given the possible sources of error: differences in recovery factors for the TTHM- and chloroform–GAC analyses; uncertainties in parameters needed to calculate TTHM–GAC surface concentrations from the TTHM data, specifically the flow through the pilot columns and the mass of GAC in individual columns, corrected for losses from backwashing.

PCBs. Chromatograms for the PCBs adsorbed on the GAC columns (Figure 7) show that Aroclor 1254 was adsorbed primarily according to its commercial composition, with little evidence of selectivity. However, a few volatile halogenated compounds that were not eliminated by the Florisil cleanup procedure appear interspersed with Aroclor 1016 in the chromatograms.

Profiles for the distribution of Aroclors 1016 and 1254 (Figure 8) indicate that they were concentrated at the inlet to the first GAC column. Analysis of samples in triplicate confirmed the depletion of the PCBs at the midpoint of the first column, followed by a small but noticeable increase at the outlet of that column (cf. Figures 7 and 8). Only Aroclor 1254 was found above minimum detectable concentrations downstream of the first column. All of the GAC samples were screened for PCBs at a minimum detectable concentration of 0.05 μg/g of GAC. This figure is based on the working range of our PCB standards from 0.1 to 2.5 mg/L and on 10-mL final volume of solvent extracts from 20-g GAC samples. Extracts from the inlet GAC samples had to be diluted volumetrically for analysis. Although our detection limit was inordinately low, there is considerable certainty in the fact that the PCBs were not present at significant concentrations downstream of the first column.

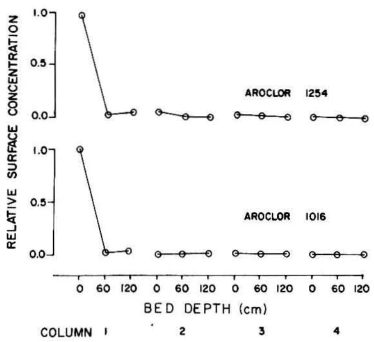

Figure 8. Profiles for distribution of Aroclors 1016 and 1254 on columns 1–4.

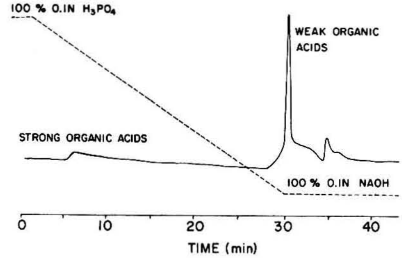

Figure 9. High-performance liquid chromatogram of organic acids extracted from GAC at inlet of column 2.

In retrospect, it would have been advantageous to have analyzed 1-g GAC samples and to have subsectioned the first 20 cm of GAC from column 1 in smaller 1-cm increments. Maximum PCB–GAC surface concentrations found were 7.6 ± 0.2 μg/g of GAC for Aroclor 1016 and 5.6 ± 1.0 μg/g of GAC for Aroclor 1254. These concentrations are substantially below batch isotherm capacities of 2.14 mg/g of GAC for Aroclor 1016 and 0.61 mg/g of GAC for Aroclor 1254, reported at equilibrium concentrations of 0.5 μg/L (*18*). It can be deduced that some of this discrepancy may have arisen from subdivision of the GAC bed into 20-cm sections. The calculated mass input of PCBs corresponds to 165 mg each of Aroclors 1016 and 1254 during the pilot columns' operation. On the basis of adsorption isotherm capacities, approximately 77 g of GAC and 270 g of GAC should have been saturated with Aroclors 1016 and 1254, respectively. Given 3900 g of GAC per column with a bed depth of 120 cm, there were approximately 32 g of GAC/cm. Hence the GAC should have been saturated to a depth of only 2.4 cm by Aroclor 1016 and 8.4 cm by Aroclor 1254. Although these calculations neglect any effect of competition on GAC adsorption capacity, they show that the bed depth saturated by the PCBs was probably less than the 20-cm sections in which the GAC columns were subdivided. Smaller GAC sections would have enabled a more precise determination of the gradient in PCB concentrations at the column 1 inlet, as well as a more accurate determination of maximum PCB–GAC surface concentrations.

Organic Acids. A typical HPLC chromatogram for the acids extracted from the GAC samples is shown in Figure 9. The various peaks are concluded to represent successive elution of compounds with decreasing acidity. The intensity of the late-eluting peak for weak organic acids suggests that they were either more abundant or more chromophoric than the strong organic acids. The chromatograms resemble those obtained under similar analytical conditions for humic substances, where the separate peaks were interpreted to represent differences in the

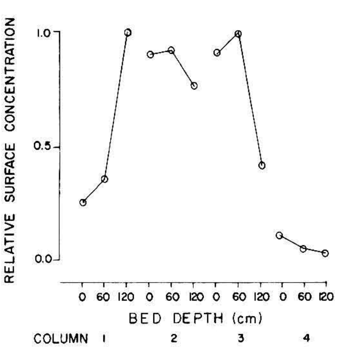

Figure 10. Profile for distribution of weak organic acids on columns 1–4.

relative abundance of carboxylic and phenolic functional groups (*12*).

In this and other respects the organic acids adsorbed on the GAC columns are considered related to fulvic and/or humic substances found in surface water suplies. When chlorinated, the weak organic acids were found to have a chlorine demand of 0.6 ± 0.2 mol of chlorine/mol of carbon and a chloroform yield of 32 ± 4 mg of $CHCl_3$/g of DOC. Values reported in the literature for chlorination of fulvic and humic acids range from 46 to 207 mg of $CHCl_3$/g of TOC (*19–23*). Our experiments differ by a somewhat shorter reaction time, 72 h compared to 90–120 h, but also by a more optimal pH for formation of chloroform, 12 compared to 6.5–9.2. In addition to having a chloroform formation potential, some of our organic acid–GAC extracts have been observed to coagulate when left to stand in the laboratory. Also, the organic acids extracted from the GAC have exhibited little affinity for a reverse-phase RP-8 column used to separate low molecular weight phenols, cresols, and chlorophenols (*16*). Finally, the UV spectrum for the weak organic acids was similar to that reported for humic substances, with a maximum at 240 nm, followed by a monotonic decrease in absorbance with increasing wavelength (*24*).

The profile for the weak organic acids (Figure 10) indicates that they had reached saturation on a substantial part of the GAC system. However, the weak organic acids were depleted at the inlet to the first column. The profile for the strong organic acids is not given because their intensity was too low to reproducibly verify their abundance. The maximum surface concentration of the weak organic acids was determined to be 3 mg of DOC/g of GAC, by successively extracting the strong and weak acids from the GAC in 0.01 and 0.1 NaOH, respectively. Batch isotherm capacities for humic substances range from 10 to 100 mg of TOC/g of GAC in solutions of humic acids containing 0.1–10 mg of TOC/L (*25*).

Relative Distributions of Organics, Determining Factors, and Sampling Strategies

The distribution profiles for chloroform, PCBs, and weak organic acids are considered to reflect basic differences in their influent concentrations and GAC capacities. The data summarized in Table I suggest that because of comparatively high influent concentrations (and therefore mass loads) and low GAC capacities for chloroform and the weak organic acids, they advanced well through the pilot columns, whereas the PCBs accumulated at the inlet.

Table I

	cumulative input	GAC capacities K_F	GAC capacities $1/n$
$CHCl_3$	10.6 g of TTHM	0.096	0.75
PCBs	165 mg of Aroclor 1016	3.44	0.66 (18)
	165 mg of Aroclor 1254	0.73	1.14 (18)
organic acids	2700 g of TOC[a] (*26*)		(25)

[a] This figure is an estimate based on TOC analyses and is not specific to organic acids.

In addition, distribution profiles obtained for chloroform and the weak organic acids suggest their displacement from the GAC inlet, but the cause of this behavior is more difficult to deduce. In the case of chloroform, at least, it was possible to verify its displacement by calculating cumulative adsorption curves (Figure 5) and the final TTHM distribution profile (Figure 6) from independently acquired breakthrough data. Displacement of chloroform has also been reported for other systems where effluent concentrations were found in excess of influent concentrations (*27, 28*). Chromatograms for the Waterford GAC samples (Figures 1 and 2) suggest that displacement of chloroform may result from accumulation of less volatile compounds, including the PCBs, at the GAC inlet. Organic and inorganic chlorine and calcium were also found at the pilot columns' inlet (*9*). Because of the 120-cm separation between sampling sites for TTHM analyses, it is difficult to identify fluctuations in TTHM influent concentrations (Figure 4) as a cause of TTHM displacement. Although dramatic fluctuations in TTHM influent concentrations occurred during the first 6 weeks (Figure 4), the first column was effectively in a net adsorptive phase as seen from the point of monitoring (Figure 5). Lesser fluctuations in TTHM influent concentrations occurred between 6 and 26 weeks, during which the first column was seen to be in a virtually continuous desorptive phase (Figure 5). Therefore the TTHM data do not provide clear evidence of a relationship between fluctuations in influent concentration and TTHM displacement. It should be possible with further experiments and use of mathematical models to resolve the extent to which chemical competition and/or fluctuations in influent compositions are the cause(s) of chloroform displacement.

We conclude from the the present work that the trihalomethanes and organic acids are two classes of chemicals for which GAC adsorption under treatment plant conditions should be considered a dynamic process. Further studies of their adsorption will benefit from judicious selection of bed depth sampling positions to monitor for dynamic conditions. For example, if the four GAC columns at Waterford had been sampled just at the inlet and outlet (0 and 480 cm), the only conclusion would have been that after 26 weeks 94% of the TTHMs were removed and the column effluent had reached initial breakthrough (6%). With sample ports at intervals of 120 cm, it was possible to obtain evidence for displacement of TTHMs, but the effluent's response to fluctutions in influent THM levels was obscured. Nonetheless the TTHM data revealed that after 26 weeks 75% of THMs adsorbed on the first 120 cm had been displaced downstream (and readsorbed), corresponding to a shift of 20% of the total mass input of TTHMs. Sectioning the GAC columns in increments of 20 cm (albeit for postrun analysis) resulted in a more detailed picture of fluctuations in GAC surface concentrations for $CHCl_3$ and weak organic acids but was not sufficient to precisely determine the sharp decline in PCB concentrations near the inlet or screen for competitive effects in PCB adsorption. For GAC systems with design parameters and mass input rates similar to the columns described in this paper, sample sites spaced 20 cm apart should suffice to study dynamic adsorption of THMs and organic acids. Smaller distances between sampling sites would be necessary to monitor dynamic adsorption of PCBs, and similar compounds, present at very low influent concentrations, but characterized by very favorable adsorption capacities; however, sample ports very close together (e.g., 1 cm) may represent a practical problem for column design and operation.

Other aspects of the sampling strategy are the sample type and sampling frequency. Analyses of GAC and water samples collected from the same location at the same time permit results to be cross-checked for accuracy. For this paper, it was useful to be able to compare results based on $CHCl_3$-GAC analyses and TTHM-water analyses in order to interpret the postrun distribution profiles. Since relatively good agreement was obtained, the key factor was not whether GAC or water samples were used but that the water samples were collected at various times during pilot column operation. In retrospect, analysis of weekly samples of either type would have improved the quality of the data base used to establish breakthrough (or saturation) curves, corresponding distribution profiles, and in the end, experimental evidence for displacement.

Conclusions

The results provided in this paper show that diverse organic substances accumulate on GAC columns in surface water supplies, trihalomethanes and organic acids in particular. Distribution profiles for these substances based on postrun GAC analyses are nonuniform: depletion of chloroform and organic acids at the GAC inlet contrast with their increased accumulation on the GAC downstream. These depletions were not found in distribution profiles for other volatile and semivolatile organics, including Aroclors 1016 and 1254 added as a spike to the GAC influent. Therefore, the depletions raise the question of time-dependent displacement of chloroform and organic acids from the GAC inlet. Evaluation of trihalomethane data from water samples collected during pilot column operation revealed that the trihalomethanes had been displaced from the GAC inlet: the final distribution of trihalomethanes was in agreement with the profile based on postrun GAC analyses. Results presented in this paper illustrate how sampling and analytical protocols could be designed to monitor for dynamic adsorption of trihalomethanes and organic acids on GAC, to obtain experimentally a better understanding of the conditions under which displacement occurs.

Acknowledgments

We are grateful to Italo Carcich and Jim Tofflemire of the New York State Department of Environmental Conservation, who supervised this project, and to Thomas Tomayo and Edwin Tifft of O'Brien and Gere for contributiong the GAC from the pilot column study. We also thank Chris Maeder and Joan Kaczmarczyk, who helped complete these analyses, and Jim Daly for use of his gas chromatograph to obtain profiles for the PCBs.

Registry No. Aroclor 1016, 12674-11-2; Aroclor 1254, 11097-69-1; chloroform, 67-66-3.

Literature Cited

(1) Zogorski, J.; Faust, S. In "Carbon Adsorption Handbook"; Cheremisinoff, P., Ellerbach, F., Eds.; Ann Arbor Science: Ann Arbor, MI, 1978; pp 753–777.
(2) Meijers, A.; Rook, J.; Schultink, B.; Smeenk, J.; van der Laan, J.; Poels, C. *J. Am. Water Works Assoc.* **1979**, *71*, 628.
(3) Kolle, W.; Sontheimer, H.; Stieglitz, L. *Vom Wasser* **1975**, *44*, 203.
(4) Yohe, T.; Suffet, I. Proceedings of the 99th American Water Works Association Meeting, June 1979, AWWA, Denver, CO, 1979; pp 553–577.
(5) McCreary, J.; Snoeyink, V. *Environ. Sci. Technol.* **1981**, *15*, 193.
(6) Kuhn, W.; Sontheimer, H. *Vom Wasser* **1973**, *41*, 66.
(7) O'Brien and Gere Engineers, Inc. "Hudson River Water PCB Treatability Study"; N.Y. State Contract No. D-141953, O'Brien and Gere Engineers, Inc., Syracuse, NY, Jan 1982).
(8) Alben, K.; Shpirt, E. In "Chemistry in Water Reuse";Cooper, W., Ed.; Ann Arbor Science: Ann Arbor, MI, 1981; pp 269–284.
(9) Alben, K.; Shpirt, E.; Perrins, N. In "Treatment of Water by Granular Activated Carbon"; McGuire, M., Suffet, I., Eds.; American Chemical Society: Washington DC, in press.
(10) *Fed. Regist.* **1979**, *44*, 68624.
(11) *Fed. Regist.* **1979**, *44*, 69464.
(12) MacCarthy, P.; Peterson, M.; Malcolm, R.; Thurman, E. *Anal. Chem.* **1979**, *51*, 2041.
(13) "Standard Methods for the Examination of Water and Waste Water"; American Public Health Association, American Water Works Association, Water Pollution Control Federation, Washington, DC, 15th ed., 1980.
(14) Pfaender, F.; Jones, R.; Stevens, A.; Moore, L.; Haas, J. *Environ. Sci. Technol.* **1978**, *12*, 438.
(15) Chudyk, W.; Snoeyink, V.; Beckman, D.; Temperly, T. *J. Am. Water Works Assoc.* **1979**, *72*, 529.
(16) Alben, K. New York State Department of Health, Albany, NY, unpublished data, 1982.
(17) Millington, D.; Bertino, D.; Kamei, T.; Christman, R. In "Water Chlorination: Environmental Impact and Health Effects"; Jolley, R., Ed.; Ann Arbor Science: Ann Arbor, MI; Vol. 4, in press).
(18) Pirbazari, M.; Weber, W. In "Chemistry in Water Reuse"; Cooper, W., Ed.; Ann Arbor Science: Ann Arbor, MI, 1981; pp 309–340.
(19) Stevens, A.; Slocum, C.; Seeger, D.; Robeck, G. *J. Am. Water Works Assoc.* **1976**, *68*, 615.
(20) Rook, J. J. *Environ. Sci. Technol.* **1977**, *11*, 478.
(21) Snoeyink, V.; McCreary, J.; Murin, C. EPA Report 600/2–77–223, U.S. EPA: Cincinnati, OH, Dec 1977.
(22) Babcock, D.; Singer, P. *J. Am. Water Works Assoc.* **1979**, *71*, 149.
(23) Scheuch, L.; Edzwald, J. *J. Am. Water Works Assoc.* **1981**, *73*, 497.
(24) Schnitzer, M.; Khan, S. "Humic Substances in the Environment"; Marcel Dekker: New York, 1972; pp 55–67.
(25) Boening, P.; Beckmann, D.; Snoeyink, V. *J. Am. Water Works Assoc.* **1980**, *72*, 54.
(26) Environmental Health Institute, New York State Department of Health, Albany, NY, unpublished data. 1977–1982.
(27) Sontheimer, H. *J. Am. Water Works Assoc.* **1979**, *71*, 618.
(28) Doyle, W.; Holdren, G., presented at the 181st National Meeting of the American Chemical Society, Atlanta, GA, March 29–April 3, 1981; ENVR 52.

Received for review November 12, 1980. Revised manuscript received December 6, 1982. Accepted December 23, 1982. Portions of this research were supported by New York State Department of Environmental Conservation, through Contract D-141953 to O'Brien and Gere Engineers, Inc.

Environ. Sci. Technol. 1983, 17, 193–198

Mobility in Soil and Plant Availability of Metals Derived from Incinerated Municipal Refuse

Paul M. Giordano,* Allan D. Behel, Jr., J. Edward Lawrence, Jr., John M. Soileau, and Billy N. Bradford

Tennessee Valley Authority, Division of Agricultural Development, National Fertilizer Development Center, Muscle Shoals, Alabama 35660

■ Fly ash residues from several sites in which solid municipal refuse is being incinerated for energy production were found to contain excessive amounts of cadmium and/or lead according to an empirical extraction test (0.5 N acetic acid) developed by the Environmental Protection Agency. Samples of associated bottom ashes contained acceptable levels of Cd and Pb, but several were marginal with respect to Pb content. Leaching tests clearly demonstrated that Cd and, to a lesser extent, Pb were mobile in soil when applied in a fly ash matrix. The high chloride content (10–12%), which is characteristic of these ashes, resulted in metal complexation and enhanced Cd and Pb mobility in soil. Normally these elements are relatively immobile in soils when applied as inorganic salts or contained in municipal sewage sludge. Plant uptake of Cd and Pb in a greenhouse test was marked when fly or finely ground bottom ashes were soil applied. Phytotoxicity of fly ash appeared to be associated with the high salt content rather than with a specific metal.

Introduction

Waste-to-energy conversion plants are attracting considerable attention in many U.S. cities because of the sharp rise in energy cost, increased expense in solid-waste management, and recent scarcity of suitable landfill sites (*4*). This approach, however, is not without problems. Although up to 75% of municipal solid waste is combustible and the volume reduction is about 90%, such environmental concerns as potential pollution to the atmosphere, water supply, and vegetation must be considered. Landfilling of ash residues, which are characteristically high in heavy metals (and occasionally toxic organics), may be a problem due to leaching and accumulation by vegetation (*2*).

The purpose of this study was to characterize the heavy-metal content of ash residues (bottom and fly) from several plants using thermal conversion processes. An extraction test (*3*) designed to identify potentially toxic or hazardous materials was used along with a series of leaching experiments to characterize ash constituents that might render the ash unsafe for conventional landfilling. Plant uptake of heavy metals also was determined from soil-applied ashes to estimate the possible impact of metal entrance into the food chain.

Experimental Section

Ash Extraction and Characterization. A variation of the technique described in ref 3 was developed and used to characterize both fly and bottom ash residues obtained from seven thermal conversion plants in the United States and Canada (identified as incinerator sites A–G). The procedure was as follows:

A. Air-dried samples (five 10.0-g replicates) of fly ash or bottom ash (crushed), able to pass through a 3.0-mm stainless steel screen, were weighed into flat-bottomed Nalgene bottles.

B. Deionized H_2O (160 mL) was added to each bottle and the contents agitated on a horizontal shaker for 30 min before 0.5 N acetic acid was added to adjust the pH to 5.0 ± 0.2.

C. After 24-h extraction, the solution volume was brought to 200 mL and filtered, and the filtrate was analyzed for Ag, As, Cd, Cr, Hg, Pb, and Se by atomic absorption spectroscopy.

Samples of fly ash also were subjected to analysis by X-ray fluorescence (XRF) and diffraction (XRD), optical microscopy (PLM), infrared spectroscopy (IR), and scanning electron microscope/energy dispersive X-ray (SEM/EDX) to characterize the residue with respect to matrix structure and elemental composition. Relative effectiveness of refuse combustion was estimated by drying 10-g samples of bottom ash at 100 °C for 2 h and igniting at 1000 °C in a muffle furnace for 1 h. The resulting weight loss after drying at 100 °C was assumed to be the unburned portion of the ash residue.

Metal Leaching from Ash Applied to Soil. A leaching apparatus consisting of a series of 15 cm (i.d.) × 60 cm (length) plastic well casings fitted with ceramic porous plates was used in conjunction with a vacuum system to reduce soil moisture to one-third bar percentage. An experiment was conducted to determine the mobility of Cd and Pb derived from fly ash (incinerator site A) in three soils varying in chemical and physical properties. The soils selected were Lakeland sand (Typic Quartzipsamment: pH 5.0, CEC 1.32 mequiv/100 g of soil, organic C 0.5%), Decatur silt loam (Rhodic Paleudult: pH 5.2, CEC 9.3 mequiv/100 g of soil, organic C 0.7%), and a calcareous Webster silty clay loam (Typic Haplaquoll: pH 7.5, CEC 30.6 mequiv/100 g of soil, organic C 5.1%). The above columns were filled with 40 cm of screened soil (<2 mm) and packed to a bulk density of about 1.5 g/cm^3. An 8-cm layer of fly ash (400 g) was added to the soil column and an additional 8 cm of soil added to the top. The equivalent of 30 cm of rainfall was leached through the prewet columns in increments over a 2-week period. Leachates were collected and stored under refrigeration until analyzed for cations, anions, pH, and organic C. Data from the Decatur soil were subsequently incorporated into the computer program GEOCHEM to determine metal equilibria and speciation with primary ligands (*4*).

A second experiment was conducted with Decatur soil in the TVA rhizotron lysimeter facility (*5*), utilizing soil bins of 1.82 × 1.22 × 1.02 m volume. Metal leaching from 30-cm thick surface soil-applied fly and bottom ashes (incinerator site A) under conditions of natural rainfall was monitored over an 18-month period. In addition sericea lespedeza (*Lespedeza cuneata* L. sericea) was sown to determine uptake of metals from the ash residues over two-crop seasons.

Plant Uptake of Metals from Soil-Applied Ashes. Decatur silt loam (pH 5.5 or limed to pH 6.5) was adequately fertilized with N, P, and K as a preplant application prior to seeding corn (*Zea mays*) and Swiss chard (*Beta vulgaris* var. cicla) in a greenhouse study. Each pot contained 2 kg of fertilized soil plus 300 g of fly ash or 600 g of crushed and screened (<2 mm) bottom ash (incinerator site A) as a surface layer, middepth layer, or mixed

Table I. Content of 0.5 N Acetic Acid Extractable Cd and Pb in Several Incinerator Ashes

incinerator site	μg/mL of extract[a] fly Cd	fly Pb	bottom Cd	bottom Pb
A	28.9	52.0	0.05	3.4
B	6.7	4.6		
C	5.7	4.4	0.05	0.85
D	0.64	0.47	<0.01	<0.01
E			0.27	4.6
F			0.09	1.9
G			0.04	4.2

[a] Waste is classified as hazardous if 0.5 N acetic acid extract contains concentrations that exceed the following levels (μg/mL): Cd, 1.0; Pb, 5.0.

full depth with the soil. Because of the high salt content of the ashes, that portion which was surface applied was previously leached with a large volume of deionized H_2O before use to ensure seed germination.

Corn and Swiss chard seeds were planted and later thinned to 5 and 8 plants per pot, respectively. Corn was harvested after 8 weeks, and chard was clipped at 3-week intervals for a total of 5 clippings. The plant tissue was dried at 70 °C, weighed, and ground in a Wiley mill equipped with stainless steel knives and screens. Heavy-metal analysis was done by atomic absorption spectroscopy after dry ashing 2-g samples at 470 °C for 5 h. Soil samples were taken after corn harvest from the no-ash controls and from mixed bottom and fly ash pots at both pH levels. Ten-gram samples of air dried soil were extracted with 50 mL of 1 N HCl or H_2O for 30 min and filtered. The filtrate was then analyzed for heavy metals by atomic absorption spectroscopy.

Results and Discussion

Ash Extraction and Characterization. Data in Table I indicate considerable variability among incinerator sites with respect to 0.5 N acetic acid extractable Cd and Pb from ash residues. Highest values were found in fly ash from site A. Monthly samples taken over a 14-month period were analyzed and found to have concentrations of Cd and Pb in fly ash ranging from 8 to 40 and 21 to 91 μg/mL, respectively, and in bottom ash from 0.03 to 3 and 0.2 to 13 μg/mL, respectively. The relatively high concentrations of Cd and Pb in the bottom ash have been reported elsewhere (*6*) even though these volatile elements would be expected to exit with the flue gases.

Since the elemental composition of the ashes is a reflection of the influent waste, much of the variability may be due to seasonal and weather-related factors (*1*). Cadmium and lead, as well as several other metals, are derived from the noncombustible as well as the combustible fraction of the refuse, and it has been suggested that emissions of these metals may be reduced significantly by recycling of the noncombustibles prior to burning (*7*). Another means by which ashes may be rendered acceptable in terms of meeting the EPA extraction standards is by mixing of fly with bottom ash during or after the incineration process (*8*). The law requires that fly and bottom ashes be combined before landfilling, thus reducing the impact of the more metal-rich fly ash.

No metals designated by EPA as hazardous contaminants other than Cd and Pb exceeded the critical concentrations in the 0.5 N acetic acid extracts of fly and bottom ashes from incinerator site A (data not shown). Although total (nitric acid–perchloric acid digestion) contents of Ag and Cr were high in both fly and bottom ashes (147 and 48 μg of Ag/g and 555 and 234 μg of Cr/g, respectively), the solubility in 0.5 N acetic acid of both metals was well below the established critical limits.

Table II. Mobility in Soil of Cd and Pb Contained in Fly Ash

soil type	range in leachate concn, μg/mL Cd	range in leachate concn, μg/mL Pb	recovery in leachate, % Cd	recovery in leachate, % Pb
	Soil Columns[a]			
Lakeland sand	2.20–56	0.7–109	40.1	7.0
Decatur clay loam	0.02–14	0.1–1.8	11.0	0.5
Webster silty clay loam	0.02–0.2	0.2–1.8	0.2	0.7
	Rhizotron Lysimeter[b]			
Decatur clay loam	50–270	2–131	79.5	6.0

[a] Columns contained 50 cm of sieved (<2 mm) soil and were subjected to the equivalent of 30 cm of rainfall in eight increments as deionized H_2O in the laboratory.

[b] Rhizotron lysimeter bins contained 140 cm of screened soil (<6 mm) and received approximately 150 cm of natural rainfall over an 18-month period.

Further characterization of the site A fly ash indicated that about 40% of the ash dissolved in boiling H_2O after 3 h. Although a qualitative XRF scan detected several metals in the material, including Cd, Pb, Zn, and Cu, only Cd was leached in a significant amount (approximately 30%). The soluble portion of the ash consisted largely of Na, K, Ca, S, and Cl.

X-ray diffraction patterns were obtained from the original sample and the dried, H_2O-soluble material. Sodium chloride and KCl were the predominant patterns seen in the original sample along with one or more unidentified crystalline phases. The predominant phases in solids after removal of the soluble phase were gypsum ($CaSO_4 \cdot 2H_2O$) and $CaSO_4 \cdot 0.5H_2O$. The hemihydrate resulted from partial dehydration of some of the gypsum. The presence of NaCl and KCl in the original samples explains the high levels of H_2O-soluble Na, K, and Cl.

Optical examination with the PLM showed 50–80% of the material to be opaque fibers or irregularly shaped particles; some of the latter were magnetic. When treated with HCl, a few of the particles evolved gas bubbles, indicating the presence of carbonates. Trace amounts of quartz and at least two unidentified crystalline phases were observed.

SEM/EDX analysis of the original solids detected the same elements as the XRF analysis except for Sn and Cd. Tin was below the level detectable by EDX, and Cd X-ray lines were obscured by other, more abundant elements. Lead was ubiquitous in the fly ash sample and not concentrated in any of the phases present. A few regularly shaped particles—spherical fly ash beads and fiberglass particles—were present.

Metal Leaching from Ash Applied to Soil. Recovery of Cd in leachate from the soil columns increased in the order Webster < Decatur < Lakeland (Table II). Highest Cd concentrations (43–56 μg/mL) appeared in leachate from the fourth and fifth increment of H_2O added to the Lakeland and from the fifth and sixth increment added to the Decatur soils (13–14 μg/mL). Recovery of Pb was lower than that of Cd and was appreciable only from the Lakeland sand.

Much higher recovery of Cd (80%), but a similar amount of Pb (6%), was obtained in the rhizotron compared with the soil columns. Differences may be explained in part by the greater amount of H_2O passing through the rhizotron system and the lower bulk density of the rhizotron soil (about 1.35 g/cm^3) relative to the packed soil columns. No Cd or Pb appeared for 2 months after ash application or until about 150 L of leachate had been collected. Very high concentrations of Cd and Pb were found throughout the 18 months of the experiment with peak concentrations occurring at the sixth month. A total of 150 cm of rainfall occurred over this period.

Despite the apparent high degree of Cd and Pb solubility in the fly ash, mobility in soil of these elements was not anticipated to be significant. An earlier study showed very little movement of Cd or Pb in columns of Decatur soil when applied as sewage sludge or sulfate salts (*9*). However, Taylor and Griffin (*10*) found Cd to be far more mobile than Pb in a Paxton fine sandy loam when applied to the soil surface as nitrate salts and leached intermittently for 30 weeks.

Hulett et al. (*11*) characterized several fly ash specimens and separated them into amorphous glass, mullite quartz (3 Al_2O_3·2 SiO_2), and magnetic spinel (Fe_3O_4) matrices. They hypothesized that removal of the glass and magnetic spinel components would likely reduce the long-term leaching of the transition elements such as Cd and Pb. Since the Cd and Pb in fly ash are associated with the glass phase, the possibility that movement occurred through the soil via physical transport in H_2O rather than chemical processes was explored. To test this possibility, ash leachates were analyzed for Cd and Pb before and after filtration through a 0.2-μm Millipore filter. No net change in concentration was obtained, suggesting that both elements were soluble and not associated with the solid phase.

High concentrations of Ca, Mg, Na, Cl, SO_4, and F were found in the ash residues, and similar levels have been documented elsewhere (*12*). This observation suggested that enhanced Cd and Pb mobility from the ash sources might be a result of displacement from soil exchange sites by cations such as Ca, Mg, and Na or possibly metal complexation by anions. Egozy (*13*) reported that Cd adsorption on Wyoming montmorillonite was very low in highly concentrated Cl solutions (>1 M) because of Cl complex formation. Adsorption was diminished further as pH was increased. Accordingly, Doner (*14*) found Cd mobility to be greater in soils in the presence of NaCl than in perchlorate solutions.

Columns prepared with Decatur soil and containing inorganic Cd, Ca, and Mg salts at concentrations equivalent to those in 400 g of fly ash from site A were leached with deionized H_2O. No Cd was detected in the leachate from incremental additions (150 mL) totaling 1200 mL (data not shown). However, leaching with a 1 M NaCl solution resulted in quantitative recovery of the applied Cd. Similar soil columns containing Cd, Ca, and Mg as well as 48 g of Cl as NaCl (amount based on 12% Cl content of the fly ash) were leached with H_2O. Again, over 90% of the applied Cd was displaced, supporting the metal Cl complexation theory. Other salts including $NaNO_3$, Na_2SO_4, and NaF were tested and found to be ineffective in promoting Cd movement through soil.

The distribution of dominant Cd, Pb, and other metal species in leachate from fly-ash-treated Decatur soil as computed by the GEOCHEM program is given in Table III. Of the metals detected in significant amounts in the solution, Cd and Pb exhibited greatest complexation by Cl; other metals were complexed by Cl to varying degrees. Sulfate and F complexation were relatively minor in all instances with the free metal ions accounting for the major portion of the metals not complexed by Cl. Behel et al. (*15*) found that Cd existed mainly in the free ion in solutions displaced from sewage-sludge-treated soil. However, the Cl content of the soil solution was less than 60 μg/mL, and the pH values of the solutions were less than 5.5, thus resulting in conditions unsuitable for metal Cl complex formation. Hahne and Kroontje (*16*) determined that MCl^+ species of Cd and Pb formed at Cl concentrations above 35 μg/mL and MCl_2 complexes at concentrations above 350 μg of Cl/mL. The MCl_3^- and MCl_4^{2-} species become important above 3500 μg of Cl/mL. In the present study, solution Cl concentrations were between 20 and 25 000 μg/mL with about 72% of the complexed metal being in the forms $CdCl^+$ and $CdCl_2$ and the remainder as $CdCl_3^-$ and $CdCl_4^{2-}$. The predominant Cl complex of Pb was the form $PbCl^+$ followed by $PbCl_2$, $PbCl_3^-$, and $PbCl_4^{2-}$.

Table III. Distribution (as Calculated by GEOCHEM) of Metals in Leachate from Decatur Soil Amended with Fly Ash from Incinerator Site A

		% of total			
			complexed by		
metal	total metal concn, μg/mL[a]	calcd free metal	Cl^-	SO_4^{2-}	F^-
Cd^{2+}	67.7	3.2	96.6	3.3	0.9
Pb^{2+}	3.9	11.4	87.7	0.7	0.1
Sr^{2+}	5.7	59.9	38.5	1.5	0.1
Ca^{2+}	4 300.0	64.7	33.0	2.0	0.3
Mg^{2+}	402.0	67.0	29.1	1.6	2.2
Ni^{2+}	0.8	72.6	24.6	2.2	0.5
Na^+	13 883.0	84.3	14.2	1.5	
Zn^{2+}	284.7	84.4	11.5	3.3	0.9
Mn^{2+}	465.7	87.3	10.0	2.7	
Ba^{2+}	9.7	87.2	10.0	2.7	0.1
K^+	23 667.0	89.2	9.5	1.3	
Cr^{3+}	0.8	0.4	0.2		94.8
Al^{3+}	4.3				100.0

[a] Measured average from three replicated soil columns.

Dry matter production of sericea lespedeza over two seasons in the rhizotron-lysimeter totaled 1.49, 1.31, and 1.15 kg when grown on the untreated, bottom-ash-treated, and fly-ash-treated soil, respectively. Corresponding uptake of Cd was 0.61, 0.55, and 4.24 mg and of Pb was 7.90, 7.22, and 10.89 mg. Although much of the Cd and Pb was present in an acetic acid soluble form in both fly and finely ground bottom ashes, plant availability was considerably greater from the former due likely to the smaller particle size, and, hence, greater reactivity. It is unlikely that landfilling of bottom ashes, especially if deposited as large clinker-type aggregates, would constitute a hazard to covering vegetation.

Plant Uptake of Metals from Soil-Applied Ashes. Surface application of preleached bottom ash resulted in dry matter production of corn similar to that where ash residues were not applied (Table IV). Mixing bottom ash (not leached) with soil resulted in extreme toxicity, while the same material layered at middepth was less damaging but still quite toxic. Leached fly ash reduced dry matter production when surface applied; however, mixed and middepth placements resulted in complete kill. Concentrations of Cd and Pb were highest from mixed bottom ash, whereas surface applications of bottom and fly ashes resulted in lower concentrations but greatest uptake because of higher yields. Soil pH level had no influence on dry matter production or metal uptake.

Cumulative dry weight yields of Swiss chard were slightly higher at an initial soil pH of 6.5 than at 5.5 (Table V). Furthermore, chard displayed a significant positive growth response to bottom ash treatment regardless of

Table IV. Dry Weights of Corn and Concentrations of Cd and Pb as Affected by Soil pH and Type and Placement of Incinerator Ashes

soil pH	type of ash	ash placement[a]	dry wt, g/pot	concn in corn plants, μg/g Cd	concn in corn plants, μg/g Pb	uptake, μg/pot Cd	uptake, μg/pot Pb
5.5	none		15.1	0.92	4.79	14	72
	bottom	surface	15.0	2.83	10.96	42	164
		center layer	5.5	8.84	8.25	49	45
		mixed	0.6	19.31	30.71	12	18
	fly	surface	10.8	2.09	15.46	23	167
		center layer	*b*				
		mixed	*b*				
6.5	none		15.1	0.92	6.09	14	92
	bottom	surface	13.0	2.75	12.75	36	166
		center layer	2.8	7.51	8.27	21	21
		mixed	0.8	29.41	21.75	24	17
	fly	surface	9.4	2.13	17.59	20	165
		center layer	*b*				
		mixed	*b*				
		$S_{\bar{x}}$	(1.1)	(1.81)	(1.62)	(2)	(12)

[a] Only ashes for surface application were leached with deionized H_2O prior to use. [b] Seed germinated but plants did not survive.

Table V. Cumulative Dry Weights of Swiss Chard as Affected by Soil pH and Type and Placement of Incinerator Ashes

soil pH	type of ash	ash placement[a]	dry weight/clipping, g/pot 1	2	3	4	5	total
5.5	none		3.8	5.1	4.1	4.8	5.8	23.6
	bottom	surface	4.9	9.0	8.3	8.5	6.8	37.5
		center layer	1.4	1.7	4.5	16.9	12.2	36.7
		mixed	1.5	2.1	5.0	16.8	12.5	37.9
	fly	surface	3.0	7.2	8.1	10.7	6.7	35.7
		center layer	*b*					
		mixed	*b*					
6.5	none		4.1	7.4	7.1	6.3	5.4	30.3
	bottom	surface	4.6	9.8	9.5	9.2	7.3	40.4
		center layer	1.7	2.5	7.0	19.0	13.7	43.9
		mixed	1.2	1.8	3.9	18.0	13.7	38.6
	fly	surface	3.5	7.9	7.6	11.8	7.6	38.4
		center layer	*b*					
		mixed	*b*					
		$S_{\bar{x}}$	(0.3)	(0.6)	(0.5)	(0.9)	(0.6)	(0.4)

[a] Only ashes for surface application were leached with deionized H_2O prior to use. [b] Seed germinated but plants did not survive.

Table VI. Concentration of Cd in Swiss Chard as Affected by Soil pH and Type and Placement of Incinerator Ashes

soil pH	type of ash	ash placement[a]	Cd concentration/clipping, μg/g 1	2	3	4	5	total
5.5	none		2.3 (9)[b]	3.0 (15)	3.5 (14)	3.2 (15)	1.8 (10)	(63)
	bottom	surface	5.0 (25)	3.5 (32)	6.8 (56)	13.7 (116)	18.7 (127)	(356)
		center layer	44.4 (62)	46.4 (79)	37.6 (169)	21.8 (368)	23.4 (286)	(964)
		mixed	42.6 (64)	44.1 (93)	35.8 (179)	26.5 (445)	36.1 (451)	(1232)
	fly	surface	5.1 (15)	5.1 (37)	7.0 (57)	10.9 (117)	18.6 (125)	(336)
6.5	none		1.9 (8)	1.8 (13)	1.6 (11)	1.7 (11)	1.4 (8)	(51)
	bottom	surface	3.6 (17)	3.2 (31)	6.7 (64)	16.8 (155)	19.9 (145)	(412)
		center layer	17.7 (29)	23.2 (58)	20.5 (144)	14.8 (281)	16.3 (223)	(735)
		mixed	44.3 (53)	43.5 (78)	30.1 (117)	22.5 (405)	34.1 (467)	(1120)
	fly	surface	4.0 (14)	4.4 (35)	6.8 (52)	8.8 (104)	15.2 (116)	(321)
		$S_{\bar{x}}$	3.4 (4)	3.5 (6)	2.5 (16)	1.5 (30)	2.1 (30)	(11)

[a] Only ashes for surface application were leached with deionized H_2O prior to use. [b] Values in parentheses represent Cd uptake in μg/pot.

placement in clippings 4 and 5, resulting in higher total yields than from the untreated pots; a similar response occurred with the preleached fly ash applied to the soil surface. This response was possibly due to one or more essential micronutrients present in the ash such as Zn, Fe, or Mn or to the increase in soil pH (Table IX).

In general, Cd uptake by chard was slightly lower at pH 6.5 than at pH 5.5 (Table VI). Concentrations of Cd from mixed bottom ash application were equal to or higher than concentrations from middepth placement; accordingly, Cd uptake was also greater with mixed placement. Surface application of ash resulted in much lower Cd concentrations, probably as a result of preleaching, which removed a significant amount of soluble Cd.

Contrasting results were obtained for Pb in that concentration and uptake were highest with surface applica-

Table VII. Concentration of Pb in Swiss Chard as Affected by Soil pH and Type and Placement of Incinerator Ashes

			Pb concentration/clipping, $\mu g/g$					
soil pH	type of ash	ash placement[a]	1	2	3	4	5	total
5.5	none		11.8 (45)[b]	9.0 (46)	7.9 (32)	7.8 (37)	6.4 (37)	(197)
	bottom	surface	23.1 (113)	12.0 (108)	10.1 (84)	11.3 (96)	17.6 (120)	(521)
		center layer	13.1 (18)	9.7 (17)	7.7 (35)	7.8 (132)	8.2 (100)	(302)
		mixed	21.2 (32)	11.6 (24)	10.4 (52)	8.3 (139)	11.3 (141)	(388)
	fly	surface	17.6 (53)	21.1 (152)	16.3 (132)	21.6 (231)	39.8 (267)	(835)
6.5	none		12.0 (49)	8.0 (59)	7.2 (51)	6.9 (44)	7.5 (41)	(244)
	bottom	surface	29.6 (136)	10.4 (102)	8.8 (84)	14.2 (130)	19.1 (139)	(591)
		center layer	15.9 (27)	9.0 (23)	7.4 (52)	7.8 (149)	9.8 (135)	(396)
		mixed	18.7 (22)	11.3 (20)	9.8 (38)	9.3 (167)	9.6 (132)	(379)
	fly	surface	24.8 (87)	13.9 (110)	16.1 (123)	18.4 (217)	30.8 (234)	(771)
		$S_{\bar{x}}$	1.3 (8)	0.9 (11)	0.7 (6)	0.9 (12)	2.0 (13)	(5)

[a] Only ashes for surface application were leached with deionized H_2O prior to use. [b] Values in parentheses represent Pb uptake in μg/pot.

Table VIII. Concentration of Several Elements in Corn and Swiss Chard as Affected by Soil pH and Type and Placement of Ash

			corn, $\mu g/g$				chard, cutting no. 1, $\mu g/g$			
soil pH	type of ash	ash placement[a]	Zn	Ni	Na	Mn	Zn	Ni	Na	Mn
5.5	none		23	2.2	245	93	68	4.8	4 838	900
	bottom	surface	83	3.2	394	75	114	4.0	45 125	355
		center layer	104	2.7	10 263	241	113	2.7	50 333	2 080
		mixed	66	0.9	4 494	49	259	4.6	45 042	52
	fly	surface	100	3.3	357	72	114	3.7	44 292	348
6.5	none		20	1.8	267	60	48	4.0	4 900	300
	bottom	surface	82	3.0	480	68	107	3.5	38 542	130
		center layer	130	2.4	22 163	181	101	4.3	53 188	449
		mixed	63	0.6	4 087	10	165	2.7	48 750	37
	fly	surface	98	2.5	318	71	111	3.6	44 458	156
		$S_{\bar{x}}$	10	0.2	3 814	123	7	0.2	1 221	13

[a] Only ashes for surface application were leached with deionized H_2O prior to use.

Table IX. Soil-Extractable Metals ($\mu g/g$ of Soil) as Affected by Soil pH and Type of Incinerator Ash

			extractant					
			H_2O			1 N HCl		
pretreatment soil pH	type of ash	postharvest soil pH	Cd	Pb	Zn	Cd	Pb	Zn
5.5	none	5.2	ND[a]	ND	ND	0.13	7.3	2.7
	bottom	7.6	0.14	0.53	0.24	19.3	98	2083
	fly	7.2	9.85	1.50	47.5	68.9	365	6475
6.5	none	6.2	ND	ND	ND	0.18	8.6	3.9
	bottom	7.6	0.14	0.43	ND	23.2	106	2483
	fly	7.1	8.74	1.52	43.2	58.5	318	5367

[a] ND = not detected in extract.

tion, especially from fly ash (Table VII). Although previous characterization of the ashes indicated little Pb removal by hot H_2O extraction, it is possible that the shallow root system associated with chard was able to extract sufficient Pb from the surface ash layer to explain these findings.

Concentrations of several other elements in corn and the first cutting of chard are shown in Table VIII. Only Na and possibly Mn were present at levels that would be considered excessive, especially in chard, which is an accumulator of most metals. Highest concentrations of Zn, Na, and Mn in corn and Na and Mn in chard were associated with the middepth placement. As with Cd, liming the soil to pH 6.5 reduced concentrations of Zn and Mn in the chard. Results suggest that the mode of ash toxicity to plants may be attributed to a cumulative effect from soluble salts rather than to a particular element.

Soil extraction of metals from mixed ash treatments after crop harvest corroborate earlier results that indicated that Cd was more soluble than Pb in the fly ash (Table IX). Whereas the amount of H_2O-soluble Pb as a percentage of the 1 N HCl fraction was similar in bottom and fly ashes, the H_2O-soluble Cd and Zn contents were much greater in the fly ash residue. Soil pH was increased markedly by ash application, especially from bottom ash. After harvest, soil pH values were 7.6 and 7.1 (from bottom and fly ashes, respectively), despite the pH differentials established prior to treatment (pH 5.5 and 6.5).

These data give preliminary indication that land application of some ash residues (especially fly ash) arising from combustion of muncipal refuse may constitute a hazard to the H_2O supply as well as to vegetation. It is clear that special treatment such as diluting fly ash in a large volume of bottom ash is necessary to meet EPA landfill requirements. However, onsite wells should be monitored to ensure that this practice effectively minimizes leachate migration. Although phytotoxicity is reduced after the ashes have been leached, uptake of Cd and Pb remains significantly high and may pose a danger if vegetation grown on these landfills should enter the food chain. Since some incineration processes appear to yield ash residues containing higher total and extractable concentrations of toxic metals than others, methods of attenuation should be developed to prevent soil and H_2O contamination. Such information would be of wide interest, since energy-recovery systems utilizing refuse are operating or planned for several locations in the United States.

Acknowledgments

We thank J. C. Duggan and M. N. Jarrett, Division of Energy Demonstrations and Technology, for their assistance in obtaining ash samples and valuable suggestions throughout the investigation. Appreciation is also extended to R. M. Scheib and D. J. Ray, Division of Chemical Development, for performing the optical analyses of ash and leachate samples.

Registry No. Cd, 7440-43-9; Pb, 7439-92-1; Sr, 7440-24-6; Ca, 7440-70-2; Mg, 7439-95-4; Ni, 7440-02-0; Na, 7440-23-5; Zn, 7440-66-6; Mn, 7439-96-5; Ba, 7440-39-3; K, 7440-09-7; Cr, 7440-47-3; Al, 7429-90-5.

Literature Cited

(1) Freeman, H. *Environ. Sci. Technol.* **1978**, *12*, 1252–56.
(2) Law, S. L. *Resource Recovery Conserv.* **1978**, *3*, 19–39.
(3) Environmental Protection Agency, *Fed. Regist.* Dec 18 **1978**, Part IV, Hazardous Waste.
(4) Mattigod, S. V.; Sposito, G. In "Chemical Modeling in Aqueous Systems"; Jenne, E. A., Ed. American Chemical Society: Washington, DC, 1979, ACS Symp. Ser. 93, pp 837–56.
(5) Soileau, J. M.; Mays, D. A.; Khasawneh, F. E.; Kilmer, V. J. *Agron. J.* **1974**, *66*, 828–32.
(6) Golembiewski, M. A.; Ananth, K. P.; Sutikno, T.; Freeman, H. M. U.S. EPA Project Summary 600/PS7-80-149, 1980.
(7) Law, S. L.; Gordon, G. E. *Environ. Sci. Technol.* **1979**, *13*, 432–38.
(8) Gunther, C. *Waste Age.* **1981**, 66–68.
(9) Giordano, P. M.; Mortvedt, J. *J. Environ. Qual.* **1976**, *5*, 165–68.
(10) Taylor, R. W.; Griffin, G. F.; *Plant Soil.* **1981**, *62*, 147–52.
(11) Hulett, L. D.; Weinberger, A. J.; Northcutt, K. J.; Ferguson, M. *Science (Washington, D.C.)* **1980**, *210*, 1356–58.
(12) Greenberg, R. R.; Gordon, G. E.; Zoller, W. H.; Jacko, R. B.; Neuendorf, D. W.; Yost, K. J. *Environ. Sci. Technol.* **1978**, *12*, 1329–32.
(13) Egozy, Y. *Clays Clay Miner.* **1980**, *28*, 311–18.
(14) Doner, H. E. *Soil Sci. Soc. Am. J.* **1978**, *42*, 882–85.
(15) Behel, A. D., Jr.; Nelson, D. W.; Sommers, L. E. *J. Environ. Qual.*, in press.
(16) Hahne, H. C. H.; Koontje, W. *J. Environ. Qual.* **1973**, *2*, 444–50.

Received for review April 21, 1982. Revised manuscript received August 30, 1982. Accepted December 16, 1982.

Environ. Sci. Technol. **1983**, *17*, 198–202

1-Nitropyrene Concentration and Bacterial Mutagenicity in On-Road Vehicle Particulate Emissions

Robert A. Gorse, Jr.,* Timothy L. Riley, Fred C. Ferris, Anna M. Pero, and Loretta M. Skewes

Ford Motor Company, Engineering and Research Staff—Research, Dearborn, Michigan 48121

■ 1-Nitropyrene (1NP) has been detected in the particulate emissions from on-road vehicles during an experiment conducted at the Allegheny Mountain Tunnel on the Pennsylvania Turnpike. 1NP emission rates and mutagenicities (Ames activities) of the emissions were determined for heavy-duty diesel trucks and for light-duty spark-ignition vehicles. The 1NP concentrations in the particulate extracts and also the 1NP emission rates are lower than would be predicted on the basis of laboratory dilution tunnel measurements either for diesels or for spark-ignition vehicles. 1NP accounts for very little of the on-road mutagenicity—indicating that other, unidentified, direct-acting mutagens are responsible for on-road vehicular exhaust mutagenicities. Recovery of 1NP from diesel particulate material appears to be independent of 1NP concentration and filter storage time at −80 °C prior to extraction.

It has been reported that organic solvent extracts of diesel and spark-ignition vehicle exhaust particulate material (*1, 2*) as well as of urban atmosphere particulate material (*3, 4*) contain direct-acting mutagens—i.e., bacterial mutagens that do not require the addition of metabolic activating enzymes to show mutagenicity—as shown in bioassays such as the Ames test using *Salmonella typhimurium* bacteria. Indirect-acting bacterial mutagens (*5*) such as benzo[*a*]pyrene and other polynuclear aromatic hydrocarbons (PAH) have long been known to be present in automobile exhaust (*6, 7*). There has been a large effort in the past few years to identify the compounds in vehicular and atmospheric particulate extracts responsible for the direct-acting bacterial mutagenicity (*1, 2, 8–12*).

Previous work in this laboratory resulted in the detection of 1-nitropyrene (1NP), a potent direct-acting bacterial mutagen, in dilution-tunnel-generated samples of light-duty diesel exhaust particulate extracts (*10, 13, 14*). Subsequently the presence of over 50 nitro-PAH compounds has been indicated by various laboratories in dilution-tunnel-generated light-duty diesel particulate extracts (*15–25*); 1NP has also been detected in spark-ignition engine particulate extracts (*22, 23*). Some studies have reported evidence of nitro-PAH compounds in urban atmosphere particulate extracts (*26–28*).

Many factors remain to be evaluated in assessing the importance of nitro-PAH to health-related issues. One crucial factor is whether on-road vehicles emit nitro-PAH at rates comparable to those measured for laboratory vehicles. To date, all observations of nitro-PAH in vehicle particulate extracts have resulted from laboratory dilution tunnel studies. The 1NP concentrations reported in light-duty diesel particulate extracts range from 25 to 2000 ppm depending on the vehicle, implying a passenger-diesel fleet average of 100–200 ppm. For some of these diesels, 1NP is reported to account for up to 25% of the total direct-acting bacterial mutagenicity (*Salmonella* strains TA98, TA100, and TA1538, these strains being the most active to vehicle particulate extracts). A study on a single heavy-duty diesel has yielded 5.1 ppm 1NP in the extract

0013-936X/83/0917-0198$01.50/0

(*24*); this would account for ~1% of the direct TA98 mutagenicity of the extract.

It is not clear how seriously the foregoing results could have been affected by nitro-PAH formed during the particulate sampling via nitration of filter-collected PAH—the so-called artifact formation of nitro-PAH (*24, 29–32*). It is generally agreed that artifact formation can occur, but the relative amounts of nitro-PAH formed in the combustion process, in the vehicle exhaust system, during the dilution process, or during particulate sampling are still unknown.

Here we report the first measurements of 1NP in particulate emissions from on-highway heavy-duty diesel and light-duty spark-ignition vehicles. Concurrently we have measured the Ames assay mutagenicities of the on-road particulate emissions from these vehicle categories, using strains TA98 and TA100.

Experimental Section

The study was performed during July 22–28, 1981, at the Allegheny Mountain Tunnel on the Pennsylvania Turnpike. The methods for particulate sampling and determination of emission factors have been described previously (*33–36*). Briefly, the air in the tunnel exit portal (two traffic lanes, eastbound tube) and the air in the tunnel supply fan rooms was sampled on Hi-Vol Teflon-coated glass fiber filters (Pallflex TX40HI20) at 0.8–1.7 m^3/min flow rate over 5.8–11.8-h periods that differed in the distribution of light-duty spark-ignition and heavy-duty diesel traffic (37–92% spark-ignition vehicles). These two vehicle categories account for >96% of the traffic volume. The ten periods resulted in 8.0×10^4 accumulated vehicle kilometers in the 1.85-km tunnel at an average speed of 84 km/h. Vehicles travelling through the tunnel are subject to an average tailwind of 5.4 m/s and an average road grade of −0.5%. Under these conditions the vehicles have a power requirement that corresponds to a no-wind, no-grade vehicle speed of ~61 km/h. The 61 km/h effective speed should be used in comparison of the on-road results with studies performed under other vehicle operating conditions.

Traffic was counted with a road-tube axle counter and visual counting of the distribution of vehicle types. The collected filters were sealed immediately and stored in the dark at −80 °C. After 1.5–3.5 months at −80 °C they were weighed and extracted in a Soxhlet apparatus with dichloromethane (DCM) for 18 h. The extract was rotary evaporated to 10-mL volume, blown to dryness under a stream of dry N_2, weighed, and redissolved in DCM, after which an aliquot was removed for Ames analysis. The remaining extract was doped with 600 ng of perdeuterio-1NP (1NP-d_9) (*37*) and fractionated by using preparative-scale normal-phase high-performance liquid chromatography (HPLC). The isolated 1NP fraction (blown to dryness, dissolved in 100 μL of DCM, and spiked with 500 ng of dibenzothiophene (DBT)) was then analyzed with a capillary gas chromatograph–mass spectrometer (GC/MS). The GC/MS retention time of 1NP and the response of characteristic ions of 1NP were used for 1NP quantitation vs. the internal standard 1NP-d_9 (corrections were made for the 0.8% 1NP impurity in the 1NP-d_9). The 1NP-d_9 was quantified relative to the internal standard DBT. Ames assays using strains TA98 and TA100, without the addition of the metabolic activation S9 mix, were performed on dimethyl sulfoxide (Me_2SO) solutions of the extracts in accordance with the Ames procedure (*38*), with additional precautions as described previously (*10, 14*). The samples were analyzed in four batches with controls (2-nitrofluorene (TA98) or sodium azide (TA100)) and with overlapping samples from the other batches. The slope of the dose–response curve was determined by linear regression analysis of the revertants/plate vs. the extract dose/plate for duplicate plates at six doses, including the blank controls in the absence of sample extract. Dose–response curves were linear over the range of doses analyzed (0–320 μg of extract/plate).

HPLC analysis was performed on a Varian 5060 HPLC with a Vista 401 data system using a 10-μm Waters μPorasil 7.8 × 300 mm column and 254-nm UV absorption (Perkin-Elmer Model LC-75) and 254-nm excitation/320-nm emission cutoff (Schoeffel Model FS970) fluorescence detectors. Solvent flow (4.5 mL/min) started with 100% hexane, at 5 min a linear gradient with DCM to 5% DCM at 10 min, a linear gradient to 100% DCM at 35 min, at 45 min a linear gradient with acetonitrile (ACN) to 100% ACN at 50 min, a step change to 100% DCM at 70 min, and a step change to 100% hexane at 80 min. Sample HPLC fractionation was preceded by HPLC of a standard containing 1NP-d_9 and then a blank solvent analysis. The sample 1NP was isolated by collecting the sample eluent during the 10-min period centered on the 1NP-d_9 elution time determined in the standard analysis.

GC/MS analysis was performed on a VG MM-16 MS interfaced to a Perkin-Elmer Model 910 GC and an INCOS 2000 data system using on-column injection (0.25 mm i.d. × 30 m SE-54 fused silica column (J & W Scientific)) with the column directly connected to the MS source. Temperature programming was from room temperature to 170 °C in 30 s and then 5 °C/min to 270 °C with a hold at 270 °C for 15 min. Helium at 40 cm/s linear velocity was used as a carrier gas. Electron impact ionization was used with positive ion detection. A magnet scan rate of 3.3 s/cycle from 450 to 80 amu was used.

The on-road emission factors were calculated by taking the tunnel minus the intake μg/m^3, multiplying by the total m^3 of air passing through the tunnel, and dividing by the total number of vehicle kilometers through the tunnel in each of the ten sampling periods. The resultant emission rates per total vehicle kilometer were then subjected to linear regression against the percentage of spark-ignition vehicles. The heavy-duty diesel emission rate equals the emission value at 0% spark-ignition vehicles, and the light-duty spark-ignition emission rate equals the values at 100% spark-ignition vehicles. This analysis procedure is valid for any emission component such as total particulate, soluble organic fraction, 1NP, or Ames activity.

From the diesel emission rates of 1NP and extractable material determined by linear regression as described above, the diesel 1NP can be expressed as ppm of the extractable diesel particulate matter. The same applies for 1NP and extractable material from spark-ignition vehicles. Similarly, Ames results can be expressed as revertants per microgram of extractable material for each vehicle type separately.

Results

The derived emission rates and mutagenicities of the particulate emissions from heavy-duty diesels and light-duty spark-ignition vehicles at Allegheny are listed in Table I. The total particulate material, soluble organic fraction and Ames activity results are each comparable to our 1979 Allegheny results and to dilution-tunnel-derived values of these parameters (*35*). However, the 1NP emission rates at Allegheny are significantly lower than have been observed in dilution-tunnel studies of either diesels or spark-ignition vehicles. The concentration (ppm) of 1NP in the extractable diesel particulate material at

Table I. On-Road Emission Factors

component	diesel[a]	spark ignition[b]	r[c]
total particulate material, mg/km	900 ± 30	20 ± 20	−0.99
soluble organic fraction, mg/km	230 ± 7	6 ± 4	−0.99
1-nitropyrene, μg/km	0.49 ± 0.06	$\leqslant$0.03[d]	−0.94
1-nitropyrene, ppm[e]	2.1	$\leqslant$5[d]	
Ames, TA98, −S9, rev/km[f]	(0.8 ± 0.1) × 10^5	(1.5 ± 0.6) × 10^4	−0.80
Ames, TA100, −S9, rev/km[f]	(1.9 ± 0.4) × 10^5	(5 ± 2) × 10^4	−0.67

[a] Predominantly heavy-duty diesel trucks, 26 metric tons average gross vehicle weight. [b] Predominantly light-duty passenger cars, ~74% catalyst-equipped (according to Turnpike fuel sales). [c] Correlation coefficient from linear regression of emission component per kilometer against percentage of gasoline vehicles for each of the ten periods. [d] Upper limit is calculated as best estimate plus 1 standard deviation. [e] Parts per million, by mass, of the extracted particulate matter; calculated from the 1NP and soluble organic fraction emission rates. [f] (Revertants/μg of extract) × (μg of extract/km).

Allegheny is 2.5 times lower than the one available dilution-tunnel result on heavy-duty diesels and up to 2 orders of magnitude lower than has been observed in dilution-tunnel samples of light-duty diesel particulate extracts. The observed on-road emission rates of 1NP account for only 0.4% and 1.3% of the direct-acting TA98 mutagenicity of the spark-ignition and diesel particulate extracts, respectively. In the case of TA100 the respective percentages are only 0.02% and 0.08%. (The Ames activity of extensively purified 1NP in this laboratory is typically ~2000 revertants/μg for TA98, − S9, and ~300 revertants/μg for TA100, − S9; these activities have been used to calculate the contribution of the on-road 1NP to the observed Ames activities by using the data in Table I.)

Looking at the individual Allegheny runs rather than the regression results, we find that the 1NP concentrations in the tunnel particulate extracts were near the ~1 ppm detection limit, ranging from below the limit to a maximum of 3 ppm. The corresponding 1NP concentrations in the tunnel air ranged between <0.04 and 0.12 ng/m^3. Corrections for the concentrations in the tunnel intake air ranged from 3% to 25% of the tunnel 1NP concentrations. Ames assay activities of the extracts varied (as a result of the varying traffic conditions) between 0.3 and 0.9 revertants/μg of extract (15–30 revertants/m^3 of tunnel air) for TA98 and between 0.8 and 2.4 revertants/μg of extract (33–85 revertants/m^3 of tunnel air) for TA100. Corrections for the Ames assay activities of the intake air ranged from 4% to 21% of the tunnel extract activity.

The 1.5–3.5-month interval at −80 °C between sample collection and extraction raises the question of chemical stability during storage. Accordingly, a series of experiments were conducted on a large filter sample of light-duty diesel exhaust particulate matter collected from a dilution tunnel. The filter was divided into 16 equal sections, and a known amount of 1NP-d_9 was added to each. Three concentration levels of 1NP-d_9 were examined, viz., approximately 3.5, 7.0, and 35 ppm in the particulate extract. The filter sections were then stored at −80 °C for periods of 1, 15, 42, and 91 days prior to extraction and analysis. Filter type, storage, extraction, and analytical procedures were the same as those used with the Allegheny samples. (The indicated 1NP-d_9 recoveries for the 3.5 ppm level were 119%, 126%, 115%, and 136%, for the 7 ppm level were 68%, 63%, 67%, and 103% (average of duplicate samples), and for the 35 ppm level were 91%, 97%, 91%, and 80%, for the respective storage times of 1, 15, 42, and 91 days. The mean recovery was 95 ± 26% with no indication of trends with storage time. We therefore conclude that sample storage time was not a factor in the Allegheny results.

Discussion

The difference between on-road and dilution-tunnel 1NP emissions (for example, 2.1 ppm on-road vs. 5.1–2000 ppm in dilution tunnels in the case of diesels, or ≤5 ppm on-road vs. 10–17 ppm in dilution tunnels in the case of light-duty spark-ignition vehicles) requires the comment that there are several differences between the on-road and laboratory conditions. There are differences in vehicle driving mode and in diesel engine design, though not in spark-ignition engine design. The limited published information relating to the question of driving mode dependence of 1NP emissions suggests that driving mode may not be important. Average emission rates of 1NP from two light-duty diesels were 4.6 μg/km on the urban driving cycle (FTP) and 4.2 μg/km on the highway fuel economy test (HWFET) (*22*). Emission rates of 1NP from 20 light-duty spark-ignition vehicles (*22*) on the FTP, HWFET, and other driving cycles showed no consistent pattern with driving cycle.

As for engine design, the on-road diesel values in Table I pertain to heavy-duty diesel trucks with direct-injection engines (mostly 4-stroke), whereas the laboratory measurements pertain to indirect-injection (prechamber) 4-stroke engines, light duty in all cases but one. Benzo[*a*]pyrene and NO$_2$ data obtained by Baines et al. (*39*) suggest that the difference between direct injection and indirect injection may not be important for 1NP formation. However, one limited comparison (*24*) does leave open the possibility of some other difference(s) between light- and heavy-duty diesels that could cause lower 1NP emissions from the latter. There would still be difficulty in reconciling the on-road results with light-duty diesel dilution-tunnel measurements. That is, the *aggregate* 1NP found at Allegheny is barely what would be expected from the light-duty diesels alone (2.8% of the light-duty vehicle traffic) even if one ignored the fact that the 1NP correlation is with the heavy-duty diesels rather than with the light-duty traffic (Table I) and arbitrarily assigned all of the on-road 1NP to the light-duty diesels. Specifically, the extreme upper limit given by this procedure is <4 μg/km, vs. ~5–10 μg/km for dilution-tunnel measurements of light-duty diesels.

Other possible effects might be considered. In the on-road study the vehicle exhaust stream is diluted by a factor of ~10^3 within the first few seconds after leaving the tailpipe, with average tunnel residence times of ~2.5 min, sample collection times of 73–256 min, and an average temperature of 19 °C; in the laboratory studies typical dilution ratios are between 5:1 and 20:1 with dilution-tunnel residence times of a few seconds, sample collection times of 23–92 minutes, filter flow rates of 2.5–3.0 m^3/min, and average temperatures of ~35 °C. Neutralization by ammonia could be a factor; if 1NP arises from classical aromatic ring nitration by H_2SO_4-mediated HNO_3 attack, then neutralization by ammonia should be more important on-road than in dilution tunnels. Aqueous extracts of the Allegheny samples were essentially pH neutral, whereas the H_2SO_4 emitted in dilution tunnels by diesels remains mostly unneutralized (*40*).

Among the above-noted differences, one that might be expected to affect 1NP emissions is the dilution difference. As a consequence of the high on-road dilution ratio, the NO_2 concentration at Allegheny (0.04–0.16 ppm average during the ten sampling periods) is much lower than is typical of dilution-tunnel studies (2–4 ppm NO_2 in the diluted exhaust). Classical nitration of aromatic compounds is kinetically first order in the nitrating agent (*41*), which in the case of vehicle exhaust is presumed to be HNO_3 or other reactants related to NO_2.

It is difficult to assess which of the effects discussed accounts for the difference in the observed on-road and dilution tunnel 1NP emission rates. However, the data do suggest that this difference cannot be entirely accounted for in terms of differences between heavy-duty and light-duty diesel systems. Furthermore, the observations appear consistent with the hypothesis that (a) low NO_2 (or other nitrating agent) concentrations result in decreased PAH nitration rates and (b) the formation of nitro-PAH in dilution tunnel experiments takes place mostly after the exhaust leaves the tailpipe. Further work is needed to explore the validity of this hypothesis. Experiments are in progress to evaluate the artifact formation of 1NP and the role of artifact formation relative to other modes of 1NP formation in vehicle exhaust.

The small role of 1NP in the on-road direct-acting mutagenicity (0.02–1.3%) means that most of the mutagenicity must result from the emission of other, unidentified, direct-acting mutagenic compounds.

We have already mentioned that the on-road emissions are similar to dilution-tunnel results with respect to particulate mass, extractable fraction, and Ames activity. Experiments at Allegheny in 1979 (*35*) show that the similarity covers not only the foregoing properties but also particle size distribution, HPLC profile, and gas chromatographic molecular weight distribution. The present study suggests that the ability of the dilution tunnel to simulate the characteristics of particulate emissions does not necessarily hold when detailed properties are considered.

Acknowledgments

We appreciate helpful discussions with W. R. Pierson, D. Schuetzle, and I. Salmeen, assistance in the field work by W. R. Pierson, W. W. Brachaczek, A. C. Szkarlat, and S. M. Japar, the cooperation of the Pennsylvania Turnpike Commission, and especially the assistance and hospitality of John R. Foor and of the crews at Allegheny Tunnel supervised by the late Robert J. Hauger.

Registry No. 1-Nitropyrene, 5522-43-0.

Literature Cited

(1) Wang, Y. Y.; Rappaport, S. M.; Sawyer, R. F.; Talcott, R. E.; Wei, E. T. *Cancer Lett.* **1978**, *5*, 39–47.

(2) Huisingh, J.; Bradow, R.; Jungers, R.; Claxton, L.; Zweidinger, R.; Tejada, S.; Bumgarner, J.; Duffield, F.; Waters, M.; Simmon, V. F.; Hare, C.; Rodriquez, C.; Snow, L. In "Application of Short-Term Bioassays in the Fractionation and the Analysis of Complex Environmental Mixtures"; Waters, M. D., Nesnow, S., Huisingh, J. L., Sandhu, S. S., Claxton, L., Eds.; EPA-600/9-78-027; Plenum Press: New York, 1978.

(3) Pitts, J. N., Jr.; Grosjean, D.; Mischke, T. M.; Simmon, V. F.; Poole, D. *Toxicol. Lett.* **1977**, *1*, 65–70.

(4) Daisey, J. M.; Kneip, T. J.; Hawryluk, I.; Mukai, F. *Environ. Sci. Technol.* **1980**, *14*, 1487–1490.

(5) Ames, B. N.; McCann, J.; Yamasaki, E. *Mutat. Res.* **1975**, *31*, 347–364.

(6) Kotin, P.; Falk, H.; Mader, P.; Thomas, M. *AMA Arch. Ind. Health* **1954**, *9*, 153–163.

(7) Kotin, P.; Falk, H.; Thomas, M. *AMA Arch. Ind. Health* **1954**, *9*, 164–177.

(8) Pitts, J. N., Jr.; Van Cauwenberghe, K.; Grosjean, D.; Schmid, J. P.; Fitz, D. R.; Belser, W. L.; Knudson, G. B.; Hynds, P. M. *Science (Washington, D.C.)* **1978**, *202*, 515–519.

(9) Rappaport, S. M.; Wang, Y. Y.; Wei, E. T.; Sawyer, R. F.; Watkins, B. E.; Rapoport, H. *Environ. Sci. Technol.* **1980**, *14*, 1505–1509.

(10) Schuetzle, D.; Lee, F. S.-C.; Prater, T. J.; Tejada, S. B. *Int. J. Environ. Anal. Chem.* **1981**, *9*, 93–144.

(11) Yu, M.; Hites, R. A. *Anal. Chem.* **1981**, *53*, 951–959.

(12) Kraft, J.; Lies, K.-H. *SAE Tech. Pap. Ser.* **1981**, *No. 810082.*

(13) Salmeen, I.; Durisin, A. M.; Prater, T. J.; Riley, T.; Schuetzle, D. *Mutat. Res.* **1982**, *104*, 17–23.

(14) Salmeen, I.; Durisin, A. M. *Mutat. Res.* **1981**, *85*, 109–118.

(15) Riley, T.; Prater, T.; Schuetzle, D.; Harvey, T. M.; Hunt, D. *Anal. Chem.* **1982**, *54*, 265–271.

(16) Xu, S. B.; Nachtman, J. P.; Jin, Z. L.; Wei, E. T.; Rappaport, S.; Burlingame, A. L., presented at EPA 1981 Diesel Emissions Symposium, Raleigh, NC, Oct 1981.

(17) Henderson, T. R.; Sun, J. D.; Royer, R. E.; Clark, C. R.; Harvey, T. M.; Hunt, D. F.; Fulford, J. E.; Lovett, A. M.; Davidson, W. R., presented at EPA 1981 Diesel Emissions Symposium, Raleigh, NC, Oct 1981.

(18) Kohan, M.; Claxton, L., presented at EPA 1981 Diesel Emissions Symposium, Raleigh, NC, Oct 1981.

(19) Nishioka, M. G.; Petersen, B. A.; Lewtas, J., presented at EPA 1981 Diesel Emissions Symposium, Raleigh, NC, Oct 1981.

(20) Newton, D. L.; Erickson, M. D.; Tomer, K. B.; Pellizzari, E. G.; Gentry, P.; Zweidinger, R. B. *Environ. Sci. Technol.* **1982**, *16*, 206–213.

(21) Pederson, T. C.; Siak, J.-S., presented at EPA 1981 Diesel Emissions Symposium, Raleigh, NC, Oct 1981.

(22) Lang, J. M.; Carlson, R. A.; Snow, L.; Black, F. M.; Zweidinger, R. B.; Tejada, S. B., presented at EPA 1981 Diesel Emissions Symposium, Raleigh, NC, Oct 1981.

(23) Zweidinger, R. B., presented at EPA 1981 Diesel Emissions Symposium, Raleigh, NC, Oct 1981.

(24) Bradow, R. L.; Zweidinger, R. B.; Black, F. M.; Dietzman, H. M. *SAE Tech. Pap. Ser.* **1982**, *No. 820182.*

(25) Pitts, J. N., Jr.; Lokensgard, D. M.; Harger, W.; Fisher, T. S.; Mejia, V.; Schuler, J. J.; Scorziell, G. M.; Katzenstein, Y. A. *Mutat. Res.* **1982**, *103*, 241–249.

(26) Löfroth, G., presented at the second EPA Symposium on Application of Short-Term Bioassays in the Analysis of Complex Environmental Mixtures, Williambsurg, VA, Mar 1980.

(27) Wang, C. Y.; Lee, M.-S.; King, C. M.; Warner, P. O. *Chemosphere* **1980**, *9*, 83–87.

(28) Jager, J. *J. Chromatogr.* **1978**, *152*, 575–578.

(29) Clark, C. R.; Truex, T. J.; Lee, F. S.-C.; Salmeen, I. *Atmos. Environ.* **1981**, *15*, 397–402.

(30) Gorse, R. A., Jr.; Salmeen, I.; Clark, C. R. *Atmos. Environ.* **1982**, *16*, 1523–1528.

(31) Herr, J. D.; Dukovich, M.; Lestz, S. S.; Yergey, J. A.; Risby, T. H.; Tejada, S. B. *SAE Tech. Pap. Ser.* **1982**, *No. 820467.*

(32) Schuetzle, D. *EHP, Environ. Health Perspect.* **1983**, *47*, 65–80.

(33) Pierson, W. R.; Brachaczek, W. W. *SAE Tech. Pap. Ser.* **1976**, *No. 760039*; *SAE Trans.* **1976**, *85*, 209–227.

(34) Pierson, W. R.; Brachaczek, W. W.; Hammerle, R. H.; McKee, D. E.; Butler, J. W. *J. Air Pollut. Control Assoc.* **1978**, *28*, 123–132.

(35) Pierson, W. R.; Gorse, R. A., Jr.; Szkarlat, A. C.; Brachaczek, W. W.; Japar, S. M.; Lee, F. S.-C.; Zweidinger, R. B.; Claxton, L. D. *Environ. Sci. Technol.* **1983**, *17*, 31–44.

(36) Gorse, R. A., Jr.; Norbeck, J. M. *J. Air Pollut. Control Assoc.* **1981**, *31*, 1094–1096.

Environ. Sci. Technol. **1983**, *17*, 202-211

(37) Schuetzle, D.; Riley, T. L.; Prater, T. J.; Salmeen, I.; Harvey, T. M. In "Analytical Techniques in Environmental Chemistry II"; Albaiges, J., Ed.; Pergamon: Oxford, 1982; pp 259–280.
(38) Ames, B. N.; Durston, W. E.; Yamasaki, E.; Lee, F. D. *Proc. Natl. Acad. Sci. U.S.A.* **1973**, *70*, 2281–2285.
(39) Baines, T. M.; Somers, J. H.; Hellman, K. H. *J. Air Pollut. Control Assoc.* **1982**, *32*, 725–728.
(40) Truex, T. J.; Pierson, W. R.; McKee, D. E. *Environ. Sci. Technol.* **1980**, *14*, 1118–1121.
(41) Frost, A. A.; Pearson, R. G. "Kinetics and Mechanism"; Wiley: New York, 1953; pp 297–309.

Received for review August 30, 1982. Accepted December 13, 1982.

Reaction Pathways of Trihalomethane Formation from the Halogenation of Dihydroxyaromatic Model Compounds for Humic Acid

Scott D. Boyce*

Department of Environmental Engineering Science, W. M. Keck Laboratories, California Institute of Technology, Pasadena, California 91125

James F. Hornig

Department of Chemistry, Dartmouth College, Hanover, New Hampshire 03755

■ The halogenation reactions of 1,3-dihydroxyaromatic compounds and simple methyl ketones in dilute aqueous solution have been investigated in order to elucidate the mechanism of analogous processes involving naturally occurring humic material. The 1,3-dihydroxyaromatic model compounds were most reactive with maximum yields of $CHCl_3$ (>90%) and $CHBr_3$ (>70%) at pH 8–10 with substrate concentrations of 10^{-5} M and halogen concentrations of 10^{-5}–10^{-4} M. At high chlorine concentrations, substantial yields of a variety of Cl-substituted carboxylic acids were detected, whereas at low $[Cl_2]$ values, a number of important polyhalogenated reaction intermediates were identified. Halogenation of resorcinol-2-^{13}C produced $^{13}CHCl_3$ and $^{13}CHBr_3$ with isotopic enrichments equivalent to that of the labeled precursor. The experimental data are generally consistent with a dominant haloform-type reaction mechanism, but some details of these results strongly suggest that several competitive pathways are also involved.

Introduction

The formation of trihalomethanes (THM's) during disinfection with chlorine is emerging as a persistent problem associated with the maintenance of potable water quality. The widespread occurrence of haloform pollutants suggests that naturally occurring humic substances constitute the dominant organic precursor of THM's (*1*). Numerous investigators have demonstrated that chlorination of fulvic and humic acids in aqueous solution produces chloroform, $CHCl_3$ (*2–10*). The corresponding Br-substituted products, $CHBrCl_2$, $CHBr_2Cl$, and $CHBr_3$, are generally thought to result from parallel bromination reactions initiated by the action of chlorine on background concentrations of bromide ion, dissolved in most natural waters (*11, 12*).

$$HOCl + Br^- \rightleftharpoons HOBr + Cl^- \qquad (1)$$

Because the structure of aquatic humic material is very complex, much research has focused on the reaction of chlorine with simple model compound systems. A survey of the literature reveals that many types of organic species such as aliphatic carboxylic acids (*13, 14*), hydroxybenzoic acids (*15*), phenols (*16*), and pyrrole nitrogen derivatives (e.g., tryptophan) (*16*) are reactive substrates for $CHCl_3$ production. Unfortunately, the available information is primarily limited to a survey of the reactivity of representative compounds in each category, over a narrow range of experimental conditions.

Christman and co-workers (*17*) conducted a systematic examination of the chlorination reactions of derivatives of vanillic acid, syringic acid, and 3,5-dihydroxybenzoic acid. These compounds were selected as representative structures for the phenolic polymer core of humic substances, based on products detected from the alkaline/$CuSO_4$ degradation of soil and aquatic organic matter (*5*). Of the substrates chosen for study, structures related to 3,5-dihydroxybenzoic acid, i.e., resorcinol and orcinol, were the most efficient precursors of $CHCl_3$. Rook (*3, 4*) had previously documented that 1,3-dihydroxybenzenes produced high yields of chloroform under alkaline conditions. Boyce and Hornig (*18*) confirmed these observations and reported that significant formation of $CHCl_3$ also occurred during reactions at low pH. Preliminary results obtained in our laboratory showed that the bromination of these substances proceeds in an analogous manner to give $CHBr_3$ (*19*). While these studies have identified several important precursor structures, many details of the conversion of these substrates to trihalomethanes require clarification.

The speciation of chlorine and bromine in aqueous solution is governed by three principal reactions (eq 2–4),

$$X_2 + H_2O \overset{K_h}{\rightleftharpoons} HOX + H^+ + X^- \qquad (2)$$

$$HOX \overset{K_a}{\rightleftharpoons} H^+ + XO^- \qquad (3)$$

$$X_2 + X^- \overset{K_c}{\rightleftharpoons} X_3^- \qquad (4)$$

where the equilibrium constants K_h, K_a, and K_c have values of 3.94×10^{-2} M^2, 3.2×10^{-8} M, and 0.18 M^{-1} for Cl_2 (*20–22*) and 5.8×10^{-9} M^2, 2.0×10^{-9} M, and 15.9 M^{-1} for Br_2 (*23–25*). Upon dissolution in water, these halogens undergo rapid hydrolysis and disproportionation to mixtures of hypohalous acid, HOX, and hypohalate anion, XO^- (*26*). The composition of the resulting solutions varies as a function of pH and the concentration of halide ion, X^-. At low X^- concentrations, hydrolysis to HOX and XO^- proceeds virtually to completion, and formation of trihalide ion, X_3^- (reaction 4), does not occur to a significant degree. Therefore, "available" chlorine and bromine exist primarily as HOCl (pK_a = 7.42) and HOBr (pK_a = 8.70) in acidic and

0013-936X/83/0917-0202$01.50/0

neutral solution. These species are strong electrophiles, which participate in addition and substitution reactions with a variety of organic molecules (*12, 27*). The action of hypochlorite as an oxidizing agent on some aliphatic and aromatic compounds in dilute aqueous systems is well understood (*15, 28*), but the corresponding reactions of bromine remain uncharacterized.

There have been a few detailed investigations of the reaction of chlorine with 1,3-dihydroxybenzenes. Zincke (*29*) reported that chlorination of resorcinol in organic solvent produced 2,2,4,4,6-pentachlorocyclohex-4-ene-1,3-dione (pentachlororesorcinol, 1), which was subsequently hydrolyzed to keto carboxylic acid 2 upon addition to water. In a much more recent study, Moye (*30*) proposed a modified degradation mechanism (eq 6). An assessment of 1,3-benzenediols as model systems for aquatic humic substances should involve experiments performed under concentration and pH conditions that more closely resemble those encountered in water treatment processes. Previous attempts to analyze the details of these reactions in dilute aqueous solution have failed to provide reproducible results (*15, 31*). Therefore, considerable uncertainty still exists as to the pathways of THM production from these substrates.

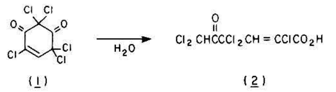

(5)

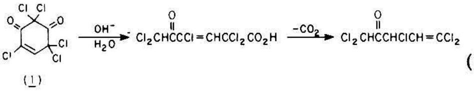

(6)

The primary objective of the current research was to conduct a systematic analysis of the halogenation reactions of a series of dihydroxyaromatic model compounds. The effects of pH and the relative reactant concentrations, $[X_2]/[\text{substrate}]$ where X = Cl and Br, on the formation of CHX_3 and other halogenated organic products in dilute aqueous media have been examined in detail. Finally, an isotopically enriched substrate, resorcinol-2-^{13}C, was synthesized, and the fate of the labeled carbon atom was followed upon reaction of the precursor with chlorine and bromine. Results of this study should help to elucidate many important features of the reaction pathways for the conversion of 1,3-dihydroxybenzenes to trihalomethanes.

Experimental Section

Instrumentation. Gas chromatographic determinations of trihalomethanes ($CHCl_3$ and $CHBr_3$) were performed on a Perkin-Elmer Model 3920B GC equipped with a ^{63}Ni electron capture detector (ECD). Peak area measurements were computed automatically with a Columbia Scientific Industries Model Supegrator 1 digital integrator. Analyses by GC/MS were conducted on a Finnigan Model 9610 gas chromatograph interfaced to a Finnigan Series 4000 mass spectrometer. Acquisition and analysis of mass spectral data were accomplished by using a Data General Nova 3 minicomputer programmed with the Finnigan/INCOS software system. Ultraviolet spectra were recorded on a Perkin-Elmer Model 571 UV/vis spectrophotometer, and infrared spectra were measured with a Perkin-Elmer Model 599 IR spectrophotometer. A JEOL FX 60 Q Fourier transform NMR spectrometer was employed for the collection of ^{1}H and ^{13}C nuclear magnetic resonance data.

Synthesis of 1,3-Dihydroxybenzene-*2*-^{13}*C*. The preparation of 1,3-dihydroxybenzene-2-^{13}C was carried out by using standard techniques as outlined in Figure 1. Boyce et al. have described the detailed procedures used in this synthesis (*19, 32*). The synthetic scheme involved cyclization of methyl 5-oxohexanoate-*6*-^{13}*C* (4). This keto ester starting material was prepared by a Grignard reaction of the mixed carboxylic anhydride 3 with methyl-^{13}*C*-magnesium iodide, $^{13}CH_3MgI$, according to the method of Terasawa and Okada (*33*). Preparation of anhydride 3 was achieved by treatment of *o*-methoxybenzoic acid (Aldrich) with methyl 4-(chloroformyl)butyrate (Aldrich) in the presence of triethylamine, Et_3N (Eastman). The isotopically labeled Grignard reagent was generated from 25% iodomethane-^{13}*C* (Stöhler Isotopes). An intramoleculer Claisen condensation reaction of methyl 5-oxohexanoate-*6*-^{13}*C* (4) with sodium methoxide, $NaOCH_3$, yielded 1,3-cyclohexanedione-*2*-^{13}*C* (5). Subsequent dehydrogenation of 1,3-cyclohexanedione over a palladium–carbon catalyst, Pd/C (Alfa), produced resorcinol-*2*-^{13}*C* (6). The cyclization and dehydrogenation reactions were performed by uitilizing techniques developed from published procedures (*34, 35*).

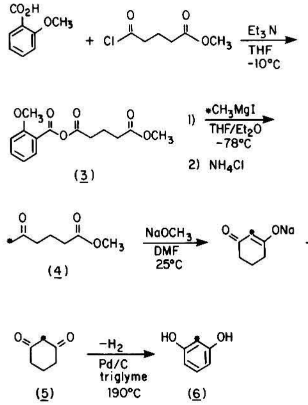

Figure 1. Synthetic scheme for the preparation of 1,3-dihydroxybenzene-*2*-^{13}*C*.

The ^{13}C-enriched reaction products were characterized by IR, UV, NMR (^{1}H and ^{13}C), and mass spectrometry. Spectra obtained for each isotopically labeled compound matched data recorded from a genuine sample of the corresponding unlabeled substance. Comparison of sample spectra and physical properties (boiling points, melting points, etc.) with published measurements (*36–40*) provided final confirmation of each ^{13}C-labeled intermediate and the final product structures.

Halogenation Reactions. A series of dihydroxybenzenes and aliphatic ketones were selected for study (Figure 2). Substrate solutions were prepared from reagent grade chemicals, which were used without further purification. Reagent grade phosphoric acid, potassium phosphate monobasic, sodium phosphate dibasic, sodium phosphate tribasic, and sodium hydroxide (all from Fisher) were employed to prepare the pH buffer solutions. Glass-distilled/deionized water (18 MΩ cm resistivity) obtained from a Nanopure purification system (Barnstead) was utilized in the preparation of all reagent solutions. The procedure used for the halogenation of model compounds and the analysis of $CHCl_3$ and $CHBr_3$ have been described in detail by Boyce and Hornig (*18, 41*). In these experiments, substrate concentrations were 10^{-5} M, and $[Cl_2]$ and $[Br_2]$ ($[X_2]$) ranged from 10^{-5} to 10^{-4} M. The reactions were conducted at 10 °C in 0.2 M phosphate buffer solutions. After 24 h, unreacted halogen was reduced to X^- by the

Table I. Trihalomethane Yields (mol of THM/mol of Substrate) from the Halogenation of Dihydroxyaromatic and Methyl Ketone Substrates[a] ([Substrate] = 1×10^{-5} M, $[X_2] = 1 \times 10^{-4}$ M)

	chloroform						bromoform		
	pH 4		pH 7		pH 10		pH 4	pH 7	pH 10
substrate	DAI[b]	SE[c]	DAI	SE	DAI	SE	SE	SE	SE
dihydroxyaromatics									
1,2-dihydroxybenzene	0.14	<0.01	<0.01	<0.01	0.24	0.23	<0.01	0.04	0.29
1,3-dihydroxybenzene	0.24	0.06	0.79	0.86	0.87	0.95	<0.01	<0.01	0.37
1,4-dihydroxybenzene	<0.01	<0.01	0.03	0.03	0.30	0.34	0.16	0.51	0.74
2,6-dihydroxytoluene	0.01	<0.01	0.08	0.07	0.17	0.24	<0.01	0.20	0.19
3,5-dihydroxytoluene	0.17	<0.01	0.58	0.51	0.90	1.00	<0.01	0.11	0.47
1,3-dihydroxynaphthalene	0.03	<0.01	0.70	0.63	0.88	0.80	<0.01	0.12	0.27
3,5-dihydroxybenzoic acid	0.39	0.01	0.73	0.70	0.47	0.54	0.02	0.07	0.63
2,4-dihydroxybenzoic acid	0.17	0.08	0.68	0.73	0.90	0.94	0.19	0.46	0.79
2,6-dihydroxybenzoic acid	1.12		1.15		1.21		0.13	0.45	0.76
methyl ketones									
acetone	<0.01	<0.01	<0.01	<0.01	<0.01	<0.01	<0.01	0.05	0.67
2-butanone	<0.01	<0.01	<0.01	<0.01	<0.01	<0.01	<0.01	<0.01	0.29
2-pentanone	<0.01	<0.01	<0.01	<0.01	<0.01	<0.01	<0.01	0.02	0.35

[a] Multiple determinations indicate a precision of 6-7% in THM yield. [b] DAI denotes THM yields determined by direct aqueous injection. [c] SE denotes THM yields determined by solvent extraction.

addition of excess sodium sulfite, and the yields of $CHCl_3$ and $CHBr_3$ were determined by GC with electron capture detection. Samples were analyzed both by direct aqueous injection (DAI) and after solvent extraction (SE) with cyclohexane (Fisher Spectranalyzed). A Chromosorb 101 column (Johns-Manville) was used for the DAI analyses, and Porapak Q (Waters) was employed for the solvent extracts. The GC columns were operated under isothermal conditions, and the injection port and ECD temperatures were maintained at 250 and 300 °C, respectively.

The halogenation of resorcinol-2-^{13}C and selected dihydroxyaromatic substrates was also carried out at higher initial reactant concentrations to permit the isolation of sufficient amounts of products for characterization by GC/MS. Chlorination reactions were performed at pH 4, 7, and 10 by using substrate concentrations of 5×10^{-4} or 1×10^{-4} M and $[Cl_2]$ ranging from 5×10^{-4} to 1×10^{-2} M, added as NaOCl (Mallinckrodt). A series of 1×10^{-4} M substrate solutions were treated with bromine at $[Br_2]/[\text{substrate}]$ ratios of 1, 5, and 10. Lower reactant concentrations were utilized in the bromination experiments due to the limited solubility of Br_2 (relative to chlorine) in water. As before, constant pH was maintained during the reactions through the use of phosphate buffers.

After 3 h, each reaction was quenched by addition of sodium sulfite, and the product solution was acidified to pH 1 with concentrated HCl. Reaction products were extracted from aqueous solution with diethyl ether (Mallinckrodt). Each extract was dried over anhydrous magnesium sulfate and concentrated to <2 mL, before GC/MS analysis, by evaporation of the excess solvent under vacuum. Chemical derivatization of selected samples using either 14% BF_3/methanol (Supelco) or a mixture of hexamethyldisilazane, HMDS, and trichloromethylsilane, TCMS (Pierce), facilitated the chromatographic separation of carboxylic acid and some phenolic reaction products.

Both the derivatized and untreated products were separated on each of two glass GC columns, 6 ft × 0.25 in. o.d., packed with either 3% SP-2100 or 10% SP-1000 on Supelcoport (Supelco). Mass spectra were recorded under electron impact ionization at an energy of 70 eV. The ion source was operated at 10^{-7} torr and 250 °C.

Results and Discussion

The results of the initial survey of $CHCl_3$ and $CHBr_3$ formation from dihydroxyaromatic and methyl ketone substances are summarized in Table I. Chlorination and bromination of 1,3-dihydroxybenzenes produced high yields of chloroform and bromoform at neutral and alkaline pH, whereas significant conversion of 1,2- and 1,4-benzenediols and methyl ketones to THM's occurred only under strongly alkaline conditions. The presence of an unsubstituted carbon atom at the ortho position with respect to both phenolic hydroxyl substituents seems to be

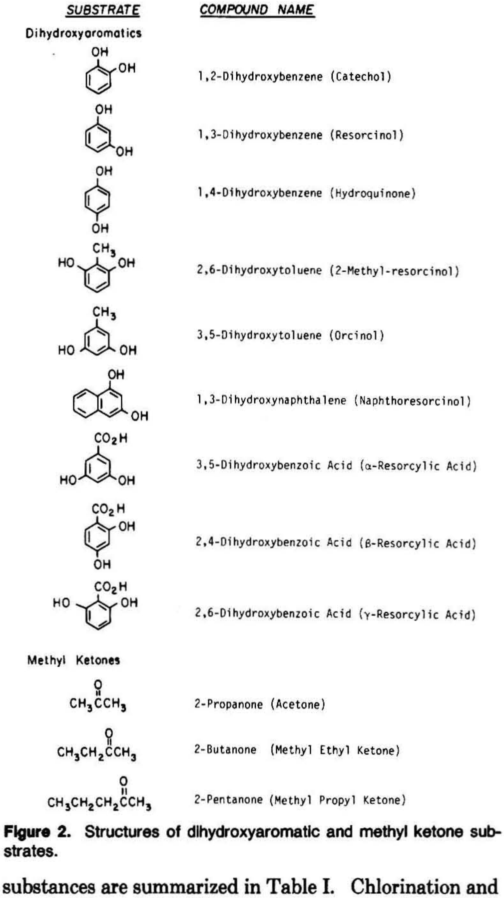

Figure 2. Structures of dihydroxyaromatic and methyl ketone substrates.

Table II. Reactant and Product (THM) Stoichiometry (mol/mol of Substrate) for the Halogenation of 1,3-Dihydroxyaromatic Model Compounds in Aqueous Solution ([Substrate] = 1 × 10^{-5} M)

substrate	pH	Cl_2/substrate	$CHCl_3$	Br_2/substrate	$CHBr_3$
1,3-dihydroxybenzene	4	6.7[a]	0.83[a]		
		6.4[b]	0.04[b]		
	7	7.1[a]	1.07[a]		
		7.1[b]	0.72[b]	7.1[b]	0.52[b]
	10	7.9[a]	0.73[a]		
		7.9[b]	0.73[b]	6.0[b]	0.72[b]
3,5-dihydroxytoluene	4	6.5[a]	0.11[a]		
	7	8.1[a]	0.74[a]		
		7.9[b]	0.69[b]	7.8[b]	0.09[b]
	10	7.2[a]	1.02[a]		
		7.2[b]	1.02[b]	6.3[b]	0.47[b]
1,3-dihydroxynaphthalene	7	5.1[a]	0.68[a]		
		5.1[b]	0.68[b]	5.0[b]	0.13[b]
3,5-dihydroxybenzoic acid	7	6.9[a]	0.97[a]		
		7.1[b]	0.74[b]	7.1[b]	0.27[b]
2,4-dihydroxybenzoic acid	7	7.1[a]	1.00		
		7.5[b]	0.80	7.0[b]	0.48[b]
2,6-dihydroxybenzoic acid	7			7.0[b]	0.47[b]

[a] Denotes results based on DAI analysis of trihalomethanes. [b] Denotes results based on solvent extraction anlaysis.

required for the efficient reaction of 1,3-aromatic diols. The only exception to this generalization was the apparent high reactivity of 2,6-dihydroxybenzoic acid. Analysis by GC/MS confirmed that chlorination of this substrate involved decarboxylation to form chlororesorcinols as originally proposed by Larson and Rockwell (*15*). These observations are indicative of an electrophilic substitution mechanism, which is highly favored when both OH groups are located at an appropriate orientation to stabilize the transition state of the reaction through the donation of electron density (*42*). Rook (*3, 4*) and Christman et al. (*17*) have each noted an analogous dependency of $CHCl_3$ production on substrate structure.

A series of experiments were conducted to determine the reactant and product (THM) stoichiometry of the halogenation reactions involving the 1,3-dihydroxyaromatic substrates. Each compound exhibited increased haloform production up to $[X_2]/[\text{substrate}]$ reactant ratios ranging from 6 to 8, except for naphthalenediol, for which a maximum yield of $CHCl_3$ and $CHBr_3$ was achieved at approximately 5:1 (Figure 3, Table II). These results agree closely with the "end points" previously reported for the chlorination of resorcinol, orcinol, and α-resorcylic acid (*5, 17, 31*). Except for a decline in the formation of chloroform in acidic solution, the observed reaction stoichiometry did not vary significantly as a function of pH. The high relative stoichiometric coefficient for the halogens is consistent with a pathway for conversion of the aromatic diol precursors to CHX_3 that involves a number of addition and substitution steps as well as oxidation reactions. The lower value for the corresponding dihydroxynaphthalene reactions reflects the fused-ring structure of the molecule, which renders one of the aromatic carbon sites adjacent to the C_1-hydroxyl group inert to electrophilic substitution by bromine or chlorine.

The direct aqueous injection and solvent extraction analyses gave equivalent results for the production of $CHBr_3$ from all the bromination reactions. This is in marked contrast to the model compound reactions with chlorine, in which the DAI-measured yields of $CHCl_3$ were consistently higher for each dihydroxyaromatic substrate at low pH (Table I and Figure 4). Other investigators have observed analogous differences upon application of the purge-and-trap and DAI techniques to the determination of trihalomethane concentrations in chlorinated natural waters (*43–45*). The discrepancy between the DAI and SE results can be readily attributed to the formation of metastable intermediates in acidic and neutral solution, which subsequently decompose to $CHCl_3$ upon injection of the aqueous sample into the hot injection port of the gas chromatograph. In support of this hypothesis, several trichloromethyl-substituted compounds including trichloroacetic acid, trichloroacetaldehyde (chloral) hydrate, and pentachloroacetone were identified unambiguously by GC/MS as chlorination products of 1,3-dihydroxybenzenes at pH 4 and 7. Boyce and Hornig (*18, 41*) and Rook (*31*) have suggested that these species arise from a series of reactions in competition with the main reaction pathway leading to chloroform.

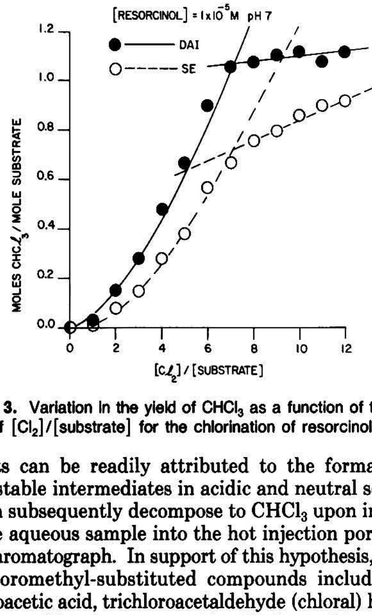

Figure 3. Variation in the yield of $CHCl_3$ as a function of the molar ratio of $[Cl_2]/[\text{substrate}]$ for the chlorination of resorcinol at pH 7.

The pH dependence for the formation of $CHCl_3$ and $CHBr_3$ is unusually complicated, as depicted in Figure 4. The shape of these curves, which was replicated for the halogenation of each 1,3-aromatic diol except 2,6-dihydroxytoluene, demonstrated that maximum conversion of the substrate to chloroform (>90%) and bromoform (>70%) was attained at pH 8–10, accompanied by a decrease in product formation in more strongly basic solution (pH 11–12). Conversely, acetone, 2-butanone, and 2-pentanone gave higher yields of $CHBr_3$ upon bromination under progressively more alkaline conditions. The reaction of these methyl ketones with chlorine failed to produce measurable yields of $CHCl_3$ under the experimental con-

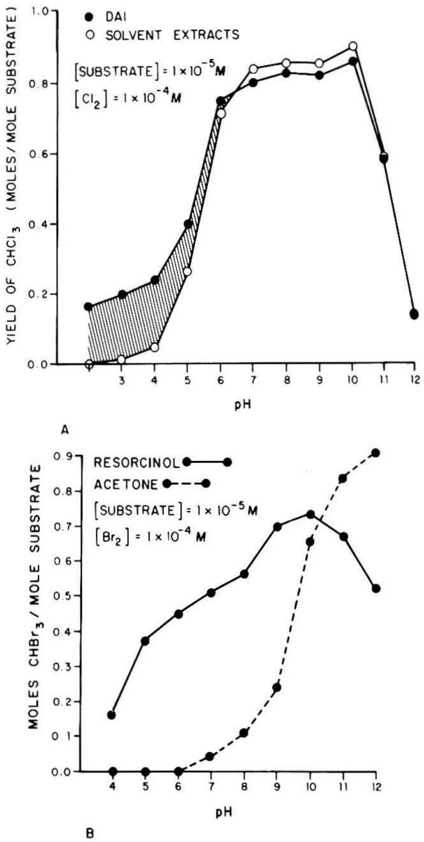

Figure 4. (A) pH dependence for the production of $CHCl_3$ from the chlorination of resorcinol. (B) pH dependence for the production of $CHBr_3$ from the bromination of resorcinol and acetone.

ditions employed in the current study. The observed decline in THM yield from 1,3-dihydroxybenzenes in strongly basic solution suggests that other reaction pathways may compete with the postulated haloform mechanism at high pH. For example, oxidative coupling of resorcinol and orcinol could occur under alkaline pH conditions following initial one-electron oxidation of the substrate without incorporation of Cl or Br. However, it seems more likely that the observed trend indicates that the intermediate precursors of $CHCl_3$ are not formed as rapidly from ClO^-, the predominant form of chlorine in alkaline media, as from HOCl. Consequently, the haloform reaction may still be the predominant route for the production of chloroform.

The second part of the current study focused on the identification of reaction products other than $CHCl_3$ and $CHBr_3$. The following discussion emphasizes results obtained from the chlorination of model compounds; however, parallel trends in reactivity were observed in the experiments with bromine. The nature of chlorinated products was determined for reactions of resorcinol, orcinol, 1,3-dihydroxynaphthalene, and the three isomers of resorcylic acid at each of four different chlorine dosages, $[Cl_2]/[\text{substrate}] = 1, 3, 5$, and 10. Experiments conducted in acidic, neutral, and alkaline solution enabled us to also examine the effects of pH on the distribution of products. Structural characterization by GC/MS was facilitated through computer matching of the product spectrum with a reference file of mass/intensity data. In several cases (see Table III), a comparison of the chromatographic retention time and fragmentation pattern with measurements of a standard sample under identical instrumental conditions provided unambiguous confirmation of the assigned structure. Other identifications are considered to be tentative.

The reaction products, which have been identified from the chlorination of resorcinol, are listed in Table III and Figure 5. These compounds are representative of the species produced from each dihydroxyaromatic precursor and illustrate the general characteristics of halogenation reactions for a variety of experimental conditions. The distribution of specific types of chlorinated products is strongly dependent on both the pH and the relative concentrations of chlorine and substrate in solution. High chlorine dosages, $[Cl_2]/[\text{substrate}] = 10$, promoted conversion of the substrate to a number of highly oxidized organochlorine compounds in addition to $CHCl_3$. The large yield of Cl-substituted carboxylic acids (relative to $CHCl_3$) at pH 4 may reflect the preponderance of hypochlorous acid as the reactive form of dissolved Cl_2 in acidic solution and its extensive participation in electrophilic addition and substitution reactions. At pH 7 and 10, the less strongly electrophilic hypochlorite anion dominates the aqueous speciation of Cl_2. Under these conditions available chlorine is consumed primarily in the formation of $CHCl_3$ through hydrolysis reactions, which are favored in weakly alkaline solution.

Christman et al. (*17*) have also noted that chlorination of resorcinol at high Cl_2/substrate ratios enhanced the accumulation of chlorinated organic acids. The authors identified chlorobutenedioic acid **7** as the major byproduct of the reaction of 1,3-dihydroxybenzene with excess HOCl at pH 7. We were unable to detect this compound under the conditions described in Table III; however, chloromaleic acid (**8**) did form in neutral solution at 10^{-3} M resorcinol and 10^{-2} M Cl_2. This observation indicates that alternative reaction pathways may direct the formation of oxidation products other than $CHCl_3$ depending on the absolute initial concentration of reactants. Therefore, slight differences in experimental procedure can be expected to account for the apparent inconsistency in the results of each study. In this context, it should be mentioned that reaction of chlorine with 1,3-dihydroxynaphthalene and 3,5-dihydroxytoluene produced measurable yields of *o*-phthalic acid (**9**) and a peak giving a mass spectrum corresponding to 2-chloro-3-methylmaleic acid (**10**), respectively. Also, bromination of resorcinol and orcinol at pH 10 gave species exhibiting spectral fragmentation patterns characteristic of the Br-substituted dicarboxylic anhydrides **11** and **12**.

$HO_2C{-}CH{=}CCl{-}CO_2H$

(7)

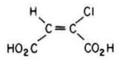

(8)

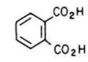

(9)

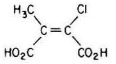

(10)

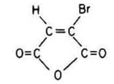

(11)

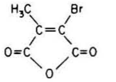

(12)

Chlorination of resorcinol at equimolar reactant concentrations yielded mono-, di-, and trichloro-1,3-dihydroxybenzenes. Several researchers have detected chlorinated aromatic species in this reaction system but have not assigned chromatographic and spectroscopic data to specific chlororesorcinol isomers (*5, 17, 31, 46*). In

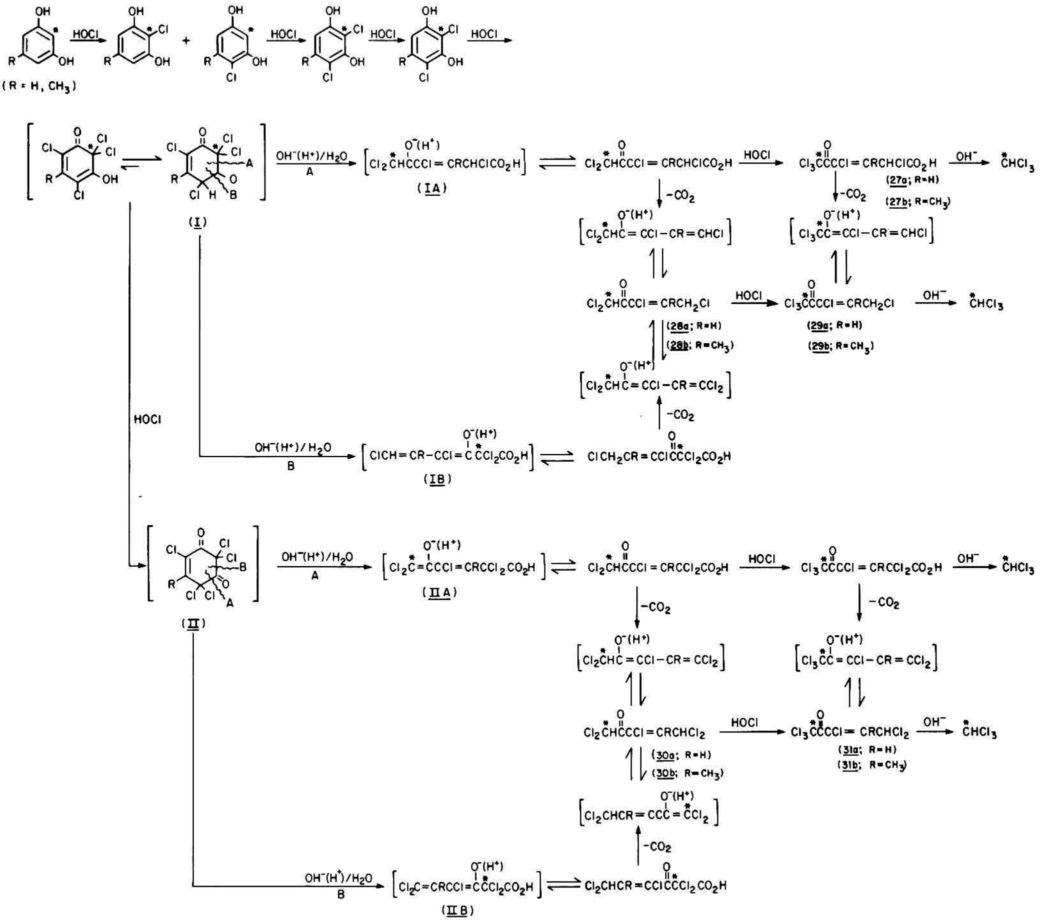

Figure 5. Reaction pathways for the conversion of 1,3-dihydroxyaromatic substrates to $CHCl_3$. Structures outlined by brackets denote proposed intermediates that were not detected by GC/MS.

analogous fashion, addition of hypochlorite to solutions of each of the other 1,3-aromatic diols resulted in the formation of electrophilic substitution products 13–17.

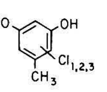
(13)

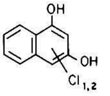
(14)

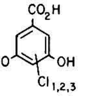
(15)

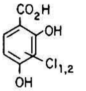
(16)

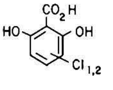
(17)

In addition to direct aromatic substitution, two of the aromatic acid substrates, β- and γ-resorcylic acid, underwent decarboxylation during reaction with HOCl. For example, 2,4-dihydroxybenzoic acid gave a mixture of 2-chlororesorcinol, 4-chlororesorcinol, 2,4-dichlororesorcinol, and 2,4,6-trichlororesorcinol. Formation of the latter three compounds is consistent with the mechanism proposed by Larson and Rockwell (*14, 15*) for the conversion of simple hydroxybenzoic acids to chlorinated phenols (reaction 7). However, the production of 2-chloro-1,3-dihydroxybenzene implies that the reaction may also proceed via a pathway involving an intermediate such as 19 in which the Cl and CO_2H substituents occupy different aromatic carbon sites (reaction 8). Oxidative decarboxylation of 3,5-dihydroxybenzoic acid was not observed because the orientation of hydroxyl groups at both meta positions relative to the carboxyl functionality pre-

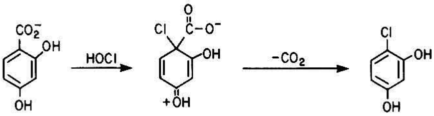

(18)

(7)

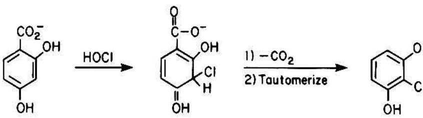

(19)

(8)

Table III. Reaction Products Identified from the Chlorination of Resorcinol ([Resorcinol] = 5×10^{-4} M, [Cl_2] = 5.10^{-4} to 5×10^{-3} M, T = 10 °C)

		pH	
resorcinol	4	7	10
1	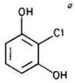 [a] 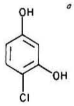 [a] 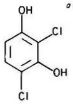 [a] 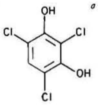 [a] 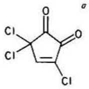 [a] $Cl_2CHC(O)CCl{=}CHCH_2Cl$	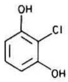 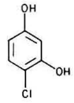 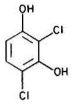 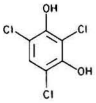 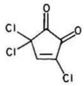 $CHCl_3$[a]	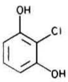 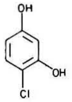 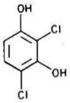 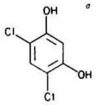 [a] 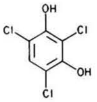 $CHCl_3$
3	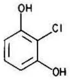 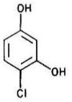 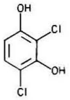 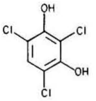 $Cl_2CHC(O)CCl{=}CHCH_2Cl$	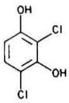 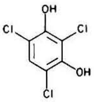 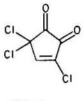 $CHCl_3$	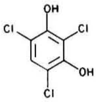 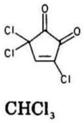 $CHCl_3$
5	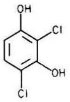 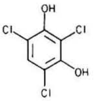 $Cl_2CHC(O)CCl{=}CHCHCl_2$ $Cl_2CHC(O)CCl{=}CHCHCl_2$ $CHCl_3$	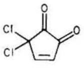 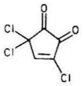 $CHCl_3$	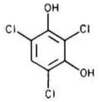 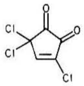 $CHCl_3$
10	$Cl_3CC(O)CCl{=}CHCH_2Cl$ $Cl_3CC(O)CCl{=}CHCHCl_2$ $Cl_3CCH(OH)_2$[a] $Cl_3CC(O)CHCl_2$[a] $CHCl_3$ six chlorinated carboxylic acids incl Cl_2CHCO_2H[a] Cl_3CCO_2H[a] $Cl_3CC(O)CCl{=}CHCHClCO_2H$	$CHCl_3$ chlorinated acids Cl_3CCO_2H 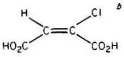 [b]	$CHCl_3$ Cl_3CCO_2H

[a] Structure of compound confirmed through matching of GC retention time and mass spectrum with analysis of standard sample. Other structural assignments are considered to be tentative. [b] Detected by GC/MS in ether extracts obtained at reactant concentrations of resorcinol = 1×10^{-3} M and Cl_2 = 1×10^{-2} M.

cludes formation of the requisite cyclohexadienone intermediates.

At intermediate [Cl_2]/[substrate] ratios (3:1 and 5:1), resorcinol was converted to a complex mixture of chlorinated compounds, which corresponded to the degradation products of 2,4,6-trichloro-1,3-dihydroxybenzene. The distribution of species varied dramatically as a function of pH. At pH 7 and 10, the most abundant components,

Table IV. Physical Constants and Spectral Data for 3,5,5-Trichlorocyclopent-3-ene-1,2-dione[a] ([Resorcinol] = 1.1×10^{-2} M, [Cl_2] = 5.5×10^{-2} M, pH 7)

MS (High Resolution)[b]			
m/e(obsd)	*m/e*(calcd)	elemental comp	ion
197.90542	197.90422	$C_5HO_2{}^{35}Cl_3$	M^+
199.90118	199.90127	C_5HO_2-$^{35}Cl_2{}^{37}Cl$	$[M + 2]^+$
201.90021	201.89832	C_5HO_2-$^{35}Cl^{37}Cl_2$	$[M + 4]^+$
169.90949	169.90931	C_4HOCl_3	$[M - CO]^+$
141.91684	141.91493	C_3HCl_3	$[M - 2(CO)]^+$
109.93231	109.93262	C_2OCl_2	$[M - (CH{=}CClCOO)]^+$

^1H NMR ($CDCl_3$, relative to Me_4Si) δ 6.36 (H_a)
IR (KBr pellet) 1790 (C=O), 1555 cm^{-1} (C=C)
UV (MeOH) 295 nm
mp 52-53 °C (sharp)

[a] Isolated by preparative gas chromatography under the following conditions: copper column, 10 ft × 0.25 in. packed w/10% SF-96 on 80/100 mesh Chromosorb WAW. Temperatures (°C): injector 210, column 180, detector 225. Carrier He, 100 mL/min. [b] Performed by Department of Chemistry, Massachusetts Institute of Technology.

as measured by GC peak area, were chloroform and a Cl-substituted intermediate having a mass spectrum consistent with 3,5,5-trichlorocyclopent-3-ene-1,2-dione (**20**).

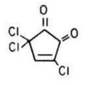
(20)

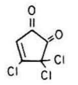
(21)

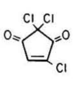
(22)

Christman and co-workers (*17*) have tentatively identified this compound on the basis of mass-analyzed ion kinetic energy spectroscopic (MIKES) measurements.

Experimental conditions were designed to optimize the formation of the C_5 diketone intermediate in order to obtain a sample for complete spectroscopic analysis. After extraction from aqueous solution with ether, the compound was isolated by preparative-scale gas chromatography. Final purification gave a white crystalline product in less than 1% yield (based on resorcinol), with a molecular formula $C_5HCl_3O_2$, which was determined by high-resolution mass spectrometry. Each of three possible cyclic alkenone structures, **20–22**, appeared to fit the observed elemental composition and ion fragmentation pattern. The physical properties and spectrophotometric measurements (Table IV) closely resembled the available literature data (*47–53*) for analogues of dione **20**. Unfortunately, the ^1H NMR data did not provide a sufficiently clear distinction between the olefinic proton environments of isomers **20** and **21**. A sample of this compound has been submitted for X-ray crystallographic analysis in order to provide unequivocal identification of the product structure. Chlorination of orcinol and dihydroxynaphthalene also formed a series of related Cl-substituted diketones **23–26**. Further support for the assigned structures was also obtained from the recent work of Tomita et al. (*54*), who have also reported the separation and characterization of chloroindanediones **25** and **26**.

Analysis by GC/MS showed several additional components in the ether extracts from the reaction of resorcinol with HOCl at pH 4. The mass spectra of these compounds conform to structures **28a–31a** in Figure 5, which illustrates a plausible mechanism for the halogenation of 1,3-dihydroxybenzenes. β- and γ-resorcylic acids also yield these products after an initial series of decarboxylation reactions (eq 7 and 8). The methyl-substituted compounds **28b–31b**

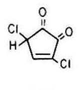
(23)

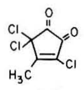
(24)

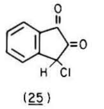
(25)

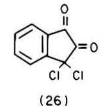
(26)

were formed as the dominant species upon chlorination of orcinol at [Cl_2]/[substrate] ratios of 3 and 5 under acidic and neutral conditions. Analogous species **32** and **33** were

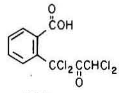
(32)

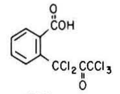
(33)

also detected in the experiments with naphthoresorcinol. We believe that these compounds are representative examples of the intermediates that participate in the general pathway of conversion of aromatic diol substrates to $CHCl_3$ as well as a variety of other CCl_3 derivatives such as trichloroacetic acid.

The proposed reaction scheme given in Figure 5 involves the basic features previously described by Zincke (*29*), Moye (*30*), and Rook (*31*). Initial electrophilic substitution yields trichloro-1,3-dihydroxybenzenes. Further addition of chlorine forms the cyclohexenedione intermediates I and II and is followed by hydrolysis and oxidative bond cleavage (A or B) about the C_2 site of the ring structure via a complex series of steps to yield carboxyenolate species such as IA, IB, IIA, and IIB. The corresponding keto carboxylic acids such as **27a** and **27b** are expected to be fairly stable in acidic solution. Therefore, it was not surprising that these products were detected from reactions of resorcinol and orcinol with HOCl at pH 4. In neutral and alkaline solution, decarboxylation is probably accompanied by direct incorporation of Cl to give, for example, chlorinated pentenones **29** and **31**. These trichloromethyl ketones then undergo base-catalyzed hydrolysis to chloroform. Decarboxylation and chlorination of intermediates such as IA, IIA, IB, and IIB may constitute the rate-limiting processes in this mechanism. Halogenation reactions involving a variety of 1,3-dicarbonyl compounds (β-keto acids and β-diketones) also occur rapidly in this fashion (*15, 55*).

In order to verify that THM products originate from the activated C_2 site of 1,3-benzenediols, a series of halogenation experiments was carried out by using isotopically labeled resorcinol. At pH 4, 7, and 10, treatment of 1,3-dihydroxybenzene-*2*-^{13}C with a 10-fold excess of Cl_2 and Br_2 produced $^{13}CHCl_3$ and $^{13}CHBr_3$. As shown by the data in Table V, the ^{13}C enrichment of the substrate and haloform reaction products (calculated from mass spectral measurements) is approximately equivalent. These results confirm that chloroform and bromoform are produced almost exclusively by a reaction pathway(s) involving carbon–carbon cleavage about the C_2 position of the ring structure of the aromatic precursor. In addition, chlorination of resorcinol-*2*-^{13}C at pH 4 yielded trichloroacetic-*2*-^{13}C acid, which seems to support the assertion that the formation of trichloromethyl-substituted byproducts occurs in acidic solution via the same general scheme.

Other ^{13}C-substituted reaction products have also been detected from the chlorination of labeled dihydroxybenzene. For example, reaction of resorcinol-*2*-^{13}C with

Table V. ^{13}C Enrichments of Isotopically Labeled Resorcinol and Halogenated Reaction Products[a]

compd	pH	% ^{13}C
1,3-Dihydroxybenzene-*2*-^{13}C		21.4
$^{13}CHCl_3$[c]	4	21.8
	7	19.6
	10	22.5
$^{13}CHBr_3$[d]	4	22.4
	7	24.9
	10	23.4
3,5,5-trichlorocyclopent-3-ene-1,2 dione-*2*-^{13}C (34)	7	23.5

[a] Carbon-13 content calculated from mass spectral measurements. Reported values denote ^{13}C enrichment after subtraction of natural ^{13}C isotopic abundance as determined from the mass spectrum of the corresponding unlabeled compound. [b] Calculated from parent ion: $[M + 1]^+/M^+$, i.e., relative intensity (*m/e* 111/*m/e* 110). [c] Calculated from $CHCl_2^+$ fragment ion: relative intensity (*m/e* 84/*m/e* 83). [d] Calculated from $CHBr_2^+$ fragment ion: relative intensity (*m/e* 172/*m/e* 171). [e] Calculated from parent ion: relative intensity (*m/e* 199/*m/e* 198).

chlorine ($[Cl_2]/[substrate] = 5$) gave 2,4,6-trichloro-1,3-dihydroxybenzene-*2*-^{13}C and a product that has been tentatively assigned the structure 3,5,5-trichlorocyclopent-3-ene-1,2-dione-*5*-^{13}C (**34**). Given the fact that the corresponding unlabeled compound **20** is only a minor product, the current finding lends credence to the hypothesis that the *o*-diketone species arise from a reaction pathway in competition with that leading to $CHCl_3$.

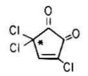

(34)

Conclusions

Derivatives of resorcinol are highly efficient precursors of trihalomethanes upon halogenation in dilute aqueous solution at neutral and weakly alkaline pH. The 1,2- and 1,4-dihydroxybenzenes are less active substrates, which undergo significant reaction only under strongly basic conditions.

Analysis by GC/MS showed that 1,3-aromatic diols were converted to several metastable trichloromethyl-substituted intermediates during reaction with chlorine in acidic solution. These compounds subsequently decomposed to $CHCl_3$ upon direct aqueous injection GC analysis. There was no evidence for the formation of the corresponding CBr_3 derivatives in the bromination experiments.

The pH dependence and reaction stoichiometry of $CHCl_3$ and $CHBr_3$ production are similar, which indicates that the reaction of 1,3-dihydroxybenzenes with Cl_2 and Br_2 proceeds to give THM's via the same general pathway. The distribution of other halogenated reaction products varied dramatically as a function of pH and the relative concentrations of halogen and substrate. Experiments conducted at a variety of $[Cl_2]/[substrate]$ ratios permitted us to characterize several intermediates involved in the formation of $CHCl_3$.

The data indicate that the conversion of 1,3-dihydroxyaromatic precursors to THM's occurs in two stages. Extensive incorporation of halogen by electrophilic substitution and addition processes is followed by a complex series of hydrolysis and decarboxylation steps leading to $CHCl_3$ and $CHBr_3$ via carbon–carbon bond cleavage about the C_2-site of the aromatic ring. The identification of $^{13}CHCl_3$ and $^{13}CHBr_3$ from the chlorination and bromination of resorcinol-*2*-^{13}C supports this conclusion. It is hoped that the results of this study offer a detailed basis for a future examination of the kinetics of this model compound system.

Acknowledgments

We gratefully acknowledge the experimental assistance of A. C. Barefoot in the synthesis of resorcinol-*2*-^{13}C and subsequent halogenation reactions and D. R. Britton for the isolation and analysis of 3,5,5-trichlorocyclopent-3-ene-1,2-dione. We also thank Michael R. Hoffmann for his helpful comments during the preparation of the manuscript.

Registry No. 20, 67951-44-4; $Cl_3CCOCHCl_2$, 1768-31-6; $Cl_3CCH(OH)_2$, 302-17-0; Cl_2CHCO_2H, 79-43-6; Cl_3CCO_2H, 76-03-9; catechol, 120-80-9; resorcinol, 108-46-3; hydroquinone, 123-31-9; 2-methylresorcinol, 608-25-3; orcinol, 504-15-4; naphthoresorcinol, 132-86-5; α-resorcylic acid, 99-10-5; β-resorcylic acid, 89-86-1; γ-resorcylic acid, 303-07-1; acetone, 67-64-1; methyl ethyl ketone, 78-93-3; methyl propyl ketone, 107-87-9; 1-chloro-2,6-dihydroxybenzene, 6201-65-6; 1-chloro-2,4-dihydroxybenzene, 95-88-5; 1,3-dichloro-2,4-dihydroxybenzene, 16606-61-4; 2,3,5-trichloro-2,4-dihydroxybenzene, 26378-73-4; chloroform, 67-66-3; bromoform, 75-25-2.

Literature Cited

(1) Symons, J. M.; Bellar, T. A.; Carswell, J. K.; DeMarco, J.; Kropp, B. K.; Robeck, G. G.; Seeger, D. R.; Slocum, C. J.; Smith, B. L.; Stevens, A. A. *J. Am. Water Works Assoc.* **1975**, *67*, 635.

(2) Stevens, A. A.; Slocum, C. J.; Seeger, D. R.; Robeck, G. G. In "Water Chlorination: Environmental Impact and Health Effects"; Jolley, R. L., Ed.; Ann Arbor Science Publishers: Ann Arbor, MI, 1978; Vol. 1, pp 77–101.

(3) Rook, J. J. *J. Am. Water Works Assoc.* **1976**, *68*, 168.

(4) Rook, J. J. *Environ. Sci. Technol.* **1977**, *11*, 478.

(5) Christman, R. F.; Johnson, J. D.; Hass, J. R.; Pfaender, F. K.; Liao, W. T.; Norwood, D. L.; Alexander, H. J. In "Water Chlorination: Environmental Impact and Health Effects"; Jolley, R. L., et al., Eds.; Ann Arbor Science Publishers: Ann Arbor, MI, 1978; Vol. 2, pp 15–28.

(6) Noack, M. G.; Doerr, R. L. In "Water Chlorination: Environmental Impact and Health Effects"; Jolley, R. L., et al., Eds.; Ann Arbor Science Publishers: Ann Arbor, MI, 1978; Vol. 2, pp 49–58.

(7) Oliver, B. G. In "Water Chlorination: Environmental Impact and Health Effects"; Jolley, R. L., et al., Eds.; Ann Arbor Science Publishers: Ann Arbor, MI, 1980; Vol. 3, pp 141–149.

(8) Youssefi, M.; Zenchelsky, S. T.; Faust, S. D. *J. Environ. Sci. Health, Part A* **1978**, *A13*, 629.

(9) Babcock, D. B.; Singer, P. C. *J. Am. Water Works Assoc.* **1979**, *71*, 149.

(10) Quimby, B. D.; Delaney, M. F.; Uden, P. C.; Banes, R. M. *Anal. Chem.* **1980**, *52*, 259.

(11) Rook, J. J. *Water Treatment Examin.* **1974**, *23*, 234.

(12) Morris, J. C. In "Water Chlorination: Environmental Impact and Health Effects"; Jolley, R. L., Ed.; Ann Arbor Science Publishers: Ann Arbor, MI, 1978; Vol. 1, pp 21–33.

(13) Larson, R. A.; Rockwell, A. L. *Naturwissenschaften* **1978**, *65*, 490.

(14) Rockwell, A. L.; Larson, R. A. In "Water Chlorination: Environmental Impact and Health Effects"; Jolley, R. L. et al., Eds.; Ann Arbor Science Publishers: Ann Arbor, MI, 1978; Vol. 2, pp 67–74.

(15) Larson, R. A.; Rockwell, A. L. *Environ. Sci. Technol.* **1979**, *13*, 325.

(16) Morris, J. C.; Baum, B. In "Water Chlorination: Environmental Impact and Health Effects"; Jolley, R. L., et al., Eds.; Ann Arbor Science Publishers: Ann Arbor, MI, 1978; Vol. 2, pp 29–48.

(17) Norwood, D. L.; Johnson, J. D.; Christman, R. F.; Hass, J. R.; Bobenrieth, M. J. *Environ. Sci. Technol.* **1980**, *14*, 187.

(18) Boyce, S. D.; Hornig, J. F. In "Water Chlorination: Environmental Impact and Health Effects"; Jolley, R. L., et

Environ. Sci. Technol. **1983,** *17,* 211–217

al., Eds.; Ann Arbor Science Publishers: Ann Arbor, MI, 1980; Vol. 3, pp 131–140.
(19) Boyce, S. D.; Barefoot, A. C.; Britton, D. R.; Hornig, J. F. In "Water Chlorination: Environmental Impact and Health Effects"; Jolley, R. L., et al., Eds.; Ann Arbor Science Publishers: Ann Arbor, MI; Vol. 4, in press.
(20) Connick, R. C.; Chia, Y. *J. Am. Chem. Soc.* **1959,** *81,* 1290.
(21) Morris, J. C. *J. Phys. Chem.* **1966,** *70,* 3798.
(22) Lifshitz, A.; Perlmutter-Hayman, B. *J. Phys. Chem.* **1962,** *66,* 701.
(23) Jones, G.; Backstrom, S. *J. Am. Chem. Soc.* **1934,** *56,* 1517.
(24) Farkas, L. *J. Am. Chem. Soc.* **1950,** *72,* 5766.
(25) Griffith, R. O.; McKeown, A.; Winn, A. G. *Trans. Faraday Soc.* **1932,** *28,* 101.
(26) Cotton, F. A.; Wilkinson, G. "Advanced Inorganic Chemistry"; Interscience: New York, 1972; p 476.
(27) Johnson, M. D. In "Bromine and Its Compounds"; Jolles, Z. E., Ed.; Academic Press: New York, 1966; pp 255–317.
(28) Smith, J. G.; Lee, S. F.; Netzer, A. *Water Res.* **1976,** *10,* 985.
(29) Zincke, T. *Ber. Dtsch. Chem. Ges.* **1890,** *23,* 3766.
(30) Moye, C. J. *Chem. Commun.* **1967,** 1966.
(31) Rook, J. J. In "Water Chlorination: Environmental Impact and Health Effects"; Jolley, R. L., et al., Eds.; Ann Arbor Science Publishers: Ann Arbor, MI, 1980; Vol. 3, pp 85–98.
(32) Boyce, S. D.; Barefoot, A. C.; Hornig, J. F. U.S. Environmental Protection Agency: Cincinnati, OH, 1981; EPA C3049 NAET.
(33) Terasawa, T.; Okada, T. *Tetrahedron* **1977,** *33,* 595.
(34) Mueller, W. Patent, Federal Republic of Germany, 2 245 270, Mar 1974.
(35) Mueller, W. H.; Riedel, K.; Kiekeler, H. Patent, Federal Republic of Germany, 2 437 1983, Feb 1976.
(36) Williams, D. H.; Howe, I. *Arch. Mass Spectral Data* **1970,** *1,* 120.
(37) Grasselli, J. G., Ed. "Atlas of Spectral Data and Physical Constants for Organic Compounds"; Chemical Rubber: Cleveland, OH, 1973; p B-229.
(38) Olah, G. A.; Grant, J. L.; Westerman, P. W. *J. Org. Chem.* **1975,** *40* 2102.
(39) Grasselli, J. G., Ed. "Atlas of Spectral Data and Physical Constants for Organic Compounds"; Chemical Rubber: Cleveland, OH, 1973; p B-450.
(40) Mukoyama, Y.; Tauno, T.; Yokokawa, H.; Fleming, J. *J. Polym. Sci.* **1973,** *11,* 3193.
(41) Boyce, S. D. Ph.D. Thesis, Dartmouth, College, Hanover, NH, 1980.
(42) Hendrickson, J. B.; Cram, D. J.; Hammond, G. S. "Organic Chemistry"; McGraw-Hill: New York, 1970; p 655.
(43) Nicholson, A. A.; Meresz, O. "Organics in Ontario Drinking Waters, Part I. The Occurrence and Determination of Free and Total Potential Haloforms"; Pittsburgh Conference on Analytical Chemistry and Applied Spectroscopy, Mar 3, 1976.
(44) Nicholson, A. A.; Meresz, O.; Lemyk, B. *Anal. Chem.* **1977,** *49,* 814.
(45) Pfaender, F. K.; Jonas, R. B.; Stevens, A. A.; Moore, L.; Hass, J. R. *Environ. Sci. Technol.* **1978,** *12,* 438.
(46) Onodera, S. M.; Tabata, M.; Suzuki, S.; Ishikura, S. *J. Chromatogr.* **1980,** *200,* 137.
(47) DePuy, C. H.; Zaweski, E. F. *J. Am. Chem. Soc.* **1959,** *81,* 4920.
(48) DePuy, C. H.; Lyons, C. E.; Rodewald, L. B. *J. Chem. Eng. Data* **1966,** *11,* 102.
(49) Wells, P. R. *Aust. J. Chem.* **1963,** *16,* 165.
(50) Scribner, R. M. *J. Org. Chem.* **1965,** *30,* 3657.
(51) Volbrecht, L.; Huysmans, W. G. B.; Mijs, W. J.; Hagerman, H. J. *Tetrahedron* **1965,** *24,* 6265.
(52) Maignan, C.; Grandguillot, J. C.; Rouessac, F. *Bull. Soc. Chim. Fr.* **1970,** *5,* 2019.
(53) Svec, P.; Sorensen, A. M.; Zibrovsky, M. *Org. Prep. Proc. Int.* **1973,** *5,* 209.
(54) Tomita, M.; Manabe, H.; Homma, K.; Hamada, A. *J. Pharmacobio-Dyn.* **1981,** *4,* S-59.
(55) Vickery, B.; Keberia, F. *Experentia* **1979,** *35,* 299.

Received for review April 14, 1982. Accepted December 9, 1982. Funding for the synthesis of the isotopically labeled resorcinol was provided under EPA Contract C3049NAET.

Mass Transfer Coefficient Correlations for Volatilization of Organic Solutes from Water

Donald Mackay* and Andrew T. K. Yeun

Department of Chemical Engineering and Applied Chemistry, University of Toronto, Toronto, Ontario, Canada M5S 1A4

■ Volatilization rates were measured in a 6-m wind-wave tank for 11 organic compounds of varying Henry's law constants. The data yielded correlations for the liquid- and vapor-phase mass transfer coefficients, confirmed the validity of the two-resistance model, and showed that no interactions occur when solutes volatilize simultaneously. The correlations are expressed in terms of the air friction velocity and the Schmidt number of the compound in air and water, thus providing characterization of the effects of windspeed (through a drag coefficient correlation with friction velocity), solute diffusivity, and temperature. The results suggest that environmental transfer coefficients will be generally lower than those measured in the laboratory.

Introduction

Volatilization may be an important environmental pathway for organic compounds that have relatively high Henry's law constants or air–water partition coefficients. The generally accepted method of calculating volatilization rates is the two-resistance model originally devised by Whitman (*1*) and applied to environmental volatilization first by Liss and Slater (*2*) and later by Mackay and Leinonen (*3*) and Smith et al. (*4*). The model expresses mass flux N (mol/(m^2 s)) of the volatilizating solute as

$$N = K_{\mathrm{OL}}(C_{\mathrm{W}} - P/H) \qquad (1)$$

where

$$1/K_{\mathrm{OL}} = 1/K_{\mathrm{L}} + RT/HK_{\mathrm{G}} \qquad (2)$$

where K_L, K_G, and K_{OL} are the liquid, gas, and overall liquid mass transfer coefficients (m/s), H is the Henry's law constant (atm m^3/mol), R is the gas constant (82×10^{-6} atm m^3/(mol K)), T is absolute temperature (K), C_W is the solute concentration in water (mol/m^3), and P is the solute partial pressure in the atmosphere (atm).

The critical variables are H (which may be obtained from solubility and vapor-pressure data or may be measured directly by gas stripping (5)) and the transport terms K_L and K_G. Several laboratory and field measurements have been made of K_L and K_G for solutes such as oxygen, CO_2, radon, and various organic solutes, and correlations have been proposed (*6–11*). K_L and K_G depend on the prevailing turbulence level as determined by water currents or wind, on temperature, and on properties of the solute such as diffusivity or molecular size.

0013-936X/83/0917-0211$01.50/0 © 1983 American Chemical Society

Table I. Physical and Transport Properties of the Compounds at 20 °C

compound	solubility, mol/m^3	vapor pressure, atm	H_3, atm m^3/mol	D_G, cm^2/s	$10^5 D_L$, cm^2/s	Sc_G	Sc_L
benzene	22.8	0.100	4.39×10^{-3}	0.088	0.957	1.99	1021
toluene	5.59	0.029	5.18×10^{-3}	0.079	0.844	2.22	1155
1,2-dichloropropane	25.0	0.052	2.07×10^{-3}	0.081	1.070	2.17	939
1,2-dibromoethane	23.0	0.015	6.29×10^{-4}	0.075	0.909	2.34	1075
chlorobenzene	4.44	0.012	2.61×10^{-3}	0.080	0.858	2.19	1137
carbon tetrachloride	5.20	0.118	2.27×10^{-2}	0.081	0.919	2.17	1062
2-pentanone	500	0.016	3.16×10^{-5}	0.081	0.871	2.17	1120
2-heptanone	38.0	0.0034	9.00×10^{-5}	0.068	0.722	2.58	1340
1-pentanol	307	0.0037	1.03×10^{-5}	0.079	0.828	2.22	1177
2-methyl-1-propanol	1280	0.0132	1.03×10^{-5}	0.088	0.926	1.99	1056
1-butanol	1040	0.0058	5.57×10^{-6}	0.088	0.966	1.99	1305

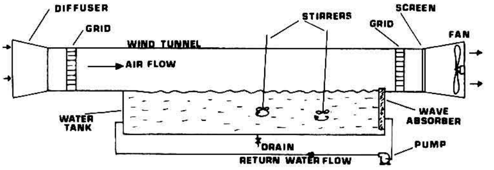

Figure 1. Schematic diagram of the wind-wave tank.

In this work laboratory wind-wave tank experiments are described in which the volatilization rates of solutes of varying Henry's law constant were studied with the objectives of (i) confirming the validity of the two-resistance model when applied to wind-wave tank volatilization, (ii) devising new correlations for K_G and K_L as a function of windspeed and molecular properties, especially at high windspeeds , (iii) investigating the possibility of interactions between solutes that are volatilizing simultaneously, and (iv) elucidating the apparent difference between volatilization rates in the environment and in laboratory tanks as has been noted by Schwartzenbach et al. (*12*). The validity of the two-resistance model cannot be regarded as being in doubt, but there are few studies in which it has been tested on environmental air–water systems. A recent example of such a test is the work of Atlas et al. (*13*). The work described here is part of a larger report on volatilization processes (*14*).

Experimental Section

The wind-wave tank used for the volatilization study, shown in Figure 1, was 6 m long, 0.61 m deep, and 0.60 m wide and was located under a wind channel 9.35 m long equipped with diffusers at both ends to smooth out the turbulence of the airflow. Honeycomb structures of thin-wall paper tubes were installed at both ends of the wind tunnel to eliminate the swirling motion of the airflow produced by the fan. Wooden screens of different porosity were used to control the airspeed. An aluminum plate 0.5 m long was attached to the end of the upwind section and inclined at an angle of 5° to the water surface to provide a smooth transition between the adjoining air- and waterflow. Water was circulated to maintain a uniform concentration along the tank, by a 1.5-HP pump with a gate valve for adjusting the recirculation rate. In addition, two stirrers (Canlab high torque) were mounted on the tank to enhance the water mixing process. A wave absorber was attached to the downwind end of the tank to dissipate the wave energy and minimize reflection.

Velocity profiles of the gas phase were measured at two locations, 1.4 and 4.2 m from the leading edge of the tank, by using a Pitot tube of Prandtl design that was mounted on a motor-driven traverse mechanism. The height of the Pitot tube from the water surface was measured by a cathetometer. The drift velocity of the wind-driven current was measured by timing small pieces of wax paper as they moved along the surface. Air humidity was measured at both upwind and downwind ends of the tank. The interfacial temperature was measured approximately by dipping a thermometer (accurate to 0.1 °C) 0.5 cm below the water surface.

The water evaporation rates were measured by using a constant-water-level device operated on the "chicken feeder" principle. The length of these experiments usually lasted over 48 h to obtain a reasonable amount of evaporation and hence accurate transfer coefficients.

Volatilization experiments of 11 organic compounds at various windspeeds were carried out, Table I giving a list of the compounds and their physical and chemical properties. Diffusivities were calculated from the Fuller, Schettler, Giddings correlation (air) and the Wilke, Chang correlation (water) (Reid et al. (*25*)). The chemicals were usually dissolved in the water by using a sump pump, but for compounds that were slightly soluble and denser than water, saturated solutions were first prepared and then diluted in the water tank. The duration of the experiments varied from 8 h for chlorinated compounds to over 50 h for alcohols. The initial concentration of the solutes in the tank varied depending on the water solubilities. For chlorinated compounds, which have low solubility, the initial concentrations ranged from 0.1 to 0.01 mol/m^3. For alcohols and ketones, which have a much higher solubility, the initial concentrations were usually 0.5 mol/m^3. In a typical run, a 10-fold change in the solute concentration would occur.

Water samples were analyzed by a gas chromatograph (Hewlett-Packard Model 5840A) equipped with a flame ionization detector. The column used was a 0.5 mm o.d., 50 m long open tubular glass column (WCOT) coated with SE 30 (methylsilicone polymer). The compound in the water was extracted by a "purge and trap" sampler (Hewlett-Packard Model 7675A) using nitrogen for 10 min and was absorbed by a short Tenax GC column followed by themodesorption at 200 °C before being directly introduced into the capillary column. For single compound analysis, the oven condition was set isothermally at the boiling point of the compound. In analyzing a mixture, the oven condition was set initially at 80 °C and the temperature programmed at a rate of 10 °C/min up to 200 °C. The detector temperature was 300 °C.

Results

Velocity profiles were measured in the wind-wave tank for windspeeds from 5.96 to 13.2 m/s. Differences were found for the profiles measured at the two locations but at the same windspeed, thus average values of the profile parameters were used. In particular, the friction velocity at the downwind location showed an increase of 15–25%

Table II. Hydrodynamic Parameter Results

U_∞, m/s	U^*, m/s	Z_0, cm	drift velocity, m/s	Re^*	10^3C_D
13.20	0.993	0.0906	0.395	54.2	5.08
11.67	0.849	0.0713	0.344	36.5	4.79
10.31	0.675	0.0429	0.290	17.5	4.77
8.57	0.455	0.0209	0.222	5.73	3.93
7.09	0.381	0.0127	0.200	2.91	3.37
5.96	0.271	0.0044	0.158	0.72	2.66

over the upwind location. The data indicated that the airflow generally developed behavior characteristic of turbulent flow in a boundary layer over a roughened surface. The logarithmic velocity law below was found to describe the data adequately where

$$U/U^* = (1/K)\ \ln\ (Z/Z_0) \tag{3}$$

where U is the velocity (m/s) at an anemometer height of Z (m), U^* (m/s) is the air side friction velocity; Z_0 (m) is the roughness height, and K is the Von Karman constant, equal to 0.4. The average drag or friction coefficient C_D, which can be calculated from the friction velocity and the windspeed, is defined as

$$C_D = \tau_a/\rho_a U_\infty^2 = (U^*/U_\infty)^2 \tag{4}$$

where τ_a (N/m^2) is the wind stress, ρ_a (kg/m^3) is the air density, and U_∞ is the free stream velocity. The fluid mechanical parameters, which included the friction velocity, roughness height, drag coefficient, and drift velocity, are given in Table II.

A component mass balance of the solute in the water gives the following integral equation, which had been simplified by assuming that the average and initial water concentrations were much greater than the concentration in equilibrium with the air phase:

$$C = C_0 \exp(-K_{OL}t/h) \tag{5}$$

where C and C_0 (mol/m^3) are the average concentration and initial concentrations of the compound in the water phase and h (m) is the mean depth of water. The data from a mass transfer run were analyzed by using linear regression to calculate K_{OL} from the slope. The data obtained for alcohols and ketones showed a fair amount of scatter. The reason may be the analytical difficulties encountered in which the stripping efficiency for this class of compounds at room temperature is low. Figure 2 shows the decay of concentration in benzene and 1-butanol volatilization experiments. Values of K_{OL} measured for different compounds at various windspeeds are given in Table III. A few runs were carried out using a mixture of compounds in which the individual mass transfer coefficients have been measured to study if any interactions among the compounds exist. It was found that the difference between the two values were within 10% error, thus interactions at such a low concentration are unlikely to exist. The data are given in Table IV.

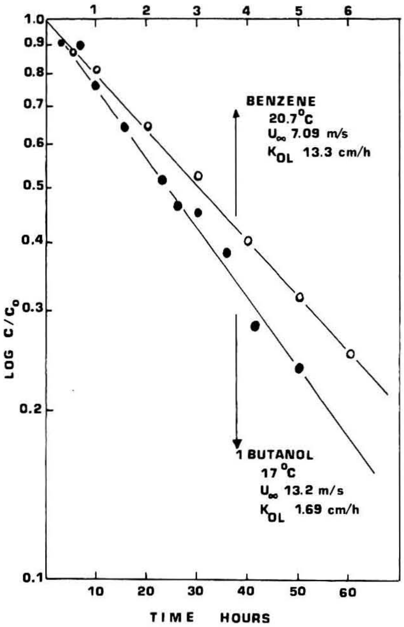

Figure 2. First-order decay in concentration for benzene and 1-butanol.

Water transfer coefficients at different speeds were estimated by measuring the amount of water evaporated by using the "chicken feeder" apparatus, the humidity of the air phase, and at the interface from the following expression:

$$K_G = \Delta V/\{(C_i - C_G)V_W A \Delta t\} \tag{6}$$

where ΔV (m^3) is the volume of water evaporated, C_i and C_G (mol/m^3) are the concentration of water at the interface and at the gas phase, V_W is the molar volume of water, A (m^2) is the normal surface area, and Δt (h) is the duration of the experiment. The measured K_G values are given in Table III.

Discussion

The drag coefficients show a definite trend of increasing with windspeed as is generally observed. The absolute

Table III. Mass Transfer Coefficients from the Wind-Wave Tank Expressed in 10^6 m/s with Correlated Values in Parentheses

	windspeed, m/s					
compound	13.2	11.67	10.31	8.57	7.09	5.96
benzene	94.4 (99.1)	73.3 (82.4)	62.5 (68.4)	51.1 (51.8)	36.9 (39.0)	31.6 (30.0)
toluene	93.6 (93.4)	79.4 (77.6)	68.9 (64.4)	51.6 (48.9)	46.9 (36.7)	26.6 (28.3)
1,2-dichloropropane	93.9 (89.2)		63.9 (61.6)		35.8 (35.1)	28.9 (27.0)
chlorobenzene	89.7 (89.7)	78.0 (74.6)		55.0 (46.9)	41.9 (35.3)	
1,2-dibromomethane	77.2 (83.1)		54.7 (57.4)	45.3 (43.5)		23.6 (25.2)
carbon tetrachloride		79.4 (77.5)	63.3 (64.4)	51.1 (48.8)	39.1 (36.7)	
2-pentanone	33.1 (28.6)	29.7 (23.8)		21.1 (14.9)		13.3 (8.67)
2-heptanone	42.7 (44.9)	31.6 (37.3)		23.0 (23.5)		16.9 (13.6)
1-pentanol	8.11 (8.06)			5.75 (4.22)		3.80 (2.45)
2-methyl-1-propanol	7.30 (10.5)		5.75 (7.28)		3.81 (4.15)	
1-butanol	4.69 (7.64)			3.58 (3.99)		2.02 (2.31)
water evaporation	71 100	55 200	39 200	29 700	22 200	19 400

Table IV. **Volatilization of Mixtures: Values in Parentheses Are for the Substances Alone under Identical Conditions**

windspeed, m/s	K_{OL}, cm/h							
	2-butanol	2-methylpropanol	2-heptanone	benzene	chlorobenzene	1,2-dichloropropane	benzene	toluene
6.0	0.820 (0.724)	1.06 (ca. 1.2)	5.71 (6.07)	12.50 (11.40)	11.50 (ca. 11.0)	11.20 (10.35)		
8.6	1.36 (1.26)	1.66 (ca. 1.6)	8.77 (8.26)	16.7 (18.4)	15.7 (19.8)	15.6 (ca. 18.0)		
10.7							24.6 (22.5)	24.1 (24.8)

values are higher than those that occur environmentally (which rarely exceed 3×10^{-3}) (*15*). This increase in C_D has also been observed by Hidy and Plate (*16*). An interpretation of this effect is that the airflow is exerting a greater force on the water in the laboratory because at short fetches the velocity profile or flow characteristics have not settled to a stable configuration, the water being accelerated by the airflow rather than maintained at constant velocity. The surface drift velocity measurements showed that the water surface was accelerating but had reached 2.8% of windspeed by the end of the tank. The roughness Reynolds numbers are in the transition and rough regions (i.e., >2.0), and thus it is unwise to extrapolate from these results to lower windspeeds, at which quite different hydrodynamic conditions may prevail. The presence of a mass transfer transition from a "calm" low-speed regime to a "rough" high-speed regime was observed by Cohen et al. (*6*).

It can be noted that the Charnock group $Z_0 g/U^{*2}$ shows fair constancy except at the lowest windspeed, a mean value of 0.0093 applying above 6 m/s. This is in good agreement with the 0.010 suggested by Smith (*17*) and provides confirmation that the surface roughness values are reasonable. The low-windspeed discrepancy may be an indication of a regime change.

These results suggest that it may be possible to link laboratory and environmental hydrodynamics and correlate both mass transfer rates by using friction velocity U^* or roughness Reynolds number (Re^*), the friction velocity being measured in the laboratory (and correlated against velocity) and estimated for environmental conditions by using, for example, the correlation of Smith (*17*) against 10-m windspeed:

$$C_D = 10^{-4}(6.1 + 0.63U_{10}) \qquad (7)$$

The correlation obtained here was

$$C_D = 4.0 \times 10^{-4} U_\infty \qquad (8)$$

Since U^* is $U_\infty C_D^{0.5}$, U^* can be easily estimated. Z_0 can be estimated if desired from the Charnock group for equilibrium conditions.

Examination of the predominantly liquid-phase resistant mass transfer data showed that K_L is well correlated with U^* and that there is little merit in including Re^* since the power on Re^* is only −0.03. Similar results were obtained when fitting the gas-phase resistant water evaporation data and the data for compounds in which there is resistance in both phases. It was found that

$$K_L = 1.02 \times 10^{-4} U^* \text{ (benzene and toluene)} \qquad (9)$$

$$K_G = 6.5 \times 10^{-2} U^* \text{ (water)} \qquad (10)$$

This unique dependence on U^* (water) is in agreement with the recent work of Wolff and van der Heijde (*8*) and of Cohen (*26*).

The entire data set was then fitted by using these equations, but it then became necessary to correct K_L and K_G for solute diffusivity, molecular size, or molecular weight. Although other molecular properties can be used to correct for differences between solutes, there is overwhelming evidence that the correct quantity is Schmidt number (Sc), which is the dimensionless ratio of viscosity/(density × diffusivity) and is typically in the range 0.5–2.0 for gases but 500–2000 for liquids (*18*). An attractive feature of Sc is that it can also express temperature dependence, notably for liquids in which case Sc decreases rapidly with increasing temperature as diffusivity rises and viscosity falls.

It should be noted that K_G will depend also on the stability conditions, i.e., the relative air and water temperatures. This dependence is not expressed here.

For steady-state film diffusion, the power on Sc should be −1.0, but since the process observed here is probably unsteady-state penetration mass transfer to eddies or roll cells of fluid, a lower dependence is indicated, −0.5 applying to penetration-type transfer. From an examination of the data obtained here, related studies (*14*) and the work of Tamir and Merchuk (*18, 19*) for K_G, Tsivoglou (*7*) for K_L, and Downing and Truesdale for temperature dependence of K_L (*20*), and other studies in the chemical engineering literature (*27*), it is concluded that the most likely dependencies are

$$K_L \propto Sc_L^{-0.5} \qquad K_G \propto Sc_G^{-0.67}$$

It is noteworthy that the careful study by Tsivoglou (*7*), which gave a dependence of K_L inversely on molecular diameter, is consistent with the above since diffusivity is proportional to molar volume to the power −0.6 and molar volume is proportional to diameter to the power 3, and thus $Sc^{-0.5}$ is proportional to diameter to the power −0.9. The Downing and Truesdale temperature dependence of 1.52–3.12% per degree agrees well with 2.8% per degree predicted by using $Sc_L^{-0.5}$.

Accordingly, correlation equations containing this dependence were fitted to the entire data set to yield

$$K_L = 34.1 \times 10^{-4} U^* Sc_L^{-0.5} \qquad (11)$$

$$K_G = 46.2 \times 10^{-3} U^* Sc_G^{-0.67} \qquad (12)$$

Combining these correlations with the C_D correlations relating U_{10} and U_∞ to U^* yields separate correlations for the laboratory tests and environmental conditions, namely

$$K_L = 68.2 \times 10^{-6} U_\infty^{1.5} Sc_L^{-0.5} \text{(laboratory)} \qquad (13)$$

$$K_L = 34.1 \times 10^{-6}(6.1 + 0.63U_{10})^{0.5} U_{10}\, Sc_L^{-0.5} \text{ (environment)} \qquad (14)$$

$$K_G = 92.4 \times 10^{-5} U_\infty^{1.5} Sc_G^{-0.67} \text{ (laboratory)} \qquad (15)$$

$$K_G = 46.2 \times 10^{-5}(6.1 + 0.63U_{10})^{0.5} U_{10}\, Sc_G^{-0.67} \text{ (environment)} \qquad (16)$$

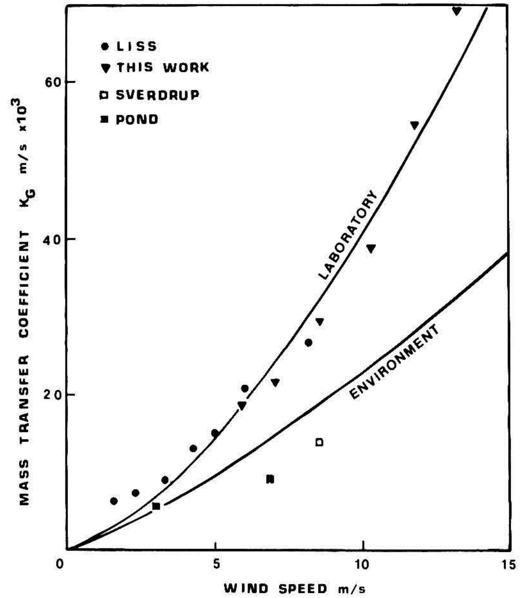

Figure 3. K_G data corrected to a Schmidt number of 0.6 plotted vs. windspeed.

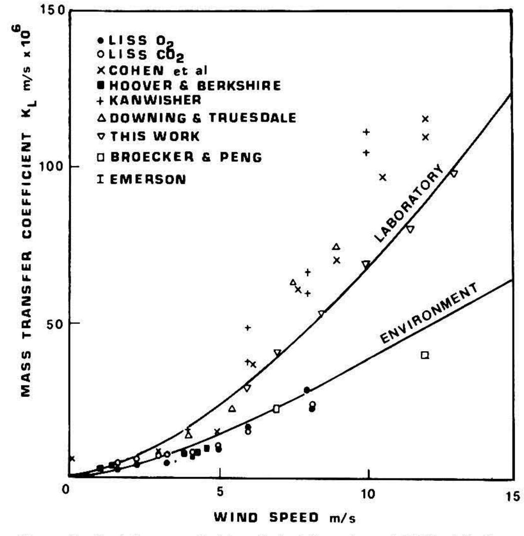

Figure 4. K_L data corrected to a Schmidt number of 1000 plotted vs. windspeed.

It is believed that these equations apply to windspeeds above approximately 5 m/s or to U^* greater than 0.3 m/s. At lower windspeeds, the equations may be inaccurate.

An implication of these results is that at the same windspeed, there will generally be larger K_G and K_L values in small laboratory tanks, thus partly explaining the discrepancy observed by Schwartzenbach et al. (*12*). Obviously, direct application of laboratory mass transfer coefficients to the environment using windspeed as the only determinant is inaccurate.

Comparison of the experimental and correlated values for all the solutes is a test of the validity of the two-resistance model since the coefficients are "weighted" according to the Henry's law constant. The data in Table III showed that the model is supported.

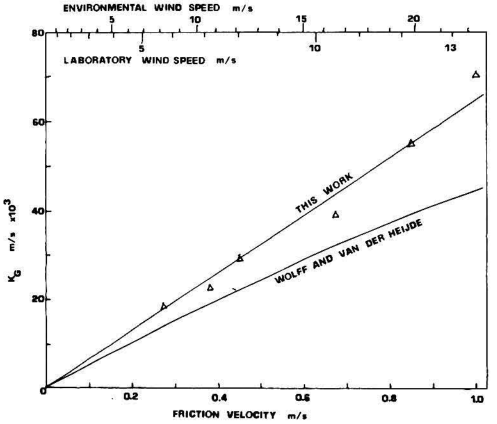

Figure 5. Present K_G correlation (Schmidt number 0.6) and that of Wolff and van der Heijde (*8*).

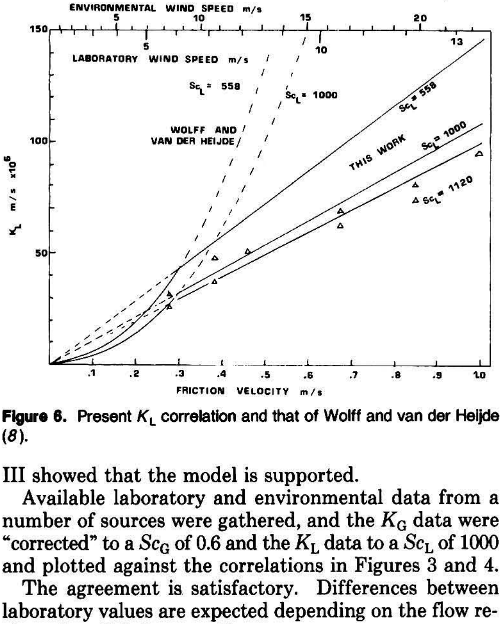

Figure 6. Present K_L correlation and that of Wolff and van der Heijde (*8*).

Available laboratory and environmental data from a number of sources were gathered, and the K_G data were "corrected" to a Sc_G of 0.6 and the K_L data to a Sc_L of 1000 and plotted against the correlations in Figures 3 and 4.

The agreement is satisfactory. Differences between laboratory values are expected depending on the flow regime since it influences C_D.

Recently Wolff and van der Heijde (8) have proposed friction velocity correlations for K_L and K_G in the form of expressions for the stagnant film thickness defined as the molecular diffusivity divided by the mass transfer coefficient. Such a formulation is inconsistent with a fractional power on the Schmidt number. Figures 5 and 6 show these correlations and eq 11 and 12 as plots of K_G and K_L vs. U^* with laboratory and 10-m windspeeds inserted as separate scales. The K_G curves are similar in form, but the present values are consistently higher. The reason is not known. The Wolff–van der Heijde K_L correlation gives lower K_L values below a U^* of 0.3 m/s, but since it contains a power of 2.2 on U^* as distinct from 1.0 used here, it greatly overpredicts K_L at high windspeeds. The present correlation is believed to be more accurate at high windspeeds, but the Wolff–van der Heijde correlation is believed to be better below a U^* of 0.3 m/s. The available environmental K_L data at low windspeeds are in better accord with the Wolff–van der Heijde equation. Expressing this equation in Schmidt number form and forcing a power of -0.5 on Sc_L yields

$$K_L = 6.2 \times 10^{-7} + 6.11 \times 10^{-4}U^{*2.2} \quad (Sc(O_2) = 558) \tag{17}$$

or

$$K_L = 6.2 \times 10^{-7} + 0.0144U^{*2.2}\, Sc_L^{-0.5} \tag{18}$$

The friction velocity can be replaced by 10-m windspeed with use of the correlation for C_D such as those of Smith (*17*) or Wu (*15*).

At zero windspeeds the above K_L correlation indicates a "still-air" value of 6.2×10^{-7} m/s or 0.22 cm/h, corresponding to a stagnant film thickness of 3.2 mm. It is likely that K_G also tends to a still-air value at zero windspeed, Wolff and van der Heijde suggesting 2×10^{-4} m/s or 72 cm/h. This corresponds to a stagnant film thickness of 12 cm, which seems intuitively to be too large. Their film thickness at U^* of 0.05 m/s is approximately 1 cm, and thus it seems unlikely that it increases 12-fold in this velocity region. Our best estimates of these still-air values based on these data and a perusal of the literature are

$$K_L = (1.0 \pm 0.5) \times 10^{-6} \text{ m/s}$$

$$K_G = (1.0 \pm 0.5) \times 10^{-3} \text{ m/s}$$

These terms can be included in the correlation. They make a negligible contribution at most windspeeds. To be completely rigorous, they should contain a diffusivity dependence, but its nature has not been established.

At high wind speeds (i.e., $U^* > 1.0$ or $U_{10} > 22$ m/s) these equations may fail due to frequent wave breaking and spray transfer. Fortunately these conditions prevail for only brief periods of time.

In summary we suggest that for laboratory and environmental calculations the following equations be used:

$$K_G = 1.0 \times 10^{-3} + 46.2 \times 10^{-3}U^*\, Sc_G^{-0.67} \tag{19}$$

$$K_L = 1.0 \times 10^{-6} + 34.1 \times 10^{-4}U^*\, Sc_L^{-0.5}\ (U^* > 0.3) \tag{20}$$

$$K_L = 1.0 \times 10^{-6} + 144 \times 10^{-4}U^{*2.2}\, Sc_L^{-0.5}\ (U^* < 0.3) \tag{21}$$

where $U^* = (6.1 + 0.63U_{10})^{0.5}U_{10}$(environment) or for these laboratory conditions

$$U^* = 2.0 \times 10^{-2}U_\infty^{1.5}$$

For other laboratory conditions different $U^* - U_\infty$ relations will apply.

The tests with solute mixtures confirm the intuitively reasonable assumption that the solutes volatilize independently. No interaction is expected at these concentrations.

A cautionary note is appropriate when applying these correlations to environmental conditions. The presence of organic or mineral sorbing suspended solids will reduce the solute fugacity or partial pressure and correspondingly reduce the volatilization rate. This has been of relatively little concern until recently since the sorbents are usually present at very low concentrations. The recent studies by O'Connor and Connolly (*21*) and Means and Wijayaratne (*22*) show that sorbents at low concentrations display unusually variable and large partition coefficients and thus the calculation of the fraction of solute that is in true solution is more difficult and less reliable than has been assumed. This is obviously an area in which a better understanding of the fundamental sorption phenomenon is required in order that more reliable volatilization calculations can be made. Particularly important is the role of sorbents in trapping or transporting the solute close to the interface.

Finally, it is recognized that these correlations have several weaknesses and can be improved. The low windspeed and still-air values may have a different diffusivity dependence than is indicated here. The water friction velocity is a preferable correlating parameter for K_L. The stability dependence of K_G is not included. These and other aspects of characterizing transfer across a sheared, wavy interface have been reviewed recently by Cohen (*26*). Including these dependencies introduces greater accuracy and complexity. It is likely that there will emerge a series of volatilization correlations varying in complexity and accuracy from which selection can be made, appropriate to the requirements of the environmental situation being quantified. These correlations are regarded as a reasonably simple set that can be used for general environmental modeling purposes and contain the dominant determinants of volatilization rate.

Conclusions

Wind-wave tank volatilization data for 11 solutes of varying Henry's law constant have been obtained at high windspeeds. The data confirm the validity of the two-resistance model for mass transfer and show that no interaction occurs when solutes are volatilized simultaneously. New correlations have been obtained in which friction velocity is used as the hydrodynamic parameter and the Schmidt number characterizes the solute diffusion properties and temperature dependence. By relating friction velocity to windspeed through the drag coefficient, it is possible to correlate liquid and vapor mass transfer coefficients against windspeed. This approach indicates that laboratory test conditions will generally result in higher mass transfer coefficients that occur in the environment at the same windspeed. It is suggested that the correlations devised here be used in conjunction with the low-windspeed Wolff–van der Heijde correlation to cover the range of environmental wind conditions.

Acknowledgments

We are grateful to Y. Cohen for constructively critical comments.

Literature Cited

(1) Whitman, W. G. *Chem. Metal. Eng.* **1923**, *29*, 146.
(2) Liss, P. S.; Slater, P. G. *Nature (London)* **1974**, *247*, 181.
(3) Mackay, D.; Leinonen, P. J. *Environ. Sci. Technol.* **1975**, *9*, 1178.
(4) Smith, J. H.; Bomberger, D. C.; Haynes, D. L. *Environ. Sci. Technol.* **1980**, *14*, 1332.
(5) Mackay, D.; Shiu, W. Y.; Sutherland, R. P. *Environ. Sci. Technol.* **1979**, *13*, 333.
(6) Cohen, Y.; Cocchio, W.; Mackay, D. *Environ. Sci. Technol.* **1978**, *12*, 558.
(7) Tsivoglou, E. C.; O'Connell, R. L.; Walter, C. M.; Godsil, P. J.; Langdon, G. S. *J. Water Pollut. Control Fed.* **1965**, *37*, 1343.
(8) Wolff, C. J. M.; van der Heijde, H. B. *Chemosphere* **1982**, *11*, 103–117.
(9) Deacon, E. L. *Tellus* **1977**, *29*, 363.
(10) Broecker, W. S.; Peng, T. H. *Tellus* **1974**, *26*, 21.
(11) Emerson, S. *Limnol. Oceanogr.* **1975**, *20*, 754.
(12) Schwartzenbach, R. P. K.; Kubica, E. M.; Giger, W.; Wakehorn, S. C. *Environ. Sci. Technol.* **1979**, *13*, 1307.
(13) Atlas, E.; Foster, R.; Giam, C. S. *Environ. Sci. Technol* **1982**, *16*, 283–286.
(14) Mackay, D.; Shiu, W. Y.; Bobra, A.; Billington, J.; Chau, E. C.; Yeun, A.; Ng, C.; Szeto, F. U.S. EPA Report EDA 600/S3-82-019, 1982, NTIS PB 82-230-939.

Environ. Sci. Technol. **1983**, *17*, 217–223

(15) Wu, J. *J. Geophys. Res.* **1969**, *74*, 444.
(16) Hidy, G. M.; Plate, E. J. *J. Fluid Mech.* **1966**, *26*, 651.
(17) Smith, S. D. *J. Phys. Oceanogr.* **1980**, *10*, 709.
(18) Tamir, A.; Merchuk, J. D. *Chem. Eng. Sci.* **1978**, *33*, 1371.
(19) Tamir, A.; Merchuk, J. D. *Chem. Eng. Sci.* **1979**, *34*, 1077.
(20) Downing, A. L.; Truesdale, G. A. *J. Appl. Chem.* **1955**, *5*, 570.
(21) O'Connor, D. J.; Connolly, J. P. *Water Res.* **1980**, *14*, 1517–1523.
(22) Means, J. C.; Wijayaratne, R. Science (*Washington, D.C.*) **1982**, *215*, 968–970.
(23) Pond, S.; Phelps, G. T.; Paquin, J. E.; McBean, G.; Steward, R. W. *J. Atmos. Sci.* **1971**, *28*, 901.
(24) Sverdrup, H. V. *J. Mar. Res.* **1937**, *1*, 3.
(25) Reid, R. C.; Sherwood, J. M.; Prausnitz, T. K. "The Properties of Gases and Liquids", 3rd ed.; McGraw-Hill: New York, 1977.
(26) Cohen, Y. Report N CITR 82-4 of National Center for Intermedia Transport, University of California, Los Angeles, CA, 1982.
(27) Sherwood, T. K.; Pigford, R. L.; Wilke, C. R. "Mass Transfer"; McGraw-Hill: New York, 1975.

Received for review June 21, 1982. Accepted December 27, 1982. We are grateful to the U.S. Environmental Protection Agency and the Ontario Ministry of the Environment for financial support.

Chemical Changes in Concentrated, Acidic, Metal-Bearing Wastewaters When Treated with Lime

Dennis R. Jenke and Gordon K. Pagenkopf*

Department of Chemistry, Montana State University, Bozeman, Montana 59717

Frank E. Diebold

Department of Chemistry, Montana College of Mineral Science and Technology, Butte, Montana 59701

■ Lime neutralization of acidic wastewaters can prove to be an effective treatment process provided sufficient lime is added. The chemical changes that occur in the system are extensive and varied. Precipitation is predominant with complexation, oxidation, and adsorption playing major roles. Total chemical analyses have identified the chemical changes, and controlled laboratory simulations have identified the relative importance of the physical–chemical processes. Exchange of oxygen and carbon dioxide are discussed, and optimum lime addition rates are predicted by thermodynamic computer simulation.

Appropriate disposal of acid-bearing waters resulting from base-metal industrial works and coal mine drainage has and continues to be a major problem. There are many situations where inappropriate disposal of industrial wastes has resulted in severe degradation of surface water and groundwater quality (*1–6*). Previous metal mining operations have also resulted in major alterations in water quality (*7–10*); this has been documented for coal mine drainage (*11*).

The techniques that have been developed for treatment of these waters includes flash distillation (*12*), freezing (*13*), foam fractionation (*14*), electrochemical oxidation (*15*), reverse osmosis (*16*), ion exchange (*17*), biological concentration (*18*), sulfide precipitation (*19*), and lime neutralization. Because of economic considerations lime neutralization with subsequent precipitation is one of the most popular.

The chemistry associated with the lime neutralization process is diverse and includes a variety of physical–chemical reactions. The application of equilibrium thermodynamics to the neutralization of acidic water originating from a coal mine and laboratory simulations has been successful for prediction of solution pH (*20*) and the salts present in the sludge (*21*). The focus of this report is an interpretation of the chemistry that occurs when highly concentrated acidic waters resulting from the Anaconda Mining Company's Butte, MT, operation are lime neutralized. The reactions include acid–base, precipitation, complexation, oxidation, gas exchange, adsorption, and ion exchange.

Systems Description

Treatment Process. The process employed by the Anaconda Mining Co. at its Butte, MT, operation utilizes lime-fortified froth flotating concentrator tailings to neutralize approximately 1.1×10^7 L (3×10^6 gallons) of acidic solution daily. A schematic description is shown in Figure 1. The acid solutions, which represent water pumped from the lower level of the underground mine system and effluent from an electrolytic copper recovery plant, are mixed with the concentrator slurry in a large wooden mixbox and are directed to a settling basin. After sedimentation the solution is either recycled through the concentrator system or discharged to the surface water through a decant tower system. The mixbox consists of a mixing chamber (1.8 m by 2.4 m by 3.7 m deep) and an exit slide that is 0.9 m wide, 0.9 m deep, and 62.5 m long. The slide is inclined at 11° and baffled to promote turbulence. The residence time in the mixbox is approximately 15 s; residence time in the settling basin is on the order of 2 days.

Laboratory Simulation. The field process was simulated by titration of the acid waste solution with fortified concentrator solution under controlled laboratory conditions. The amount of CaO added to fortify the concentrator solution varied such that mixing with the acid solution produced slurries that had pH values ranging from 4 to 10. Specifically, 75 mL of fortified concentrator solution was added to 40 mL of filtered effluent from the copper recovery plant. The solution was mixed for 1 min, analyzed for pH, transferred to a centrifuge bottle, and centrifuged at 5000 rpm for 5 min. The supernate was filtered through 0.45-μm paper, analyzed for pH, chemically quenched by the addition of 2 mL of concentrated HCl, and stored for further analysis. The precipitates were dried at 150 °C for 5 h and dissolved in 20 mL of 4 M HCl for analysis. Solutions and precipitates were analyzed, and the acid-neutralizing capacity of the fortified concentrator solution was determined by titration with 0.050 N HCl.

0013-936X/83/0917-0217$01.50/0

Table I. Chemical Composition (mg/L) of Acid Influents

	precipitation plant effluent[a]		Kelly mine water[a]	
	range	av	range	av
Al	490-650	575 ± 47	85-150	124 ± 22
Ca	120-375	153 ± 75	135-290	214 ± 39
Cu	60-95	126 ± 31	23-34	29 ± 4
Fe^{2+}	900-1800	1225 ± 205	480-1500	813 ± 300
Fe^{3+}	5-25	15 ± 5	1-5	3 ± 2
K	0.2-2.3	0.8 ± 0.6	14.2-25.5	21.7 ± 4.1
Mg	525-655	592 ± 45	170-260	227 ± 33
Mn	185-245	202 ± 35	65-105	88 ± 15
Na	14.3-31.9	21.4 ± 5.0	14.2-100	72.1 ± 34.4
Si	41-67	48 ± 7	18-27	22 ± 2
Zn	555-790	660 ± 66	105-75	155 ± 23
SO_4^{2-}	6250-11425	9975 ± 1475	2900-570	4750 ± 720
flow, g/min	4200-5400	4690 ± 575	2700-6200	4470 ± 1050
flow, L/s	265-340	295 ± 36	170-391	282 ± 66
pH	1.2-3.4	2.3 ± 0.7	2.1-3.2	2.5 ± 0.3

[a] Data for 16 sampling trips.

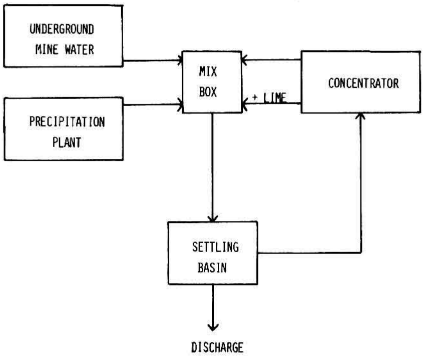

Figure 1. Schematic of the Anaconda Company's Butte, MT, wastewater treatment process.

Computer Simulation. The aqueous chemical equilibrium computer program REDEQL·EPAK (*22*) was modified to allow modeling of the mixing processes and the addition of chemical reagents to the aqueous systems. While a more detailed characterization of the computational algorithm used in this program has been presented elsewhere (*23*), the program in general assumes thermodynamic equilibrium and solves stability constant expressions with Newton–Raphson iteration. The input data include total chemical composition, flow-rate data of each influent stream, and estimates of lime addition rates. Electroneutrality was achieved by adjustment of total sulfate concentration. Calculated thermodynamic supersaturation of the influents was allowed to persist; however, for all mixtures produced and all simulations performed, thermodynamic equilibrium was assumed and precipitation occurred. For simulation of the treatment process, the lime added (weight per unit volume) was assigned a stoichiometry of $Ca(OH)_2$. The output provides an identification of solid phases, distribution of mass between solid and solution, speciation within the solution phase, and the solution pH.

Experimental Section

Sample Collection. The treatment process involves mixing of two acid and two concentrator solutions, each of which was routinely sampled. In addition, samples were obtained after mixing and from the settling pond. The acid solutions were collected by passing a rinsed, narrow-mouthed galvanized steel scoop through the liquid as it falls from the transport pipe into the mixbox and were transferred to polyethylene bottles for storage. In order to ensure sample representability, the high suspended solid solutions (concentrator slurry and mixbox effluent) were sampled by partial flow diversion with use of a 2.5-cm diameter steel nozzle attached to a 2.4-m section of rubber hose that was held in the stream. Samples were collected at various points along the vertical and horizontal extent of the transport pipe and were recombined to form a single composite. Four to six samples were combined to form the composite, which appeared to provide reasonable access to the suspended solids present. The samples from the settling pond were grab sampled at the decant tower. Solution flow rates were obtained from calibrated flow meters or by mass balance calculations (*24*).

Analysis. The pH of the samples was determined in the field with an Orion Model 405A Ionanalyzer using a glass/SCE combination electrode. Upon receipt from the field, samples were immediately filtered through 0.45-μm Nuclepore polycarbonate filters (high suspended solid samples were subjected to preliminary filtration through Whatman 42 cellulose media) and were analyzed for Al, Ca, Cu, Fe, K, Mg, Mn, Ni, Si, and Zn by inductively coupled plasma emission or atomic absorption spectroscopy. Analysis for Cl^-, F^-, NO_3^-, and SO_4^{2-} was by ion chromatography, and total suspended solids were determined gravimetrically. Ferrous iron was determined colorimetrically with phenanthroline (*25*), and ferric iron was calculated from total iron and iron(II). Carbonate content was determined from standard alkalinity titration (*25*). The hydrolyzable metal content in the concentrator solutions was low by comparison and introduced minimal uncertainty in the alkalinity. Sample analysis was completed within 2 h of sample receipt, and therefore no preservation was used. Filtered suspended solid samples were dried at 110 °C for 24 h, pulverized to −200 mesh, digested by using the mixed acid/high-pressure decomposition technique of Bernas (*26*), and analyzed as described above. Powdered samples of these materials were characterized mineralogically by X-ray diffraction. Carbonate content of the solids was determined by evolution of CO_2 in a closed system after acid addition; the CO_2 evolved was collected in a 0.1 M NaOH scavenger solution and analyzed by acid titration.

Results and Discussion

Chemical Description. Acid Waters. The chemical analysis data for the two sources of acid water are presented in Table I. The composition range for these waters

Table II. Chemical Composition (mg/L) of Concentrator Influents

	with lime[a]		without lime[a]	
	range	av	range	av
Al	0.1-1.8	0.2 ± 0.3	0.1-0.3	0.1 ± 0.2
Ca	540-1015	845 ± 134	203-828	517 ± 169
Cu	0.02-0.46	0.14 ± 0.12	0.01-0.30	0.08 ± 0.08
Fe	0.01-0.16	0.07 ± 0.07	0.01-0.23	0.06 ± 0.04
K	37.5-57.6	46.6 ± 6.3	23.0-54.4	39.1 ± 9.7
Mg	0.01-0.21	0.06 ± 0.06	0.02-0.30	0.12 ± 0.07
Mn	0.01-0.05	0.02 ± 0.02	0.01-0.05	0.01 ± 0.02
Na	30.0-50.0	41.7 ± 5.0	22.8-48.8	38.1 ± 9.2
Si	0.1-2.7	1.0 ± 0.9	0.1-3.9	1.7 ± 1.5
Zn	0.01-0.29	0.13 ± 0.08	0.01-0.42	0.09 ± 0.12
SO_4^{2-}	1590-2215	1760 ± 235	1230-2565	1750 ± 275
flow, L/s	7620-17450	11250 ± 2945	655-20000	9940 ± 4620
flow, g/min	480-1099	709 ± 185	413-1260	625 ± 290
pH	10.4-12.6	11.6 ± 0.6	10.4-12.6	11.4 ± 0.6

[a] Data for 16 sampling trips, uncertainty values are 1 standard deviation.

Table III. Chemical Composition of Systems Effluent[a]

	mixbox effluent		incomplete treatment mixbox effluent, sample		decant discharge	
	range	av	1	2	range	av
Al	0.1-0.7		113	0.5	0.1-3.5	1.4
Ca	370-875	606 ± 168	325	562	598-795	635
Cu	0.01-0.06	0.03 ± 0.01	163	1.1	0.01-0.20	0.02
Fe	0.01-0.13	0.04 ± 0.04	565	47.2	0.07-3.70	0.20
K	30.0-46.7	39.0 ± 5.0	32.5	39.3	29.6-63.4	45.1
Mg	0.07-70.0	13.0 ± 23.9	285	170	2.1-8.4	5.0
Mn	0.01-1.1	0.19 ± 0.36	97.5	52.5	0.01-0.96	0.22
Na	38.5-57.5	49.3 ± 6.5	52.5	450	37.3-91.6	53.7
Si	0.8-1.0	0.9 ± 0.1	21.0	7.1	1.0-6.6	3.5
Zn	0.01-1.26	0.07 ± 0.08	285	51.4	0.1-1.6	0.4
SO_4^{2-}	1550-2330	2105 ± 325	6370	3130	1400-2520	2520
pH	7.0-11.2	9.9 ± 1.4	4.2	6.3	7.4-11.0	9.3

[a] Data for 14 sampling trips; concentration in mg/L; uncertainty values are 1 standard deviation.

is sizable; however, general consistency is better as evidenced by a standard deviations of about ±10%. Both acid solutions are dominated by divalent iron and sulfate. In addition, they include sizable quantities of alkali, alkaline earth, and transition metals. The precipitation plant's effluent (PPE) contains roughly 1.7 times as much total dissolved solids as the mine water. Computer-calculated chemical speciation indicates that the mono- and disulfate complexes of the transition and alkaline earth metals are important in the solution chemistry and account for almost 40% of the total dissolved metal load. This speciation causes a major decrease in the ionic strength from what one predicts on the basis of total composition analysis.

Alkali metals are present as the free aquated ions. The iron(II)/iron(III) distribution, which is extensively dominated by Fe(II), is in agreement with predictions based on pH and oxygen partial pressure (*27*). Similarly, it is expected that manganese should be dominated by Mn(II). The inorganic carbon content of these solutions is minimal and is controlled by the water solubility of CO_2.

Concentrator Water. The waters from the concentrator are dominated by calcium and sulfate (Table II). The solubility of aluminum and transition-metal hydroxides regulate the concentration of these metals in solution. For Cu and Zn, the formation of hydroxide complexes in the pH 10–12 region increases their solubility into the submilligram per liter range. These waters experience extensive formation of $CaSO_4(aq)$ in solution, and as a consequence, the ionic strength is reduced. In addition, they are nominally supersaturated with respect to gypsum. The high pH of these solutions would suggest the presence of considerable amounts of bicarbonate, carbonate, and solid calcium carbonate. Alkalinity titration and analysis of the solids indicates an inorganic carbon alkalinity of less than 10 mg/L as $CaCO_3$, which is at least 2 orders of magnitude lower than the equilibrium predicted values. The inorganic carbon content in the solid phase is approximately 1%, as $CaCO_3$. Apparently contact time with the atmosphere prior to mixing is insufficient to generate sizable amounts of HCO_3^- and CO_3^{2-} in solution.

Concentrator solutions contain organic floating and frothing agents that are left from the concentrating process. These agents, zanthantes and long-chain alcohols, which may be present in up to 2 × 10^{-4} M in the concentrator plant, are removed with the ore-containing froth. The amount present in the effluent waters was not determined; however, it is significantly less than what was present in the concentrator plant and does not appear to play a major role in the chemistry.

The concentrator slurries are approximately 30% by weight suspended solids, which are dominated by quartz and pyrite, but contain recognizable amounts of kaolinite, montmorillonite, muscovite, biotite, and lime. The lime, which is added at a rate of approximately 5 g/L, represents a major fraction of the acid-neutralizing capacity of the waters.

Effluent Waters. If the objectives of the lime neutralization process are to be realized, the concentrations of the transition metals in the effluent waters will be significantly lower than those observed in the acid waters. The data in Table III indicate that when the pH of the effluent water is greater than 7, this is the case. Major reductions are observed for Al, Cu, Fe, Mg, Mn, Si, and Zn. If insufficient quantities of lime are added to the concentrator waters, incomplete treatment is observed and the reduction in metal content is not as pronounced. This was observed for one set of samples, and the data are summarized in columns 4 and 5 of Table III. The treatment process leaves Ca, Na, and K as the major cations in solution and sulfate as the predominant anion. The concentrations of calcium and sulfate are sufficient to result in the formation of $CaSO_4(aq)$.

The major chemical change occurring in the settling basin is the absorption of atmospheric carbon dioxide, which results in a decrease in pH and allows the chemical system to move toward thermodynamic equilibrium.

Process Mechanism. There are at least five processes that can be identified as contributors to the removal of metals from the acid solutions. These include dilution, precipitation, oxidation, surface adsorption, and ion exchange. The dilution factor encountered upon mixing of the acid waters and the concentrator waters will reduce the total metal concentrations by about 60%. This is small in comparison to what is observed, and since the concentrations of the metals are high in the acid waters, this process provides minimal impact.

An increase in the pH of the metal-bearing waters provides the opportunity for the precipitation of hydrous oxides, carbonates, mixed silicates, and sulfates. Which of these is preferred is of interest since it will dictate treatment strategies. Laboratory observations, field studies, and thermodynamic calculations indicate that hydrous oxides of some of these metals will precipitate. The question then becomes which ones and to what extent. The formation of sulfate salts, with the exception of gypsum, is unlikely since they are fairly soluble. The concentration of silica in the acid waters is below the solubility limit; however, the formation of mixed salts of the type $Al_2(SiO_3)_2(OH)_2$ is possible.

The relative stability of the carbonate salts, as compared to other salts, makes them a potential sink for the transition and alkaline earth metals, but their formation will be limited by the transfer of inorganic carbon to the system. As previously noted, the concentrator streams are undersaturated with respect to inorganic carbon and do not represent a significant carbonate source. Inorganic carbon must, therefore, be introduced into this system by atmospheric exchange. The reactions for the transfer of carbon dioxide from the atmosphere are given in eq 1 and 2.

$$CO_2(g) \xrightarrow{H_2O} CO_2(aq) \qquad (1)$$

$$CO_2(aq) + OH^- \rightarrow HCO_3^- \qquad (2)$$

The rate constant for reaction 2 is 8.5×10^3 M^{-1} s^{-1} (*28*). If reaction 2 represents the rate-limiting process for the generation of inorganic carbon in solution, one can calculate the amount of inorganic carbon that enters the system during the 15-s reaction time interval. Using finite difference

$$\Delta[HCO_3^-] = k[CO_2(aq)][OH^-][\Delta t] \qquad (3)$$

and with

$$[CO_2(aq)] = P_{CO_2}K_H = (10^{-3.5})(10^{-1.46}) \qquad (4)$$

where K_H is the Henry's law constant and $[OH^-] = 10^{-4}$ it follows that

$$\Delta[HCO_3^-] = (8.5 \times 10^3)(10^{-3.5})(10^{-1.46})(10^{-4})(15) = 1.5 \times 10^{-4} \text{ mol/L} \qquad (5)$$

This is the maximum amount expected since if reaction 1 were rate limiting, the system would become undersaturated with respect to $CO_2(aq)$ and correspondingly generate less HCO_3^-. Conversion of HCO_3^- to CO_3^{2-} is a diffusion-controlled process and will be fast by comparison. Since the total available metal content is approximately 0.02 M, it can be concluded that insufficient inorganic carbon enters the system during the reaction time interval and minimal metal carbonate precipitation occurs.

Hydroxide precipitation is complicated by the fact that iron and manganese can exist in more than one oxidation state. In the acid waters Fe(II) and Mn(II) are the stable ions, whereas at pH 10 Fe(III) and Mn(IV) are preferred. Oxidation is thus anticipated during the precipitation process.

The rate expression for the oxidation of iron(II) by dissolved oxygen is shown in equation 6 where k_{Fe} equals

$$-d[Fe(II)]/dt = k_{Fe}[Fe(II)][O_2(aq)]/[H^+]^2 \qquad (6)$$

3×10^{-12} M min^{-1} (*29*). With initial concentrations of $Fe(II) = 2 \times 10^{-2}$ M and $[O_2(aq)] = 2.9 \times 10^{-4}$ M and pH = 10.0, the calculated oxidation rate is 1.75×10^3 M/min. With this rate, all of the iron(II) in the mixed solution is predicted to oxidize to Fe(III) in less than 1 ms. This rate represents an exaggerated estimate for several reasons. In the first place, the rate calculation ignores the influence of sulfate. The formation of an $FeSO_4(aq)$ ion pair reduces the activity of Fe(II) in solution and correspondingly will reduce the rate of oxidation (*30*). Second, the system is not buffered in Fe(II), and thus its concentration will decrease with time and correspondingly the rate will decrease. Of critical concern is whether sufficient oxygen will be available to oxidize the iron(II) during this 15-s time interval.

The rate of oxygen solubilization is dependent upon the turbulence of the stream flow. A typical oxygen transfer rate of 5.3×10^{-4} mg/(m^2 s) has been reported for a stream 2-ft deep with a flow velocity of 6.1 m/s (Reynolds number $\sim 10^8$) (*31*). These conditions approximate those of the mixbox, and with a residence time of 15 s, 3.35×10^{-4} mol of O_2 could dissolve in each liter of solution. This is sufficient to oxidize 78 mg/L of iron(II) and would produce a sluge containing approximately equal weights of Fe(II) and Fe(III), which is consistent with the field observations.

Manganese(II) oxidation is much slower than iron(II) oxidation (*32*). If the potential for transition-metal catalysis of this process is considered, it becomes difficult to precisely define the contribution of Mn(II) oxidation to the overall reaction process. It is probable that Fe(II) will utilize virtually all of the available oxygen, and thus the major reactions involving Mn^{2+} are precipitation as $Mn(OH_2)$ and adsorption.

The ability of hydrous metal oxides to remove trace metals from solution by adsorption is well documented (*33–37*), and since these waters contain sizable quantities of $Fe(OH)_3$, $Al(OH)_3$, and $SiO_2{\cdot}2H_2O$, adsorption is of potential significance in the treatment process. These waters also contain sizable amounts of suspended material prior to the rapid pH increase. This provides an opportunity for adsorption, coprecipitation, and discrete precipitation. Analysis of the products confirms that these physical–chemical processes have occurred; however, it provides no indication of their relative contributions or the time frame during which they occur. Recent laboratory studies (*34*) indicate that adsorption and coprecipitation are indistinguishable for this type of system. In addition, the surfaces are composed of a variety of reaction sites as reflected by variation in adsorption free-energy changes as the concentration of adsorbate is varied. The laboratory

Table IV. Chemical Composition of Precipitate Produced in Laboratory Simulation[a]

simulation	final pH	Cu	Al	Mg	Mn	Zn	Fe^{2+}	Fe^{3+}	Ca	Si	SO_4
0	3.8	ND	2.5	ND	ND	0.3	4.2	39.72	ND	1.5	<0.5
1	4.2	0.06	10.7	0.14	0.07	0.33	2.4	25.60	ND	1.1	7.4
2	4.6	0.20	14.8	0.02	ND	0.28	0.84	18.91	ND	1.21	9.6
3	5.5	0.99	14.4	1.03	0.38	12.2	1.3	19.2	0.7	2.5	6.1
4	5.1	0.77	14.5	0.34	0.12	4.0	0.71	18.91	0.1	2.2	1.2
5	7.0	0.46	7.7	2.98	3.20	12.7	2.73	15.07	2.9	2.2	6.3
6	10.3	0.33	5.3	7.48	3.36	8.2	1.87	10.78	6.6	1.7	3.7

[a] ND = not detected, values are percent of totals. The ratio of Al/SO_4 in the solid and Al removed from solution were used to calculate the amount of SO_4 removed from solution for Figure 4.

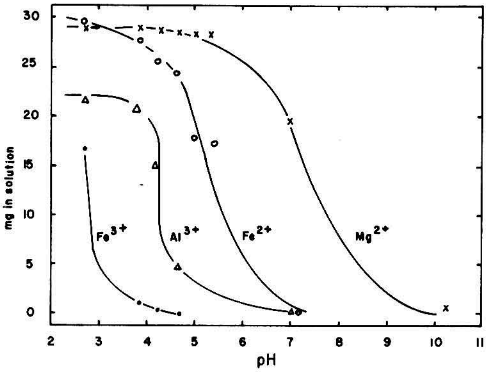

Figure 2. Removal of Al^{3+}, Fe^{3+}, Fe^{2+}, and Mg^{2+} from solution as a function of the pH of the treatment process (total volume 115 mL).

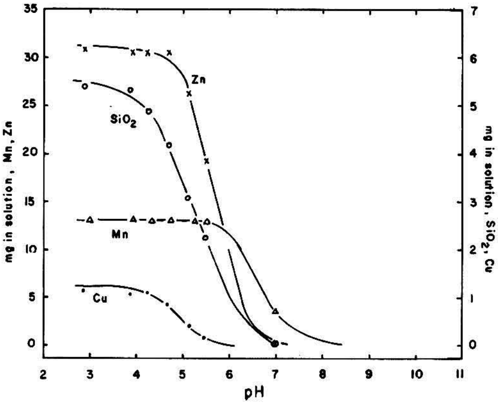

Figure 3. Removal of Cu^{2+}, Mn^{2+}, SiO_2, and Zn^{2+} from solution as a function of the pH of the treatment process (total volume 115 mL).

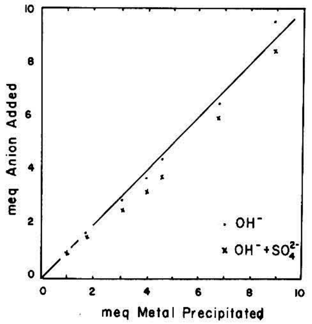

Figure 4. Stoichiometric relationship between the equivalents of anions added and the equivalents of metal precipitated: (●) consideration of OH^- only; (X) consideration of OH^- and SO_4^{2-}.

simulation studies, which will be presented subsequently, provide an opportunity to more precisely define what may be occurring.

It has been noted that the major source of base in the field process is not the concentrator solution but the reservoir of lime contained in the suspended solids. Leaching of the concentrator solid with various acids indicates that this material contains a small amount of labile Na and K, which presumably is present in the aluminosilicate exchange sites. Exchange of these species with hydrogen ion at low pH is a potential contributor to the neutralization process.

The chemical processes that occur as the solution leaves the area of active mixing are limited to movement toward thermodynamic equilibrium. Specifically, precipitation of gypsum and the adsorption of atmospheric CO_2 are important. The latter is reflected by a pH decrease and the former by a decreased sulfate content. While both gypsum and calcite precipitation decrease the calcium concentration, it is noted that the calcium content of the discharge solution is actually somewhat higher than that of the mixbox effluent. This difference reflects continued dissolution of residual lime present in the settling sludge.

Laboratory Simulation. Laboratory simulation of the treatment process involves controlled neutralization of the acidic metal-bearing waters. This provided seven mixture solutions with final pH values ranging from 3.8 to 10.3. Both precipitates and supernates were chemically analyzed. The weight percents of the metals in the precipitate are listed in Table IV. The first precipitate was dominated by Fe(III), and this reflects the composition of the acidic waters and the relative thermodynamic stability of the hydroxides. The concentrations of the metals in solution and how they decrease as the pH of the reaction mixture increases are shown in Figures 2 and 3. As mentioned previously, Fe^{3+} precipitates first, and the process is virtually complete by pH 3.5. Aluminum precipitation is complete by pH ~5 and copper is gone by pH 6. Zinc and Fe^{2+} exhibit similar behavior with 50% loss occurring in the pH range 5.5–6. Half of the Mn^{2+} is gone by pH 6.5, and magnesium, as expected, is the last to precipitate. Loss of $SiO_2 \cdot 2H_2O$ is intermediate between that observed for Al^{3+} and Zn^{2+}. On the basis of thermodynamic stability of the hydroxides and the initial metal concentrations, one predicts that 50% of the metals would be lost from solution by the following pH values: Fe^{3+}, 3; Al^{3+}, 4; Cu^{2+}, 6.1; Zn^{2+}, 6.6; Fe^{2+}, 8.3; Mn^{2+}, 9.1; Mg^{2+}, 9.8. The observed results indicate that Fe^{3+}, Al^{3+}, and Cu^{2+} are in agreement with the thermodynamic prediction and Zn^{2+} is fairly close. Fe^{2+}, Mn^{2+}, and Mg^{2+} are lost from solution at pH values significantly lower than what is predicted on the basis of their hydroxide solubility. Oxidation of Fe^{2+} to Fe^{3+} and Mn^{2+} to Mn^{4+} could account

Table V. Chemical Composition of a Solution as a Function of Lime Addition: Computer Simulation of Total Concentration in Solution (mg/L)[a]

	Amount of Lime Added										
mg/L	0	0.8	1.6	2.4	3.2	4.0	4.7	5.5	6.3	7.9	
lb/min	0	2	4	6	8	10	12	14	16	20	
species											mixbox effluent
Al	87.3	44.6					0.7	1.2	15	165.1	0.7
Ca	539	542	547	556	568	580	594	613	659	812	650
Cu	30.2	30.2	26.6							0.6	
Fe	358	358	358	261	129	29.3					
K	33.0	33.0	3.0	33.0	33.0	33.0	33.0	33.0	33.0	33.0	37.5
Mg	114.5	113.5	113.5	113.5	11.35	113.5	89.0	28.6	2.2		5.4
Mn	42.6	42.6	42.6	42.6	42.6	42.6	4.5	1.5	0.4		0.1
Na	38.2	38.2	38.2	38.2	38.2	38.2	38.2	38.2	28.2	28.2	55.0
$SiO_2 \cdot 2H_2O$	15.2	0.4	0.4	0.4	0.4	0.4	0.4	0.4	0.4	0.4	0.5
SO_4^{2-}	3250	3010	2773	3548	2328	2001	1801	1692	1554	1424	1750
Zn	111.9	111.9	111.9	88.0	74.5	19.2	2.7	2.8	4.6	12.3	0.2
pH	3.58	4.20	6.32	7.84	8.00	8.31	9.88	10.12	11.21	11.84	10.1

[a] Blank spaces denote concentrations of less than 0.1 mg/L.

for the loss of these two species; however, the loss of Mg^{2+} indicates another process.

A plot of hydroxide added vs. cations precipitated is shown in Figure 4. The solid line represents the one to one relationship, and there is good agreement at the extremes. A small but significant difference occurs in the pH 5–7 region. Other precipitated anions include SiO_3^{2-} and SO_4^{2-}. The inclusion of SiO_3^{2-} to interpret Figure 4 does not help since the reference state is $SiO_2 \cdot 2H_2O$ and thus negative charge in the system is conserved. This is not the case for SO_4^{2-}, and inclusion of precipitated sulfate in Figure 4 improves the agreement. Adsorption of trace-metal cations onto the hydrous oxide surfaces with nonstoichiometric release of hydrogen ion would account for the remaining difference, and this has been observed for several systems in this pH range (*33, 37*). The solid species $Al(OH)SO_4$ has also been identified in acid coal mine drainage (*38*), and several silicates are predicted to be stable.

The observed removal of Fe^{2+}, Mn^{2+}, and particularly Mg^{2+} from solutions at pH values below what is predicted on the basis of their hydroxide solubility indicates that they are nonstoichiometrically adsorbed by the solid surface and thus scavanged from solution.

Computer Simulation. Modeling this treatment process as a sequence of chemical reactions utilizing thermodynamically driven equilibrium conditions provides an indication of what could happen if there were no kinetic constraints. The general flow of the computer simulations involves mixing of two solutions and a minimization of the free energy of the system. This procedure identifies the most stable heterogeneous phases and also evaluates the species distribution in solution. In an attempt to provide a model that is comparable to that observed in the laboratory simulation and also one comparable to that observed in the field, the rate of lime addition was varied from 0 to 7.9 mg/L (0–7 × 10^{-4} lb/gal.). The bulk chemistry of the solution to which this lime is added, as shown in the first column of Table V, represents the results of mixing of mine, precipitation plant, and concentrator solutions having an average composition (in a ratio that reflects their average flow rates). The calculated results are shown in Table V.

The calculated pH values are used as a guideline for comparison to the laboratory and field data. As was observed in the laboratory studies, Al^{3+}, Fe^{3+}, and Cu^{2+} are lost at low pH. These calculations did not include the oxidation of Fe^{2+} to Fe^{3+}, and thus loss of iron is through the precipitation of $Fe(OH)_2$, which is predicted to occur at higher pH values than what was observed in the laboratory experiments. The same conclusion applies to Mn^{2+}. The predicted loss of Zn^{2+} and Mg^{2+} also occurs at pH values greater than what is observed. The loss of $SiO_2 \cdot 2H_2O$ is in agreement with the experimental data. Calcium and sulfate are predominantly regulated by the precipitation of gypsum.

The predicted concentrations, at a lime loading rate of 5.5 mg/L (4.6 × 10^{-4} lb/gal.) is in good agreement with what is observed in the mixbox solutions. The pH values are the same within experimental and modeling error, and thus if the model is a reasonable approximation, the concentrations of the other species should also be comparable. This is observed to be the case for Al, Ca, Cu, Fe, K, Na, Si, and sulfate. As has been identified previously, Mg, Mn, and Zn are lower in the experimental observations that what is predicted without including adsorption.

The calculations could have included surface complexation, but they did not since the uncertainty in assigning the concentrations of the surface sites and in the magnitudes of effective stability constants for the mixed system is too large. In a qualitative sense, however, surface complexation would cause removal of Fe^{2+}, Mn^{2+}, and Zn^{2+} at lower pH values than what is shown in Table V. When the addition of lime exceeds 5.5 mg/L, sufficient hydroxide is being added to the system to form soluble hydroxide complexes, and thus the trace-metal content of the solutions will increase as the pH rises from 10 to 12.

Summary

Laboratory and theoretical simulations have been developed for an industrial base-metal treatment process. The laboratory simulations, which involve controlled precipitation, provide excellent agreement with the field treatment process and, in addition, identify the sequence of chemical events. The major reactions involve precipitation of stoichiometric hydroxides. The transfer of O_2 and CO_2 from the atmosphere does not play a major role in the chemistry of transferring the metals from solution to the solid phase during mixbox treatment. The time interval is too short and the gas–liquid interfacial area is too small to permit sufficient quantities of these two reagents to enter the system. Adsorption–coprecipitation is indicated as the process that greatly facilitates the removal of Fe^{2+}, Mg^{2+}, Mn^{2+}, and possibly Zn^{2+} from solution. Thermodynamic calculations predict the optimum rate of lime addition for the industrial treatment process.

Acknowledgments

Appreciation is extended to the Anaconda Mining Co. for access to their facility and cooperation during sampling and to Sara Ingle and Mike O'Leary for assistance in the generation of the computer model.

Registry No. Copper, 7440-50-8; oxygen, 7782-44-7; carbon dioxide, 124-38-9; aluminum, 7429-90-5; iron, 7439-89-6; magnesium, 7439-95-4; manganese, 7439-96-5; zinc, 7440-66-6.

Literature Cited

(1) Emrich, G. H.; Merritt, G. L. *Ground Water* **1969**, *7*, 27.
(2) Gang, M. W.; Langmuir, D. *Proc. Fifth Symp. Coal Mine Drainage Res., Natl. Coal Assoc.* (*Washington, DC*) **1974**, 39.
(3) Wentz, D. A. *Colo. Water Resour. Circ.* **1974**, *No. 21*.
(4) Plass, W. T. *Proc. Third Symp. Surface Mining and Reclamation, Natl. Coal Assoc./Bitumn. Coal Res. Inc.* (*Louisville, KY*) **1975**, 152.
(5) Minear, R. A.; Tschantz, B. A. *J. Water Pollut. Control Fed.* **1976**, *48*, 2549.
(6) Greenfield, R. J.; Stoyer, C. H. *Trans.—Soc. Min. Eng. AIME* **1976**, *260*, 20.
(7) Boyes, J. M.; Cain, D.; Alley, W.; Klusman, R. W. In "Water Resources Problems Related to Mining"; Hadley, R. F., Snow, D. T., Eds.; American Water Works Association: Minneapolis, MN, 1974; pp 41–53.
(8) Wentz, D. A., ref 7, pp 158–173.
(9) Norbeck, P. N.; Mink, L. L.; Williams, R. E., ref 7, pp 149–157.
(10) Wildeman, T. R.; Cain, D.; Ramiriz, A. J., ref 7, pp 219–229.
(11) Fed. Wat. Poll. Cont. Assoc., "Stream Pollution by Coal Mine Drainage in Appalacia"; U.S. Department of the Interior; Cincinnati, OH, 1969.
(12) O'Brien, W. Ph.D. Thesis; West Virginia University, Morgantown, WV, 1972.
(13) Applied Science Laboratories Inc. Water Pollut. Control Res. *Ser.*, No. 14010 DRZ 02/71, U.S. Environmental Protection Agency: Washington, DC, 1971.
(14) Hansen, P. J. *Fourth Symp. Coal Mine Drainage Res.*; *Bituminous Coal Research Inc.* (*Monroeville, PA*) **1973**, 157–178.
(15) Jasinski, R.; Gaines, L. Water Pollut. Contr. Res. Ser., No. 14010 FNQ 02/72, U.S. Environmental Protection Agency: Washington, DC, 1972.
(16) Wilmoth, R. C.; Mason, D. G.; Gupta, M. *Fourth Symp. Coal Mine Drainage Res.*; *Bituminous Coal Research Inc.* (*Monroeville, PA*) **1973**, 115–157.
(17) Holmes, J.; Schmidt, K., ref 16, pp 179–200.
(18) Rice, P. A.; Rabolini, F., ref 16, pp 293–306.
(19) Ross, L. W. Environmental Protection Agency Report 670/2-73-080, 1973.
(20) O'Brien, W. S.; Galli, A. F.; Wen, C. Y. *Proc. Fifth Symp. Coal Mine Drainage Res., Natl. Coal Assoc.* (*Washington, DC*) **1974**, 192–204.
(21) Morow, R. E.; Wentz, D. A., ref 7, pp 54–65.
(22) Ingle, S. E.; Keniston, J. A.; Schults, D. W. EPA Report 600/3-80-044, 1980.
(23) Morel, F. M.; Morgan, J. J. *Environ. Sci. Technol.* **1972**, *6*, 58.
(24) Jenke, D. R. M. S. Thesis, Montana College of Mineral Science and Technology, Butte, MT, 1978.
(25) Standard Methods for the Examination of Water and Wastewater, American Public Health Association: Washington, DC, 1971.
(26) Bernas, B. *Anal. Chem.* **1968**, *40*, 1682.
(27) Hem, J. D. U.S. Geol. Surv. Water Supply Paper No. 1473, 1970.
(28) Kern, D. M. *J. Chem. Educ.* **1960**, *37*, 14.
(29) Stumm, W.; Lee, G. F. *Ind. Eng. Chem.* **1961**, *53*, 143.
(30) Sung, W.; Morgan, J. J. *Environ. Sci. Technol.* **1980**, *14*, 561.
(31) Hogan, W. T.; Reed, F. E.; Starbird, A. W. EPA Report No. 160-80D00-7/70, 1970.
(32) Coughlin, R. W.; Matsui, I. *J. Catal.* **1976**, *41*, 108.
(33) Davis, J. A.; Leckie, J. O. *J. Colloid Interface Sci.* **1978**, *67*, 90.
(34) Benjamin, M. M. Ph.D. Thesis, Stanford University, Stanford, CA, 1978.
(35) Kurbatov, M. H.; Wood, G. B.; Kurbatov, J. D. *J. Phys. Chem.* **1951**, *55*, 1171.
(36) Brunnix, E. *Philips Res. Rep.* **1975**, *30*, 177.
(37) Benjamin, M. M.; Leckie, J. O. *J. Colloid Interface Sci.* **1981**, *79*, 209.
(38) van Breeman, N. *Soil Sci. Soc. Am. Proc.* **1973**, *37*, 694.

Received for review May 10, 1982, Accepted December 13, 1982. This research was supported in part by Grant 0264022 from the U.S. Bureau of Mines.

Environ. Sci. Technol. 1983, 17, 224–227

Photochemical Ozone Formation in Urban and Point-Source Plumes

Ken Sexton*

School of Public Health, Department of Environmental Health Sciences, Harvard University, Boston, Massachusetts 02115

Hal Westberg

Department of Chemical Engineering, Air Resources Section, Washington State University, Pullman, Washington 99164

■ Results of aerial measurements in plumes from large urban areas, petroleum refineries, automotive-painting operations, fossil-fuel power plants, and controlled burning of forest slash are presented. Field monitoring studies occurred during summer months between 1974 and 1980 and emphasized collection of data on in-plume ozone buildup and associated precursor concentrations. Photochemical ozone formation in excess of ambient background levels was documented in all plumes studied, with the exception of power-plant emissions. Examination of NMHC/NO_x ratios indicates ozone production, or depletion in the case of power-plant effluents, was consistent with the traditional HC–NO_x–UV light model. Urban non-methane hydrocarbon composition was similar for the cities monitored, but marked variation was observed between plumes from other sources.

Introduction

During 1974–1980, surface and aerial measurements of ozone, non-methane hydrocarbons (NMHC), and nitrogen oxides were recorded downwind of a number of urban and point sources. The ambient monitoring program was specifically aimed at investigating the relationship between ozone and ozone precursors in plumes from large metropolitan areas, petroleum refineries, automotive-painting facilities, fossil-fuel power plants, and controlled burning of forest slash. Results are presented emphasizing the relative magnitude of photochemical ozone formation over time periods of 6–8 h and associated in-plume concentrations of hydrocarbon and nitrogen oxides precursors.

Experimental Section

Ground-level measurements were centered around a 23-ft instrumented trailer which served as a field laboratory. Typically, the trailer was located near the emissions source being investigated. Continuous monitoring of O_3, NO, NO_2, NO_x, CH_4, CO, total hydrocarbon, selected halocarbons, and a variety of meteorological parameters was accomplished at this site. Non-methane hydrocarbon samples were collected at the surface and by an instrumented aircraft in Teflon bags or stainless steel canisters and then returned to the field laboratory. Individual hydrocarbon identification was accomplished by using two Perkin-Elmer gas chromatographs. From 1974 to 1975 only C_2–C_6 NMHC were measured, but after 1975 C_2–C_{10} hydrocarbon compounds were analyzed for all samples.

Instruments carried by the aircraft allowed for continuous measurement of O_3, NO, NO_2, NO_x, visual range, condensation nuclei, temperature, and relevant flight parameters (e.g., airspeed, altitude). Beginning in 1977, a pulsed fluorescent SO_2 analyzer provided continuous data on ambient SO_2 levels. Hydrocarbon grab samples were also collected and returned to the field laboratory for analysis. A Metrodata acquisition system was employed in both the trailer and the aircraft, allowing for storage of continuous data on nine-track magnetic tape. A more complete description of study designs, instrument manufacturers, measurement techniques, and calibration procedures is available elsewhere (1–6).

Results

Pollutant measurements in selected urban and point-source plumes during the first 6–8 h of transport were conducted by using an instrumented aircraft. Field studies occurred during summer months (1974–1980) and focused on documenting in-plume photochemical transformations. Research efforts emphasized collection of data on ozone enhancement (or depletion), concentration and composition of non-methane hydrocarbons, and levels of nitrogen oxides. Sources investigated included large urban areas (Chicago, IL; Milwaukee, WI; Houston, TX), petroleum refineries (Benicia, CA; Lawrenceville and Robinson, IL), an automotive-painting facility (Janesville, WI), fossil-fuel power plants (western shore of Lake Michigan), and controlled burning of forest slash (rural areas in Washington State).

Large Urban Centers. Airborne emissions downwind of Chicago, Milwaukee, and Houston were monitored in order to provide a comparison of ozone and ozone precursor levels. Chicago and Milwaukee are located in the Great Lakes region and have not been as well studied as some other urban centers. Houston is situated along the Gulf Coast and has been the subject of several air pollution studies.

Measurements in the Chicago and Milwaukee plumes were obtained in conjunction with field studies in 1976 (*7*) and 1977 (*4*). Migratory high-pressure systems dominate summertime and fall meteorology in this region, and the relationship between anticyclones and air quality in the Midwest has been well documented (*8*). Mesoscale lake breezes have been shown to have a significant impact on pollutant concentrations in areas immediately adjacent to Lake Michigan, especially downwind of Chicago and Milwaukee (*9–11*).

The Chicago plume was observed on several occasions to be transported downwind as a discernible entity for more than 100 miles. During periods of synoptic air flow from the southeast, emissions from the Chicago–Gary urban complex were shown to have a significant effect on local pollutant levels in southern Wisconsin (*12*). Peak in-plume ozone enhancement under these conditions was on the order of 80 ppb above background levels, while NMHC and NO_x concentrations 60 miles from Chicago were approximately 75 ppbC and 15 ppb, respectively. In samples collected just downwind of the city, hydrocarbon values typically were greater than 500 ppbC and NO_x levels were near 100 ppb.

Highest ozone concentrations were commonly recorded along the Lake Michigan shoreline to the north of Chicago during lake breeze fumigation. In the most frequently observed scenario, primary emissions from the Chicago–Gary area drifted to the northeast over Lake Michigan during the morning hours. Secondary pollutants were formed in the polluted air mass over the lake and then advected onshore by the afternoon lake breeze winds.

0013-936X/83/0917-0224$01.50/0

Table I. Summary of O_3, NO_x, and NMHC Data from Urban and Point-Source Plumes

parameter	Chicago plume (*11*)	Milwaukee plume (*11*)	Houston plume (*13*)	Marathon oil refinery (*5*)	GM painting plant (*16*)	power plants (*7*)	forest-slash burn (*19*)
ΔO_3,[a] ppb	100–200	100–150	100–250	15–30	5–15	depletion	40–50
NMHC/NO_x[b]	5–10	5–15	7–10	10–20	10–15	<1	5–10
NO_x,[b] ppb	50–100	<50	50–100	25	20–30	100–400	50–100
NMHC,[b] ppbC	550	250	750	350	250	near background[c]	700
olefins, %	11	10	8	5	6	<5	45
aromatics, %	22	25	11	10	35	5–15	25
paraffins, %	67	65	80	85	58	85	25
plume width,[b] miles	20–30	10–15	10–20	3–5	3–5	3–5	1–4
time req'd for O_3 buildup,[d] min	<30	<30	<30	60–120	60–120	NA[e]	<5

[a] Observed maximum ozone enhancement above background levels. [b] Typical value recorded in region of peak ozone buildup. [c] Less than 100 ppbC in most cases. [d] Approximate time from precursor release to production of photochemical O_3 in excess of local ambient background concentrations. [e] Not applicable.

Peak afternoon ozone values in the shoreline region of fumigation typically exceeded 200 ppb at ground level (100 ppb above background), and concentrations as high as 300 ppb were recorded by the instrumented aircraft. Associated hydrocarbon and NO_x levels were about 300–500 ppbC and 25–100 ppb, respectively.

Milwaukee is a smaller, less industrialized city than Chicago, located approximately 50 miles north along the shore of Lake Michigan. As in the case of the Chicago plume, emissions from Milwaukee were shown to produce elevated levels of photochemical ozone as they drifted over the lake. On several occasions, fumigation of the shoreline by the Milwaukee plume resulted in peak ozone concentrations in excess of 200 ppb near Sheboygan, 50 miles north of the city. Precursor concentrations measured in the effluent from Milwaukee were routinely less than for Chicago, with NMHC levels between 200 and 300 ppbC and NO_x less than 50 ppb. It is important to note that although excess ozone concentrations in the Milwaukee and Chicago plumes were similar (100–150 ppb), the Chicago plume was normally larger.

Observations of pollutant levels in the Houston plume were obtained during an intensive monitoring study in 1978 (*6*). During the period of investigation in Aug and Sept, relatively low pollution concentrations were advected into the Houston area; however, afternoon ozone buildup downwind of the city was consistently recorded. Ozone concentrations in the urban plume typically exceeded ambient background levels by 100–250 ppb, with elevated values persisting for more than 100 miles downwind.

Peak photochemical ozone formation was associated with NMHC concentrations of 700–800 ppbC and NO_x levels of approximately 50 ppb. Highest ozone concentrations were noted when easterly winds caused industrial discharges from the ship-channel region to mix rapidly with Houston urban emissions. Attempts to quantify relative contributions of NMHC and NO_x precursors from Houston, the ship channel, and nearby industrialized locations, such as Baytown and Texas City, have not been successful to date. Yet all these sources undoubtedly contribute to emissions which are labeled as the "Houston plume" (*13*). Data from the urban plumes discussed above are summarized in Table I.

Petroleum Refineries. A 2-week study near the Texaco refinery at Lawrenceville, IL, in June 1974 indicated that in-plume pollutant values were on the order of 1–2 ppm NMHC, 30 ppb NO_x and 3–5 ppm CO. Although elevated NMHC values, primarily alkanes, were recorded out to 30 miles from the plant, no evidence of in-plume ozone enhancement was observed (*1*).

In Sept 1975, a 2-week investigation was conducted to measure in-plume pollutant concentrations in the plume from the Exxon refinery at Benicia, CA (*2, 14*). Because of interferences from nearby industrial sources, Exxon emissions could be tracked for only about 8 miles (approximately 30-min irradiation time). In-plume ozone values were either less than or equal to background levels out to that distance. Non-methane hydrocarbon concentrations in the plume were in the range 500–1000 ppbC and NO_x levels varied from 50 to 150 ppb. Ozone buildup was consistently recorded in the delta region of the Sacramento river, approximately 30 miles downwind. However, it was not possible to define the contribution of Exxon emissions.

During July 1977, a field monitoring program near the Marathon refinery at Robinson, IL (*3, 5*), revealed ground-level NMHC and NO_x concentrations on the order of 5000 ppbC and 25 ppb, respectively. Downwind of the plant, NMHC values were typically 1000–2000 ppbC at less than 2 miles, decreasing to 300–400 ppbC at 5 miles and 100–150 ppbC at 10 miles. In-plume NO_x levels were commonly 10–25 ppb, with elevated NO_x and NMHC recorded out to 20 miles from the refinery. Excess ozone formation was observed in conjunction with the Marathon plume during some afternoon flights. Peak ozone levels were typically between 15 and 30 ppb above background concentrations and were most frequently observed in the region 5–15 miles downwind of the plant. The data pertinent to ozone formation in petroleum-refinery plumes are given in Table I.

Automotive-Painting Plant. Photochemical ozone generation near the General Motors Assembly Division plant at Janesville, WI, was examined in 1977 and 1978 (*4, 15, 16*). The majority of organic volatiles measured in the GM plume consisted of hydrocarbons in the C_7–C_{10} molecular weight range, with toluene, C_8 alkanes, ethylbenzene, and the three isomeric xylenes predominating. Ground-level measurements near the plant revealed NMHC concentrations of 3000 ppbC, while downwind levels were approximately 200–300 ppbC at 5–10 miles. Aerial measurements showed NO_x values varying from 20 to 30 ppb within plume boundaries. Isolated instances of elevated ozone concentrations attributable to GM emissions were recorded in both 1977 and 1978. Excess ozone formation was consistently between 5 and 15 ppb above background. Information from the GM study is given in Table I.

Fossil-Fuel Power Plants. Ozone production in power-plant plumes along the western shore of Lake

Michigan was examined in 1976 (7). Ozone concentrations in the definable portion of the plume were commonly depleted compared to background levels due to scavenging by nitric oxide. Non-methane hydrocarbon values within plume boundaries were on the same order as existing background concentrations. Elevated in-plume NO_x levels were always observed. Although no instances of photochemical ozone production due solely to power-plant emissions were noted, other investigators have reported ozone buildup in power-plant effluents (*17, 18*). Measurements of O_3, NO_x, and NMHC concentrations in fossil-fuel power-plant plumes are given in Table I.

Controlled Burning of Forest Slash. Measurements in slash-burn plumes from predominantly rural regions of Washington State revealed consistent ozone buildup of 40–50 ppb (*19*). Ozone production appeared to occur very rapidly in the plume, with excess O_3 frequently recorded directly over the forest burn. Hydrocarbon analysis showed that many photochemically reactive olefins were present in airborne emissions and favorable NMHC/NO_x and NO_2/NO ratios were often observed. Nitrogen oxides concentrations between 50 and 100 ppb were commonly associated with the plume, while NMHC values as high as 600–700 ppbC were recorded. The olefinic compounds propene, 1-butene, 2-methylpropene, *cis*-2-butene, and *trans*-2-butene typically constituted about 20% of the total NMHC. Data from forest-slash burning are summarized in Table I.

Discussion

Factors such as UV radiation, temperature, irradiation time, absolute NMHC concentrations, NO_2/NO ratio, and especially the NMHC/NO_x ratio have been shown to be important determinants of photochemical ozone generation. Due to the difficulties of aerial monitoring in narrow plumes, determining the effects of these variables on ozone buildup in real atmospheres is not straightforward. The situation is further complicated by the fact that precursor concentrations vary both spatially and temporally due to changing meteorological parameters and fluctuating emission rates. The data in Table I show maximum ozone enhancement recorded within various plumes and concentrations of NMHC and NO_x measured in conjunction with these peak values. In all instances where ozone buildup due to urban or point-source emissions was documented, NMHC/NO_x ratios were in the region between 5 and 20. This is the range (typically between 8 and 15) where maximum ozone production is expected to occur (*20*). Results are surprisingly consistent given the complex nature of photochemical processes and limitations of available monitoring devices. The fact that no in-plume ozone enhancement was attributable to fossil-fuel power-plant emissions was probably due to low NMHC/NO_x ratios and O_3 scavenging by nitric oxide.

The composition of NMHC in urban plumes was relatively consistent, particularly for Chicago and Milwaukee. The lower proportion of aromatics and higher percentage of paraffins recorded in the Houston plume are not unexpected since petrochemical industrial emissions account for a significant fraction of that city's emission inventory. As shown in Table I, NMHC levels in the Houston effluent are similar in makeup to those recorded downwind of the Marathon petroleum refinery. In contrast to the similarities in NMHC composition between urban areas, the hydrocarbon mix in plumes from oil refineries, painting plants, and slash burns shows marked variation. Petroleum-refinery emissions are composed principally of paraffinic compounds with few olefins. Painting discharges contain few olefins, but over a third of the total is aromatics. Forest-burn emissions are almost half olefins, with the remaining fraction divided evenly between aromatics and paraffins.

Because of differences in hydrocarbon reactivities, the variations observed in hydrocarbon composition are potentially important in influencing maximum ozone production. Olefins have been shown to be the most reactive class of hydrocarbon compounds and will be the fastest promoters of ozone buildup. Aromatics are the next most reactive category followed by paraffins. While the paraffinic species are the slowest reacting group, they can contribute to ozone formation over longer time periods and may be important photochemical ozone precursors in cases of long-range multiday transport. The rapid generation of ozone recorded in slash-burn plumes is partially a result of the high olefin content in burn emissions. Conversely, ozone buildup in petroleum-refinery plumes was only noted after 1–2 h of transport. Since the vast majority of refinery emissions are slow-reacting paraffins, more irradiation time was required before in-plume ozone concentrations exceeded background levels.

Photochemical ozone formation in urban plumes is a somewhat different situation than that for point sources. In petroleum refineries, for instance, hydrocarbon emissions occur primarily at ground level due to evaporation and have little thermal buoyancy. Nitrogen oxides emissions result from processing operations and commonly are vented to the atmosphere from a stack. Only after these primary pollutants have mixed together downwind of the plant will NMHC/NO_x ratios favor ozone formation. Similarly, nitrogen oxides and other pollutants are released from fossil-fuel power plants through tall stacks and are not expected to exhibit excess ozone formation unless entrainment of background NMHC is sufficient to cause favorable NMHC/NO_x ratios.

Urban emissions, on the other hand, occur over a wide area with NMHC and NO_x often emitted near ground level and in close proximity (e.g., automotive emissions). These pollutants mix with discharges from industrial sources and together make up the urban plume. Maximum ozone concentrations associated with urban emissions are observed typically 1–2 h downwind. However, the bulk of in-plume ozone was consistently recorded over or directly downwind of urban centers. The rapid production of ozone was probably due to the high olefinic content of automotive emissions, the close proximity of NMHC and NO_x sources at or near ground level, and the disperse nature of these sources, which allowed for rapid mixing across a wide area.

Conclusions

Observations in urban and point-source plumes under a variety of meteorological conditions indicate that photochemical ozone formation is qualitatively consistent in all cases with the traditional HC–NO_x–UV light model. In-plume ozone buildup occurred when NMHC/NO_x ratios were in the range 5–20, and longer irradiation periods were required for emissions containing mainly slower reacting hydrocarbons. Although non-methane hydrocarbon composition was found to vary between plumes from petroleum refineries, painting operations, power plants, and forest burning, urban NMHC emissions were similar for the cities studied.

Registry No. O_3, 10028-15-6; NO_x, 11104-93-1.

Literature Cited

(1) Westberg, H.; Allwine, K. J.; Robinson, E. May 1977, EPA Report 600/7-77-049.

(2) Sexton, K.; Westberg, H. Feb 1980, EPA Report 600/7-80-028.

(3) Sexton, K.; Westberg, H. "Ambient Hydrocarbons and Ozone Concentrations Near a Refinery: Robinson, Illinois 1977"; Final Report to the U.S. Environmental Protection Agency, for Grant 805376, 1982.
(4) Westberg, H.; Sexton, K.; Holdren, M. Aug 1978, General Motors Report for Contract EA-148705.
(5) Sexton, K.; Westberg, H. *Atmos. Environ.* **1983**, *17*, 467.
(6) Westberg, H.; Sexton, K.; Holdren, M. "Measurement of Ambient Hydrocarbons and Oxidant Transport, Volume I-Houston Study, 1978"; Final EPA Report for Grant R805343.
(7) Allwine, K. J.; Westberg, H. Wisconsin Public Service Commission Report for Contract 8110, 1976.
(8) Vukovic, F. M.; Boch, W. D., Jr.; Chrissman, B. W.; King, W. J. *Atmos. Environ.*, **1977**, *11*, 967.
(9) Lyons, W. A. In "Lectures on Air Pollution and Environmental Impact Analysis"; American Meteorological Society: Boston, MA, 1975; pp 136–202.
(10) Lyons, W. A.; Cole, H. S. *J. Appl. Meteor.*, **1976**, *15*, 733.
(11) Westberg, H.; Sexton, K.; Roberts, E. *J. Air Pollut. Control Assoc.*, **1981**, *31*, 385.
(12) Sexton, K.; Westberg, H. *J. Air Pollut. Control Assoc.*, **1980**, *30*, 911.
(13) Sexton, K.; Westberg, H. *Proceedings* of 73rd Annual Meeting of Air Pollution Control Association, paper 80-39.5, Montreal, Quebec, June 1980.
(14) Sexton, K.; Westberg, H. *J. Air Pollut. Control Assoc.*, **1979**, *29*, 1149.
(15) Sexton, K.; Westberg, H. General Motors Report for Contract EA-148705, 1979.
(16) Sexton, K.; Westberg, H. *Environ. Sci. Technol.*, **1980**, *14*, 329.
(17) Davis, D. D.; Smith, G.; Klauber, G. *Science (Washington, D.C.)* **1974**, *186*, 733.
(18) Miller, D. F.; Alkezweeny, A. J.; Hales, J. M.; Lee, R. N. *Science (Washington, D.C)* **1978**, *202*, 1186.
(19) Westberg, H.; Sexton, K.; Flyckt, D. *J. Air Pollut. Control Assoc.*, **1981**, *31*, 661.
(20) Sexton, K.; Westberg, H. submitted for publication in *J. Air Pollut. Control Assoc.*

Received for review June 23, 1982. Revised manuscript received December 1, 1982. Accepted December 27, 1982. This research was made possible through funding provided by the U.S. Environmental Protection Agency (Environmental Sciences Research Laboratory) and General Motors Corp. (Environmental Activities Staff).

Partition Equilibria of Nonionic Organic Compounds between Soil Organic Matter and Water[†]

Cary T. Chiou,* Paul E. Porter, and David W. Schmedding

Environmental Health Sciences Center and Department of Agricultural Chemistry,
Oregon State University, Corvallis, Oregon 97331

■ Equilibrium isotherms for the simultaneous uptake of binary nonionic organic compounds from water on soil indicated no competitive effect between the two solutes. This observation supports the hypothesis that partition to the soil organic phase is the primary process for sorption of nonionic organic compounds from water on soil. The partition process between soil organic matter and water was analyzed by using the conventional solution concept for solutes in water and the Flory–Huggins treatment for solutes in the polymeric humic phase. Sorption determined for 12 aromatic compounds on a Woodburn soil shows that the extent of solute insolubility in water (S) is the primary factor affecting the soil organic matter–water partition coefficient (K_{om}) and that the effect of solute incompatibility with soil organic matter is significant but secondary. This explains the commonly observed correlations of log K_{om} vs. log S and log K_{om} vs. log K_{ow} (octanol–water).

Introduction

Earlier publications (*1, 2*) provided evidence that sorption of nonionic organic compounds from water on soil consists primarily of partition into the soil organic phase; adsorption by the soil mineral fraction is relatively unimportant in wet soils presumably because of the strong dipole interaction between soil minerals and water, which excludes neutral organic solutes from this portion of the soil. We here report further support for the partition hypothesis in soil–water systems and present a novel analysis of partition equilibria between soil organic phase and water, taking into account the solute solubility in polymeric humic substances.

Partitioning of organic solutes between the soil organic phase and water may be treated in a manner similar to that between an organic solvent phase and water (*3, 4*). To analyze the relative effects on partition coefficient of solute solubility in water, compatibility with soil organic phase, and alteration of water solubility by soil organic components dissolved in water, a reference "ideal line" (*3*) relating sorption coefficient with water solubility is needed. We assume that the effect of soil–water mutual saturation on the solute's water solubility is insignificant with topsoil since the fraction of water-soluble organic components (which may have a potential effect on solute solubility) is usually negligible. We consider the major components of soil humus to be amorphous polymeric (macromolecular) substances and therefore adapt the Flory–Huggins theory (*5, 6*) to account for the solute activity in an amorphous polymer. The partition process with soil organic matter is conceived to be analogous to that involved with synthetic resins used in ion-exclusion, salting-out, and solubilization chromatography for separating nonionic species (*7–10*).

The relation between partition coefficient and water solubility for slightly water-soluble organic solutes in an organic solvent–water mixture, in which the solvent has small solubility in water, is given by (*3*)

$$\log K = -\log S - \log \bar{V}_0{}^* - \log \gamma_0{}^* + \log (\gamma_w{}^*/\gamma_w) \quad (1)$$

where K is the solute partition coefficient, S is the molar water solubility of the liquid or supercooled liquid solute, $\bar{V}_0{}^*$ is the molar volume of water-saturated organic phase, $\gamma_0{}^*$ is the solute activity coefficient (Raoult's law convention) in water-saturated solvent phase, $\gamma_w{}^*$ is the solute activity coefficient in solvent-saturated water, and γ_w is

---

[†] Oregon State Agricultural Experiment Station Technical Paper No. 6480.

the solute activity coefficient in water. The ideal line for the solutes partitioned between an organic solvent (such as octanol) and water is thus

$$\log K^\circ = -\log S - \log \bar{V}_0^* \qquad (2)$$

where K° represents the partition coefficient when solutes form ideal solutions in the (water-saturated) solvent phase and when the solute solubility in water is not affected by the solvent dissolved in water.

When the organic phase is polymer, as are soil humic substances, γ_0^* in eq 1 (defined on a mole-fraction basis) must be modified to account for the large disparity in molecular volumes of solute and polymer, an effect that introduces large negative deviations from Raoult's law without associated heat effects (*5, 6*). The Flory–Huggins theory (*5, 6, 11, 12*) treats the activity of solutes at dilute concentrations in an amorphous polymer as

$$\ln a = \ln \phi + \phi_p(1 - \bar{V}/\bar{V}_p) + \chi\phi_p^2 \qquad (3)$$

where a is the activity of solute, ϕ is the volume fraction of solute, ϕ_p is the volume fraction of polymer, $\bar{V}$ is the molar volume of solute, $\bar{V}_p$ is the average molar volume of polymeric substances, and χ is the Flory–Huggins interaction parameter, a sum of excess enthalpic (χ_H) and excess entropic (χ_S) contributions of the solute–polymer interaction (*13, 14*). When water is sorbed to the polymer phase, as for water-saturated soil organic matter, the properties of a, ϕ, ϕ_p, $\bar{V}_p$, and χ are those corrected for the effect of water sorbed. Thus, for instance, ϕ_p is the volume fraction of soil organic matter and sorbed water (i.e., $\phi_p = 1 - \phi$) and $\bar{V}_p$ is the average molar volume of water-saturated soil organic matter ($\bar{V}_p = \bar{V}_p^*$).

To obtain the solute activity coefficient (γ_0^*) at given mole fraction in water-saturated soil organic phase, ln a in eq 3 may be set equal to $\ln x\gamma_0^*$, where x is the mole fraction of solute in water-saturated soil organic phase. At dilute concentrations of solute in this phase, x and ϕ can be approximated as

$$x = n/(n + n_p) \simeq n/n_p \qquad (4)$$

and

$$\phi = n\bar{V}/(n\bar{V} + n_p\bar{V}_p) \simeq n\bar{V}/(n_p\bar{V}_p) \qquad (5)$$

where n is the moles of solute and n_p is the moles of soil humus and sorbed water. Substituting eq 4 and 5 into eq 3 gives

$$\ln \gamma_0^* = \ln \bar{V} - \ln \bar{V}_p^* + \phi_p(1 - \bar{V}/\bar{V}_p^*) + \chi\phi_p^2 \qquad (6)$$

The solute partition coefficient between soil organic phase and bulk water can then be derived by substituting eq 6 into eq 1 with $\bar{V}_p^* = \bar{V}_o^*$ and $\phi_p \simeq 1$ along with the assumption of $\gamma_w^*/\gamma_w \simeq 1$ and $\bar{V}/\bar{V}_p^* \ll 1$, giving

$$\log K_{om} = -\log S\bar{V} - \log \rho - (1 + \chi)/2.303 \qquad (7)$$

where K_{om} is the solute partition coefficient between soil organic phase and water and ρ is the density of the organic matter introduced to express K_{om} in a more usual weight basis.

According to Hildebrand et al. (*13*) and Scott (*14*), if the contribution to the incompatibility of a solute in a polymer, other than that of size difference, is given by the regular solution theory, the component χ_H of χ can be reasonably correlated by the solubility parameters of solute and polymer. In this case

$$\chi = \chi_S + (\bar{V}/RT)(\delta - \delta_p)^2 \qquad (8)$$

where χ_S is approximately the reciprocal of the coordination number of the polymer subunits, δ is the solubility parameter of solute, and δ_p is the apparent (total) solubility parameter of water-saturated polymer. The value of χ_S depends presumably on the characteristics of the polymer network (crosslinking and chain length). Scott (*14*) treated χ_S as an empirical constant, assumed to be about 0.25 for high polymers. The ideal line for compounds with negligible heats of interaction ($\chi = \chi_S$) in the polymer phase would thus be

$$\log K_{om}^\circ = -\log S\bar{V} - \log \rho - (1 + \chi_S)/2.303 \qquad (9)$$

where K_{om}° is the partition coefficient when $\chi = \chi_S$ and ρ is assumed for soil organic matter to be 1.2 by comparison with values for similar polymeric materials (*15*). With use of eq 9 as the ideal line and the experimental data of log K_{om}, the incompatibility of a compound with (water-saturated) soil organic matter is $(\chi - \chi_S)/2.303 = \log (K_{om}^\circ/K_{om})$. If $(\chi - \chi_S)/2.303$ is small compared to $\log S\bar{V}$ for a group of solutes partitioned to the organic matter phase of a soil, the relation between log K_{om} and $\log S\bar{V}$ should be linear.

This study investigates the sorption of some aromatic compounds (benzene derivatives and PCBs) from both single-solute and binary-solute aqueous solutions on a Woodburn soil and discusses the relation of log K_{om} vs. $\log S\bar{V}$, log K_{om} vs. log S, and log K_{om} vs. log K_{ow} (octanol–water) for the selected compounds.

Experimental Section

All sorption experiments were conducted with a Woodburn silt loam soil, which has the following compositions: 1.9% organic matter, 68% silt, 21% clay, and 9% sand, with a cation-exchange capacity of 14 mequiv/100 g of soil. Test compounds were reagent grades or analytical standards from Analabs, Aldrich, and Mallinckrodt and used as received except for some chlorinated biphenyls (PCBs) that were recrystallized in methanol to remove impurities.

Stock aqueous solutions were prepared by saturating each chemical with water at approximately 50 °C and then allowing the suspensions to stand at 20 °C. Excess chemicals in suspension were removed by centrifugation and saturated aqueous phases separated. A series of more dilute solutions were prepared for equilibration with appropriate amounts of soil. Soil–solution mixtures were equilibrated at 20 °C in 30-mL screw-capped centrifuge tubes (equipped with Teflon-lined lids) for 24 h on a mechanical shaker. Samples were centrifuged at 20 °C for 1 h in a controlled-temperature centrifuge to spin down soil particulates. To avoid vapor losses in transferring aqueous solutions to the sample tubes, a series of tubes with weighed amounts of soils were prepared and solutions quickly introduced to the tubes and capped. Reweighing established the volume of the solution in each tube.

With benzene, ethylbenzene, and chlorobenzene, vapor loss from the equilibrated aqueous phases was avoided by sampling through the septum in the caps using a gas-tight syringe. Aqueous samples of benzene and ethylbenzene were injected directly into a gas chromatograph while chlorobenzene solutions were extracted with suitable amounts of hexane prior to analysis with the gas chromatograph. In each case, small corrections were made for the amounts of chemicals in the air space of the original sample tubes, based on the known Henry's law constants and the air volumes. Other chemicals were sampled with pipets and the solutions extracted with hexane for subsequent analyses.

In the study of the simultaneous sorption of 1,3-dichlorobenzene and 1,2,4-trichlorobenzene by soil, the

Table I. Water Solubilities (S), Molar Volumes ($\bar{V}$), Octanol-Water Partition Coefficients (K_{ow}), and Soil Organic Matter-Water Distribution Coefficients (K_{om}) of Selected Organic Solutes

compound	log S,[a] mol/L	$\bar{V}$,[b] L/mol	log $S\bar{V}$	log K_{om}	log K_{ow}[c]
benzene	−1.64	0.0894	−2.69	1.26	2.13
anisole	−1.85	0.109	−2.82	1.30	2.11
chlorobenzene	−2.36	0.102	−3.35	1.68	2.84
ethylbenzene	−2.84	0.123	−3.75	1.98	3.15
1,2-dichlorobenzene	−2.98	0.113	−3.98	2.27	3.38
1,3-dichlorobenzene	−3.04	0.114	−3.98	2.23	3.38
1,4-dichlorobenzene	(−3.03)	0.118	−3.96	2.20	3.39
1,2,4-trichlorobenzene	−3.57	0.125	−4.47	2.70	4.02
2-PCB	(−4.57)	0.174	−5.33	3.23	4.51
2,2′-PCB	(−5.08)	0.189	−5.57	3.68	4.80
2,4′-PCB	(−5.28)	0.189	−5.97	3.89	5.10
2,4,4′-PCB	(−5.98)	0.204	−6.67	4.38	5.62

[a] The listed solubilities are the 20–25 °C values cited in ref 3 except for anisole from ref 20 and PCBs (at 20 °C) from this work. The numbers in parentheses are the supercooled liquid solute solubilities estimated according to the method described in ref 3. For 2-, 2,2′-, 2,4′-, and 2,4,4′-PCB, the calculations were based on their solid solubilities of 3760, 717, 637, and 115 μg/L at 20 °C, respectively, and an assumption of 13.5 cal/(mol K) for their entropies of fusion. [b] The molar volumes of PCBs are estimated by using the densities of liquid Aroclor mixtures that have approximately the same chlorine atoms as the individual PCBs. [c] The K_{ow} values of PCBs (except for 2-PCB) are the experimental data from this work, and the values for the remaining compounds are from ref 3 and 21.

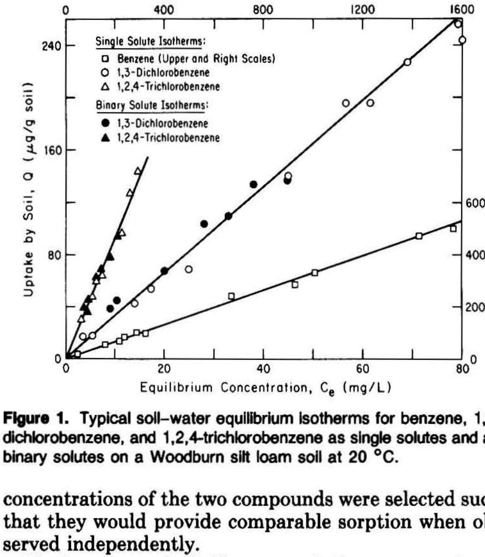

Figure 1. Typical soil-water equilibrium isotherms for benzene, 1,3-dichlorobenzene, and 1,2,4-trichlorobenzene as single solutes and as binary solutes on a Woodburn silt loam soil at 20 °C.

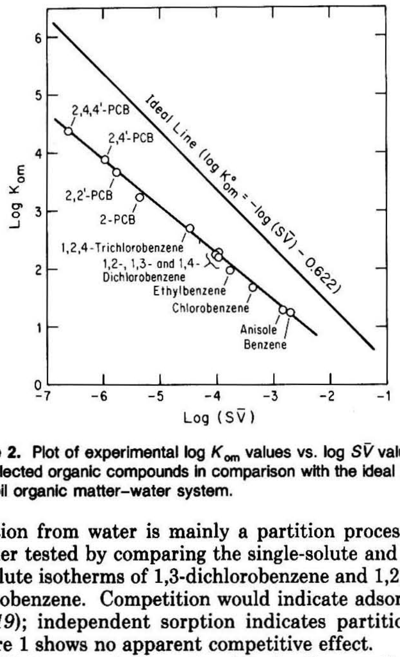

Figure 2. Plot of experimental log K_{om} values vs. log $S\bar{V}$ values for the selected organic compounds in comparison with the ideal line for the soil organic matter–water system.

concentrations of the two compounds were selected such that they would provide comparable sorption when observed independently.

The benzene and ethylbenzene solutions were analyzed by a Tracor 550 gas chromatograph with a Chromosorb 105 column and hydrogen flame detector. Anisole solutions were analyzed by UV absorption using a Cary 11 spectrophotometer. The remaining compounds were analyzed with the Tracor 550 gas chromatograph with a Carbowax 20 M column and EC detector. The amount sorbed was based on the difference in aqueous concentrations before and after equilibration. The amount of chemicals retained by the glass wall was found insignificant compared to the amount sorbed by soil, and hence no correction was made.

Results and Discussion

Typical isotherms from water at 20 °C for benzene, 1,3-dichlorobenzene, and 1,2,4-trichlorobenzene as single components and for the last two in combination on a Woodburn silt loam soil are shown in Figure 1. No indication of isotherm curvature at equilibrium concentrations extending to 60–90% of saturation was found. This characteristic complies with the criteria for solute partition in the soil organic matter phase (*1, 2, 4*). The idea that sorption from water is mainly a partition process was further tested by comparing the single-solute and binary-solute isotherms of 1,3-dichlorobenzene and 1,2,4-trichlorobenzene. Competition would indicate adsorption (*16–19*); independent sorption indicates partitioning. Figure 1 shows no apparent competitive effect.

Table I summarizes sorption data for 12 aromatic compounds on the same soil along with related physical properties. The K_{om} values are obtained from the slopes of the isotherms divided by the organic matter content of the soil. While these data are for a single soil, many investigators (*1, 4, 22–29*) have shown that the sorptive characteristics of the organic components of soils of widely differing types and sources are comparable. The results in Table I can therefore be considered reasonably representative of many soils. Figure 2 is a plot of log K_{om} vs. log $S\bar{V}$ along with the ideal line from eq 9. The regression equation of data from the 12 organic compounds is

$$\log K_{om} = -0.813 \log (S\bar{V}) - 0.993 \qquad (10)$$

with a correlation coefficient $r^2 = 0.995$, where S is in moles per liter and $\bar{V}$ in liters per mole. Similar to the partition of organic solutes in octanol–water systems (in which log

$K_{ow} = -0.862 \log S + 0.710$) (*3, 4*), the experimental log K_{om} values show a systematic deviation from the ideal line, making the slope of the experimental line significantly different from −1. However, while the effect of log $S\bar{V}$ is more important than the effect of solute incompatability with soil organic phase, i.e., $(\chi - \chi_S)/2.303$, the latter is greater than the corresponding effect (log γ_0*, eq 1) for the same compounds with the octanol phase (*3, 4*). The finding that soil organic matter is inferior to octanol as partition phase for relatively nonpolar organic compounds is quite reasonable as the soil organic matter is generally more polar than octanol. This difference in polarity is illustrated by the observation that soil humus can sorb a significant amount of water (*30*), whereas octanol holds only about 5% water by weight (*31*).

Using eq 8 to account for the deviations from the ideal line (log $K_{om}°$ − log K_{om}) for the compounds for which solubility parameters are available (*32*) (benzene $\delta = 9.2$; chlorobenzene, 9.5; ethylbenzene, 8.8; 1,2-dichlorobenzene, 10.0), δ_p is calculated to be 12.7, 13.2, 12.3, and 13.6 for the (water-saturated) humic substances of the studied soil. The average value ($\delta_p = 13.0$) appears to fall into a reasonable range for soil humus that contains certain polar groups and water in its network, indicating that its polarity is between acetal resin ($\delta_p = 11.1$) and polyacrylonitrile ($\delta_p = 15.4$) and perhaps close to nylon 66 ($\delta_p = 13.6$) (*33*). The calculated δ_p value for the organic matter of the studied soil is appreciably higher than $\delta = 10.3$ for octanol, although the δ value for the octanol phase of the octanol–water mixture would be somewhat greater because of water saturation. The calculated δ_p could be inaccurate as eq 3, 6, and 8 are derived with certain assumptions and approximations.

Since variability of $\bar{V}$ is small compared to that of S, the correlation between log K_{om} and log S should be essentially linear, as reported previously (*1, 4, 22–28*). Omitting the molar volume term, the present study leads to

$$\log K_{om} = -0.729 \log S + 0.001 \qquad (11)$$

with $r^2 = 0.996$, where S is in moles per liter. In eq 10 and 11, the S values for solid solutes are the estimated solubilities of the corresponding supercooled liquids. The reason for this adjustment is discussed later.

Because water insolubility is the major factor affecting the values of K_{om} and the values of K_{ow} (octanol–water) for slightly water-soluble organic solutes (*3*), a practically linear relationship should also exist between log K_{om} and log K_{ow}, as observed for various compounds in different soils (*22–29*). In this study, the regression gives

$$\log K_{om} = 0.904 \log K_{ow} - 0.779 \qquad (12)$$

with $n = 12$ and $r^2 = 0.989$. The coefficient of log K_{ow} for a selected group of compounds should approximate the ratio of the change of log K_{om} with log S to that of log K_{ow} with log S. The ratio of −0.729 in eq 11 to −0.799 in log K_{ow} vs. log S for the 12 compounds in Table I yields 0.912, in good agreement with eq 12.

Since the effect of melting point contributes to part of the solute insolubility without affecting the partition coefficient (*3, 34*), we have converted the water solubilities of the solid solutes to the estimated solubilities of the corresponding supercooled liquids by standard thermodynamic methods (*3, 13*). This procedure normalizes all solute solubilities in terms of their liquid forms. Consistent with the partition criteria, 1,4-dichlorobenzene as a supercooled liquid and 1,2- and 1,3-dichlorobenzenes as liquids, now having about equal solubilities, give about the same values in K_{ow} (*21*) and in K_{om}. Similarly, anthracene and phenanthrene as supercooled liquids have about the same water solubilities (*3*) and K_{ow} (*21*) and K_{om} (*22*) values, despite a large difference in their solubilities as solids (*3*). In general, the Flory–Huggins treatment for solute solubility in a polymer phase and the melting-point correction for solid solubilities lead to an improved understanding of the correlations of log K_{om} vs. log $S\bar{V}$, log K_{om} vs. log S, and log K_{om} vs. log K_{ow}. From the partition standpoint, one can expect the K_{om} values and hence the correlation equations with log K_{om} for given compounds in different soils to be affected by the composition of the soil organic matter. A characterization of structural variations of humic substances in soils (sediments) is an important step toward defining the range of variability of K_{om} values.

Finally, the partition concept for soil–water systems appears to parallel the theory for reversed-phase high-pressure liquid chromatography (HPLC). Both processes involve partition of the solute into the polymeric (organic) phase. The mineral fraction of soil and the column support interact preferentially with the polar solvent (water) and are thus relatively inert to nonionic organic compounds. Just as the composition of the stationary phase in reverse-phase HPLC affects the retention, K_{om} is affected by the network and polarity of soil humus as it varies with oxidation and ambient conditions. Thus, although the water solubility of an organic solute appears to be the primary factor determining K_{om}, it would be of interest to investigate how humic components vary in different soils and how their capacity to remove solutes from water depends on these chemical and physical differences, including the effect of water sorbed to humic components.

Registry No. H_2O, 7732-18-5; 2-PCB, 2051-60-7; 2,2′-PCB, 13029-08-8; 2,4′-PCB, 34883-43-7; 2,4,4′-PCB, 7012-37-5; benzene, 71-43-2; anisole, 100-66-3; chlorobenzene, 108-90-7; ethylbenzene, 100-41-4; 1,2-dichlorobenzene, 95-50-1; 1,3-dichlorobenzene, 541-73-1; 1,4-dichlorobenzene, 106-46-7; 1,2,4-trichlorobenzene, 120-82-1; 1-octanol, 111-87-5.

Literature Cited

(1) Chiou, C. T.; Peters, L. J.; Freed, V. H. *Science (Washington, D.C.)* **1979**, *206*, 831.
(2) Chiou, C. T.; Peters, L. J.; Freed, V. H. *Science (Washington, D.C.)* **1981**, *213*, 684.
(3) Chiou, C. T.; Schmedding, D. W.; Manes, M. *Environ. Sci. Technol.* **1982**, *16*, 4.
(4) Chiou, C. T. In "Hazard Assessment of Chemicals: Current Developments"; Saxena, J., Fisher, F., Eds.; Academic Press: New York, 1981; Vol. I, pp 117–153.
(5) Flory, P. J. *J. Chem. Phys.* **1942**, *10*, 51.
(6) Huggins, M. L. *Ann. N.Y. Acad. Sci.* **1942**, *43*, 1.
(7) Rieman, W.; Walton, H. F. "Ion Exchangers in Analytical Chemistry"; Pergamon Press: New York, 1970.
(8) Horvath, C.; Melander, W. Molnar, I. *J. Chromatogr.* **1976**, *125*, 129.
(9) Horvath, C.; Melander, W. *J. Chromatogr. Sci.* **1977**, *15*, 393.
(10) Freeman, D. H.; Cheung, L. S. *Science (Washington, D.C.)* **1981**, *214*, 790.
(11) Flory, P. J. "Principles of Polymer Chemistry"; Cornell University Press: Ithaca, NY, 1953; pp 495–520.
(12) Tijssen, R.; Billiet, H. A. H.; Schoemakers, P. J. *J. Chromatogr.* **1976**, *122*, 185.
(13) Hildebrand, J. H.; Prausnitz, J. M.; Scott, R. L. "Regular and Related Solutions"; Van Nostrand-Reinholdt: New York, 1970.
(14) Scott, R. L. *J. Chem. Phys.* **1949**, *17*, 268.
(15) Weast, R. C. "Handbook of Chemistry and Physics", 53rd ed.; CRC Press: Cleveland, OH, 1972.
(16) Rosene, M. R.; Manes, M. *J. Phys. Chem.* **1976**, *80*, 953.
(17) Rosene, M. R.; Özcan, M.; Manes, M. *J. Phys. Chem.* **1976**, *80*, 2586.
(18) Rosene, M. R.; Manes, M. *J. Phys. Chem.* **1977**, *81*, 1646.

Environ. Sci. Technol. **1983**, *17*, 231–237

(19) Manes, M. In "Activated Carbon Adsorption of Organics from the Aqueous Phase"; Suffet, I. H., McGuire, M. J., Eds.; Ann Arbor Science: Ann Arbor, MI, 1980; Vol. I, pp 43–64.

(20) McGowan, J. C.; Atkinson, P. N.; Ruddle, L. H. *J. Appl. Chem.* **1966**, *16*, 99.

(21) Hansch, C.; Leo, A. "Substituent Constants for Correlation Analysis in Chemistry and Biology"; Wiley: New York, 1979.

(22) Karickhoff, S. W.; Brown, D. S.; Scott, T. A. *Water Res.* **1979**, *13*, 241.

(23) Kenaga, E. E.; Goring, C. A. I. In "Aquatic Toxicology"; Eaton, J. C., Parrish, P. R., Hendricks, A. C., Eds.; American Society for Testing and Materials: Philadelphia, PA, 1980; pp 78–115.

(24) Karickhoff, S. W. *Chemosphere* **1981**, *10*, 833.

(25) Hassett, J. J.; Banwart, W. L.; Wood, S. G.; Means, J. C. *Soil Sci. Soc. Am. J.* **1981**, *45*, 38.

(26) Means, J. C.; Wood, S. G.; Hassett, J. J.; Banwart, W. L. *Environ. Sci. Technol.* **1980**, *14*, 1524.

(27) Means, J. C.; Wood, S. G.; Hassett, J. J.; Banwart, W. L. *Environ. Sci. Technol.* **1982**, *16*, 93.

(28) Briggs, G. G. *J. Agric. Food Chem.* **1981**, *29*, 1050.

(29) Schwarzenbach, R. P.; Westall, J. *Environ. Sci. Technol.* **1981**, *15*, 1360.

(30) Boelter, D. H. *Soil Sci. Soc. Am. J.* **1964**, *28*, 433.

(31) Leo, A.; Hansch, C.; Elkins, D. *Chem. Rev.* **1971**, *71*, 525.

(32) Barton, A. F. M. *Chem. Rev.* **1975**, *75*, 731.

(33) Deanin, R. D. "Polymer Structure Properties and Applications"; Cahners Books: Boston, MA, 1972; p 293.

(34) Mackay, D. *Environ. Sci. Technol.* **1977**, *11*, 1219.

Received for review August 13, 1982. Revised manuscript received December 6, 1982. Accepted December 30, 1982. This work was supported by EPA Cooperative Research CR-808046 from the EPA Environmental Research Laboratory at Corvallis, OR, and by NIH Grants ES-02400 and ES-00210.

Partitioning of Strontium-90 among Aqueous and Mineral Species in a Contaminated Aquifer

Richard E. Jackson* and Karen J. Inch

River Road Laboratories, National Hydrology Research Institute, Inland Waters Directorate,
Environment Canada, Ottawa, K1A 0E7, Canada

■ The geochemical partitioning of a toxic metal contaminant, ^{90}Sr, during its migration through a shallow sand aquifer is discussed. Adsorption of ^{90}Sr from the contaminated groundwaters (pH ~6, I ~0.001) causes it to have a migration velocity of only 3% of that of transporting groundwater. Five microscopically identified adsorbents were isolated in the aquifer sediments and showed the following affinity sequence for ^{90}Sr: vermiculite > feldspar > biotite > muscovite > quartz. While ~80% of the adsorbed ^{90}Sr is exchangeable with 0.1 M $SrCl_2$, the residual adsorbed ^{90}Sr is strongly correlated with extractable Fe, Al, and Mn, suggesting specific adsorption by these metal oxides. An equilibrium adsorption model was used to determine the partitioning of ^{90}Sr between adsorbents and between solid and solution phases. Over 90% of all ^{90}Sr in the aquifer is adsorbed. Approximately 90% of all adsorbed ^{90}Sr is equally divided between vermiculite and feldspar minerals.

Introduction

The radionuclide ^{90}Sr was disposed of in shallow trenches in the recharge area of an aquifer at the Chalk River Nuclear Laboratories (200 km northwest of Ottawa, Ontario, Canada) during the mid-1950s in experiments to determine the consequences of the escape of radionuclides from waste-management facilities. Since that time the ^{90}Sr has migrated through the sand aquifer (Figures 1 and 2) at a velocity approximately 3% of that of the transporting groundwater (*1, 2*). This phenomena can be used to illustrate how a metal contaminant is geochemically partitioned during its migration through a sand aquifer.

All reports of ^{90}Sr migration in aquifers, whether porous or fractured, indicate that ^{90}Sr is strongly retarded relative to the mean groundwater velocity (*1–9*). Adsorption and/or precipitation processes are undoubtedly responsible.

In the simplest case retardation may be due to electrostatic adsorption involving clay minerals and cation exchange. In such systems Sr(II) adsorbs ideally in that mass-action equilibria equations adequately describe the reactions (*10–13*). However, natural aquifer materials that are effective adsorbents include not only clay minerals but also hydrous metal oxides, primary aluminosilicates and organic matter. In aquifer sediments, two or more of these phases may be present in a single grain, and each phase may be of variable composition. Furthermore Sr(II) adsorption by any particular adsorbent may be due to a composite of electrostatic, covalent, and perhaps other forces (*14*).

Of the other adsorbents only hydrous metal oxides have received significant attention as Sr(II) sinks (*15–25*). Experiments show that Sr(II) is specifically adsorbed by Al(III) and Fe(III) oxide gels (*22, 23*) and perhaps MnO_2 (*24*). Hence it is probable that ^{90}Sr is retained by these oxides in aquatic sediments. Our own work (*1, 2*) supports this thesis, as does that of Cerling and Turner (*25*), who have noted that Fe/Mn oxide coatings on streambed sediments near the Oak Ridge National Laboratory, TN, contain ^{90}Sr in a nonexchangeable form.

In addition to adsorption mechanisms Sr(II) may be retarded during groundwater transport by precipitation processes, either as $SrCO_3$ (*26*) or by coprecipitation with $CaCO_3$ (*27*).

The purpose of this study was to determine how ^{90}Sr is partitioned within a shallow, sand aquifer typical of those used for municipal and industrial water supply and waste disposal. This was accomplished by (1) characterizing the hydrogeological and mineralogical properties of the contaminated aquifer sediments, (2) determining the extent of ^{90}Sr migration within the aquifer and the distribution of ^{90}Sr between solid and aqueous phases, (3) defining the aqueous geochemistry of ^{90}Sr in the contaminated zone, (4) identifying the portion of adsorbed ^{90}Sr associated with various grain-size fractions and mineral adsorbents, (5) conducting desorption experiments on contaminated aquifer sediments to estimate the relative amounts of electrostatically and specifically adsorbed ^{90}Sr, and (6)

0013-936X/83/0917-0231$01.50/0

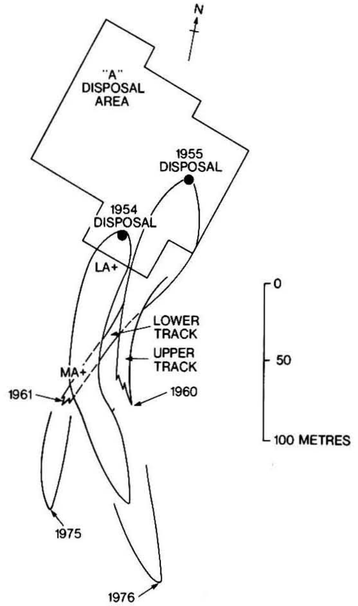

Figure 1. Plan view of ^{90}Sr migration paths showing dates of advance. The outline of the plumes is defined by radioactivities of 1000 dpm/g.

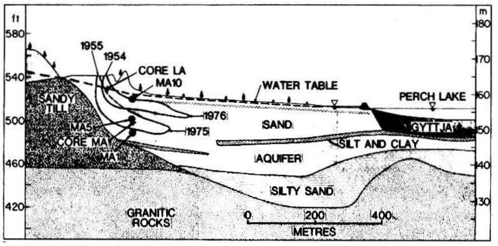

Figure 2. Cross-sectional view of ^{90}Sr migration paths. The outline of the plumes is defined by radioactivities of 1000 dpm/g. Locations of cores (LA, MA) and groundwater samples (MA10, 5, 1) are identified.

incorporating the above results into a partitioning model to obtain an approximation of the distribution of the contaminant among microscopically identified adsorbents.

Experimental Section

Groundwaters were pumped from radioactively contaminated parts of the aquifer by using a portable peristaltic pump and multilevel sampling devices composed of polypropylene tubes (0.3-cm diameter) contained inside a PVC pipe, each tube protruding through the wall of the pipe at a different depth, at which elevation it serves as a point water sampler (*9*). After measuring groundwater temperature and specific electrical conductance (YSI SCT meter), pH and E_H were measured in the field by using air-exclusion flow cells and combination glass and platinum electrodes connected to a voltmeter (Orion 407A). Dissolved oxygen was measured with a ppb oxygen analyzer (Orbisphere). Groundwater samples for chemical analysis were collected in a Millipore Plexiglass sampler and then forced under N_2 pressure through a 0.45-μm prerinsed, in-line Swinnex filter (Millipore HA) into an acid-rinsed, N_2-filled polyethylene bottle. A portion of the filtrate was acidified for cation analysis, the remainder being kept for anion analysis. Metals were determined by atomic absorption (K, Mg, Fe, Mn) and flame emission (Ca, Na, Sr) spectrophotometry, alkalinity by potentiometric titration, sulfate by colorimetric titration, and chloride by specific-ion potentiometry. Total inorganic carbon was measured with an Oceanography International total carbon analyzer with an IR detector (*1*, *28*).

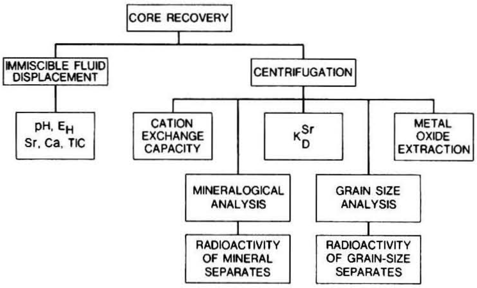

Figure 3. Flow chart of procedures of analysis of contaminated aquifer sediments.

Undisturbed samples of contaminated aquifer sediments were recovered from shallow depths (1–12 m) by using a cohesionless sediment sampler to which was attached a 5-cm i.d. thin-walled aluminum tube of 1.5-m length. Part of the core was used for the extraction of the interstitial waters by immiscible-fluid displacement (*29*) to determine the state of $CaCO_3$ and $SrCO_3$ saturation. In the rest of the core interstitial waters were separated from aquifer sediments by centrifugation, and subsequently chemical and mineralogical analyses were conducted on the contaminated waters and sediments (*2*). Grain-size and mineralogical analyses of the contaminated aquifer sediments were conducted by using dry sieving and either optical or X-ray diffraction (XRD) techniques, respectively. Cation-exchange capacities were measured by using a modification of the USGS method (*30*) employing ^{60}Co and an automatic γ counter (*2*). These procedures are summarized in Figure 3.

Desorption experiments were undertaken on ^{90}Sr-contaminated aquifer sediments in order to determine the amounts of adsorbed radioactivity that were (1) exchangeable with 0.1 M $SrCl_2$, (2) associated with oxides of Al, Fe, and Mn, and (3) still fixed following these steps. A procedure based on that of Suarez and Langmuir (*31*) was developed in which 30 g of contaminated sediment was first counted for total β emissions and then placed in an Erlenmeyer flask to which was added 100 mL of 0.1 M $SrCl_2$. The flask was gently agitated, avoiding grain abrasion, on a shaker for 3 days, after which time the sediments were retained on a filter, washed with distilled water, and measured for residual adsorbed radioactivity. A 1-g portion of sediment that had been extracted with $SrCl_2$ was dried and placed in a scintillation vial with 15 mL of an acidified reducing agent, 0.1 M hydroxylamine hydrochloride in 0.1 M potassium tetroxalate (pH $\simeq$1.5). The vial was agitated for 3 days, following which either the sediment was decanted, washed, and counted for fixed radioactivity or the aqueous extract was recovered and counted for desorbed radioactivity. In the latter case the aqueous extract was also analyzed for Al, Fe, and Mn by atomic absorption spectrophotometry in order to estimate the amount of the respective hydrous metal oxides dissolved by the acidified reducing agent that were presumably acting as radiostrontium adsorbents.

The radiochemical separation of ^{90}Sr from other radionuclides was achieved by carbonate precipitation of Sr(II) in groundwater or sediment extract followed by fuming HNO_3 separation employing 25 mL of water and 1 g of sediment (2 N HNO_3 extraction) (*32*). The distribution coefficient was calculated by

$$K_D^{Sr} = \frac{dpm/g}{dpm/mL} \qquad (1)$$

where dpm/g and dpm/mL are the radioactivities expressed in disintegrations per minute per gram of sediment and per milliliter of interstitial water, respectively. The radioactivity of (1) grain-size and mineral separates and (2) aqueous extracts and sediments from the desorption experiments and the distribution coefficient measurements were counted in a low-background β counter after 15 days to permit the growth of the ^{90}Y daughter (detection limit ~27 dpm).

Contaminated Aquifer

Hydrogeology and Mineralogy. The aquifer system in the vicinity of the A disposal area at the Chalk River Nuclear Laboratories is composed of a sequence of fluvial and aeolian sands that are typically fine grained (0.25–0.125 mm) with less than 5% silt and clay. The aquifer system contains several discontinuous silt and clay units up to 1 m thick (*1*).

Approximately 80% of all sand-sized grains are either quartz or feldspar with minor amounts of biotite (partially altered to vermiculite), hornblende, muscovite, chlorite, sericite, and magnetite. Trace amounts of calcite (<0.01% by weight), iron sulfide, organic matter (~0.01% by weight), and hydrous oxides of aluminum (~0.1% by weight extractable metal), iron (~0.1%), and manganese (~0.001%) have also been detected in the aquifer sediments (*1, 28*).

The hydraulic conductivity of the aquifer sands is in the range 2×10^{-3} to 2×10^{-2} cm/s (*9*), the mean porosity is 0.38 (*33*), and the bulk density is about 1.7 g/cm^3 (*9*). Groundwater recharge to the aquifer occurs in the upland region around the A disposal area. In general, flow is horizontal in the sand aquifer and groundwater discharges into Perch Lake. On the basis of borehole-dilution tests the mean groundwater flow velocity at the leading edge of the ^{90}Sr plumes is about 5–25 cm/day (*34*). The residence time for groundwater in the shallow flow system is approximately 10–20 years, computed on the basis of tritium dating and velocity measurements (*1*).

^{90}Sr Migration and Distribution Coefficients. Three disposals of ^{90}Sr were conducted at A disposal area in the 1950s. The first, in 1952, contained 1000 Ci of ^{90}Sr in 5000 m^3 of water disposed into a trench system. In 1954, 7 m^3 of liquid radioactive waste containing 60 Ci of ^{90}Sr plus other mixed fission products in solution with 700 kg of HNO_3 and 2000 kg of NH_4NO_3 was disposed into a pit 3 m deep containing lime and limestone. In 1955, a solution containing 300 Ci of ^{90}Sr plus other mixed fission products dissolved in 500 m^3 of 2.5 N HNO_3 was disposed into a pit without neutralization (*35*). In the period immediately following 1955, ^{90}Sr migrated rapidly through the aquifer due to the low pH and high ionic strength conditions. Figures 1 and 2 show the approximate positions of the ^{90}Sr front at different dates as defined by the total count rate of all β emitters (β_T) of 1000 dpm/g (*1, 36*). Since 1960 the ^{90}Sr has migrated at approximately 3% of the velocity of the groundwater.

From eq 1 the mean value of the distribution coefficient of ^{90}Sr for ten samples from the LA and MA sampling sites was K_D^{Sr} = 9.6 mL/g with a standard deviation σ = 4.9 mL/g. Batch K_D^{Sr} values determined by Patterson and Spoel (*37*) using sediments from the same aquifer yielded a mean estimate of 4.5 mL/g, whereas analysis of breakthrough curves for an in situ ^{85}Sr tracer test, conducted 100 m in front of the ^{90}Sr plume, yielded K_D^{Sr} values ranging from 2.6 to 4.5 mL/g (*9*). A discussion of the causes for these relatively minor differences is given by Pickens et al. (*9*).

Table I. Chemical Analysis of Groundwaters Pumped from Multilevel Samplers (MA10, 5, 1) and Extracted from Cores of Aquifer Sediments (MA5/3, LA1/2) and Numerically Computed Speciation Data

parameter	MA10	MA5	MA1	MA5/3	LA1/2
		Chemical Analyses[a]			
pH	6.0	6.1	6.7	6.3	6.2
E_H, V	0.55	0.37	0.41	0.1	0.4
alkalinity, mequiv/L	0.2	0.4	0.7		
O_2	5.0	<0.4	≃2		
TIC	2.5	4.7	9.1	15.2	8.4
Ca^{2+}	4.2	12.0	24.4	15	12
Mg^{2+}	1.3	4.8	13.8		
Sr^{2+}	<0.01	0.06	0.11	0.06	0.05
Na^+	2.0	17.2	44.0		
K^+	1.6	2.4	3.5		
Fe^{2+}	<0.1	3.6	0.2		
Mn^{2+}	0.01	0.56	0.18		
SO_4^{2-}	7.5	11.5	18.0		
Cl^-	4.8	62	108		
		Computed Speciation[b]			
SI $SrCO_3$	<0	−5.3	−4.0	−3.4	−4.0
SI $CaCO_3$	−4.3	−3.4	−2.0	−2.4	−2.9
SI $SrSO_4$	<0	−3.0	−2.6		
pSr^{2+}		6.2	5.9	5.1	5.2
$pSrHCO_3^+$		8.9	8.2	7.2	7.7
$pSrOH^+$		13.4	12.6	12.2	12.4
$pSrSO_4^0$		7.8	7.4		

[a] Data in mg/L except where noted. TIC = total inorganic carbon. [b] SI = log IAP − log K_{SO}. $SrCO_3$: pK_{SO} = 9.00, T = 25 °C, I = 0. $CaCO_3$: pK_{SO} = 8.30. $SrSO_4$: pK_{SO} = 7.30. pSr^{2+} etc. indicates negative logarithm of concentration of aqueous species. $SrHCO_3^+$: log β = 11.5 (*38*). $SrOH^+$: log β −13.29 (*39*). $SrSO_4^0$: log β = 2.5 (*38*).

Results and Discussion

Aqueous Speciation of Sr(II). In order to establish whether the retardation of ^{90}Sr is due to solubility or adsorption processes, large-volume (~2 L) samples of groundwater were pumped from a multilevel sampling device installed in the aquifer at site MA (see Figures 1 and 2). Chemical data for three multilevel samplers are reported in Table I, as are saturation index ($CaCO_3$, $SrCO_3$, $SrSO_4$) and speciation (Sr^{2+}(aq), $SrHCO_3^+$, $SrSO_4^0$) values calculated by the computer code MINEQL (*40*). In all cases the groundwaters are unsaturated with respect to the Sr(II) compounds, and the aquo ion comprises about 98% of the total aqueous Sr(II). Furthermore the groundwaters extracted by immiscible fluid displacement from the cores of aquifer sediments taken at the MA and LA sites also display undersaturation of the metal carbonates. Consequently the retardation of ^{90}Sr must be due to the adsorption of Sr(II), most probably as the aquo ion.

Identification of Mineral Adsorbents. Cores of contaminated aquifer sediments were taken at two sites in the ^{90}Sr plume, LA and MA (see Figure 1) and were processed according to the methods in Figure 3 in order to identify the mineral adsorbents. Analysis by X-ray diffractometry confirmed the presence of the clay mineral vermiculite as well as the common minerals quartz, feldspar, and hornblende (*9, 28*). The vermiculite is concentrated in the coarse fraction of the aquifer sediment

Table II. Radioactivity (β_T) Associated with Various Grain-Size Fractions of Core MA and Their Corresponding Mineral Abundances

grain size, mm	wt %	radio-activity dpm/g	mineral abundance, %		
			quartz	feld-spar	mica[a]
>0.42	3	7100	29	28	42
0.25–0.42	28	3400	45	34	18
0.18–0.25	34	1400	47	35	15
0.15–0.18	13	1600	50	30	10
0.12–0.15	10	2300	53	29	10
0.10–0.12	7	2700	42	31	13
0.09–0.10	2	3600	40	23	10
0.07–0.09	1	7300	40	21	9

[a] Includes biotite, muscovite, and vermiculite.

and is probably the result of in situ chemical weathering of biotite (*28*), which may be written schematically as in eq 2. Thus the weathering of biotite produces an ad-

$$\underset{\text{(biotite)}}{\text{Fe(II)–cation–Al–silicate(s)}} + O_2 + H_2CO_3 + H_2O \rightarrow$$
$$\underset{\text{(vermiculite)}}{\text{Fe(III)–Al–silicate(s)}} + \text{Fe(III)–Al–oxide(s)} +$$
$$HCO_3^- + H_4SiO_4 + \text{cations} + \text{electrons} \quad (2)$$

sorbent clay mineral, which on the basis of electron microprobe data has a surface enriched in Fe(III) and Al(III) oxides (*28*). Recent work by Lyon (*41*) has demonstrated that many quartz and feldspar grains in this aquifer also contain Fe(III) oxides. The cation-exchange capacities of these two sediments are 1.2 ± 0.1 mequiv/100 g for LA and 1.1 ± 0.6 mequiv/100 g for MA.

Grain-size analysis of LA and MA, shown in Table II, revealed that the ^{90}Sr is preferentially adsorbed by the coarsest (>0.4 mm) and finest (<0.09 mm) fractions on a basis of equal weight (i.e., dpm/g). It is important to note that these two fractions comprise only about 4% of the total sediment weight and that the bulk of adsorbed radiostrontium is associated with the medium-grain-size fraction (i.e., fine and very fine sands). However, the bimodal distribution of maximum adsorbed radioactivity indicates that an adsorption process not wholly dependent on specific surface must account for the association of ^{90}Sr with the coarsest grain-size fraction. An inspection of the mineral abundances in the coarsest fraction of MA (see Table II) shows that abundant mica is present, including vermiculite.

Two-hundred medium- and coarse-sized grains of each of quartz, feldspar, vermiculite, biotite, and muscovite from core LA were separated under an optical microscope and were counted for total β activity. The relative affinity of these minerals for ^{90}Sr is given by the following sequence in which the numerical values in parentheses have the units of dpm/200 grains: vermiculite (3000) > feldspar (1900) > biotite (1600) > muscovite (~500) > quartz (~200). Therefore, vermiculite is indeed responsible for the enhanced adsorption of ^{90}Sr by the coarse-sized fraction and is the most adsorbent aquifer material on a grain-for-grain basis. This conclusion has also been reached by Lyon (*41*) in another study of mineral adsorbents elsewhere in the same aquifer.

Desorption Experiments. In order to indicate the mechanisms by which ^{90}Sr is adsorbed to the aquifer materials, selective chemical extractants were used to desorb ^{90}Sr from the LA and MA core samples.

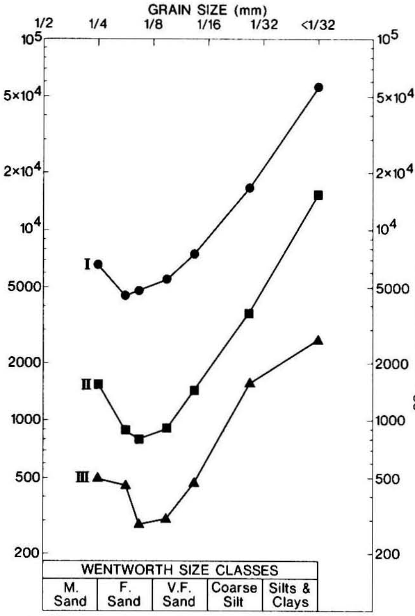

Figure 4. ^{90}Sr associated with various grain-size fractions from core LA: (I) untreated ^{90}Sr-contaminated aquifer sediment; (II) residual radioactivity following extraction with 0.1 M $SrCl_2$ for 3 days at 24 °C; (III) residual radioactivity following extraction with $SrCl_2$ and then 0.1 M $NH_2OH{\cdot}HCl$ (pH ~1.5) for 3 days at 24 °C.

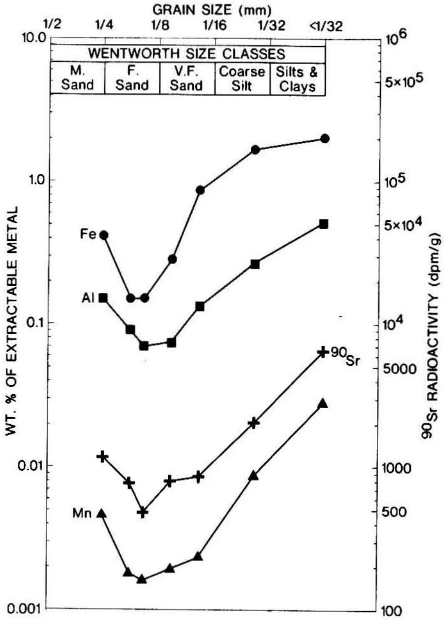

Figure 5. Amounts of ^{90}Sr, Fe, Al, and Mn extracted with acidified hydroxylamine hydrochloride from various grain-size fractions of core LA following extraction of the same samples with 0.1 M $SrCl_2$.

The effect of the desorption treatments on the LA sample is shown in Figure 4. Approximately 80% of the ^{90}Sr is exchangeable with $SrCl_2$ and is therefore assumed adsorbed by simple electrostatic bonds. Most of the residual ^{90}Sr is released by treatment with the acidified reducing agent. To confirm that it is the hydrous oxides of Al, Fe, and Mn that are actually retaining the ^{90}Sr, the extracting solutions were analyzed for Al, Fe, and Mn as

Table III. Partition Model[a] for ^{90}Sr Adsorption in a Contaminated Sand Aquifer

adsorbent	abundance,[b] %	10^3K_{AD},[c] L/g	$\{S_T\}$,[d] g/L	$K_{AD}\{S_T\}$	fractional adsorption ($K_{AD}\{S_T\}/\Sigma$)
quartz	45	0.4	1900	0.8	0.05
feldspar[e]	38	4.7	1600	7.5	0.45
biotite	4	3.7	200	0.7	0.04
vermiculite	4	37	200	7.4	0.44
muscovite	3	2.6	100	0.3	0.02
	94			$\Sigma = 16.7$	1.00

$[SrS_{ST}]/[Sr_{ST}] = \Sigma/(1 + \Sigma) = 0.94$

[a] See eq 5–7. [b] Weighted averages from Table II. [c] Reference 37. [d] Assumes bulk density = 1.7 g/cm^3 and porosity = 0.4. [e] Includes sericite.

well as for ^{90}Sr. Results of these analyses for both LA and MA desorptions are shown in Figures 5 and 6, respectively, indicating that a very strong correlation exists between ^{90}Sr and extractable Al, Fe, and Mn.

Therefore, the majority (~80%) of adsorbed ^{90}Sr is exchangeably adsorbed; most of the remainder is apparently specifically adsorbed by hydrous metal oxides and is nonexchangeable.

Partition Model. Oakley et al. (*42*) have developed an equilibrium adsorption model to describe the partitioning of trace-metal ions between different adsorbents in aquatic sediments. They consider the adsorption of a dissolved metal ion, Me, by a solid S

$$Me_T + S_T = MeS \tag{3}$$

which yields the conditional equilibrium constant (L/g)

$$K_{AD} = [MeS]/([Me_T]\{S_T\}) \tag{4}$$

where [MeS] is the concentration of adsorbed metal in moles per liter, $[Me_T]$ is the total concentration of dissolved metal ion in moles per liter, and $\{S_T\}$ is the total concentration of the adsorbent in grams per liter. Equation 4 is equivalent to the special case of the Langmuir adsorption isotherm in which $K_{AD}[Me_T] \ll 1$, resulting in a linear isotherm. For such a case K_{AD} is identical with the distribution coefficient $K_D{}^{Me}$ and may be determined from the slope of a straight-line plot of $[MeS]/\{S_T\}$ vs. $[Me_T]$.

Using eq 9–13 of Oakley et al. (*42*), it is possible to develop an expression (eq 5–7) to describe the partitioning

$$\frac{[MeS_{ST}]}{[Me_{ST}]} = \frac{\overset{k}{\sum} MeS(k)}{[Me_T] + \overset{k}{\sum} MeS(k)} \tag{5}$$

$$= \frac{\overset{k}{\sum} K_{AD}(k)\{S_T(k)\}[Me_T]}{[Me_T] + \overset{k}{\sum} K_{AD}(k)\{S_T(k)\}[Me_T]} \tag{6}$$

$$= \frac{\overset{k}{\sum} K_{AD}(k)\{S_T(k)\}}{1 + \overset{k}{\sum} K_{AD}(k)\{S_T(k)\}} \tag{7}$$

between the total metal adsorbed to the various adsorbents, $[MeS_{ST}]$, and the total metal (dissolved + adsorbed) in the system, $[Me_{ST}]$, where $[MeS(k)]$ is the concentration of the metal adsorbed to adsorbent k, $K_{AD}(k)$ and $S_T(k)$ are the conditional equilibrium constant and the concentration of the kth adsorbent, respectively, and $[Me_{ST}] = [Me_T] + [MeS_{ST}]$.

Two assumptions are required in order to employ this partition model: (1) the adsorption of ^{90}Sr by the aquifer materials under consideration is described by a linear adsorption isotherm; (2) local chemical equilibrium is attained between adsorbate and adsorbent.

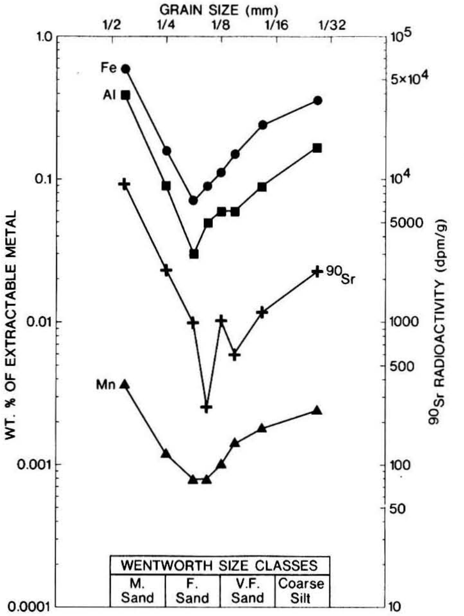

Figure 6. Amounts of ^{90}Sr, Fe, Al, and Mn extracted with acidified hydroxylamine hydrochloride from various grain-size fractions of core MA following extraction of the same samples with 0.1 M $SrCl_2$.

Oakley et al. (*42*) point out that a linear adsorption isotherm is obtained if $\lambda\{S_T\} \gg [MeS]$, where λ is the number of moles of surface sites per unit mass of adsorbent. λ is equivalent to the cation-exchange capacity. For the aquifer sediments under consideration $\lambda \sim 0.5 \times 10^{-5}$ mol of Me(II)/g, $\{S_T\} \sim 4000$ g/L, and $[MeS] \sim 2 \times 10^{-5}$ mol of Sr(II)/L. Therefore $\lambda\{S_T\} \sim 10^3[MeS]$, and the isotherm may be considered linear, consequently $K_D{}^{Sr} = K_{AD}$.

It is assumed that after 25 years of contact with these aquifer materials the observed concentrations of ^{90}Sr in the aquifer approach local chemical equilibrium values.

The results of using the partitioning model developed in eq 3–7 together with the $K_D{}^{Sr}$ values of Patterson and Spoel (*37*) and the weighted averages of the five principal mineral adsorbents of core MA are presented in Table III. As shown, the model accounts for 94% of all grains in MA and suggests that, from eq 7, 94% of ^{90}Sr in the aquifer is adsorbed to the aquifer grains, i.e., only ~6% is in solution at any one time; this implies $K_D{}^{Sr} \sim 4$ mL/g. Of the amount adsorbed approximately 90% (0.45 + 0.44 in the right-hand column of Table III) is associated with just two phases, feldspar and vermiculite.

The results presented in Table III are of special interest to hydrogeologists and groundwater geochemists and suggest that, in the migration of contaminants in groundwater flow systems, toxic metal adsorption may take place predominantly on the grains of minerals (1) that are abundant in the aquifer but have relatively small K_{AD} (or $K_D{}^{Sr}$) values, e.g., feldspar, and (2) those that are relatively scarce but have high K_{AD} (or $K_D{}^{Sr}$) values, e.g., vermiculite. This underlines the necessity for the careful examination of the mineralogy of the aquifer sediments and is a direct consequence of the linearity of the partition model. Knowledge of the relative mineral abundances allows one to estimate an approximate $K_D{}^{Sr}$ value, which demonstrates the practicality of the partition model.

The adsorbents listed in Table III were identified on the basis of X-ray diffraction and optical microscopy. They are not pure solid phases. X-ray fluorescence and electron-microprobe analyses reveal the presence of significant quantities of Fe(III) and Al(III) oxides on their surfaces. These oxides are apparently the cause of the retention of ^{90}Sr by the aquifer materials. Therefore, the adsorbents listed in Table III might better be referred to as "microscopically identified adsorbents". As such "vermiculite" should be considered as a structured mixture of Fe(III), Si(IV), and Al(III) oxides and exchangeable interlayer Mg(II) and K(I) ions with a nominal unit cell spacing of 1.43 nm and a surface randomly enriched in adsorbent Fe(III) and Al(III) oxides. Furthermore, as the ^{90}Sr plume migrates down the flow system (see Figure 2), it encounters increasingly lower dissolved O_2 conditions such that Fe(III) oxides become unstable (*28*) and may no longer play as significant a role as adsorbents.

Conclusions

Cores of contaminated aquifer sediments and samples of contaminated groundwater were taken from within a plume of ^{90}Sr that is advancing through a sand aquifer at approximately 3% of the groundwater velocity. From results of their analysis it is concluded that:

(1) The retardation of ^{90}Sr relative to that of the mean groundwater velocity is due to adsorption rather than precipitation. The vast majority of ^{90}Sr ions (98%) are present as the aquo Sr(II) ion and are presumably adsorbed as such.

(2) The propensity of ^{90}Sr to be adsorbed by any one of five optically identified adsorbents present in the aquifer sediments is given by the following sequence: vermiculite > feldspar > biotite > muscovite > quartz.

(3) Approximately 80% of adsorbed ^{90}Sr is exchangeable with 0.1 M $SrCl_2$. A strong correlation exists between the release of the residual ^{90}Sr and extractable Fe, Al, and Mn, suggesting that ~20% of the adsorbed ^{90}Sr is specifically adsorbed to oxides of these metals.

(4) An equilibrium adsorption model was used to analyze the partitioning of ^{90}Sr between the five microscopically identified adsorbents. The model estimated that >90% of all ^{90}Sr in the aquifer is adsorbed at any one time. Furthermore ~90% of all adsorbed ^{90}Sr is associated equally with feldspar and vermiculite adsorbents; the rest of the adsorbed ^{90}Sr is divided equally between quartz, biotite, and muscovite. The equal importance of the less abundant vermiculite (~4% of all aquifer grains) with feldspar (~38%) as a ^{90}Sr adsorbent is due to its proportionately higher adsorption constant (K_{AD} or $K_D{}^{Sr}$).

Acknowledgments

We acknowledge with thanks the comments and suggestions on this paper by R. J. Patterson, our colleagues at Stanford and Chalk River, and the anonymous reviewers. We express our thanks to AECL for providing laboratory and field facilities on a continuing basis.

Registry No. ^{90}Sr, 10098-97-2; vermiculite, 1318-00-9; biotite, 1302-27-8; muscovite, 1318-94-1; quartz, 14808-60-7.

Literature Cited

(1) Jackson, R. E.; Inch, K. J. "Hydrogeochemical Processes Affecting the Migration of Radionuclides in a Fluvial Sand Aquifer at the Chalk River Nuclear Laboratories"; Environment Canada, IWD Scientific Ser. No. 104, 1980.
(2) Jackson, R. E.; Inch, K. J.; Patterson, R. J.; Lyon, K.; Spoel, T.; Merritt, W. R.; Risto, B. A. In "Contaminants and Sediments"; Baker, R. A., Ed.; Ann Arbor Science: Ann Arbor, MI, 1980; pp 311–329.
(3) Ewing, B. B. *J. Sanit. Eng. Div., Am. Soc. Civ. Eng.* **1959**, *85*, 39.
(4) Kaufman, W. J.; Ewing, B. B.; Kerrigan, J. V.; Inoue, Y. *J. Water Pollut. Control Fed.* **1961**, *33*, 73.
(5) Parsons, P. J. *Health Phys.* **1963**, *9*, 333.
(6) Baetsle, L. H. *Nucl. Saf.* **1967**, *8*, 576.
(7) Tamura, T. In "Underground Waste Management and Environmental Implications"; Cook, T. D., Ed.; Memoir 18, American Association of Petroleum Geologists, Tulsa, OK, 1972; p 318.
(8) Landstrom, O.; Klockars, C.-E.; Holmberg, K.-E.; Wasterberg, S. "In-situ Experiments on Nuclide Migration in Fractured Crystalline Rocks"; Karnbranslesakerhet Tek. Rapp. 110; Stockholm 40, Sweden, 1978.
(9) Pickens, J. F.; Jackson, R. E.; Inch, K. J.; Merritt, W. F. *Water Resour. Res.* **1981**, *17*, 529.
(10) Wahlberg, J. S.; Baker, J. H.; Vernon, R. W.; Dewar, R. S. *Geol. Surv. Bull. (U.S.)* **1965**, No. 1140-C.
(11) Wahlberg, J. S.; Dewar, R. S. *Geol. Surv. Bull. (U.S.)* **1965**, No. 1140-D.
(12) Shiao, S.-Y.; Rafferty, P.; Mayer, R. E.; Rogers, W. J. In "Radioactive Waste in Geological Storage"; Fried, S., Ed.; American Chemical Society: Washington, D.C., 1979; ACS Symp. Ser. No. 100, Chapter 17.
(13) Rafferty, P.; Shiao, S.-Y.; Binz, C. M.; Meyer, R. E. *J. Inorg. Nucl. Chem.* **1981**, *43*, 797.
(14) Parks, G. A. In "Chemical Oceanography", 2nd ed.; Riley, J. P., Skirrow, G., Eds.; Academic Press: New York, 1975; Vol. 1, Chapter 4.
(15) Tamura, T. In "Transactions of 8th International Congress on Soil Science"; Bucharest, Romania, 1964; Vol. 3, pp 465–477.
(16) Belot, Y.; Gailledreau, C.; Rzekiecki, R. *Health Phys.* **1966**, *12*, 811.
(17) Bonner, W. P.; Bevis, H. A.; Morgan, J. J. *Health Phys.* **1966**, *12*, 1691.
(18) Frere, M. H.; Champion, D. F. *Soil Sci. Soc. Am. Proc.* **1967**, *31*, 188.
(19) Schulze, W.; Scheffler, M. *Fresenius' Z. Anal. Chem.* **1967**, *226*, 395.
(20) Egorov, Y. V.; Lyubimov, A. S. *Sov. Radiochem. (Engl. Transl.)* **1969**, *11*, 206.
(21) Huang, C. P.; Stumm, W. *J. Colloid Interface Sci.* **1973**, *43*, 409.
(22) Kinniburgh, D. G.; Syers, J. K.; Jackson, M. L. *Soil Sci. Soc. Am. Proc.* **1975**, *39*, 464.
(23) Kinniburgh, D. G.; Jackson, M. L.; Syers, J. K. *Soil Sci. Soc. J.* **1976**, *40*, 796.
(24) Murray, J. W. *Geochim. Cosmochim. Acta* **1975**, *39*, 505.
(25) Cerling, T. E.; Turner, R. R. *Geochim. Cosmochim. Acta* **1982**, *46*, 1333.
(26) Halevy, E.; Tzur, Y. *Soil Sci.* **1964**, *98*, 66.
(27) Jenne, E. A.; Wahlberg, J. S. *Geol. Surv. Prof. Pap. (U.S.)* **1968**, No. 433-F.
(28) Jackson, R. E.; Patterson, R. J. *Water Resour. Res.* **1982**, *18*, 1255.
(29) Patterson, R. J.; Frape, S. K.; Dykes, L. S.; McLeod, R. A. *Can. J. Earth Sci.* **1978**, *15*, 162.
(30) Beetem, W. A.; Janzer, V. J.; Wahlberg, J. S. *Geol. Surv. Bull. (U.S.)* **1962**, No. 1140-B.

(31) Suarez, D. L.; Langmuir, D. *Geochim. Cosmochim. Acta* **1976**, *40*, 589.
(32) Grummitt, W. E.; Milton, G. M. "Radiochemical Procedures for Strontium and Yttrium"; AECL-934, Chalk River Nuclear Laboratories, Chalk River, Canada, 1957.
(33) Parsons, P. J. "Movement of Radioactive Wastes Through Soil, Part 1"; AECL-1038, Chalk River Nuclear Laboratories, Chalk River, Canada, 1960.
(34) Pickens, J. F.; Cherry, J. A.; Gillham, R. W.; Merritt, W. F. In "Proceedings of the Invitational Well Testing Symposium"; Lawrence Berkeley Laboratory: Berkeley, CA, 1977; p 4.
(35) Mawson, C. A. *Prog. Nucl. Energy, Ser. 12* **1969**, *2*, 461–479.
(36) Parsons, P. J. "Movement of Radioactive Wastes Through Soil, Part III"; AECL-1525, Chalk River Nuclear Laboratories, Chalk River, Canada, 1961.
(37) Patterson, R. J.; Spoel, T. *Water Resour. Res.* **1981**, *17*, 513.
(38) Langmuir, D. In "Chemical Modeling in Aqueous Systems"; Jenne, E. A., Ed.; American Chemical Society: Washington, D.C., 1979; ACS Symp. Ser. No. 93, p 359.
(39) Baes, C. F., Jr.; Mesmer, R. E. "The Hydrolysis of Cations"; Wiley: New York, 1976; p 103.
(40) Westall, J. C.; Zachary, J. L.; Morel, F. M. M. "MINEQL. A Computer Program for the Calculation of Chemical Equilibrium Composition of Aqueous Systems"; Technical Note No. 18, Department of Civil Engineering, Massachusetts Institute of Technology, Cambridge, MA, 1976.
(41) Lyon, K. M.Sc. Thesis, Queen's University, Kingston, Ontario, Canada, 1981.
(42) Oakley, S. M.; Nelson, P. O.; Williamson, K. J. *Environ. Sci. Technol.* **1981**, *15*, 474.

Received for review April 23, 1982. Revised manuscript received November 23, 1982. Accepted December 30, 1982.

Effect of Natural Organic Coatings on the Coagulation of Particles

Ronald J. Gibbs

Center for Colloidal Science, College of Marine Studies, University of Delaware, Newark, Delaware 19711

■ Coagulation experiments with four natural samples and the same samples with the organic coatings removed were conducted in Couette- and blade-type reactors. These experiments showed that the natural coated samples coagulated significantly slower than the samples with the coatings removed. Dissolved organic material did not have a significant effect relative to the particle organic coatings.

Introduction

Fine-grained particles make up the majority of the sediments entering the marine environment. These particles carry the majority of toxic metals and organic substances carried by rivers and discharged into estuaries and the ocean. These muds are responsible for filling estuaries and marshes and for depositing deltas and submarine fans over geological time spans. Therefore, it is critical that we understand the coagulation processes related to fine particles in estuaries and deltas.

The major complicating factor in our present understanding of these processes is that when fine particles first encounter a small amount of seawater, they are attracted to each other to form aggregates or flocs. The presence of aggregates in the environment has been discussed by Berthois (*1*), Biddle and Miles (*2*), Gibbs et al. (*3*), Kranck (*4, 5*), Krone (*6*), Schubel and Kana (*7*), Sheldon (*8*), and Zabawa (*9*).

Coagulation of clay minerals in the laboratory was studied extensively by Whitehouse et al. (*10*) and later by Krone (*6, 11, 12*), Shiozawa (*13*), Hahn and Stumm (*14*), Edzwald (*15*), Edzwald et al. (*16*), Eppler et al. (*17*), Hunt (*18*), and Gibbs (*19*).

The surface electrical properties of particles undergo a change as they pass from a river environment into the ocean mainly because of the polyvalent ions present in seawater. This change has been discussed by Pravdic (*20*), Martin et al. (*21*), and Hunter and Liss (*22*). Natural organic surfactants have an effect on the properties of surfaces of natural particles in seawater through the formation of films, as proposed by Neihof and Loeb (*23–25*) and Hunter and Liss (*22*). These previous studies all measured an electrical property of the particles (electrophoresis, electroosmosis, or streaming potential or current). Specifically, they studied the effect of absorbed surface-active dissolved substances on the electrical properties of the particles.

The present study was designed to measure directly the effect that natural organic coatings have on the coagulation process of natural particles. To provide the best control on isolating this effect, a laboratory study was utilized.

Procedures

The coagulation experiments were conducted in a Coutte-type double cylinder reactor (*26*) similar to that used by Hunt (*18*) and in a blade-type reactor (*19, 27*) similar to that used by Edzwald (*15*). These two reactors are the devices most widely used in coagulation studies in a variety of disciplines. Shear was determined by measuring torque for the blade-type reactor and was calculated for the Coutte-type reactor. The mixing rate in the blade-type reactor was maintained at a shear of 60*g* and the rate in the Couette-type reactor was maintained at a shear of 17*g*.

To eliminate background counts, the water used was filtered through 0.45-μm diameter Millipore filters. Experiments using the Couette-type reactor were conducted at 150 mg/L particle concentration (typical of many turbidity maxima in estuaries) and at the critical coagulation salinity (the salinity at which coagulation increases rapidly) by using dilutions of filtered seawater (34 ‰) with pH maintained at 7 by adding small amounts of HCl. Experiments using the blade-type reactor were conducted with 150–160 mg/L particle concentrations at 1.1, 4.4, and 17.5 ‰ by using dilutions of artificial seawater (*28*), with pH maintained at 8.1 ± 0.3 by adding small amounts of HCl. The artifical seawater was free of dissolved organic substances because of either high-temperature (500 °C) treatment of the salts or ultraviolet treatment of the water and some salt solutions.

The natural samples used in the experiments using the Couette-type reactor were Amazon River material having a composition of 27% montmorillonite, 24% illite, and 38% kaolinite, Yukon River material having a composition of 20% montmorillonite, 29% illite, and 45% chlorite, and material from the continental shelf off Guiana, South

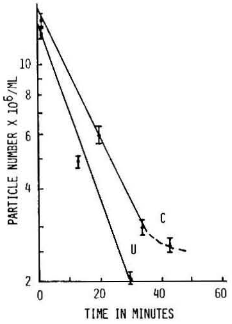

Figure 1. Relationship of particle number and time for the Amazon River sample with and without coating using 2 ‰ salinity in the Couette-type reactor.

America, having a composition of 45% montmorillonite, 18% illite, and 30% kaolinite. The samples were taken from the reactors by using a glass tube having a 2-mm diameter. Each was carefully placed in a 400 μm deep well on a microscope slide. Typically, more than 200 particles were counted, producing the high accuracy reported. Possible error is less than the size of the symbols on the graphs; when it is larger, it is given as an error bar on the graph. In order to determine the effect of organic coating on the coagulation rates, the experiments were conducted with the particles in their natural condition and after the organic coatings were removed by oxidizing with sodium hypochlorite (*29*).

Before coagulation can occur, the particles must be destabilized by compression of the double layer around each particle and/or sorption by increasing the ionic strength (especially the divalent cations) with seawater as it mixed with the river water. Once the particles are completely destabilized, a collision between two particles will produce an aggregate of two, and the process can continue until an equilibrium is attained, with the aggregate consisting of hundreds of the original particles.

There are three processes causing coagulation of destabilized particles in nature: (1) thermal agitation; (2) velocity gradient (turbulence); (3) differential settling.

In thermal agitation the collision frequency (I_B) on suspended particles is defined by Smoluchowski (*30*) as

$$I_B = 4\pi D R n_0$$

where D = diffusion coefficient, R = collision radius (particle diameter), and n_0 = number of particles per cubic centimeter. Thermal agitation in the environment occurs, for the most part, with particles less than 1 μm in diameter. In the turbulent environment of natural waters, thermal agitation would be overwhelmed by the velocity gradient mechanism for all but the $<^1/_2$-μm material.

In the studies undertaken, all of the material was $>^1/_2$-μm in diameter. Therefore, thermal agitation is not considered as an important process.

The major mechanism causing coagulation in the environment and in these studies is velocity gradient (turbulence). The equation that described coagulation under turbulent conditions was originally developed by Smoluchowski (*30*) and has been improved by a number of researchers (*31, 32*). A simple form of this rate equation is

$$\mathrm{d}n/\mathrm{d}t = -(4/\pi)\alpha\phi n G$$

where α is the collision efficiency factor, ϕ is the volume of solid material per unit volume of solution, n is the number concentration of particles, and G is the mean velocity gradient. In our experiments we measured $\mathrm{d}n/\mathrm{d}t$ (the change in particle number with time), n, and ϕ; therefore, α can be calculated. The same procedure has been utilized by other researchers in numerous coagulation studies on a wide variety of materials. The work of Edzwald (*15*) and Hahn and Stumm (*14*) discussed coagulation of clay minerals in these terms. The collision efficiency factor, α, is a measure of the particles likelihood to coagulate.

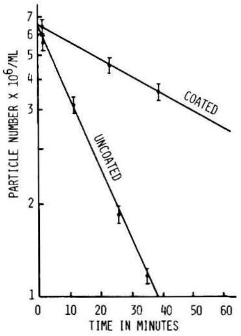

Figure 2. Relationship of particle number and time for the Yukon River sample with and without coating using 0.6 ‰ salinity in the Couette-type reactor.

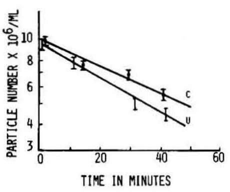

Figure 3. Relationship of particle number and time for a ocean sample with and without coating using 0.9 ‰ salinity in the Couette-type reactor.

Results

The experiments with the Couette-type reactor on the Amazon River sample material at 2 ‰ salinity (Figure 1) show that the natural sample (coated) coagulated slower (lower slope, α of 0.69) than the sample from which the coating had been removed with α of 0.82. After about 30 min, the coagulation rate of the natural sample material slowed down. The experiments with the Yukon River sample material at 0.6 ‰ using the Couette-type reactor exhibited a striking difference between the slope of the lines (Figure 2). The sample with the coating removed had a coagulation rate 4 times the rate of the natural sample. The natural sample took about 55 min for the particle number to decrease to half the starting number, called half-time ($T_{1/2}$), whereas the uncoated sample took only about 11 min. The natural sample had an α of 0.23 compared to 0.77 for the sample without the coating. The experiment using the ocean sample in the Couette-type reactor at 0.9 ‰ salinity again showed that the natural (coated) sample coagulated more slowly than did the uncoated sample (Figure 3). The natural sample had a α of 0.19 and a $T_{1/2}$ of 46 min, whereas the treated sample without the coating had an α of 0.26 and a $T_{1/2}$ of 33 min. It can be seen that all the experiments conducted in the Couette-type reactor showed that the natural samples with coatings coagulated slower than did the samples with coatings removed.

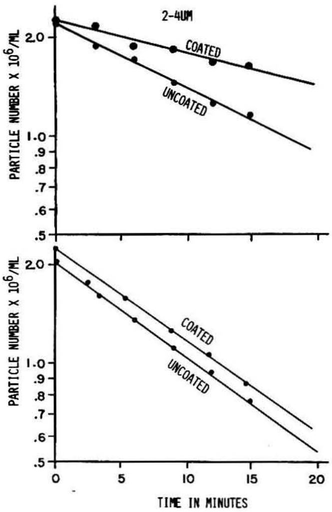

Figure 4. Relationship of particle number and time for Delaware Bay sample with and without coatings using 1.1 ‰ (4a) and 17.5 ‰ (4b) in the blade-type reactor.

The experiments in the blade-type reactor (27) using the 2–4-μm diameter fraction of the Delaware Bay sediments at 1.1 ‰ salinity showed a significant difference in the coagulation rate between the natural (coated) sample and the uncoated sample (Figure 4a). The natural sample had an α of 0.077 and a $T_{1/2}$ of 32 min, whereas the sample with the coating removed had an α of 0.145 and a $T_{1/2}$ of 19 min. Similar experiments at a salinity of 4.4 ‰ indicate that coagulation rates for coated and uncoated material are closer than at 1.1 ‰ salinity. The natural coated sample had an α of 0.207 and a $T_{1/2}$ of 14 min, and the uncoated sample had an α of 0.177 and a $T_{1/2}$ of 12 min. The experiments at 17.5 ‰ salinity (Figure 4b) indicated that coagulation rates for the natural (coated) sample are nearly the same as those for the uncoated sample. The natural coated sample had an α of 0.207 and a $T_{1/2}$ of 12.5 min, and the uncoated sample had an α of 0.216 and a $T_{1/2}$ of 11 min.

All of the experiments conducted with the blade-type reactor used organic-substance-free artificial seawater. In order to evaluate whether the natural dissolved organic substances had an effect on the coagulation processes, the blade-type reactor experiments were repeated with filtered natural seawater (retaining its natural dissolved organic substances). The results were not significantly different from the experiments using organic-free artificial sea water. From this, we can conclude that the effect of the dissolved organic substance is insignificant relative to removal of natural organic coatings and/or that the natural level of 150 mg/L of particles overwhelms the small amount of dissolved organic substances.

The effect of salinity can be studied in the blade-type reactor experiments. Figure 5 is a plot of the collision efficiency factor, α, and the salinity. It shows the large difference between coated and uncoated samples at low salinities and how the difference decreases at higher salinity. A simpler method of portraying the coagulation rate is plotting the particle half-time, $T_{1/2}$. In Figure 6 the long times and large differences between coated and uncoated material at low salinities is shown, whereas at high salinities the time is shorter and the difference between the coated and uncoated material is smaller. In the environment, this would imply that the region in which this difference in coagulation properties would be most significant is the brackish low-salinity portions and that in any region with salinity higher than about 15 ‰ this difference would be very small.

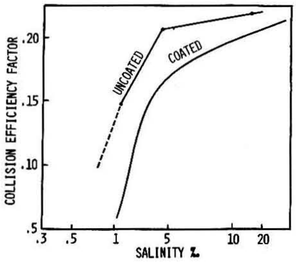

Figure 5. Relationship of collision efficiency factor (α) and salinity for Delaware Bay sample in the blade-type reactor.

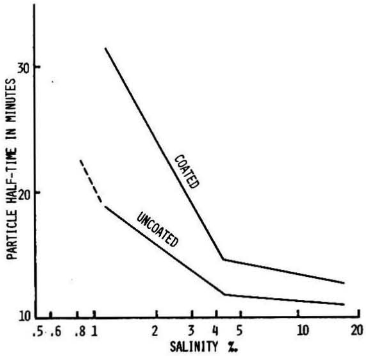

Figure 6. Relationship of particle half-time and salinity for Delaware Bay sample in the blade-type reactor.

Conclusion

The effect of the organic coatings on particles has a significant impact on the coagulation rate of natural particles. This effect is largest at low salinities and decreases with increasing salinity.

Literature Cited

(1) Berthois, L. *Rev. Geogr. Phys. Geol. Dyn.* **1961**, *1*, 39–42.
(2) Biddle, P.; Miles, J. H. *Sediment. Geol.* **1972**, *7*, 23–33.
(3) Gibbs, R. J.; Konwar, L.; Terchunian, A. *Can. J. Fish. Aquat. Sci.*, in press.
(4) Kranck, K. *Sedimentology* **1975**, *22*, 111–123.
(5) Kranck, K. *Nat. Can. (Que.)* **1979**, *106*, 163–173.
(6) Krone, R. B. Final Report, U.S. Army Corps of Engineers, San Francisco District, 1972.
(7) Schubel, J. R.; Kana, T. W. *Powder Technol.* **1972**, *6*, 9–16.
(8) Sheldon, R. W. *Limnol. Oceanogr.* **1968**, *13*, 72–83.
(9) Zabawa, C. *Science (Washington, D.C.)* **1978**, *202*, 49–51.
(10) Whitehouse, U. G.; Jeffrey, L. M.; Debrecht, J. D. *Clays Clay Miner.* **1960**, 1–76.
(11) Krone, R. B. Final Report, U.S. Army Corps of Engineers, San Francisco District, 1962.
(12) Krone, R. B. "Estuarine Transport Processes"; Kjertve, G., Ed.; University of South Carolina Press: Columbia, SC, 1978; pp 177–190.
(13) Shiozawa, T. *J. Jpn. Assoc. Miner. Petrol. Econ. Geol.* **1970**, *63*, 75–84.
(14) Hahn, H. H.; Stumm, W. *Am. J. Sci.* **1970**, *268*, 354–368.
(15) Edzwald, J. K. Publication UNC-SG-72-06, Chapel Hill, NC, 1972.
(16) Edzwald, J. K.; Upchurch, J. B.; O'Melia, C. R. *Environ. Sci. Technol.* **1974**, *8*, 58–63.

Environ. Sci. Technol. **1983**, *17*, 240-243

(17) Eppler, B.; Neis, U.; Hahn, H. H. *Prog. Water Technol.* **1975**, *7*, 207-216.
(18) Hunt, J. R. Ph.D. Dissertation, California Institute of Technology, 1980.
(19) Gibbs, R. J. *J. Sediment. Petrol.*, in press.
(20) Pravdic, V. *Limnol. Oceanogr.* **1970**, *15*, 230-233.
(21) Martin, J. M.; Jednacak, J.; Pravdic, V. *Thalassia Jugosl.* **1971**, *7*, 619-636.
(22) Hunter, K. A.; Liss, P. S. *Nature (London)* **1979**, *282*, 823-825.
(23) Neihof, R. A.; Loeb, G. I. *Limnol. Oceanogr.* **1972**, *17*, 7-16.
(24) Neihof, R. A.; Loeb, G. I. *J. Mar. Res.* 1974, *32*, 5-12.
(25) Loeb, G. I.; Niehof, R. A. In "Applied Chemistry at Protein Interfaces"; Baier, R. E., Ed.; 1975; pp 319-335.
(26) Ham, R. K.; Christman, R. F. *J. Sanit. Eng. Div. Am. Soc. Civ. Eng.* **1969**, *95*, 481-502.
(27) Lathrop, J. E. M.S. Thesis, University of Delaware, 1980.
(28) Kester, D. R.; Duedall, I. W.; Connors, D. N.; Pytkowitz, R. M. *Limnol. Oceanogr.* **1967**, *12*, 176-179.
(29) Anderson, J. V. *Clays Clay Miner.* **1963**, Tenth National Conference, 380-388.
(30) Smoluchowski, M. v. *Z. Phys. Chem.* **1971**, *92*, 129-168.
(31) Camp, T. R.; Stein, P. C. *J. Boston Soc. Civ. Eng.* **1943**, *30*, 219-237.
(32) Reeink, H.; Overbeek, J. T. *Faraday Soc. Discuss.* **1954**, *18*, 74-84.

Received for review July 14, 1982. Accepted December 27, 1982.

NOTES

Reductive Destruction of Hydrazines as an Approach to Hazard Control

George Lunn and Eric B. Sansone

Environmental Control and Research Program, NCI—Frederick Cancer Research Facility, Frederick, Maryland 21701

Larry K. Keefer*

Analytical Chemistry Section, Division of Cancer Cause and Prevention, National Cancer Institute, Bethesda, Maryland 20205

■ Hydrazine and 14 of its mono- and disubstituted alkyl, aryl, and acyl derivatives were quantitatively destroyed by using either of two nickel-based catalytic reductive procedures. Small volumes of solutions containing hydrazines were made alkaline and treated with aluminum-nickel powder; large volumes were treated with preformed Raney nickel with or without an exogenous hydrogen source. No interference was discovered except from acetone. The only products detected were ammonia and the amines corresponding to the hydrazine reduced. No benzidine could be detected when 1,2-diphenylhydrazine was reduced. These procedures appear to provide a reliable, efficient, one-step approach to conversion of potentially carcinogenic hydrazines to innocuous products in laboratory wastes or in the environment.

Hydrazine and its derivatives can enter the environment by a number of routes. Hydrazine has been used for boiler-water treatment, in the manufacture of blowing agents, agricultural chemicals, and medicinal agents, and (principally) as a propellant (*1-3*). Hydrazine may also be a product of nitrogen fixation by certain bacteria (*4*). Substituted hydrazines have been used as drugs, herbicides, and propellants (*4-9*); two hydrazine derivatives, agaritine and *N*-methyl-*N*-formylhydrazine, have been isolated from edible mushrooms (*4*).

Hydrazine and several of its derivatives are carcinogenic (*1, 8-11*). Attempts have been made to destroy residues of these compounds to prevent or reverse environmental contamination by them. Much of the emphasis in these chemical destruction studies has been on oxidative pathways, using reagents such as ozone (*12*) or hypochlorite (*2*). Unless carefully controlled, however, these pathways can lead to products that may be more hazardous than the starting material. For example, 1,1-dimethylhydrazine (UDMH), used as a propellant in a variety of military and space applications (*2, 6-8*), can be oxidized to *N*-nitrosodimethylamine (*7, 13*).

After noting that Seebach and Wykypiel (14) used Raney nickel and hydrogen to convert hydrazines and nitrosamines to amines, we studied the applicability of catalytic reductions to the decontamination of wastes containing hydrazines. In this paper we report that hydrogenolytic cleavage of hydrazine and its derivatives can be conveniently, inexpensively, and quantitatively achieved under a wide variety of conditions, according to eq 1.

$$H_2 + R^1R^2NNHR^3 \xrightarrow{\text{Ni catalyst}} R^1R^2NH + R^3NH_2 \qquad (1)$$

The results indicate that nickel-based reductive methods hold considerable promise as an approach to preventing environmental contamination by hydrazines.

Experimental Section

Materials. With three exceptions, the hydrazine and amine standards used were purchased from Aldrich Chemical Co., Milwaukee, WI. 1,1-Diethylhydrazine, 1,1-diisopropylhydrazine, and 1,1-di-*n*-butylhydrazine were prepared by reducing the corresponding nitrosamine with lithium aluminum hydride (*15*). The products were distilled before use. The boiling points of the products were 90-94 °C (1,1-diethylhydrazine), 89-90 °C (180 mmHg) (1,1-diisopropylhydrazine), and 135 °C (200 mmHg) (1,1-di-*n*-butylhydrazine). The reported boiling points of these compounds are 96-99 °C, 41 °C (16 mmHg), and 87-90 °C (21 mmHg), respectively (*15*). Satisfactory purity was indicated in each case by the boiling point and gas chromatographic homogeneity. Aluminum-nickel alloy powder (50:50, w:w) was also obtained from Aldrich.

Reduction Procedures with in Situ Generation of Hydrogen and Nickel Catalyst. In a typical reaction,

0013-936X/83/0917-0240$01.50/0

Table I. Reduction of Hydrazines ($R^1R^2NNHR^3$) to the Corresponding Amines with Nickel–Aluminum Alloy in Potassium Hydroxide Solution

R^1	R^2	R^3	yield of amine, %	residual hydrazine, %[a]	retention time, min		column[b]	column temp, °C
					amine	hydrazine		
H	H	H	*c*	<0.01[d]	*c*	*c*		
Me	Me	H	97	<1	0.7	1.6	A	80
Et	Et	H	100	<0.1	0.6	1.7	A	80
i-Pr	*i*-Pr	H	104	<0.1	0.5	2.7	A	80
n-Bu	*n*-Bu	H	93	<0.1	2.1	7.8	A	90
$-(CH_2)_5-$		H	89	<0.1	1.1	4.5	A	100
$-(CH_2)_4-$		H	101	<0.25	2.2	8.8	A	80
$-(CH_2)_2O(CH_2)_2-$		H	104	<0.1	1.7	4.5	A	130
$-(CH_2)_2N(NH_2)-(CH_2)_2-$		H	73 (piperazine)	<1	1.0	11.3	B	100
Me	H	Me	94	<0.1	0.5	2.6	C	100
Ph	Me	H	96	<0.5	1.4	2.7	D	110
Ph	H	Ph	101[e]	<0.5	1.4	3.4	D	100 (amine) 150 (hydrazine)
Ph	H	C(O)NHNHPh	96 (aniline)	*c*	1.7	*c*	B	130
Ph	H	H	98	<0.2	1.7	8.7	B	130
p-$CH_3C_6H_4$	H	H	78	<2	2.3	11.5	B	130

[a] No hydrazine was detected in any reaction mixture after 24 h. Values given are the detection limits, expressed as percentages of the initial hydrazine concentration. [b] See Experimental Section for identities of coded column packings. [c] This compound could not be detected with the chromatographic conditions used. [d] A colorimetric analytical procedure was used; see Experimental Section. [e] Benzidine was absent (detection limit = 1% of the initial hydrazobenzene concentration). The retention time was 3.4 min at 200 °C on 3% OV-1 on 80/100 Supelcoport.

5 mg of the hydrazine to be reduced was dissolved either in 1 mL of 0.5 M potassium hydroxide solution or, if the hydrazine was incompletely soluble in the aqueous medium, in a mixture of 0.5 mL of methanol and 0.5 mL of 1 M potassium hydroxide. The resulting solution was magnetically stirred in a small vial after adding 100 mg of aluminum–nickel alloy powder. The reaction mixture was monitored by injecting 2-μL aliquots without further workup onto 1.8 m × 2 mm silanized glass columns in a Hewlett-Packard 5830A gas chromatograph equipped with a flame ionization detector. Four column packings were used: (A) 10% Carbowax 20 M + 2% KOH on 80/100 Chromosorb WAW; (B) 2% Carbowax 20 M + 1% KOH on 80/100 Supelcoport; (C) 28% Pennwalt 223 + 4% KOH on 80/100 Gas Chrom R; (D) 3% SP-2401 DB on 100/120 Supelcoport. Injector temperature was 200 °C, detector temperature was 300 °C, and the carrier gas was nitrogen flowing at about 30 mL/min. The quantity of amine present was determined by comparing its peak area with that of an alcohol or polyether added to the initial reaction mixture as an internal standard. In all cases but one (see Table I), the starting hydrazine also gave a peak under the conditions used for the amine. Less than 5% of the starting material was detectable 1 h after adding the aluminum–nickel powder; after 24 h the hydrazine was completely destroyed, within the limit of detection.

Hydrazine itself was reduced under these conditions. The reaction mixture was analyzed colorimetrically according to the method of Watt and Chrisp (*16*). Less than 0.01% of the hydrazine remained after 17 h.

In contrast, when aluminum foil (22 mg) was used in place of the aluminum–nickel alloy, 92% of the initial quantity of 1,1-dimethylhydrazine remained after 5 h. Similarly, 22 mg of aluminum amalgam in 1 mL of water caused no change in the concentration of 1,1-dimethylhydrazine. Copper(I) chloride (50 mg) in 1 mL of 6 M hydrochloric acid reduced the concentration of 1,1-dimethylhydrazine by 48% after 6 h; however, the yield of dimethylamine was only 4%, and a number of unidentified products were detected.

Reduction Procedures with Raney Nickel. The nickel catalysts employed were either prepared before use from aluminum–nickel alloy (*17, 18*) or purchased from Aldrich. The Raney nickel used, whether purchased or freshly prepared, contained sufficient adsorbed hydrogen to reduce more than 1 mmol of acetone to isopropanol per gram of catalyst within 3 h.

1,1-Dimethylhydrazine (0.2 mL) was dissolved in 50 mL of water, and 2.3 g of Raney nickel catalyst (Aldrich) was added. The reaction mixture was periodically analyzed by using gas chromatography (column packing A, see above). After 1 h no hydrazine remained (<1%). When larger amounts of 1,1-dimethylhydrazine were present, some, but not all, of the hydrazine was destroyed after being stirred with the Raney nickel; with freshly prepared Raney nickel, but not with the commercial catalyst, the hydrazine remaining after 1 h could be completely degraded by continuing the stirring under an atmosphere of hydrogen gas.

Disposal. When reduction was complete, the reaction slurry was filtered with suction through a pad of Celite (*14*) on a Büchner funnel and washed thoroughly with water and/or methanol. The filter cake was not allowed to dry in the funnel because of its potential for ignition. Instead, it was placed while still wet onto a metal tray and kept away from any flammable materials for 24 h. It was then discarded with the nonflammable waste. Additional protection against fire was achieved by adding 1 mL of acetone per gram of alloy after the hydrazine reduction was complete but 24 h before filtration. Alternatively, the spent nickel could be dissolved cautiously in dilute mineral acid (*19*).

Analysis for Residual Metal Ions in Solution. The concentrations of nickel and aluminum ions remaining in solution after reduction were determined by using a Perkin-Elmer 403 flame atomic absorption spectrometer. **Warning:** Many hydrazines are carcinogenic and should be handled, stored, and discarded with due respect for their toxic potential. In the destruction reactions described in this paper, hydrogen is either added or produced in situ, so all reactions should be carried out in a properly functioning chemical fume hood. The in situ hydrogen generation reactions evolve both heat and large quantities of gas; therefore, when large-scale reactions are conducted, reaction vessels should be cooled with ice and the alloy should be added slowly in portions to the continuously stirred reaction mixture to prevent it from frothing over. The hazard potential arising from the pyrophoricity of finely divided nickel has been described above, together with control procedures.

Results

The results of treating hydrazine and several of its substituted derivatives with Raney nickel and hydrogen in water or with aluminum–nickel alloy powder in alkaline solution are summarized in Table I. In no case could residual hydrazine be detected after 24 h of exposure to excess reductant.

Amines corresponding to the hydrazine reduced were the only products detected by gas chromatography. Yields ranged from 73% to 104%; the detection limit was about 1% of the theoretical yield. When hydrazine itself was reduced, the filtered reaction mixture was distilled into a receiver containing excess hydrochloric acid. Evaporation of the receiver's contents left a residue whose weight corresponded to 53% of the theoretical yield of ammonium chloride.

Special efforts were made to detect reaction products that might themselves be hazardous. For example, no benzidine was found (detection limit = 1% of the theoretical yield, or 50 ppm in the reaction mixture) when 1,2-diphenylhydrazine was reduced. In another case, we stirred 10 g of aluminum–nickel alloy with 200 mL of 1 M sodium hydroxide for 24 h and analyzed the filtrate by atomic absorption spectrometry; no nickel was found at a detection limit of 0.5 ppm; the concentration of aluminum was 15 ppm.

Other reducing systems such as aluminum in potassium hydroxide solution, aluminum amalgam, or cuprous chloride did not efficiently destroy dialkylhydrazines.

Discussion

Hydrogenolysis of hydrazine and its derivatives at a catalytic nickel surface appears to furnish an attractive means of protecting the environment from contamination by these compounds. There are several potential advantages in this approach.

There are many catalytic nickel reducing systems (*17*). Among them they offer a variety of characteristics a chemist might use in developing specific procedures for solving both routine and exotic decontamination problems. We have successfully used two systems in this study. One employed preformed Raney nickel, with or without an exogenous source of hydrogen. The other involved in situ generation of hydrogen and spongy nickel by addition of aluminum–nickel alloy powder to an alkaline solution of the hydrazine to be destroyed. The two systems gave similar results.

Reductive destruction of hydrazines with nickel catalysts is efficient. None of the hydrazines could be found, within the limits of detection (0.01–2% of the initial hydrazine concentration), in any reaction mixture (Table I) after 24 h of exposure to reducing conditions. We conclude that nickel hydrogenolysis has the potential for reliable quantitative destruction of hydrazines. In contrast, aluminum foil in potassium hydroxide solution, aluminum amalgam in water, and copper(I) chloride in 6 M hydrochloric acid were not effective for destruction of hydrazines.

Another advantage, not shared by all decontamination procedures, is that the products detected thus far are all considered to be relatively nontoxic. As mentioned above, oxidative degradation of UDMH can lead to formation of the potent carcinogen *N*-nitrosodimethylamine, a significant deficiency for a decontamination method even if destruction of hydrazine is complete. The only products detected in the reactions summarized in Table I were ammonia and/or the amine corresponding to the hydrazine reduced, compounds ordinarily suspected of having substantial toxicity only if the amine generated contains certain types of aromatic substituents (such as 2-naphthyl (*20*)). A special case to which we devoted careful analytical attention was the cleavage of 1,2-diphenylhydrazine, a compound known to readily rearrange (*21*) under acidic reduction conditions to benzidine, another powerful carcinogen (*22*). When 1,2-diphenylhydrazine was destroyed by using aluminum–nickel alloy in alkaline solution, no trace of benzidine could be found at a detection limit of 50 ppm (1% of the theoretical yield of benzidine). In assessing the toxic potential of products generated in these reactions, it was also necessary to consider the fate of the metals added to initiate the hydrogenolysis. After treating aluminum–nickel alloy with base, no nickel could be found in solution by atomic absorption at a detection limit of 0.5 ppm; aluminum was present in the filtrate to the extent of only 15 ppm. There are no ambient water quality criteria for aluminum; however, for nickel the most restrictive criterion requires that the 24-h average concentration of nickel not exceed 7.1 μg/L (*23*). Since the volume of the reaction mixture is not large, it should not be difficult to ensure that the nickel ion concentration meets the water quality criteria.

It would be premature to conclude, however, that all products of all reactions in Table I are innocuous, because a significant amount (up to 27%) of the starting hydrazine remained unaccounted for after some of the reactions. We recommend that a complete material balance be established, with special emphasis on detecting any potentially toxic products, before any reaction is considered for use in environmental protection applications.

An important feature of these reactions is their relative lack of sensitivity to potential interferences. The data of Table I demonstrate that reduction of hydrazines proceeds quantitatively in either neutral or alkaline solution, with either endogenously or exogenously supplied catalyst–hydrogen mixtures, and in the presence or absence of added methanol. Hydrazines were also destroyed in other solvent systems such as mineral oil–pentane–water (1:1:2, v:v, a two-phase mixture), rapidly stirred olive oil–water emulsions, dichloromethane–methanol–water (1:3:1), and aqueous solutions containing dimethyl sulfoxide. In addition, previous studies (*24, 25*), in which reduction of nitrosamines using the in situ generation procedure frequently led to substantial but transient amounts of hydrazines produced as intermediates, offer indirect but persuasive evidence that hydrazine reduction proceeds readily and quantitatively in a wide variety of solvent systems, including methanol–water (9:1, v:v), dichloromethane–methanol–water (1:3:1), mineral oil–hexane–water (1:1:2, a two-phase mixture), rapidly stirred olive oil–water emulsions, and aqueous solutions containing dimethyl sulfoxide or dissolved gelatin. The only interferences discovered in a recent multilaboratory collaborative study of the nitrosamine destruction method (*26*) were those from acetone, which is preferentially reduced, and some (but not all) batches of dichloromethane (*27*).

Many other potentially hazardous compound classes containing N–N and N–O bonds are also reduced to presumably nontoxic products such as ammonia, amines, water, and alcohols under these conditions. Besides the nitrosamines and hydrazines mentioned above, studies still in progress suggest that compounds such as nitrosamides, azoxy compounds, nitramines, azo derivatives, triazenes, and N-hydroxy compounds are also cleaved quantitatively to completely reduced products at the catalytic nickel surface. This feature would be especially advantageous n disposing of waste from a carcinogenesis research laboratory (our own area of primary concern), in which simultaneous work with many such compounds may result n accumulation of mixed waste, which demands a broad-spectrum decontamination procedure.

Other significant advantages of nickel-catalyzed reductive destruction of hydrazines include its relative lack of expense (the only specialized prerequisite for most of the reactions studied was aluminum–nickel alloy, purchased for approximately 5 cents/g) and its experimental simplicity. The latter feature should be an especially important benefit. The availability of a reliable, one-step waste-treatment procedure requiring no equipment more complicated than a magnetic stirrer should be most welcome. Of course, good laboratory practice strongly suggests that the efficacy of a decontamination procedure be analytically verified periodically; for this purpose, specialized equipment and considerable expertise in analytical chemistry will normally be required.

As to the relative advantages of the preformed Raney nickel procedure vs. addition of aluminum–nickel alloy powder to aqueous base, we consider the latter to be preferable in most cases because it avoids the use of catalytic preparations and hydrogen, which are flammable, as starting materials. Generation of the reducing system n situ, however, does require that the medium be strongly alkaline (0.5–1 M in hydroxide) to achieve useful reaction rates. While this requirement should not lead to any major problems in decontaminating small batches of hydrazine-containing wastes (e.g., those from the typical research aboratory), it would become economically and environmentally disadvantageous in large-scale operations such as those involved in industrial or environmental cleanup applications. In these cases, the well-established Raney nickel reduction should provide an attractive alternative. When the concentration of the hydrazines and other reducible contaminants is relatively small, it may be possible to destroy them with Raney nickel alone, using no gaseous hydrogen; the Raney nickel samples we studied contained more than 1 mmol of hydrogen per gram of catalyst, as measured by their ability to convert acetone to isopropanol. Of course, when Raney nickel alone cannot quantitatively reduce the contaminant, an atmosphere of hydrogen can be added; doing so completed the destruction of the hydrazine when freshly prepared catalyst was used.

Acknowledgments

We thank H. Issaq for the atomic absorption analyses.

Literature Cited

(1) IARC. "IARC Monographs on the Evaluation of Carcinogenic Risk of Chemicals to Man. Some Aromatic Amines, Hydrazine and Related Substances, N-Nitroso Compounds and Miscellaneous Alkylating Agents"; World Health Organization: Geneva, Switzerland, 1974; Vol. 4, pp 127–136.

(2) AFOSH, Air Force Occupational Safety and Health. "Occupational Health—Exposure to Hydrazine"; AFOSH Standard 161-13, Department of the Air Force: Washington, DC, 1979.

(3) NIOSH, National Institute for Occupational Safety and Health, "Criteria for a Recommended Standard—Occupational Exposure to Hydrazines"; NIOSH Publication No. 78-172, U.S. DHEW: Washington, DC, 1978.

(4) Toth, B. *J. Cancer Res. Clin. Oncol.* **1980**, *97*, 97–108.

(5) Beisler, J. A.; Peng, G. W.; Driscoll, J. S. *J. Pharm. Sci.* **1977**, *66*, 849–852.

(6) Tuazon, E. C.; Carter, W. P. L.; Winer, A. M.; Pitts, J. N., Jr. *Environ. Sci. Technol.* **1981**, *15*, 823–828.

(7) Carter, W. P. L.; Tuazon, E. C.; Winer, A. M.; Pitts, J. N., Jr. In "*N*-Nitroso Compounds"; Scanlan, R. A., Tannenbaum, S. R., Eds.; American Chemical Society: Washington, DC, 1981; ACS Symp. Ser. 174, pp 117–131.

(8) Reference 1, pp 137–143.

(9) Reference 1, pp 145–152.

(10) Reference 1, pp 153–157.

(11) Reference 1, pp 159–172.

(12) Sierka, R. A.; Cowen, W. F. *Proc. Ind. Waste Conf.* **1981**, *35*, 406–415.

(13) Simoneit, B. R.; Burlingame, A. L. *Nature* (*London*) **1971**, *234*, 210–211.

(14) Seebach, D.; Wykypiel, W. *Synthesis* **1979**, 423–424.

(15) Zimmer, H.; Audrieth, L. F.; Zimmer, M.; Rowe, R. A. *J. Am. Chem. Soc.* **1955**, *77*, 790–793.

(16) Watt, G. W.; Chrisp, J. D. *Anal. Chem.* **1952**, *24*, 2006–2008.

(17) Augustine, R. L. "Catalytic Hydrogenation"; Marcel Dekker: New York, 1965; p 26.

(18) Enders, D.; Pieter, R.; Renger, B.; Seebach, D. *Org. Synth.* **1978**, *58*, 113–122.

(19) Schwenk, E.; Papa, D.; Hankin, H.; Ginsberg, H. "Organic Syntheses"; Wiley: New York, 1955; Collect. Vol. 3, pp 742–744.

(20) Reference 1, pp 97–111.

(21) Dewar, M. J. S. In "Molecular Rearrangements"; de Mayo, P., Ed.; Wiley: New York, 1963; pp 295–344.

(22) IARC. "IARC Monographs on the Evaluation of Carcinogenic Risk of Chemicals to Man"; World Health Organization: Geneva, Switzerland, 1972; Vol 1, pp 80–86.

(23) EPA. "Ambient Water Quality Criteria for Nickel"; EPA Report 440/580-060, U.S. EPA: Washington, DC, 1980.

(24) Lunn, G.; Sansone, E. B.; Keefer, L. K. *Food Cosmet. Toxicol.* **1981**, *19*, 493–494.

(25) Sansone, E. B.; Lunn, G.; Jonas, L. A.; Keefer, L. K. In "*N*-Nitroso Compounds: Occurrence and Biological Effects"; Bartsch, H., O'Neill, I. K., Castegnaro, M., Okada, M., Eds.; IARC Scientific Publications No. 41, World Health Organization, Geneva, Switzerland, 1982; pp 137–149.

(26) Castegnaro, M.; Eisenbrand, G.; Ellen, G.; Keefer, L.; Klein, D.; Sansone, E. B.; Spincer, D.; Telling, G.; Webb, K., Eds.; "Laboratory Decontamination and Destruction of Carcinogens in Laboratory Wastes: Some *N*-Nitrosamines"; IARC Scientific Publications No. 43, World Health Organization: Geneva, Switzerland, 1982.

(27) M. Castegnaro, International Agency for Research on Cancer, Lyon, France, personal communication, 1982.

Received for review April 23, 1982. Revised manuscript received November 22, 1982. Accepted January 7, 1983. Research was sponsored in part by the National Cancer Institute under Contract N01-CO-75380 with Litton Bionetics, Inc., and Contract N01-CO-23910 with Program Resources, Inc.

Environ. Sci. Technol. 1983, 17, 244–245

Impact of Fossil Fuel Combustion on Sediments of Lake Michigan: A Reprise

John J. Griffin and Edward D. Goldberg*

Scripps Institution of Oceanography, La Jolla, California 92093

■ The size distribution of charcoals in sediments of Lake Michigan reflects the onset of the industrial revolution and the increased intensities of fossil fuel combustion during the twentieth century. Prior to 1900 the less than 1-μm fraction was dominant, and its source was primarily biomass burning. In the subsequent years coal and oil burning became evident with larger particles, especially greater than 32 μm, making larger contributions to the total charcoal concentrations. The input of the larger particles is a consequence of near fallout of particles from energy-producing plants near the lake.

Previously, we have proposed that the amounts of charcoal found in the sedimentary record reflect the intensity of combustion processes at the earth's surface, both natural and anthropogenic (*1*). For the case of Lake Michigan, the fluxes of charcoal from wood, coal, and oil burning changed over the past century and reflected the onset of industrial activity (Table I). The first strong evidence of coal utilization appeared about 1900. In addition, our results indicated that there was a decrease in charcoal concentrations in the deposits from about 1960 to the present, which we attributed to improved controls of emissions from the stacks of power plants and industrial facilities. We had analyzed the greater than 38-μm size class of the charcoals inasmuch as these particles possessed in their morphologies characteristics of the source material—oil, coal, or wood (*2*).

Further, the twentieth-century urbanization of the lower Lake Michigan region, with its increasing production of energy needed for the production of goods and services to support an ever increasing population, impinged upon the lake environment. The places of commerce were sited along or near the lake, so as to take advantage of its natural resources, i.e., water and transportation. One manifestation of this impingement is the associated increase in the concentration of anthropogenic carbon in the lake sediments. Prior to 1900 the primary source of charcoal in the sediments was from burning of biomass.

Two size classes of carbon particles are generated in burning coal, oil, and wood. The coarse fraction, generally greater than a few microns in diameter, is produced from incomplete combustion or pyrolysis of fuel particles. This carbon has been called charcoal, char, and coke. The second type includes the submicron particles produced from the vapor-phase condensation of carbon. This has been called soot and is composed of submicron spheres agglomerated into random chain-like structures (Figure 1). In this presentation we use the term charcoal to include both types of carbon.

If we assume the fallout ratio of the two types is a function of particle size for a particular site, then a particle size gradient with the larger size particles near the source should be observed (*3*). Thus, we have determined the size distribution of charcoals in Lake Michigan Box Core LM-780914, collected from a water depth of 64 m at 43°00′ N and 86°22′ W. This is the same sediment utilized in our previous studies in which the chronology of the strata, metal and charcoal concentrations, and mineral levels were determined (*1*).

Table I. Total Charcoal Concentrations in the Lake Michigan Deposit

period of deposition	charcoal (dry weight), %	period of deposition	charcoal (dry weight), %
1976-1978	0.60	1920-1923	0.29
1973-1976	0.62	1918-1920	0.25
1970-1973	0.59	1916-1918	0.21
1968-1970	0.57	1913-1916	0.13
1968-1970	0.57	1910-1913	0.12
1963-1968	0.64	1908-1910	0.13
1960-1963	0.61	1906-1908	0.15
1958-1960	0.63	1898-1903	0.11
1956-1958	0.74	1893-1898	0.11
1953-1956	0.71	1883-1893	0.10
1948-1953	0.66	1873-1883	0.12
1943-1948	0.73	1863-1873	0.11
1938-1943	0.51	1853-1863	0.07
1933-1938	0.58	1843-1857	0.17
1928-1933	0.40	1837-1843	0.10
1923-1928	0.32	1827-1837	0.11

We recognize that a single core cannot be used to study the integrated fluxes and the mass balances for sedimentary components in a water body the size of Lake Michigan. Still, a single core can reveal relative changes in fluxes, where the sedimentary strata can be dated, as was demonstrated in our previous work (*1*). Our aim is to ascertain if there has been a change in size distribution over the past century and a half, during which period there was a change in fluxes of charcoal from a variety of sources as a consequence of the industrial revolution.

The charcoal is isolated from the sediment in the following way. Oven-dried (110 °C) sediment samples were leached in hot 6 N HCl from 2 to 4 h and subsequently carefully washed with H_2O. The residue was digested for about 2 weeks in a mixture of 300 mL of 10 N HF and 50 mL of concentrated HCl at room temperature. The supernate is removed by careful centrifugation, and the residue is leached with hot 6 N HCl. The residue is then washed with H_2O in preparation for oxidation, which is accomplished by dispersing the residue in 100 mL of 6 N KOH and by the careful addition in small increments of 800 mL of 30% H_2O_2. After oxidation the residue is leached with hot 6 N HCl and washed with H_2O in preparation for particle size analysis. Stokes settling techniques were used to separate the particles into the different size classes. The carbon particles were assumed to have a density of 2 g/cm^3 and the settling medium was H_2O. Each size fraction was collected, oven-dried, and weighed and the charcoal concentration determined by infrared assay (*4*). Samples that were too small for infrared assay had their charcoal contents determined by loss on ignition at 600 °C. Duplicate runs on the same sample showed both techniques give results within ±10% of each other.

Particle size distributions as a function of age of the strata are shown in Figure 2. The greater than 38-μm and the less than 1-μm fractions show trends over a time interval that was dated by the ^{210}Pb geochronology (*1*). As previously noted (*2*), the greater than 38-μm particle concentration showed an increase beginning about 1900. Furthermore, these charcoals had morphologies indicative of coal sources and to a lesser extent those of oil, whereas the contribution from wood charcoal decreased from 1900

0013-936X/83/0917-0244$01.50/0

Environ. Sci. Technol. 1983, 17, 245-248

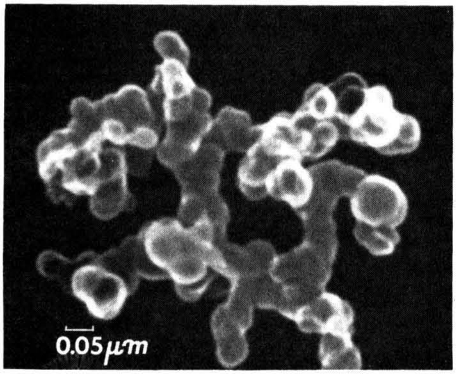

Figure 1. Morphology of the very fine-grained charcoal. Small spheres have aggregated into irregular chains.

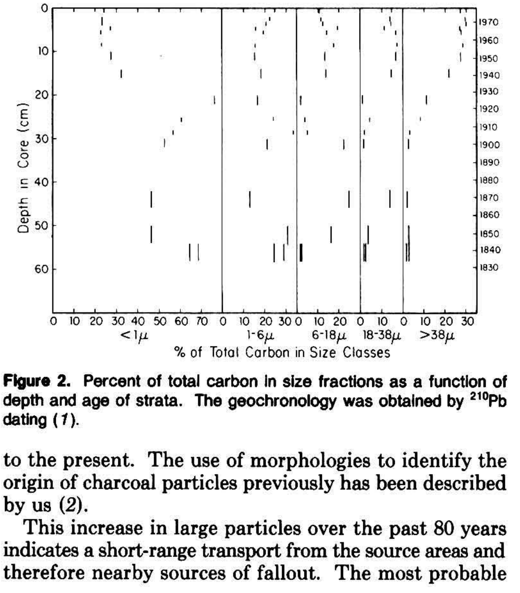

Figure 2. Percent of total carbon in size fractions as a function of depth and age of strata. The geochronology was obtained by ^{210}Pb dating (*1*).

to the present. The use of morphologies to identify the origin of charcoal particles previously has been described by us (*2*).

This increase in large particles over the past 80 years indicates a short-range transport from the source areas and therefore nearby sources of fallout. The most probable sources of this fallout would be the energy-producing plants sited along the shore of the lower Lake Michigan basin. As the region's economic activities and population matured and stabilized over the past decades, these stationary energy-producing sources proved to be a stable source of particles whose variations are affected by the economy and/or improvements in combustion and pollution-control technology.

The fine fraction (less than 1 μm) has a rather constant concentration (20–30%) during the past 40 years, whereas the older strata show a concentration increase that is variable with no distinct trends. The low values during the past 40 years are the result of dilution by the large particles with a fossil fuel origin. The increase in the fine fraction in older sediment is correlated with the very low concentration of large particles. These large particles have morphologies indicating a wood origin and probably have their origins in burning of biomass by man and through natural phenomena. This biomass burning would not be limited to a few fixed geographic areas but would range over the entire lower Lake Michigan basin. The same volume of biomass would not be regularly combusted but would vary depending upon available fuel and upon favorable conditions for burning. The fine-grained nature indicates a more distant source and represents long-distance transport and fallout. This would be in keeping with the early development of the region as it transformed from a prairie to an agricultural area and then to its present industrial economy.

Thus we have identified a number of parameters associated with charcoals that may be useful in reconstructing burning histories from the sedimentary record: charcoal concentrations, morphologies, and size distributions.

Literature Cited

(1) Goldberg, E. D.; Hodge, V. F.; Griffin, J. J.; Koide, M. *Environ. Sci. Technol.* **1981**, *15*, 466–471.
(2) Griffin, J. J.; Goldberg, E. D. *Science (Washington, D.C.)* **1979**, *206*, 563–565.
(3) Windom, H. L. *Bull. Geol. Soc. Am.* **1969**, *80*, 761–782.
(4) Smith, D. M.; Griffin, J. J.; Goldberg, E. D. *Anal. Chem.*, **1975**, *47*, 233–238.

Received for review June 11, 1982. Accepted December 27, 1982. Research funded by the National Science Foundation, Geochemistry Program (EAR80-17491).

Electrolytic Preparation of [^{36}Cl]Chlorine Dioxide from H^{36}Cl

Hossein A. Ghanbari,* Willis B. Wheeler, and James R. Kirk

Department of Food Science and Human Nutrition, Institute of Food and Agricultural Sciences, University of Florida, Gainesville, Florida 32611

■ Electrolysis of KOH-neutralized H^{36}Cl resulted in greater than 90% conversion of K^{36}Cl to K^{36}ClO$_3$. Reduction of K^{36}ClO$_3$ with oxalic acid in a closed gas-generation system yielded ^{36}ClO$_2$ gas. The generated gas was passed through a Na$_2$CO$_3$ column, which effectively absorbed the contaminants Cl$_2$ and CO$_2$, and the purified ^{36}ClO$_2$ was then dissolved in water. This procedure is an effective laboratory preparation of ^{36}ClO$_2$ and is characterized by high yield, purity, and specific activity.

Wide use of ClO$_2$ as a disinfectant has led to studies involving the metabolism of ClO$_2$ (*1, 2*), the mode of bacterial or viral inactivation (*3–9*), and the fate of chlorine (*10*). These studies and others such as ClO$_2$ toxicity and the mechanism of bactericidal action would be greatly facilitated if ^{36}ClO$_2$ were either commercially available or could be synthesized easily in the laboratory. In order to study the reactivity of ClO$_2$ with biological molecules radioactive chlorine dioxide was used. Radioactive chlorine dioxide is not commercially available as a stock item, and chlorine-36 is marketed primarily as H^{36}Cl. This paper describes an electrolytic method for the preparation of high-purity, high specific activity ^{36}ClO$_2$ in good yield from commercially available H^{36}Cl.

0013-936X/83/0917-0245$01.50/0 © 1983 American Chemical Society

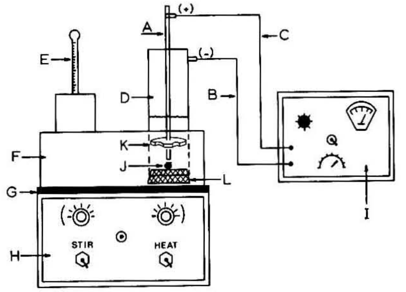

Figure 1. Electrolysis apparatus: (A) carbon rod; (B) cathod; (C) anode; (D) stainless steel tubing (1-in. outer diameter), one end closed with rubber stopper; (E) thermometer; (F) heating block with 1-in. wells; (G) insulator sheet; (H) heater–stirrer with thermostat; (I) power supply; (J) magnetic stirring bar; (K) Teflon spacer; (L) rubber stopper.

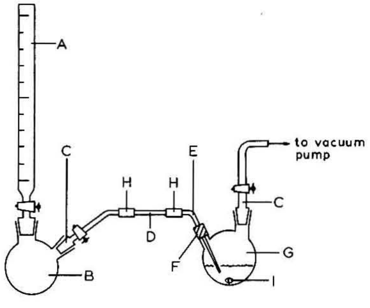

Figure 2. Apparatus for Cl_2 and ClO_2 gas generation: (A) separatory funnel, 10 mL, 14/20 neck (Bantam-Ware, Kontes K299000-0010); (B) two-neck boiling flask, 25 mL 14/20 neck (Kontes K294990-0025); (C) flow control adapter, 14/20 neck (Kontes 275200); (D) glass tubing, 15 cm long (4 mm i.d.), used for column packing when required; (E) inlet tube (Kontes K-275501); (F) rubber adapter (Kontes K-773900); (G) two-neck boiling flask (25 mL, Kontes K299000-0010; 50 mL, Kontes 294990-0050; 100 mL, K605020-0224); (H) Tygon tubing; (I) Stirring bar.

Experimental Section

A practical way to generate ClO_2 from HCl is to prepare chlorate from HCl and then reduce the chlorate to ClO_2 (*1, 10–13*). Chlorate was prepared electrolytically as follows:

$H^{36}Cl$ (New England Nuclear) was adjusted to pH 7.5–8.0 with 1 N KOH and diluted with deionized water to make a final concentration of 0.5 M $K^{36}Cl$. The electrolysis cell was a piece of stainless steel tube (10 cm long, 2.5 cm in diameter), and one end was plugged by using a rubber stopper. Brine (10 mL, 0.5 M $K^{36}Cl$, pH 7.5–8.0) was placed in the cell, which served as the container and the cathode. A 0.63-cm diameter graphite welding rod with the copper-clad covering removed was used as the anode (Figure 1; Arcair, Lancaster, OH 43130). An E-C Apparatus power supply (E-C Apparatus Corp., Philadelphia, PA) supplied power at current settings of 100–500 mA with an anode surface area of about 400 mm². During electrolysis, the temperature was maintained at 65–70 °C, and the solution was gently stirred by using a small Teflon-coated bar.

Potassium chlorate was formed by the reaction of chlorine produced at the anode and hydroxide ion produced at the cathode (reactions 1–3). The equation for

$$2Cl^- \rightarrow Cl_2 + 2e^- \qquad (1)$$

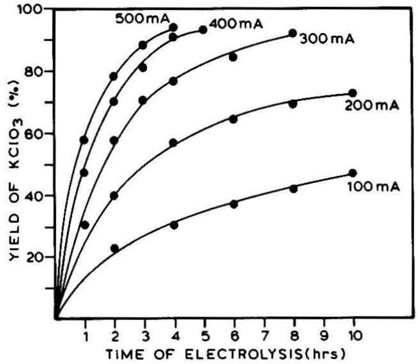

Figure 3. Relationship of duration of electrolysis and current to yield of $KClO_3$. Electrolysis was carried out in a stainless steel–carbon cell containing 10 mL of 0.5 M KCl, pH 7.5–8.0, with temperature maintained at 65–70°C. The yield of $KClO_3$ was calculated by using the formula in the text.

$$2e^- + 2H_2O \rightarrow 2OH^- + H_2 \qquad (2)$$

$$3Cl_2 + 6OH^- \rightarrow 5Cl^- + ClO^-_3 + 3H_2O \qquad (3)$$

the overall process is shown in reaction 4.

$$Cl^- + 3H_2O \rightarrow ClO^-_3 + 3H_2 \qquad (4)$$

Following electrolysis, the liquid in the cell was centrifuged in a clinical centrifuge for 5 min at high speed to remove carbon particles arising from the anode. The supernatant was incubated at 65–70 °C in a 25-mL Erlenmeyer flask and taken to dryness to yield sodium chlorate and sodium chloride crystals.

Chlorine dioxide was then generated from the chlorate salts in a gas-generation apparatus (Figure 2). Dried crystals of chlorates prepared by reactions 1–3 were dissolved in 10 mL of H_2O. A 1-mL aliquot of chlorate solution was placed in flask B containing 25 mg of oxalic acid crystals. Flask G contained 10 mL of organic-free deionized water. With the system under vacuum, 18 M H_2SO_4 was added dropwise to flask B (the reaction is violent), and chlorine dioxide was liberated according to the reaction

$$2KClO_3 + (COOH)_2 + 2H_2SO_4 \rightarrow 2ClO_2 + 2CO_2 + 2H_2O + 2KHSO_4 \qquad (5)$$

Chlorine dioxide, a light orange gas, was readily dissolved in the water in flask G (Figure 1), which was held at 0–4 °C. The exothermic reaction in flask B drives the reaction and expels ClO_2 from the reaction flask. As the reaction nears completion, gentle heating of flask B with a hair dryer increased the yield appreciably.

Chlorine dioxide was determined by an iodometric titration (*14, 15*). Radioactivity was determined by scintillation counting in Aquasol (New England Nuclear) using a Searle Analytic 92 liquid scintillation system, with windows set at 50–800. The number of disintegrations per minute (dpm) was calculated from a quench curve constructed by relating external standard ratios to percentage counting efficiencies.

Results and Discussion

Chemical procedures for the preparation of [^{36}Cl]-chlorate result in very low yields. As an alternative approach, the electrolytic process for preparing chlorates using a carbon–stainless steel electrode electrolysis cell (*10, 12*) was selected. Reaction conditions such as KCl con-

Table I. Fate of ^{36}Cl during the Process of Electrolysis and ClO_2 Generation[a]

column and wt of contents	radioactivity after electrolysis, %		radioactivity after ClO_2 generation, %			
	carbon pellet[b]	$K^{36}ClO_3$ soln	reaction flask	column	$^{36}ClO_2$ trap	void[c] space
none	4	96	6	0	78	16
Na_2CO_3 (1 g)	4	96	6	23	43	14

[a] Details of the procedures are given in the text. Radioactivity present initially in 1 mL of $K^{36}Cl$ solution is given in a relative value of 100 (actual amount 1.2×10^6 to 3.2×10^6 dpm), and subsequent amounts are expressed relative to this value. [b] Pellet obtained by centrifugation of the brine after electrolysis. [c] This value was calculated. Void volume was about 10 times larger than the trap volume.

Table II. Purity and Specific Activity of ^{36}Cl in ClO_2 Solutions. Chlorine Equivalent Concentration Was Determined by the Iodotitrometric Method

column	Cl equivalent at pH 7, dpm/cpm	Cl equivalent at pH 7 to that at pH 2, ratio of ppm	ClO_2, % of Cl equivalent at pH 7	ClO_2-Cl equivalent, dpm/ppm
none	99.5	1:3.7	67.5	67.2
Na_2CO_3	70.6	1:4.9	97.5	68.8

centration, pH, temperature, and distance between the electrodes were selected on the basis of reaction requirements and practical considerations.

Yield of product was calculated according to the following formula:

$$\text{percent yield of } KClO_3 = \frac{DW_t - DW_0}{3MW_0} \div \frac{DW_0}{MW_{KCl}} 100 \qquad (6)$$

where DW_0 is the dry weight of KCl before electrolysis, DW_t is the dry weight of the salts after electrolysis for t min, MW_0 is the formula weight of oxygen, and MW_{KCl} is the formula weight of KCl.

This formula is based on the assumptions that each mole of KCl produces 1 mol of $KClO_3$ and that the increase in weight is due to the addition of 3 mol equiv of oxygen. Although the increase in pH (up to 2 units) observed during the course of electrolysis suggests such possibilities as loss of chlorine as Cl_2, experiments using $K^{36}Cl$ showed no detectable loss of Cl_2.

Experimental results presented in Figure 3 showing yield vs. time at selected amperages led to the recommendation of a 400-mA current (7–9 V) and a duration of 4 h for electrolysis.

In the event some of the KCl was left unreacted, it was possible to separate $KClO_3$ from KCl by their solubility characteristics (*11*, *12*). Pure crystals of $KClO_3$ were formed by dissolving the solids after electrolysis in a small volume of hot water and then cooling the solution. In our laboratory-scale system this step was not helpful, but in the commercial preparation of large amounts of $KClO_3$ it may be economically feasible to salvage unreacted $K^{36}Cl$ by using this technique. It should be noted that $NaClO_3$ is much more soluble than $KClO_3$ (*11*).

The reduction of chlorate can be carried out by oxidative acidification in the presence of sodium chloride, sulfurous anhydride, or oxalic acid (*15*). In this method of ClO_2 synthesis, sodium chloride was not used because Cl^- would be oxidized to Cl_2 and would contaminate the product. The use of SO_2 gas was not practical because of the closed vacuum system. Thus, oxalic acid was the reducing agent of choice. Good product yields routinely resulted in solutions of 500 ppm ClO_2 (2500 ppm chloride equivalent) being routinely prepared.

Contamination of ClO_2 should be minimized during generation, and contaminants such as Cl_2 must be removed before dissolving ClO_2 in water. Either side reactions or acidification of hypochlorites still present in the chlorate solution may form Cl_2. Of the reducing agents that can be used to generate chlorates, oxalic acid produced the least Cl_2; however, the ClO_2 still required purification. During passage of the generated gas mixture through a column of $NaClO_2$, a common practice in the general purification of ClO_2 (*14–16*), it was found that $^{36}ClO_2$ exchanged with the $NaClO_2$ of the column with resultant loss of most of the radioactivity from the gas phase. Substitution of a Na_2CO_3 column eliminated the poor recovery and yielded pure ClO_2 of high specific activity. The sodium carbonate acts as a caustic scrubber, immobilizes Cl_2 as hypochlorite, absorbs CO_2, and has great capacity to absorb impurities. The fate of ^{36}Cl during the process of electrolysis, ClO_2 generation, and purification of $NaClO_2$ is summarized in Table I. These data indicate that more than 90% of ^{36}Cl was evolved from the reaction flask as ClO_2 gas. The solution remaining in the reaction flask (1.9 mL) contained some $^{36}ClO_2$ as dissolved gas as evidenced by the pale yellow color. Since KCl did not produce ClO_2 when treated identically, formation of $KClO_3$ by electrolysis was more than 90% complete and confirms the data for nonlabeled $KClO_3$ shown in Figure 3.

The purity and specific activity of a radioactive compound are the final criteria for the effectiveness of a procedure. A test for purity of ClO_2 in solution is the iodometric titration of chlorine equivalents at pH 7.0 (0.1 N phosphate buffer) and at pH ≤2.0 (glacial acetic acid). In a pure aqueous solution of ClO_2, the following relationship exists:

Five chlorine equivalents at pH 7 = one chlorine equivalent at pH 2.

If ClO_2 is contaminated with Cl_2, HOCl, and/or OCl^-, the percentage ClO_2 chlorine equivalent, calculated from the following formula, will be low:

$$\%\ ClO_2 \text{ chlorine equivalent} = \frac{\text{ppm at pH 2} - \text{ppm at pH 7}}{4} 100 \qquad (7)$$

Purified chlorine dioxide was 97.5% pure, and its specific activity (expressed as dpm/ppm ClO_2 chlorine equivalent) was as high as the ClO_2 prepared without column purification (Table II).

Acknowledgments

We thank J. Bosworth for his technical assistance.

Registry No. $^{36}ClO_2$, 84418-47-3; $K^{36}ClO_3$, 84418-48-4; $H^{36}Cl$, 36640-18-3; oxalic acid, 144-62-7.

Environ. Sci. Technol. **1983**, *17*, 248–250

Literature Cited

(1) Abdel-Rahman, M. S.; Couri, D.; Jones, J. D. *J. Environ. Pathol. Toxicol.* **1980**, *3*, 421–430.
(2) Abdel-Rahman, M. S.; Couri, D.; Bull, R. J. *J. Environ. Pathol. Toxicol.* **1980**, *3*, 431–449.
(3) Ridenour, G. M.; Ingols, R. S. *J. Water Works Assoc.* **1947**, *39*, 561–567.
(4) Ridenour, G. M.; Armbruster, E. H. *J. Water Works Assoc.* **1949**, *41*, 537–550.
(5) Benarde, M. A.; Israel, B. M.; Oliveri, V. P.; Granstrom, M. L. *Appl. Microbiol.* **1965**, *13*, 776–780.
(6) Roller, S. D.; Oliveri, V. P.; Kawata, K. *Water Res.* **1980**, *14*, 635–641.
(7) Cronier, S.; Scarpino, P. V.; Zink, M. L.; Hoff, J. C., presented at the 77th Annual Meeting of the American Society for Microbiology, New Orleans, LA, May 1977.
(8) Ridenour, G. M.; Ingols, R. S.; Armbruster, E. H. *Water Sewage Works* **1949**, *96*, 279–283.
(9) Stevens, A. A.; Seeger, D. R.; Slocum, C. J. In "Ozone/Chlorine Dioxide Oxidation Products of Organic Materials"; Rice, R. G., Cotouro, J. A., Eds.; International Ozone Institute: Cleveland, OH, 1978; pp 383–395.
(10) Incoviello, S. A.; Thomas, R. J. "Migration Data for Chlorine Dioxide-Cl^{36} in Potatoes and Tomatoes"; a report by Olin Research Center, New Haven, CT, 1979.
(11) Robson, H. L. *Encycl. Chem. Technol.* **1949**, *3*, 707–716.
(12) Pitman, A. L.; McLaren, J.; Davis, F. H.; Groggins, P. H. *Chem. Metall. Eng.* **1938**, *45*, 692–696.
(13) Masters, B. J. In "Inorganic Isotopic Synthesis"; Herber, R. H., Ed.; W. A. Benjamin: New York, 1962; pp 215–226.
(14) Franson, M. A., Ed. "Standard Methods for the Examination of Water and Waste Water", 14th ed.; American Public Health Association: Washington, D.C., 1976.
(15) Masschelein, W. J. "Chlorine Dioxide: Chemistry and Environmental Impact of Oxychlorine Compounds"; Ann Arbor Science, Ann Arbor, MI, 1979.
(16) White, G. C. "Handbook of Chlorination"; Van Nostrand-Reinhold: New York, 1979.
(17) Dodgen, H.; Taube, H. *J. Am. Chem. Soc.* **1949**, *71*, 2501–2504.

Received for review December 22, 1980. Revised manuscript received November 8, 1981. Accepted December 6, 1982. This work was supported in part by National Science Foundation Grant PFR 78-27067.

Application of γ–γ-Directional Correlation Measurements for Speciation Studies in Environmental Research

Marcel de Bruin* and Peter Bode

Interuniversity Reactor Institute, Mekelweg 15, 2629 JB Delft, The Netherlands

■ Photons and/or particles emitted consecutively in the decay of a radionuclide exhibit a specific directional correlation pattern. This pattern is subject to perturbations due to interactions between the decaying nuclei and their chemical and physical environment. For molecules in solution, the degree of perturbation depends on the size of the molecule in which the nucleus is incorporated, while the presence of a time dependency of the perturbation is an indication for the occurrence of chemical or physical reactions. The experimental characteristics of perturbed directional correlation (PDC) experiments make the technique very suitable for studies of trace-element behavior in very dilute systems, e.g., that present in biological and environmental systems. This is illustrated with results from a PDC experiment involving trace-element uptake by roots of a tomato plant seedling.

Introduction

Most characteristics of nuclear transformations of radionuclides are virtually independent of the chemical and physical status of the decaying atom. As an exception, an influence of the chemical form on the decay constant has been observed for decay through internal conversion or electron capture since in this case the orbital electrons are involved. However, these differences are small and hard to measure. Stronger effects of chemical binding on nuclear decay characteristics can be observed in the directional correlation pattern existing between particles and/or photons emitted in consecutive decay processes. For certain elements (see Table I) the delay time t_i between these emissions is such that an appreciable disorientation of the nuclear spin may occur (*1*), resulting in a perturbation of the directional correlation expressed as the perturbation factor *G*. The perturbation depends on the chemical and physical status of the decaying atoms such as, e.g., structure and composition of the surrounding of atoms incorporated in solids or size of the molecule the atoms are bound to and viscosity for atoms present in solution (Figures 1 and 2). Changes in the chemical status of a radioactive species will be reflected in the effective directional correlation (*2–5*).

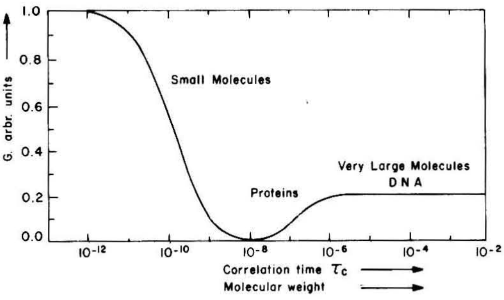

Figure 1. Dependence of *G* on molecular weight and associated rotational correlation time (*6*).

For practical applications of perturbed directional correlation (PDC) measurements, the use of γ-ray-emitting nuclides is most suitable; the directions of charged particles (β^-, α) are strongly altered by interactions between these particles and sample or container material. γ–γ-Directional correlation functions can be measured with the use of two detectors (Figure 3). The viewing angle θ between the two detectors can be varied, and the number of events detected in coincidence in both detectors is recorded as function of θ. The directional correlation often depends on the time elapsed between the two correlated γ-ray emissions. It can be measured as a function of the delay

0013-936X/83/0917-0248$01.50/0

Table I. Characteristic Properties of Some Radionuclides Suitable for Trace-Element Studies Using PDC Measurements

nuclide	half-life	decay mode	γ-γ cascade, keV-keV	cascade abundance,[a] %	t_i,[b] ns	method of production	max spec act., μCi/μg	min concn, ppb
^{57}Co	270 days	EC	122-14	85	98	accelerator		<1
^{67}Ga	78 h	EC	209-184	27	1.0	accelerator		<1
^{75}Se	118.5 days	EC	121-279	16	0.3	reactor	70	2
^{111m}Cd	49 min	IT	151-245	33	85	reactor	1	100
^{115}Cd	53 h	β^-	35-492	0.4	6	reactor	3	3000
^{133}Ba	10.7 years	EC	356-81	62	6	reactor	0.2	200
^{181}Hf	42 days	β^-	133-482	40	11	reactor	20	3
^{188}Re	17 h	β^-	486-155	1	0.7	reactor	350	10
^{199m}Hg	43 min	IT	374-158	12	2.4	reactor	0.2	1000
^{204m}Pb	67 min	IT	911-374	97	270	accelerator		<1
^{237}U	6.7 days	β^-	208-59	23	68	reactor	40	3

[a] Reference 8. [b] t_i = lifetime of intermediate state between the consecutive emission.

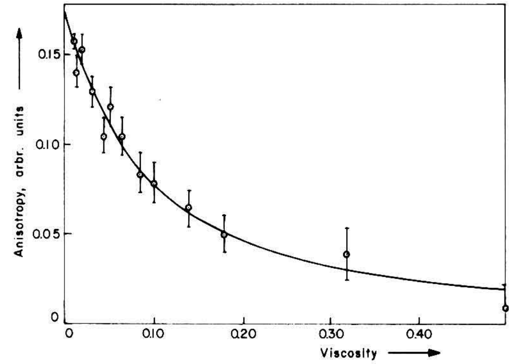

Figure 2. Time-integrated anisotropy of the ^{111}Cd γ-γ-directional correlation as a function of the viscosity of the ^{111}In source (*7*).

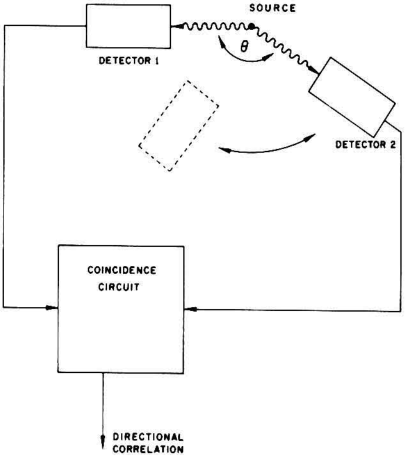

Figure 3. Schematic setup of coincidence spectrometer for γ-γ-directional correlation measurements.

time between the two γ-ray emissions (time differentiated) or as the integral for all correlated γ-ray emissions, independent of delay time (time integrated). Some of the elements suitable for PDC measurements and their relevant nuclear properties are listed in Table I.

When compared to other techniques for observing the chemical status of atoms, PDC measurements show some advantages inherent to the measurement of γ radiation emitted by radionuclides:

γ–γ-Directional correlations can be measured from outside the system under study, without any direct contact and/or chemical or physical disturbance. Moreover, because of the penetrating power of γ radiation, little demands are made on the system containment. These conditions allow for dynamic experiments with easily disturbed systems such as dilute solutions, mixtures in state of equilibrium, and even living organisms.

The mass of an element in a sample can be small, as long as its radioactivity allows for sufficiently precise measurement of the directional correlation. The mass minimally required for an experiment mainly depends on the specific activity of the radionuclide. For accelerator-produced nuclides the specific activity can be very high and is mostly limited by purposely added inactive material. Table I includes the specific activities of radionuclides produced by reactor activation, assuming a thermal neutron flux of 10^{14} ns^{-1} cm^{-2} and irradiation times of 1 half-life with a maximum of 10 days. The table also lists, for a sample volume of 10 cm^3, the element concentrations minimally required for a PDC measurement.

Application of PDC Experiments in Environmental Trace Element Research

The experimental characteristics discussed in the previous section and the applicability to potentially toxic elements such as Se, Cd, and Hg make PDC measurements especially suitable for studies of trace-element behavior as part of environmental research. This includes the speciation of trace elements in various matrices such as natural water and wastewater or soils and studies of adsorption and desorption phenomena in water–soil mixtures. Because of its noninvasive character, the PDC technique can be used in dynamic measurements of uptake and metabolism of trace elements by living organisms like small animals and plants.

The latter application can be illustrated with the first results recently obtained with the IRI PDC spectrometer designed for this purpose in a study of the uptake of ^{181}Hf in roots of plants. Figure 4A shows the time-differentiated directional correlation for ^{181}Hf in a solution containing 1 ppm Hf as $HfOCl_2$. Figure 4B represents the pattern for the same ^{181}Hf after uptake in the roots of a tomato plant seedling grown for 1 day in the Hf solution. It was observed that the Hf appeared to be immobilized in the root and that it is not transported into the stem. A clear difference can be noticed between the two patterns, indicating a difference in chemical status of the Hf before and after uptake in the roots. The periodic pattern observed in the latter case suggests the presence of (part of) the Hf on or in a solid phase, probably the cell membranes.

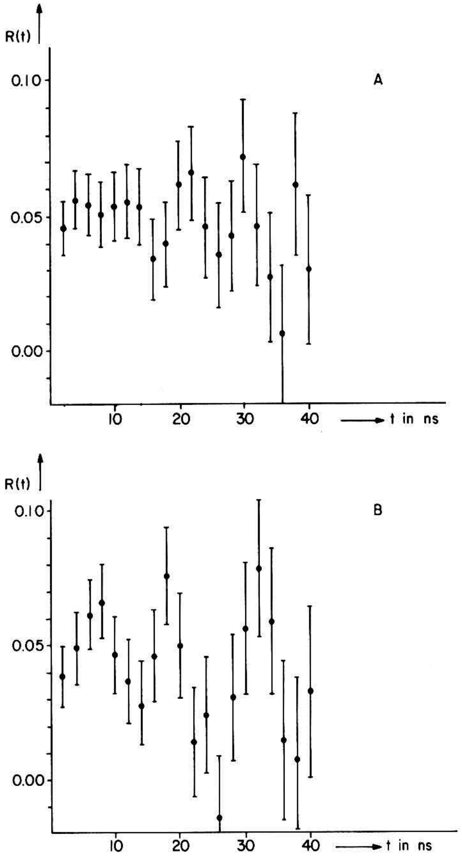

Figure 4. Time-differentiated anisotropy $R(t)$, calculated from a number of coincidences N observed for θ = 90 and 180° according to $R(t) = (N_{90}-N_{180})/N_{90}$ for (a) ^{181}Hf in aqueous solution and (b) ^{181}Hf after uptake in roots of a tomato plant seedling.

This assumption is in agreement with the observation that depositions of immobile elements are located in the cell walls (*9*, *10*).

Concluding Remarks

There is an extensive amount of theoretical and experimental evidence that measurements of perturbed directional correlations may yield information on the chemical status of the decaying atom. Measurement technique and sensitivity make PDC measurements particularly suitable for studies of trace elements. The nature of the usable elements points to the potential importance of the technique in environmental, geochemical, biological, and medical research. It can be expected that in those fields PDC measurements can answer some of the questions on trace-element behavior where commonly used techniques fail because of experimental limitations. Moreover, special attention should be paid to the possibility of dynamic observation of the status of elements inside sensitive systems such as living organisms, which are easily disturbed when applying other experimental techniques.

Registry No. Hf, 7440-58-6.

Literature Cited

(1) Karlsson, E., Matthias, E., Siegbahn, K., Eds. "Perturbed Angular Correlation", supplemented by Proceedings of the Uppsala Meeting on Extranuclear Perturbations in Angular Correlations, 1963; North-Holland: Amsterdam, 1964.
(2) Graf, G.; Glass, J. C.; Richer, L. L. *Adv. Exp. Med. Biol.* **1974**, *48*, 639–679.
(3) Adloff, J. P. *Radiochim. Acta* **1978**, *25*, 57–74.
(4) Rinneberg, H. H. *At. Energy Rev.* **1979**, *27*, 477–595.
(5) van Krugten, H., van Nooyen, B., Eds. "Angular Correlations in Nuclear Desintegration", Proceedings of the Symposium on Angular Correlations in Nuclear Desintegration 1971; Rotterdam University Press: Groningen, The Netherlands, 1974.
(6) Sastry, K. S. R.; Hallee, G. J., presented at the Int. Symp. on Biomolecular Structure, Conformation, Function and Evolution, Madras, India, 1978.
(7) Hemmig, P. B.; Steffen, R. M. *Phys. Rev.* **1953**, *92*, 832.
(8) Lederer, C. M., Shirley, V. S.; Eds. "Tables of Isotopes", 7th ed.; Wiley: New York, 1978.
(9) Läuchli, A. *Planta (Berlin)* **1968**, *83* 137–149.
(10) Rasmussen, H. P. *Planta (Berlin)* **1968**, *81*, 28–37.

Received for review April 8, 1982. Revised manuscript received September 27, 1982. Accepted December 6, 1982.

Introducing the Books that Order Themselves!

With American Chemical Society's *PACT* plan, you'll never have to order a book again!

We have a plan for book purchasing that can make your job a lot easier. It's called **PACT—** Primary Access to Chemistry Titles. And it's easy. Just tell us your chemical subject categories, and we'll send you all the new ACS books in those areas . . . just as soon as they're published.

Know what that means? No more endless paperwork as you order individual books. No more disappointing "out-of-stock" notices. No more wading through scores of book reviews just to find the titles that are relevant to you.

Just one purchase order . . . and the satisfaction of knowing your collections are complete.

Just Choose Your Subjects

Pick one or all of the following subject categories in chemistry from the ACS Advances Series, Symposium Series and Monograph Series:

- **Analytical**
- **Agriculture/Pesticide**
- **Carbohydrate**
- **Cellulose/Paper/Textile**
- **Colloid/Surface**
- **Energy/Fuel/Petroleum/ Geochemistry**
- **Environmental/Health & Safety**
- **Food/Flavor**
- **Industrial/Engineering**
- **Inorganic**
- **Medicinal/ Pharmaceutical**
- **Nuclear**
- **Organic**
- **Polymers/Applied Polymer Science**
- **Physical**

And then be assured of prompt, automatic delivery throughout the year of select books as soon as they're published . . . of just those books that perfectly suit your needs.

No-Worry Guarantee

Your PACT is flexible, too. If at any point you wish to cancel or modify this plan, just say the word. No strings attached! And any book sent to you may be returned for full credit within thirty days.

Want to know more? Call us toll free at (800) 424-6747. Or clip the coupon and send it in today.

Mail to **PACT—Primary Access to Chemistry Titles**
American Chemical Society Sales Office
1155 Sixteenth Street, N.W., Washington, D.C. 20036

YES! I want further information about no-hassle book purchasing through PACT.

Name ______________________________

Organization ______________________ Business Phone ______________

Address ______________________________

City, State, Zip ______________________________

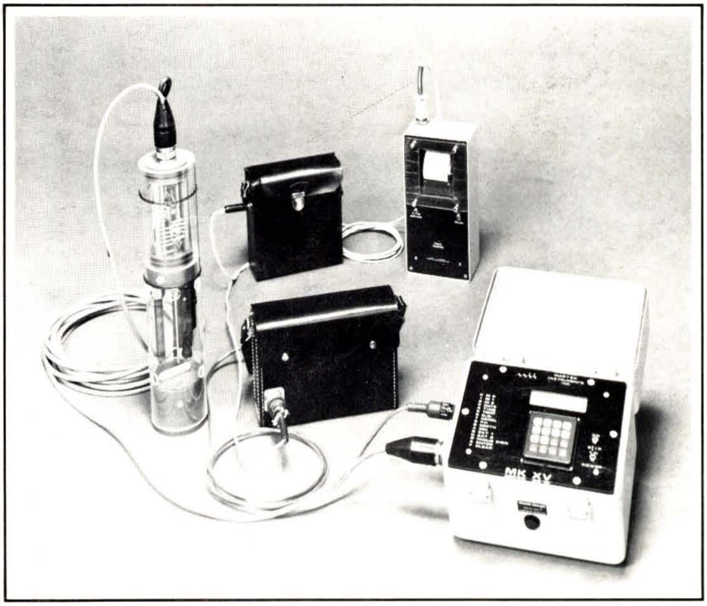
MK XV